Microbial Dynamics and Activity in Mineral Bioleaching Systems: Novel Insights for Improved Process Performance in the Presence of Metallic Toxins

Adedolapo Adeyemi

In fulfilment of the requirements for the degree of
Master of Science in Engineering

Supervisor: Prof Susan T.L. Harrison
Co-Supervisors: Dr Christopher G. Bryan & Dr Mariette Smart

Department of Chemical Engineering
Faculty of Engineering and the Built Environment
University of Cape Town

February 2024

Plagiarism Declaration

1. I know that plagiarism is wrong. Plagiarism is to use another's work and to pretend that it is one's own.
2. I have used the Harvard system for citation and referencing. Each significant contribution to, and quotation in, this report from the work, or works, of other people has been attributed, and has been cited and referenced.
3. This report is my own unaided work, except for assistance received from the teaching staff.
4. I have not allowed, and will not allow, anyone to copy my work with the intention of passing it off as his or her own work.

Signed by candidate

Signature

Abstract

Owing to a decrease in the availability of mined ores as primary mineral sources and a push towards more environmentally sustainable production in the mining sector, there has been an increased interest in the use of historic tailings and electronic wastes for metal retrieval. Bioleaching is considered a suitable method for metal recovery from these wastes. This is because of its perceived low cost, environmental astuteness and its ability to nullify the potential environmental degradation that can occur as a result of these wastes accumulating. However, utilising these wastes is not without its challenges as lower-grade minerals often contain an abundance of metals and other compounds which could be toxic to bioleaching microorganisms and potentially impact performance. While studies on individual iron- and sulfur-oxidising species and their tolerance to metals have been reported for a subset of microbial species of interest, currently, minimal work has been done to quantify the negative effects of these metals when using mixed microbial communities. This information is important as mixed communities are used commercially. Understanding the dynamics and behaviours of the microorganisms within the bioleaching cultures has the potential to increase bioleaching performance and efficiencies as a better understanding would allow for better control of systems and their robustness.

To better understand the impact these inhibitory metals may have on microorganisms, bioleaching tests were conducted. The aim of these tests was to determine the extent to which two chosen metals, nickel and chromium, affected the microbial consortia that were being used. Nickel and chromium were selected because they are metals found within e-wastes such as waste printed circuit boards (PCBs) that could potentially inhibit microorganisms at high enough concentrations. Two similar microbial communities were utilised (BRGM-KCC and BIOX® culture) consisting of different proportions of *Leptospirillum ferriphilum*, *Acidithiobacillus caldus*, *Sulfobacillus benefaciens*, *Ferroplasma acidiphilum* and other microbes. The tests performed included batch small-scale tests in 12-well Microwell plates (MWPs) with only an iron source, tests in MWPs with both an iron and sulfur source, and a semi-continuous test in 1 L bioreactors with a pyritic tailings material. In all studies, increasing concentrations of Ni^{2+} and Cr^{3+} were tested to investigate how these metals influenced microbial-facilitated iron oxidation, microbial growth, pH, redox potential and the microbial speciation of the cultures.

Results show the significance of a single component in the system: for the MWP tests in the presence of no sulfur, nickel was more toxic to the microbes of both consortia, but when sulfur was present, the opposite was seen. Considering the BRGM-KCC culture, the maximum tolerated concentrations (MTCs) in the MWPs without sulfur were 4 and 7.5 g/L for nickel and chromium, respectively, and in the MWPs with sulfur, they were > 4 and < 2 g/L for nickel and chromium, respectively. Studies of the ability of the BRGM-KCC culture to tolerate increasing nickel and chromium concentrations in the semi-continuous bioreactor system in the presence of pyritic tailings confirmed that the microorganisms could tolerate nickel more readily than chromium in the presence of reduced sulfur. At 24 g/L nickel, the change in growth and oxidation was small. Conversely, at 4 g/L of chromium, most microbes were severely inhibited with cell numbers decreasing and iron oxidation ceasing. An important consideration observed in the project was the decoupling of microbial growth and iron oxidation, demonstrated previously in stress environments. In some tests, the iron oxidation achieved in the presence of chromium was higher than tests containing nickel; however, the cell numbers were significantly lower. This indicates that increased iron oxidation may occur as a stress response where microorganisms oxidise more iron to obtain more energy for cell maintenance. The implication of this is that in certain bioreactors, metals can be purposefully added (below the MTC) to increase iron oxidation without the requirement for additional CO_2 supply. However, for this to be sustainable in systems requiring continuous operation, sufficient microbial growth is needed to sustain the population and this was not observed under conditions of chromium inhibition.

Another important finding is related to the microorganism, *Fp. acidiphilum.* In almost all experiments, this microbe was able to maintain its numbers, regardless of the metal inhibitor, metal concentration and increased or decreased numbers of other microorganisms. Even in the semi-continuous bioreactor tests where all other microorganisms experienced a decrease in cell numbers at 6 g/L chromium, *Fp. acidiphilum* was able to maintain its numbers at around 7.16×10^7 cells/mL. *Fp. acidiphilum* has also been observed in commercial bioreactors, with some previously bacterial-dominated cultures seeing a shift towards the archaeon. *Fp. acidiphilum* is clearly a robust microbe found in many instances in laboratories and industrially, and thus understanding its behaviour and tolerance levels is becoming increasingly important. The results show the dynamic nature of bioleaching microorganisms.

The work presented here contributes to knowledge on acidophilic bioleaching microorganisms so that systems can be designed where bioleaching efficiency can be maximised, and wastes can become a more utilised commodity. This work adds value by increasing the amount of information available on common bioleaching microorganisms with regards to metal tolerance.

Acknowledgements

Firstly, I would like to thank my two current supervisors, Prof Sue Harrison and Dr Chris Bryan. Thank you for all your time, effort and support that you provided me with along the way. It was a pleasure getting to see and hear your wealth of experience and knowledge.

Dr Mariette Smart, thank you for all the support in the beginning of my journey, and helping me to learn my way around the lab.

Catherine Edward, thank you for being so willing to answer my questions and help me out in the lab.

Thank you to the National Research Foundation (Grant Reference: MND200605528445) for your financial support over the course of my studies. I would also like to thank BRGM and the UCT Chemical Engineering Department for their financial contributions.

To the CeBER staff: Thank you for being available to help out when things would go wrong (even at the oddest hours).

To my CeBER buddies, it has been so lovely meeting you all and getting to experience the research space with you. You all made this journey so much better and even more fulfilling and I am very happy to be able to call you all my friends. I will always think fondly of our “1 hour” lunch-time breaks.

To my wonderful family, I am so incredibly grateful for your patience, love and support while I completed my studies. Your eagerness to help and your kind, encouraging words were always so soothing in times when I was down and I am truly blessed to have you all in my life. Thank you Mom, Dad and Dipo.

Lastly, I would like to express my gratitude to the Almighty for giving me the strength to carry on.

Table of Contents

List of Figures

List of Tables

Acronyms and Abbreviations

General	
ARD	Acid rock drainage
CeBER	Centre for Bioprocess Engineering Research
EC	Electronic components
EPS	Extracellular polymeric substance
E-waste	Electronic waste
ICP-AES	Inductively coupled plasma atomic emission spectroscopy
MTC	Maximum tolerated concentration
MWP	Microwell plate
PAH	Polyaromatic hydrocarbon
PCB	Printed circuit
PHAH	Poly-halogenated hydrocarbons
qPCR	Quantitative real-time polymerase chain reaction
TSF	Tailings storage facility
VOC	Volatile organic compounds
XRF	X-ray Fluorescence

Microbial Genus	
A.	*Acidiphilium*
Ad.	*Acidianus*
Ap.	*Acidiplasma*
At.	*Acidithiobacillus*
Fp.	*Ferroplasma*
L.	*Leptospirillum*
S.	*Sulfolobus*
Sb.	*Sulfobacillus*
Tp.	*Thermoplasma*

Chapter 1: Introduction

1.1 Background

In recent years, there has been an increased interest in the use of wastes as mineral resources in mining activities. This is due to the depletion of high-grade, simple ores, coupled with a growing focus on waste valorisation (Ahmadi et al., 2015; Joulian et al., 2020; Mäkinen et al., 2020). Global demand for metals is continuously rising, and it is expected for resource requirements to double between 2010 and 2030 (Kinnunen and Kaksonen, 2019). There is demand for a variety of valuable metals, including, but not limited to, copper, nickel, cobalt, manganese and magnesium. These metals are considered critical raw materials or strategic raw materials in the European Union and many other countries, and have high risk associated with their supply (European Union, 2023; Huerta-Rosas et al., 2020). Unfortunately, primary resource availability is decreasing and alternative resources are therefore required to meet the growing metal demands. Historic tailings are a proposed source of these metals, and are in abundance. However, to date, tailings have not been significantly utilised and the mining industry remains heavily focused on the linear economy, extracting value and discarding metals that are more difficult to recover (Ahmadi et al., 2015; Bryan et al., 2011; Kinnunen and Kaksonen, 2019; Liu et al., 2008; Mäkinen et al., 2020; Zhang et al., 2020).

Tailings can be defined as waste residue that originates from mineral processing plants after valuable material has been extracted, and it tends to be fine grain material (Kinnunen and Kaksonen, 2019). Mohanty et al. (2010) claims that approximately 2 – 12 tons of waste is generally produced per ton of metal extracted from ores; however, it is well recognised that the ration of waste to metal depends directly on the grade of ore being processed, with the move to lower grade ores resulting in higher quantities of waste (Harrison, 2018). It is also noted that these numbers vary greatly depending on the ore type, and this is seen with some gold ores where only a few grams of gold may be extracted per ton of ore processed (Costa et al., 2022). These approximations result in an estimated production of tailings in the range of 5 – 14 billion tons produced across the globe per annum (Mäkinen et al., 2020). If these tailings are sulfidic and are improperly managed, it may cause issues such as acid rock drainage (ARD) and metal deportment which are detrimental to the environment (Gao et al., 2021). As described in Owor et al. (2007), when left for long enough periods of time, metals and sulfates within tailings are mobilised into the surrounding environment and have the potential to contaminate groundwater and surrounding lands. Thus, it is beneficial for the volume of this waste to be minimised and the risk associated with it, owing to its potential reactivity, to be reduced. The valorisation of tailings is also noted to align with multiple of the United Nations Sustainable Development Goals (SDGs) and associated goals of the Africa Union's Agenda 2063 which act as blueprints to achieve a more sustainable future through addressing global challenges. The utilisation of tailings contributes to SDG11 (Sustainable Cities and Communities), and SDG12 (Responsible Production and Consumption) in particular (Kinnunen and Kaksonen, 2019; United Nations, 2021) as well as SDG7, associated with clean energy owing to the role of metals in low carbon processes.

Yet another ecological issue related to tailings is the instability of the plentiful tailings storage facilities (TSFs). There are currently 29 000 – 35 000 existing active, inactive and abandoned TSFs internationally (Minetek, 2023). A number of severe TSF incidents have occurred across the globe. Examples include in Spain (Aznalcollar in 1998), Romania (Baia Mare in 2000), Canada (Mt Polley in 2014), Brazil (Fundao in 2015) and recently in South Africa (Jagersfontein in 2022) (Kinnunen and Kaksonen, 2019; Minetek, 2023). Tailings are an immense liability to mining companies and TSFs require good design and constant maintenance. Thus, it is advantageous to decrease the volumes present in TSFs (Kinnunen and Kaksonen, 2019).

An additional advantage related to the use of tailings as a mineral for metal extraction is the fact that it generally possesses a small particle size. Bryan et al. (2011), Ahmadi et al. (2015), Huerta-Rosas et al. (2020), Mäkinen et al. (2020) and Zhang et al. (2020) all utilise different tailings sources that have a P80 < 50 µm as these have already gone through the mineral processing steps of being quarried, crushed and in some instances milled. This then decreases or alleviates the need for comminution which in turn results in decreased costs associated with mineral retrieval and comminution. This has the potential to significantly decrease expenditure as mining and processing can make up between 40 – 60% of the total cost of mineral processing (Kinnunen and Kaksonen, 2019).

Besides the environmental and process benefits associated with the use of tailings, there is also the potential for economic gain. According to Ahmadi et al. (2015), for certain metals, three quarters of their total reserves can be found within tailings. Additionally, it is thought that a single tailings area can possess valuable and critical metals to the value of up to hundreds of millions of euros (Kinnunen and Kaksonen, 2019). However, it is noted that tailings sources are variable and while one may be rich in resources, another may be scarce with minimal metal for recovery. Despite this, all may pose potential environmental issues.

There are a number of different mechanisms that can been used to recover valuable metals from different mineral concentrates and ores. These include pyrometallurgical, hydrometallurgical, and biohydrometallurgical technologies such as smelting, pressure oxidation, chemical leaching, biooxidation, and bioleaching (Kinnunen and Kaksonen, 2019). In some cases, biohydrometallurgy has been considered the most environmentally astute, energy efficient and low cost option (Huerta-Rosas et al., 2020; Mäkinen et al., 2020). This is due to the fact that no harmful gases are released into the environment, and operating temperatures and pressures remain low in comparison to some of the other technologies. These low operating conditions allow for a safer working environment and reduce energy demand with pressures remaining at atmospheric levels, and temperatures generally not exceeding about 80°C (Rawlings, 2011). In addition, biohydrometallurgical technologies are able to be used when processing low metal grades and wastes where impurities may cause issues for other more traditional processing techniques (Kinnunen and Kaksonen, 2019).

One such biohydrometallurgical process that has been commercially used is bioleaching. Bioleaching is a subsection of biomining. It is a bioprocess used to recover metals of value from minerals, where the metals of interest are solubilised into the aqueous phase and subsequently recovered. The process makes use of various sulfur and iron oxidising microorganisms, the specific species present depending on leaching conditions and feed characteristics. It is becoming increasingly popular as a method for the recovery of metals from suitable wastes (Zhang et al., 2020).

While it may always be environmentally beneficial to leach tailings which act as a pollution source, financially, it may not always be deemed feasible as the cost of extraction can outweigh the value of metal obtained from tailings. This is particularly the case for tailings which possess minimal residual metals. As a result, alternative waste sources are also being investigated, one of which is electronic wastes (e-wastes) (Anaya-Garzon et al., 2021; Maluleke et al., 2024a, 2024b; Tapia et al., 2022). Like tailings, these wastes are abundant and have the potential to increase the amount of metal that can be extracted from wastes as a whole. Thus, a co-processing approach is being considered as it allows for the benefit of removing the ARD-producing potential of tailings, while still extracting desirable metals from electronic wastes and tailings where it is present (Bryan et al., 2020; Joulian et al., 2020).

The use of wastes as a metal source is not entirely without its challenges. As mentioned, the heterogeneous, low-grade nature of wastes mean that impurities can be found within its structure. These impurities are present in different forms including flotation reagents, organics, oil and grease, or certain metals (Dew et al., 1997). These impurities can act as inhibitors to bioleaching microorganisms and may then negatively affect bioleaching performance. The type and concentration of these inhibitors vary from waste to waste, but a commonality is that they all contain a certain level of metal inhibitors which at high enough concentrations can negatively impact microorganisms (Cabrera et al., 2005). Limited literature is currently available on the effect of these inhibitors on the growth of specific bioleaching microbes and the resultant shifts in species abundance as a result of exposure to these metals.

The metal content found within both tailings and e-wastes varies widely, and is dependent on many factors. Generally, e-wastes possess a higher concentration of metals, which may be at concentrations high enough to inhibit bioleaching microorganisms. E-wastes consist of many different components such as batteries, cathode ray tubes and printed circuit boards (PCBs). However, the most value can be obtained from PCBs (Bryan et al., 2020). PCB composition is variable, contingent on the type and use of its source equipment. Thus if used in bioleaching systems, there is the potential for a number of metals to be introduced into solution such as copper, nickel, cobalt, aluminium and chromium which may inhibit bioleaching (Abhilash et al., 2021).

This project aims to investigate the microbial metal tolerances of bioleaching microorganisms and study the microbial community dynamics in order to get a better understanding of these microorganisms and explore how they respond to metals in their environment. Nickel and chromium are the metals which are considered because they are present in PCBs and e-wastes in general, and limited literature is available. Mixed communities, which are robust, are considered. They are used in commercial applications, however, minimal literature is available on the effect of toxins on these multifaceted communities as a considerable amount of literature has focused on pure cultures. With a better understanding of these bioleaching microbes, there is the potential for bioleaching systems to be designed which are efficient with maximised metal recovery.

1.2 Scope and constraints

There are various microorganisms which can be used in bioleaching systems to recover different metals of value. While some information may pertain to microorganisms used in bioleaching in general, this project will focus on the BIOX® and BRGM Kasese communities, with particular focus on the BRGM Kasese microbial community. Literature shows that different strains of a single microbe can behave differently (Cabrera et al., 2005).

Another constraint on this project is related to the metals that will be considered. As mentioned, a variety of metals can be found within e-wastes and PCBs. In this project, the metals studied were limited to nickel and chromium. In a co-processing approach where tailings and PCBs are leached, the majority of the metal entering into solution will be from the PCBs. Thus, some of the metal concentrations used in this project are based on PCB compositions. While there is a small amount of nickel and chromium that can be found within tailings, these amounts are much lower than what is found in PCBs. No actual PCBs were used in this project. In addition, chemical interactions between metals within the system were not studied in detail.

1.3 Thesis structure

Chapter 2 consists of an extensive literature review. It starts off giving a definition and overview of the biohydrometallurgical process of bioleaching and provides a detailed comparison of it and other technologies that are currently being utilised to extract and recover valuable metals from different minerals. It then goes into a comprehensive explanation of the mechanism of bioleaching, detailing the dissolution process. The review then focuses on the use of wastes in bioleaching as an alternative mineral source, with particular focus on tailings and electronic wastes. Information reviewed about these wastes include the waste sources, mineralogy and composition, environmental impact of these wastes, current utilisation of the wastes and finally, examples. The literature review then switches focus to the microorganisms used in bioleaching, showing the microbial-facilitated reactions and detailing the microorganisms used in the process. More information is then given on microbial inhibition that can occur and possible causes of the inhibition. The next section in the literature review centres on the bioleaching efficiency that can be achieved with the various indicators of efficiency, and the factors affecting efficiency being described. Finally, the most important information with respect to this project is highlighted in the final section where gaps in current literature are identified in order to show the necessity for this study.

In **Chapter 3**, the research project is explicitly defined. A problem statement, objectives, key questions and hypothesis are stated. Additionally, the implications of the project are stated where it is shown what the information obtained through this project will be able to achieve.

Chapter 4 details the materials and methods section. Firstly, the microbial consortiums used are specified. Following this, methods under the 3 experimental blocks are specified, namely, the batch Microwell plate (MWP) tests without a sulfur source, the batch MWP tests with a sulfur source and the semi-continuous bioreactor tests. The general analytical methods used are then stated in a separate section at the end of **Chapter 4**.

Chapter 5, Chapter 6 and **Chapter 7** are the results and discussion for the MWP with no sulfur, MWP with sulfur and bioreactor studies, respectively. The findings obtained through experimentation are explored in this section. The MWP blocks of experiments are shorter, small-scale, preliminary studies and the bioreactor block is a larger scale, longer study. In **Chapter 5**, provision was made for iron-oxidising microorganisms only with the addition of ferrous sulfate. In **Chapter 6**, provision was made for iron and sulfur-oxidising microorganisms with the addition of ferrous sulfate and tyndallised sulfur. In **Chapter 7**, a pyritic tailings source was used in 1 L bioreactors. In all these chapters, results relating to microbial iron oxidation, microbial growth, redox potential, pH and microbial speciation are discussed.

Finally, the conclusion and recommendations are discussed in **Chapter 8**.

Chapter 2: Literature Review

2.1 Bioleaching

2.1.1 Overview

In bioleaching processes, microorganisms catalyse oxidation reactions to ensure the provision of lixiviants for biohydrometallurgical processes where metals are solubilised, extracted and recovered from different minerals and wastes (Zhang et al., 2020). Metals such as cobalt, copper, nickel and zinc can be obtained in this manner (Huerta-Rosas et al., 2020). Biooxidation, also a biohydrometallurgical process, occurs when microorganisms break down minerals occluding the metal value, with the desired metal remaining in the ore, and being dissolved and extracted into the aqueous phase with subsequent recovery. It occurs when the metal of interest is insoluble by bioleaching. Examples include gold, palladium and platinum. These desired metals may be exposed through biooxidation which solubilises the mineral sulfides present, and then extracted through a secondary treatment such as cyanidation to solubilise the target metal.

Bioleaching is not the only technology available to obtain metal value from minerals; however, in comparison to pyrometallurgical or hydrometallurgical technologies, it has often been considered the most environmentally astute, energy efficient and low cost option (Hedrich et al., 2016; Huerta-Rosas et al., 2020; Mäkinen et al., 2020), especially when handling low grade waste materials. This is due to the fact that it does not release harmful gases into the environment, and it generally operates at low temperatures and pressures in comparison to other hydrometallurgical technologies. These low operating conditions allow for a safer working environment and reduce energy demand with pressures remaining at atmospheric levels, and temperatures generally not exceeding about 80°C (Rawlings, 2011).

Bioleaching can be further divided into different subsections based on the chemical processes taking place. These subcategories are described below (Punia Bangar et al., 2022; Roberto and Schippers, 2022; Vera et al., 2022):

A. Acid bioleaching

This bioleaching refers to the use of microorganisms to produce inorganic acids such as sulfuric acid, carbonic acid and nitric acid, or organic acids such as acetic acid, lactic acid and citric acid. The acid then allows for the dissolution of ores due to the acidity and complexation of metals. This type of bioleaching is generally associated with oxide ores like limonitic laterites or metal sulfides. In cases when sulfuric acid is the acid produced, it is generated by sulfur-oxidising bacteria or archaea which use elemental sulfur when it is added, or use sulfur from the sulfur moiety when metal sulfides are being leached. Currently, the ability to clearly differentiate between acid bioleaching and oxidative bioleaching is not possible when metal sufides are being leached because their dissolution processes encompass ferric iron generated via protons and oxidation reactions.

B. Reductive bioleaching

This bioleaching refers to the dissolution of minerals through reduction catalysed by microorganisms. The major reaction taking place in this leaching is the dissimilatory reduction of ferric iron into ferrous iron. This type of bioleaching is most commonly associated with the leaching of limonitic laterites. However, with the addition of elemental sulfur as a reducing agent and a source of sulfuric acid, the distinction between reductive leaching and acid leaching that occurs is not entirely clear for laterite bioleaching. With reductive bioleaching, since the microorganisms which facilitate ferric iron reduction are simultaneously oxidising hydrogen, it is thought that hydrogen might be able to be used as a potential reducing agent in the future.

C. Oxidative bioleaching

In this bioleaching, ferrous iron and sulfur-oxidising bacteria and archaea catalyse the formation of lixiviants and the lixiviants subsequently dissolve metal sulfides. In this process, oxygen is utilised as an electron acceptor in a system of chemical reactions that can be defined by the thiosulfate pathway or the polysulfide pathway described in Section 2.1.2 below. Ferric iron acts as a lixiviant and attacks metal sulfides via electron extraction and as a result, it is reduced to ferrous iron. Iron-oxidising microorganisms then catalyse the re-oxidation of ferrous iron to ferric iron. All current commercial examples of biohydrometallurgy fall into this category.

2.1.2 Mechanisms

Considering oxidative bioleaching, two potential mechanisms were put forward by which dissolution may occur: direct leaching and indirect leaching (Bosecker, 1997). Following much debate, it is widely accepted that direct leaching does not take place (Ehrlich, 2002; Sand et al., 1995). Instead, it is recognised that indirect leaching can take place via a contact or non-contact mechanism (Coram and Rawlings, 2002).

In the non-contact mechanism, planktonic microorganisms oxidise ferrous iron in solution to ferric iron. The ferric iron that is produced needs to then come into contact with the mineral surface for dissolution to occur. Conversely, in the contact mechanism, most of the microbial cells in a population are attached to the mineral surface (Gehrke et al., 1998). The microorganisms are attached to the sulfide mineral's surface through extracellular polymeric substances (EPS) which allow for a controlled reaction area for mineral dissolution reactions.

Indirect bioleaching occurs when microorganisms generate lixiviants which act as chemical oxidants that break down metal sulfides. Generally, this lixiviant can be ferric iron, formed from ferrous iron via microbial-facilitated oxidation (Bosecker, 1997; Rawlings, 2011), protons, or both. The leaching agent can be found in solution, attached to the mineral surface or in the cells' EPS (Roberto and Schippers, 2022; Vera et al., 2022). Indirect leaching can occur via two pathways; the thiosulfate pathway or the polysulfide pathway seen in Figure 2.1.

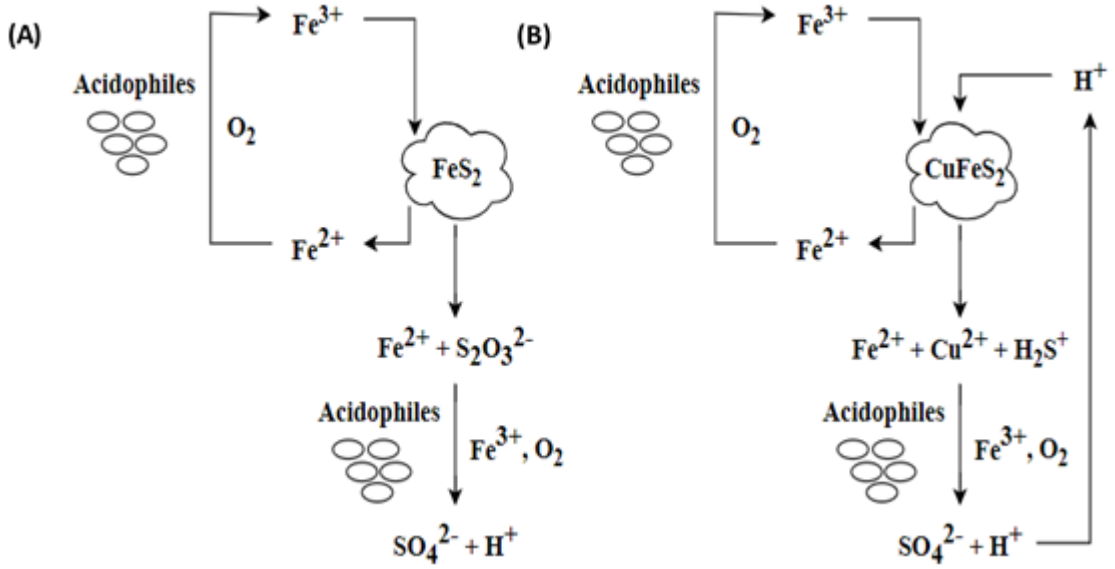

Figure 2.1: Schematic diagram of the thiosulfate (A) and polysulfide (B) pathways that occur with indirect leaching (modified from Schippers and Sand, 1999 and Vera et al., 2022). In (A), the example mineral shown is pyrite (FeS_2). In (B), the example mineral shown is chalcopyrite ($CuFeS_2$). The main electron acceptors are given on the right of the arrows. Note equations are not stoichiometric.

The thiosulfate and polysulfide pathways occur when different minerals are being leached. The thiosulfate pathway occurs when the mineral to be leached is, for example, pyrite, molybdenite or tungstenite while the polysulfide pathway occurs when metal sulfides such as chalcopyrite, zinc sulfide and lead(II) sulfide are being leached. In both pathways, ferric iron attacks the metal sulfides which in turn releases iron in the form of ferrous iron into solution, simultaneously reducing the ferric iron to ferrous iron. When the dissolution of the metal sulfide mineral occurs, both the desired metal cations and water-soluble intermediate sulfur compounds, here $S_2O_3^{2-}$ are released into solution. The ferric iron is then regenerated via microbial-facilitated oxidation of ferrous to ferric iron, using oxygen as an electron acceptor. Various iron oxidisers are responsible for this iron oxidation that takes place (Chandra and Gerson, 2010; Harahuc et al., 2000; Smith et al., 1988). This oxidation reaction can be seen in Equation 2.1.

$$2Fe^{2+} + \frac{1}{2}O_2 + 2H^+ \rightarrow 2Fe^{3+} + H_2O \tag{2.1}$$

In the thiosulfate pathway, the first sulfur intermediate compounds formed are thiosulfate ions ($S_2O_3^{2-}$) while in the polysulfide pathway, sulfaniumyl ions (H_2S^+) are formed. However, it is noted that there are more intermediary phases in the sulfur oxidation stages and other compounds such as elemental sulfur may be produced. Sulfur-oxidising bacteria and archaea are then responsible for the oxidation of these intermediates, yielding sulfuric acid. In the polysulfide pathway, where acid-soluble metal sulfides are being leached, an additional attack executed by protons in solution occurs where valence band electrons of the metal sulfides can be bound by the protons (Schippers and Sand, 1999; Vera et al., 2022). Equations 2.2 and 2.3 show the reactions that take place in the thiosulfate pathway. Equations 2.4 – 2.6 show the reactions taking place in the polysulfide pathway. Note that M in Equation 2.4 represents a general metal (such as copper in the case of chalcopyrite).

$$FeS_2 + 6Fe^{3+} + 3H_2O \rightarrow {S_2O_3}^{2-} + 7Fe^{2+} + 6H^+ \quad (2.2)$$

$${S_2O_3}^{2-} + 8Fe^{3+} + 5H_2O \rightarrow 2{SO_4}^{2-} + 8Fe^{2+} + 10H^+ \quad (2.3)$$

$$MS + Fe^{3+} + H_2O \rightarrow M^{2+} + 0.5H_2S_n + Fe^{2+} \ (n \geq 2) \quad (2.4)$$

$$0.5H_2S_n + Fe^{3+} \rightarrow 0.125S_8 + Fe^{2+} + H^+ \quad (2.5)$$

$$0.125S_8 + 1.5O_2 + H_2O \rightarrow {SO_4}^{2-} + 2H^+ \quad (2.6)$$

While the break-down reactions that cause the dissolution of minerals described above are facilitated by iron and sulfur-oxidising microorganisms through the regeneration of lixiviants, the dissolution component is abiotic and occurs in parallel to microbial oxidation. However, the overall rate at which leaching occurs has been measured to be a million times slower than when microbes are present (Ionescu et al., 2015; Kirby et al., 1999; Singer and Stumm, 1970) . This is a reason bioleaching has been considered above other abiotic leaching techniques in many mining operations.

2.1.3 Bioleaching of wastes

It has been recorded that over the last decade, primary ore and mineral stocks have been consistently decreasing while the global demand for metals has increased resulting in a deficit that needs to be filled by alternative resources (Kinnunen and Kaksonen, 2019). Historically, linear economy-based thinking and maximum value extraction at minimum cost in the mining industry has resulted in the wastes produced being stored and left to accumulate (Kinnunen and Kaksonen, 2019). However in recent years, the bioleaching of waste, as well as low grade ores, has become increasingly important and considered due to the depletion of the higher grade mined ores as well as the environmental benefit associated with decreasing the waste, particularly reactive waste, in the environment (Bryan et al., 2011; Ahmadi et al., 2015; Huerta-Rosas et al., 2020; Mäkinen et al., 2020; Zhang et al., 2020). The wastes being produced, or that are already stock-piled, are plentiful, and include tailings, electronic wastes (e-wastes), sludge, fly ash, sediment, spent catalyst and smelter waste (Zhao et al., 2021, p. 7). Tailings and e-wastes possess high potential on an industrial or commercial scale for further processing because of their large metal inventory (Abhilash et al., 2021; Ahmadi et al., 2015). These wastes are described in detail in Sections 2.2 and 2.3.

2.2 Tailings

2.2.1 Overview

Tailings comprise of finely divided waste residue originating from a mining processing plant. It is generally an effluent from concentration processes such as froth flotation, gravity separation or magnetic separation, but can be considered to be any waste material that is generated in processing plants. Bulk tailings in tailings ponds or dams can possess a wide variety of substances from different sources and are often amalgamations of materials from different effluents (IndustriALL, 2019).

Mäkinen et al. (2020) and Zhang et al. (2020) highlight mine tailings as one of the largest mining wastes in the world, spanning increasingly large areas. It is estimated that 5 – 14 billion tons tailings per annum are produced globally (Mäkinen et al., 2020). These tailings pose as an environmental hazard and more detail about the environmental effects of tailings is given in Section 2.2.2. This include issues such as acid rock drainage (ARD) (Mäkinen et al., 2020; Zhang et al., 2020), metal deportment and physical instability. Thus, from an environmental standpoint, it is beneficial to use tailings as a mineral source in bioleaching to reduce both the amount of reactive waste present in the environment which may lead to issues such as ARD as well as the amount of overall waste in the environment (Harrison et al., 2020, 2013).

Another proposed advantage of utilising tailings is their small particle size. Bryan et al. (2011), Ahmadi et al. (2015), Huerta-Rosas et al. (2020), Mäkinen et al. (2020) and Zhang et al. (2020) all consider tailings having a P80 < 50 µm. This is beneficial as comminution may then not be required as a pre-processing step (Huerta-Rosas et al., 2020; Liu et al., 2008; Zhang et al., 2020). In some studies (Mäkinen et al. (2020) for example), a form of comminution is still performed, but requiring a lower duty; the need for a size decrease is seen to be dependent on the tailings being used.

In addition to environmental and process benefits of bioleaching, metal extraction from tailings can provide both additional resource and economic benefit. Ahmadi et al. (2015) indicates that for certain metals, three quarters of their overall reserves can be found in tailings. With the high capacity available for leaching, it is favourable for more attention to be put into the leaching of tailings. However, tailings, like other mineral sources, may be a limited resource if no new tailings are being produced. Thus, any commercial application should take this into account.

2.2.2 Environmental impact

Utilising tailings as a mineral source is beneficial environmentally as it reduces the volume of tailings and thus decreases the potential for issues such as ARD where harmful material and metals may be solubilised into the surrounding environment if tailings storage facilities (TSFs) are improperly managed. ARD is formed when sulfidic minerals (most commonly pyrite) react with oxygen, water and microorganisms. While the dissolution process occurs naturally in the environment in the form of weathering, mining operations which leave large amounts of sulfidic minerals exposed to oxygen, water and microorganisms in acidic environments expedite the process which may potentially result in an accelerated breakdown referred to as ARD (McCarthy, 2011).

Many cases of ARD from tailings ponds have been reported globally. In the Free State in South Africa, gold mining tailings have decreased the quality of groundwater sources impacting local communities. Of the water samples taken, it was recorded that 40% had elevated lead concentrations and 63% had elevated iron concentrations (Belle et al., 2021). In China, the Luhun Reservoir is located downstream of a molybdenum processing area and a single element pollution factor of 2.05 was recorded for molybdenum concentrations in its waters. This is in the heavily polluted range (Song et al., 2021). In Vicosa do Ceara, Brazil, an abandoned copper mine's tailings has caused the reduction of aquatic macroinvertebrate presence and increased the amount of copper present in living organisms (Perlatti et al., 2021). Lastly, in Poland, heavy zinc pollution and moderate lead pollution of local agricultural land due to mining activities has resulted in a ban in the planting of green leafy vegetables in the area. This farming was previously an important part of the area's economic wealth and the ban has now caused some instability with the removal of that source of income. The ARD that leaches from mine tailings is not only problematic for the environment, but also reduces the amount of metals available for recovery at the time of re-processing.

Another major risk associated with TSFs is their potential for failure and subsequent collapse, releasing a large volume of slurry and causing flooding of toxic material. TSFs thus require intensive maintenance and pose a great safety risk if not managed correctly. In September 2022, the town of Jagersfontein in South Africa experienced a tailings dam failure resulting in a number of fatalities, ecological damage and millions of rands of damage (Minetek, 2023). Globally, many similar incidents have occurred. Examples include the Ajka mine in Hungary in 2010, Philex Padcal in the Philippines in 2012, the Mount Polley mine in Canada in 2014, the Cadia mine in Australia in 2018 and the Córrego do Feijão iron ore mine in Brazil in 2019 (Adiguzel et al., 2022; Owen et al., 2020). These regular TSF failure incidences leave behind large amounts of damage; it is thus beneficial to reduce the likelihood of such cases by reducing the volume of tailings present.

The use of tailings as a mineral source for bioleaching operations aligns with multiple United Nations Sustainable Development Goals (SDGs) which act as a blueprint to attain a better, more sustainable future for all by addressing multiple global challenges. SDGs 6, 12, 13 and 14 are all demonstrated, linking to Clean Water and Sanitation, Responsible Consumption and Production, Climate Action, and Life Below Water, respectively. The use of tailings in bioleaching reduces the possibility of valuable water sources and aquatic life being harmed through metal contamination, allows for responsible consumption and production with the recycling of waste material, and reduces the amount of greenhouse gases being released into the atmosphere compared to other technologies (United Nations, 2021).

2.2.3 Mineralogy

The mineralogy of sulfidic-bearing acidogenic tailings suitable for oxidative bioleaching is diverse; every tailings source has different phases and elements present in different concentrations. However, there are certain minerals present in tailings that can be seen to be common in different sources, and there are different elements associated with these minerals. For example, cobalt is regularly associated with the pyrite phase, found within its grains, while copper is present in chalcopyrite (Ahmadi et al., 2015; Bryan et al., 2011; Mäkinen et al., 2020; Zhang et al., 2020). Knowing the composition of tailings is imperative for bioleaching operations and environmental considerations because it is important to know the elements that could potentially be recovered, or which could be mobilised into surrounding environments if TSFs are mismanaged (IndustriALL, 2019; Mwesigye et al., 2016; Owor et al., 2007).

Table 2.1 provides examples of tailings found around the world, focusing on studies where the desired metals to be obtained are cobalt, nickel, copper and zinc. These are metals commonly present in sulfidic tailings at high enough concentrations to warrant bioleaching, either for recovery for value or for removal to mitigate environmental hazard.

Table 2.1: Comparison of tailings samples used in bioleaching experiments

Major phases present[1]	Desired Element Concentrations[2]	Source	Study
Pyrite, magnetite, talc, antigorite, chalcopyrite	**0.16% Cu**, **0.08% Ni**, **0.04% Co**	Reverse flotation cells from Hematite Recover Plant near Golgohar Iron Mine	Ahmadi et al., 2015
Cobaliferous pyrite	**1.35% Co**	Kasese tailings from flotation concentrate	Bryan et al., 2011
Pyrite, chalcopyrite, sphalerite, barite, galena, other sulfides, silicate	**0.12% Cu**, **0.02% Co**, 1.49% Zn	Rammelsberg bulk mine tailings, Germany	Zhang et al., 2020
Pyrite, chalcopyrite, sphalerite, barite, galena, other sulfides, silicate	**0.57% Cu**, **0.06% Co**, 4.85% Zn	Rammelsberg flotation concentrate, Germany	Zhang et al., 2020
Pyrite, pyrrhotite, quartz, sphalerite, oxidized iron-sulfide, tremolite, calcite	**4.46% Zn**, **1.17% Co**, **0.41% Cu**, **0.03%** Ni	Tailings pond (unspecified)	Mäkinen et al., 2020
Quartz, pyrite, arsenopyrite	0.06% Cu	Janggun mine tailings, South Korea	Ngoma et al., 2018
Quartz, sphalerite, pyrite, calcite, anglesite, gypsum	**0.57% Zn,** 0.02% Cu,	Lead-zinc mine tailings from Shaoguan, China	Ye et al., 2017

[1]Other materials also present, materials with highest concentrations are represented in table. [2]Bold values represent metals that were specifically tested and monitored in each study. However, other values were noted as potential metals that could also be recovered; [2]wt%

2.2.4 Current utilisation

Currently, tailings are not commonly used as a resource and hence the need for an increase in the number of TSFs required globally. The total global cumulative tailings production between 1915 and 2019 was reported to be about 225 billion tons, and this number is currently still growing (Adiguzel et al., 2022). Due to the large volume of tailings being produced, the need to reduce their volume for disposal and reduce the extent of their reactivity is important (Harrison et al., 2020, 2013). Research is underway to determine potential viable uses for tailings. One possibility, as described, is its use as a mineral source for metal recovery through bioleaching. Another possibility is use of the particulate nature of the tailings as a substratum for construction, road building and soil fabrication. The possible use for metal recovery and in the concrete industry are described briefly below with a commercial application of bioleaching being described in Section 2.2.4.2.

2.2.4.1 Concrete industry

The use of tailings in the concrete industry is being considered with tailings being a potential partial replacement for either cement or fine aggregate. This is particularly for non-sulfidic material. This means that with sulfidic tailing, there is a requirement for the material to be leached prior to being used in the concrete industry, and is thus a potential use for bioleaching residues. Studies have indicated that these tailings can be substituted for cement at between 5 to 20%, and can be substituted for fine aggregate at between 10 to 40% (Adiguzel et al., 2022; Gao et al., 2020; Gou et al., 2019). A study by Adiguzel et al. (2022) showed that there was minimal mobilisation of metals in concrete treated with tailings in cases where the concrete was in contact with water. This means there should be minimal concern for potential contamination. However, this is likely to be tailings dependent and may not be the case for all types. The compressive and flexural strength was also seen to decrease with increased concentrations of tailings in the concrete, particularly when it replaces cement. Additionally, the water permeability increased when an excess of 10% tailings was used and this is thought to compromise structural integrity (Adiguzel et al., 2022; Gao et al., 2020; Gou et al., 2019). Thus, according to these studies, a limited amount of tailings can be used. Generally, not much research has been done on the durability of concrete containing tailings. More studies are required before tailings can be used in the concrete industry at a larger scale.

2.2.4.2 Bioleaching industry: Kasese Cobalt Company Limited

The Kasese Cobalt Company Limited ran a commercial plant in Uganda in which it used tailings as a mineral source. To date, this is one of only a few large-scale industrial applications of a plant using tailings for metal recovery, in particular cobalt. Another example is in Vuonos, Finland, where Mondo Minerals talc mine's sulfidic waste stream was leached to recover nickel and arsenic (Mäkinen et al., 2020; Morin et al., 2005; Neale et al., 2017).

The Kasese plant utilised tailings from the abandoned Kilembe copper mine in Western Uganda where 270 000 tons of blister copper was produced. Kilembe was in operation from 1956 to 1978 and used ore from five distinct deposits (Abraham R and Tumwebaze, 2017). The primary sulfides leached in Kilembe consisted of pyrite, chalcopyrite and pyrrhotite in a ratio of approximately 12:7:1. Rarer minerals included linnaeite, sphalerite, diegenite, pentlandite and molybdenite. 15 million tons of waste were produced, of which 7 million tons was in the form of sulfidic flotation tailings. It was estimated that over 1.1 million tons of the waste was cobaliferous pyritic tailings with an average cobalt concentration of about 1.35% (Mwesigye et al., 2016; Owor et al., 2007). This shows the large quantity of cobalt still entrained in the tailings and shows the potential value that can be obtained (Owor et al., 2007). Details on the mineralogy of the Kilembe tailings used as a mineral source in the Kasese plant can be seen in Table 2.2.

There are numerous tailings sites in which the Kasese plant had access to, to utilise as a mineral source. These sites are located around the Kilembe and Nyamwamba River valley area and each tailings source is seen to have varying mineral compositions due to external weathering factors (Mwesigye et al., 2016). Table 2.3 indicates the concentrations of a number of the elements present in the various tailings sites, demonstrating variation in concentration across tailings sites. These tailings have been stored for a long period of time over which leaching and mobilisation of sulfate and metallic elements into the surrounding river basin and soil has occurred (Abraham R and Tumwebaze, 2017; Hartwig et al., 2005; Owor et al., 2007). Studies show that, in comparison to control water and soil samples representative of samples uncontaminated by Kilembe mine tailings, elevated concentrations of cobalt, copper, nickel, zinc, chromium, lead, cadmium, arsenic, iron and sulfates exist in river water and soil near the Kilembe tailings (Mwesigye et al., 2016; Owor et al., 2007), highlighting the negative environmental impact that can be associated with TSFs if they are not managed properly.

Table 2.2: Mineralogy of Kilembe Mine tailings using Strunz 10th Edition Classification[1]
(adapted from Cox et al., 2003; Owor et al., 2007; Mindat.org & Hudson Institute of Mineralogy, 2021)

Mineral	**Chemical formula**
Class 1: Native Elements	
Gold	Au
Class 2: Sulfides and Sulfosalts	
Chalcopyrite	$CuFeS_2$
Linnaeite	$Co^{2+}Co^{3+}S_4$
Marcasite	FeS_2
Molybdenite	MoS_2
Pentlandite	$(Ni_xFe_y)_{\Sigma 9}S_8$ (mostly Ni-rich, but Fe-rich present too
Pyrite	FeS_2
Var. Cobalt-bearing Pyrite	$(Fe,Co)S_2$
Pyrrhotite	$Fe_{1-x}S$ (x = 0 – 0.17)
Siegenite	$CoNi_2S_4$
Sphalerite	ZnS
Class 4: Oxides and Hydroxides	
Cuprite	Cu_2O
Magnetite	$Fe^{2+}Fe^{3+}{}_2O_4$
Quartz	SiO_2
Class 5: Nitrates and Carbonates	
Azurite	$Cu_3(CO_3)_2(OH)_2$
Calcite	$CaCO_3$
Malachite	$Cu_2(CO_3)(OH)_2$
Class 9: Silicates	
Chrysocolla	$Cu_{2-x}Al_x(H_{2-x}Si_2O_5)(OH)_4 \cdot nH_2O$ (x < 1)
Epidote	$\{Ca_2\}\{Al_2Fe^{3+}\}(Si_2O_7)(SiO_4)O(OH)$
Kaolinite	$Al_2(Si_2O_5)(OH)_4$
Muscovite	$KAl_2(AlSi_3O_{10})(OH)_2$
Var. Illite	$K_{0.65}Al_{2.0}[Al_{0.65}Si_{3.35}O_{10}](OH)_2$
Associated Elements	
Al, Au, C, Ca, Co, Cu, Fe, H, K, Mo, Ni, O, S, Si, Zn	

[1] *There is the possibility of other substances being present.*

Table 2.3: Element concentration in Kilembe mine tailings sites in mg.kg^{-1} (adapted from Mwesigye et al., 2016)

Tailings site	Cr	Co	Ni	Cu	Zn	As	Ag	Cd	Pb
1	152	79.7	101	2 270	29.6	11.7	0.40	0.00	6.30
2	136	148	156	1 100	68.3	2.90	0.20	0.30	7.00
3	107	110	118	5 470	41.1	11.9	0.90	0.10	16.2
4	113	152	125	10 200	36.2	5.00	0.80	0.10	4.80
5	121	101	164	165	52	6.30	0.23	0.03	13.4
6	97.4	78.2	119	691	50.9	13.6	0.60	0.10	21.8

With the Kasese tailings being exposed to the environment for about 22 years and undergoing weathering, there is the potential that a differential sulfur concentration gradient has formed within the tailings. This is an important consideration as sulfur concentration plays an important role in bioleaching operations and can affect the efficiency (Liu et al., 2008). Thus, in the use of tailings as a mineral source from TSFs, it is important to consider that tailings from the same area can vary in composition.

The Kasese plant recovered mainly cobalt, with nickel and copper obtained as additional metal value. The plant had a bioleaching efficiency of 92% which was obtained by using a mixed community of acidophilic microorganisms (Bryan et al., 2011).

The Kasese plant was shut down due to political discord and financial constraints (Monitor, 2021; Musisi, 2017; Tenywa, 2013). While there was seen to be a large quantity of tailings concentrate containing a relatively high percentage of cobalt, the amount of metal value within the tailings was not enough to sustain profitable continuous operation for an extended period of time as operating costs outweighed income received. Additionally, the steep fall in copper prices created a further discrepancy between income and expenditure (Monitor, 2021).

This could be a potential issue for a number of tailings streams where bioleaching is technically feasible, but the amount of residual metal within the tailings is not enough to be economically viable. To overcome this issue, additional waste streams can be added to the system in a co-processing approach so that waste treatment and valorisation can result in a higher product yield. A potential supplementary waste stream is electronic waste (e-waste) which is plentiful and continuously growing.

The potential viability of a co-processing approach can be seen in the CEReS project where the co-processing of mine wastes and electronic wastes took place (Bryan et al., 2020). A simplified schematic of the process can be seen in Figure 2.2. In the process, waste printed circuit boards (PCBs) and coal mine wastes were used. After pre-processing of the PCBs, the PCB char was combined with a mixture containing ferric and hydrogen ions as lixiviant, and PCB leaching occurred. The metals were extracted into a pregnant leach solution (PLS) for metal recovery. The lixiviant was produced via bioleaching mechanisms described in Section 2.1.2. The products for recovery from the PLS (and the solid residue left after leaching) include precious metals, rare earth elements, tin-lead solder, copper, gallium, tantalum and iron-based products. By-products such as liquid hydrogen fuels, halogen brine and carbon-rich concentrates are also produced and add value to the process. An additional benefit of the CEReS process is that the different residues, without specific current uses, are benign and the environmental issues associated with their pre-processing are removed (Bryan et al., 2020; NiDieu, 2019).

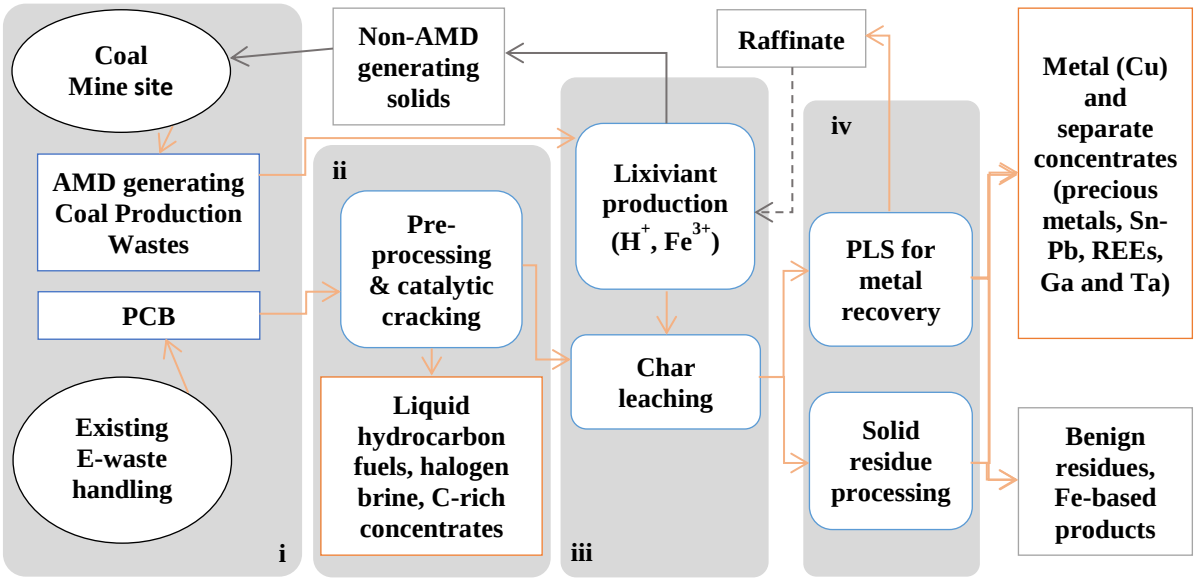

Figure 2.2: Simplified overview of CEReS co-processing project (adapted from Bryan et al. (2020))

Despite the technical process validity of the CEReS concept, it was seen to not be financially favourable as the process does not in its given form create sufficient value to cover all operating expenses. This issue may be alleviated by improving processing efficiency (Bryan et al., 2020). One approach to contribute partially is reducing the number of steps required and combining the processing of the e-waste and mining waste into one vessel. With this, the mine waste bioleaching, lixiviant production, and the PCB leaching would occur together and potentially make the process more economically feasible. However, in doing so, the bioleaching microorganisms would be in the presence of elevated inhibitor concentrations and therefore it would be important to determine how increased concentrations of metals found within these wastes affect the microorganisms.

2.3 Electronic wastes (E-wastes)

2.3.1 Overview

An emerging resource that is recognised as an important source of metals is electronic waste (e-waste) such as printed circuit boards. E-waste, also often referred to as waste electronic and electrical equipment, is the fastest growing waste stream in the developed world. The waste occurs with the advancement of different technologies resulting in old laptops, computers, televisions, telephones, printers, microwaves, and many other technologies, together with their printed circuit boards, being discarded in large stockpiles (Dissanayake, 2014). E-waste results from a variety of sources seen in Figure 2.3, with household appliances being the highest contributor (Chakraborty et al., 2022; Halim and Suharyanti, 2020). Contained within these e-wastes is a variety of metals and other toxic substances including, but not limited to, chromium, nickel, cadmium, mercury, lead, copper and cobalt. (Chakraborty et al., 2022; Dissanayake, 2014). Because of the many potentially harmful components within e-wastes, it is desirable to ensure they are not disposed to landfills, large heaps or stockpiles for long periods of time. Further, because of the limited availability of critical metals, re-use and recycling of key metals is desirable. Hence, a range of solutions to process the growing waste stream are being considered.

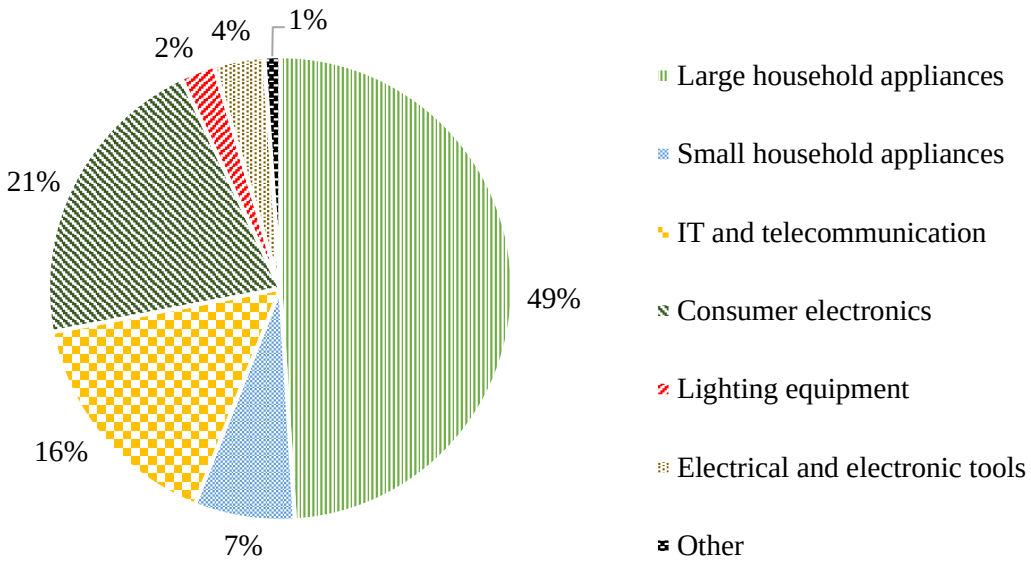

Figure 2.3: Sources of e-wastes (adapted from Halim & Suharyanti, 2020)

PCBs make up about 3 to 6 wt% of the total e-waste produced and are considered one of the more difficult to treat wastes (Wang et al., 2020). PCBs mechanically support and electrically link electronic components with the use of conductive pathways, signal traces and tracks. They are used in the manufacturing of a multitude of machinery and computers and are a vital part of most electrical and electronic devices and thus with the increase in the production of these equipment, comes an increase in waste PCBs (Zeng et al., 2012). Within PCBs, copper, nickel, chromium, aluminium, iron, silver and gold, amongst others, have the potential to be recovered (Mori de Oliveira et al., 2022; Zeng et al., 2012). Due to the large quantity of metals found within PCBs, a substantial amount of value can be extracted from this waste source. Literature shows that by combining the leaching of tailings with the leaching of e-wastes in a co-processing approach, there is the potential for systems to be created where enough metals are extracted to form a financially viable process while also decreasing the negative impact of tailings and other wastes in the environment (Joulian et al., 2020).

2.3.2 Environmental impact

Similarly to tailings, e-wastes have been seen to have a negative effect on the environment with the mobilisation of metals and other components into the surrounding environment where large quantities of these wastes are deposited (Chakraborty et al., 2022; Halim and Suharyanti, 2020; Mori de Oliveira et al., 2022; Wang et al., 2020; Zeng et al., 2012; Zhao et al., 2023). The components within e-wastes have been categorised into two contaminant groups, primary and secondary contaminants. Primary contaminants are the toxic constituents such as metals and halogenated compounds. Secondary contaminants consist of the residues or by-products produced as a result of improper recycling processes, and include polyaromatic hydrocarbons (PAHs), dioxins and poly-halogenated aromatic hydrocarbons (PHAHs) (Halim and Suharyanti, 2020). These contaminants have been seen to be an issue in areas where large quantities of e-wastes have been stockpiled, and in developing countries like Ghana, Rwanda, India, Vietnam, Indonesia and Malaysia because much of the world's e-wastes are transported to these regions and discarded. In many of these developing countries, environmental regulations are not as stringent compared to many other areas and thus inadequate waste management results in increased environmental harm (Andeobu et al., 2021; Dissanayake, 2014; Halim and Suharyanti, 2020).

Globally, there have been multiple examples of how e-wastes have caused the contamination of soil, air and water in the environment. In Vietnam, it was seen that soil and river dioxin compound concentrations were above the maximum acceptable concentration thresholds outlined by the World Health Organisation due to the open burning and open storage practices (Suzuki et al., 2016). In China, analyses conducted on soil samples from rice paddy sites were seen to have elevated copper, nickel, lead, zinc, tin, molybdenum and calcium concentrations due to the proximity to e-waste processing and open burning sites (Uchida et al., 2018). An investigation in India revealed how chromium, nickel, lead, copper and zinc concentrations as well as particulate matter levels (PM_{10}) were elevated in areas near e-wastes, and blood analyses of residents in the area also showed increased metal concentrations (Gangwar et al., 2019). Lastly, in four districts in India, groundwater sources have been seen to have an excess of cadmium concentrations and this is once again attributed to subpar e-waste processing in the form of open-air burning and illegal waste dismantling (Idrees et al., 2018). As can be seen, there are multiple cases around the world showing how growing e-waste stockpiles have a negative environmental impact, and have affected people living near the waste. Thus, it is beneficial from an environmental, health and safety standpoint for e-wastes to be processed to recover metals and to reduce potential negative effects.

2.3.3 Composition

The composition of different types of PCBs and other e-wastes vary widely with nature of device and time period of manufacture, and even electronics or electrical equipment which have the same use can have different concentrations of metals. As mentioned, multiple metals can be found within PCBs including nickel, chromium, copper, cobalt, iron and aluminium (Abhilash et al., 2021). Nickel and chromium, two metals seen to be found within PCBs (and to a much smaller extent in tailings) are metals which have the potential to be disruptive in bioleaching systems at high enough concentrations. In PCBs, nickel is one of the metals which generally has a high presence. In contrast, chromium is seen to be available at lower levels, but literature shows that even at very low levels, it can result in negative effects in leaching systems (Abhilash et al., 2021; Cabrera et al., 2005). It is noted that like nickel, other metals such as copper, iron and cobalt are also seen to be present at high concentrations within PCBs. However, through literature analysis it is seen that more information regarding microbial tolerance and reaction to these metals is available, with little information available for chromium in particular. Considering nickel and chromium concentrations within PCBs, Table 2.4 shows a number of different PCB compositions taken from different sources. Using the sources shown in Table 2.4, an average nickel to chromium ratio of 1:0.03 is calculated.

Table 2.4: Nickel and chromium concentrations within PCBs from different sources

Source	**PCB composition**[1]			
	Nickel		**Chromium**	
(Anaya-Garzon et al., 2021)	0.34	%	0.00842	%
(Kaliyaraj et al., 2019)	1.231 0.1231	mg/g %		
(Wu et al., 2018)	≤ 0.01	%		
(Tapia et al., 2022)	0.4	%	0.017	%
(Abhilash et al., 2021)	0.169	%	0.006	%
(Arshadi and Mousavi, 2015)	0.016	%		
(Choi et al., 2004)	0.25	%		
(Yamane et al., 2011)	0.02	%	91 0.0091	ppm %
(Bas et al., 2013)	1.3	%	72.4 0.00724	ppm %
(Gu et al., 2014)	0.63	%	47 0.0047	ppm
(Hong and Valix, 2014)	4.3 0.00043	ppm %		
(Yang et al., 2014)	0.41	%	0.04	%
(Bryan et al., 2015) Median	0.09 - 1.15 0.62	% %	0.2 - 1 0.00006	ppm %
(Nie et al., 2015)	0.26	%		
(Xia et al., 2018)	11.79 0.01179	ppm %		
(Annamalai and Gurumurthy, 2019)	1.15	%		
Overall Average	**0.357**	**%**	**0.012**	**%**
Ni:Cr Ratio	**1**		**0.03**	

[1]*All % represents wt %.*

In any bioleaching system where e-wastes are being processed, it is evident that microorganisms within the system would be exposed to a substantial amount of metals in view of e-waste compositions. Thus, it is important to take into consideration the potential inhibition that could occur and how the metals affect the bioleaching microorganisms.

2.3.4 Current utilisation

2.3.4.1 Reuse of electronic components

According to Zhao et al. (2023), a large quantity of undamaged electronic components (ECs) from PCBs are discarded as refuse, and most ECs in these wastes maintain an elevated level of functionality and usability. Generally, PCBs are designed for a durability of about 500 000 h, however, the average usage is only about 20 000 h which is only 4% of its capabilities. Thus, there is the potential for these components to be removed and reused, preserving their original function, and the remaining components could continue down other processing steps. This method of e-waste utilisation is beneficial as it would allow for a reduced amount of waste using minimal effort while also reducing the demand for fresh metal supply; however, knowledge on this more direct usage of e-waste is scarce, and more information and research is required to authenticate its viability.

2.3.4.2 Recycling

Currently, there are many methods of recycling in use to handle PCBs and other e-wastes. Generally, mechanical or mechanical-physical recycling methods are used; these include steps involving dismantling, crushing and separation techniques (Wang et al., 2020; Zeng et al., 2012; Zhao et al., 2023). The potential separation technologies are varied and include gravity/density separation, magnetic separation, electrostatic separation, hydraulic shaking bed separation, pyrolysis, open soldering/burning, incineration, strong acid leaching and bioleaching (Halim and Suharyanti, 2020; Wang et al., 2020; Zhao et al., 2023). The technologies are used in various combinations depending on the type of PCB or e-waste being processed and the metals targeted for recovery. Methods which require high temperature and burning are problematic due to the potential for severe Volatile Organic Compound (VOC) and other chemical contamination into the atmosphere. Additionally, these methods along with strong acid leaching and hydraulic bed separation have been seen in some cases to have low value recoveries (Halim and Suharyanti, 2020).

2.3.4.3 Bioleaching

Bioleaching can be used to extract valuable material from PCBs and other e-wastes. It has the benefit of not being energy intensive and having minimal negative impacts on the environment. The use of bioleaching as a method to retrieve valuable metals from PCBs and other e-wastes is still in its infancy. Research is ongoing to ensure it is feasible at a commercial scale (Annamalai and Gurumurthy, 2019). In terms of the technical process feasibility of the bioleaching, a wide variety of metal recoveries have been reported. Considering copper, one of the most prevalent metals found in PCBs, recoveries reported across multiple studies can be seen in Table 2.5. The wide range of recoveries result from varying temperature, acidity, type and amount of metals present in the PCB, pulp density, residence time, microorganisms used and type of reactor, amongst other parameters. Therefore, it is important to optimise these factors to ensure bioleaching systems are optimized and potential inhibitors can be accounted for.

Table 2.5: Copper recovery from PCBs in various research studies

Source	Copper recovery (%)	Microorganisms and Conditions
(Abhilash et al., 2021)	93	*A. thioxidans* & *A. ferroxidans*, 35°C, pH 2, 8% pulp density, 10 day residence time (RT), flask test
(Abhilash et al., 2021)	66	*A. niger*, 35°C, pH 2, 8% pulp density, 10 day residence time (RT), flask test
(Tapia et al., 2022)	69	*Tissierella*, *Acidiphilium* & *Leptospirillum* bacteria, 30°C, pH 2, 10 g/L pulp density, 18 day RT, stirred tank reactor
(Kaliyaraj et al., 2019)	68	*Actinobacteria* strain TN10, 28°C, pH 5 – 7, 120 hour RT, flask test
(Wu et al., 2018)	93.4	*Leptospirillum ferriphilum* & *Sulfobacillus thermosulfidooxidans*, 100 g/L pulp density, 9 day RT, flask test
(Ilyas et al., 2013)	78	*Sulfobacillus thermosulfidooxidans* & *Thermoplasma acidophilum*, 45°C, pH 2, 100 g/L pulp density,165 day RT, column reactor

2.4 Microorganisms

A variety of acidophilic microorganisms are utilised or found in bioleaching communities. These include species within the genera *Acidithiobacillus* (*At), Leptospirillum (L), Ferroplasma (Fp), Sulfolobus (S)* and *Acidianus (Ad)* (Bosecker, 1997). These microorganisms oxidise the sulfur and iron species present in the mineral or waste and thereby generate lixiviants in the process by which the metal value is solubilised. Soluble metal sulfides are converted via biochemical reactions into water-soluble metal sulfates.

2.4.1 Microorganisms used

An important decision that needs to be made in any bioleaching system is the choice of microorganism. Rawlings and Johnson (2007) speaks of two approaches to choosing microorganisms: the top-down approach where many microorganisms are placed into the system to make a robust, biodiverse microbial community and the bottom-up approach where specific microorganisms are chosen for certain characteristics. Through experiments where cobaliferous pyritic tailings from the Kasese plant in Uganda were leached, it was tested whether the top-down approach or bottom-up approach was more effective. The following bioleaching experiments were carried out: bioleaching the unsterilized and untreated Kasese tailings with no new inoculation, bioleaching treated tailings with the indigenous microbial community from the Kasese plant, bioleaching treated tailings with a reconstituted consortium consisting of the four main indigenous microorganisms (*L. ferriphilum* BRGM-1, *Sulfobacillus (Sb) benefaciens* BRGM-2, *At. caldus* BRGM-3 and *Fp. acidiphilum* BRGM-4), and bioleaching with a designed consortium where certain microorganisms were chosen for specific characteristics. The microorganisms used in the designed consortium consist of G1 (a gram positive iron and sulfur oxidiser which is a mixotroph and firmicute), *Acidimicrobium ferroxidans* TH3 (an iron oxidiser which is a mixotroph and actinobacterium), *At. thiooxidans* SDE4 (an autotrophic sulfur oxidiser), SDE2 (an iron and sulfur oxidizing firmicute) and Y008c (a gram positive iron oxidiser which is a mixotroph and is made by contaminating a culture of Y008).

The results from this study indicated that the top-down approach was most effective. The designed consortium performed the worst, having had no initial acclimation time for the microbes to adjust to the conditions of the bioleaching system. This highlights the importance of microbial readjustment periods before use in new systems.

In the Kasese plant, the microbial community used originally consisted of *L. ferriphilum*, *At. caldus* and *Sb. benefaciens* as the main components. However, over time, there was some change in the community structure to a *L. ferriphilum* dominated community with decreasing *At. caldus* and *Sb. benefaciens* (Bryan et al., 2011). In addition, the appearance of a *Ferroplasma* species was observed. The appearance was attributed to the opportunistic behaviour of the archaeon which occurs with the *Ferroplasma* sp. utilising the organic carbon produced by the other microorganisms (Bryan et al., 2011). In a study by Zhang et al. (2014), where bioaugmentation with a *Ferroplasma* species was undertaken to test *L. ferriphilum* and *At. caldus* leaching of chalcopyrite, the early leaching stages showed the same trend seen in Bryan et al. (2011), with an increase in *Ferroplasma* accredited to an increase in the other microorganisms which in turn increased dissolution. However, at later stages of leaching, with a higher *Ferroplasma* concentration, the opposite was seen in the dissolution process. In a number of microbial communities, an increased archaeal dominance is being seen. This is also the case for the BIOX® culture in commercial settings. The laboratory BIOX® culture maintained on Fairview mine concentrate in the Centre for Bioprocess Engineering Research, University of Cape Town, has been dominated by *L. ferriphilum* and *At. caldus* at standard BIOX® conditions. However, this is not the case in commercial BIOX® reactors where there has been a shift to archaeal dominance with an increase in *Fp. acidiphilum* and a *Thermoplasma sp.* (Smart et al., 2017c). These changes have been attributed to changes in operating conditions and the opportunistic nature of the archaeal species. However, there is also the potential for metals and other material within the reactors to be affecting community dynamics and this indicates the importance of understanding the effects different metal components in bioreactors have on bioleaching microorganisms.

Considering a number of commonly used and found bioleaching microorganisms, Table 2.6 below gives information on the various species and their operating ranges taken from different literature sources

Table 2.6: Characteristics of different microbial species present in bioleaching systems (Makaula, 2019; Schippers, 2007; Schippers et al., 2014; Watling, 2016)

Microorganism	Growth substrate	Optimum operating conditions
Bacteria		
Leptospirillum ferriphilum	Iron	Temperature: 30 - 37°C pH: 1.3 – 1.8
Acidithiobacillus caldus	Sulfur	Temperature: 45°C pH: 2 – 2.5
Sulfobacillus benefaciens	Iron & Sulfur	Temperature: 38.5°C pH: 1.5
Acidithiobacillus ferrooxidans	Iron & Sulfur	Temperature: 30 - 35°C pH: 2.5
Acidithiobacillus thiooxidans	Sulfur	Temperature: 28 - 30°C pH: 2 - 3
Leptospirillum ferrooxidans	Iron	Temperature: 28 - 30°C pH: 1.5 - 3
Sulfobacillus thermosulfidooxidans	Iron & Sulfur	Temperature: 45 - 48°C pH: ~ 2
Archaea		
Ferroplasma acidiphilum	Iron	Temperature: 35°C pH: 1.7
Acidiplasma cupricumulans	Iron & Sulfur	Temperature: 54°C pH: 1 – 1.2
Thermoplasma Acidophilium	Sulfur	Temperature: 56°C pH: 1.8
Acidanus brierleyi	Iron & Sulfur	Temperature: ~ 70°C pH: 1.5 - 2

2.4.2 Microbial inhibition

In reviewing the different microorganisms used in the bioleaching of tailings, it is apparent that bacterial iron oxidisers generally have dominated cultures (Bryan et al., 2011; Mäkinen et al., 2020; Zhang et al., 2020). However, as stated, there has been a shift in many communities with archaeal presence increasing. This could be due to a variety of factors such as different microorganisms favouring certain operating conditions, competition and synergy between microorganisms, or inhibitory substances. These inhibitory materials include flotation reagents, flocculants, defoamers, organics, oil and grease, chloride, or certain metals (Dew et al., 1997). Considering the metallic element inhibitors in particular, it is apparent that these toxic elements may enter the bioleaching system through the use of tailings and other waste sources like e-wastes.

While native acidophilic microbial species have generally adapted and evolved to deal with higher heavy metal concentrations in their environment by developing detoxification mechanisms, there is still a limit to the amount in which they can tolerate (Bruins et al., 2000). Some metals, such as chromium, cobalt, copper, magnesium, manganese, nickel and zinc, are required in trace concentrations for microbial metabolism to occur. Others, such as aluminium, cadmium, gold, lead, mercury and silver, are not essential. The issue arises when concentrations present in the mineral or waste source to be leached becomes too high, with an excessive amount bioavailable to the leaching microorganisms (Igiri et al., 2018). High concentrations of metals can have an intensely destructive impact on the different microbial species used in bioleaching. Table 2.7 shows the effect various metals have on bioleaching microorganisms when present at high enough concentrations.

Table 2.7: Metal toxicity to bioleaching microorganism (adapted from Igiri et al., 2018)

Metal	Effect on microbes
Arsenic (As)	Enzyme deactivation
Cadmium (Cd)	Protein denaturing, nucleic acid destruction, hindering of cell division and transcription
Chromium (Cr)	Growth inhabitation, elongation of lag phase, hinders oxygen uptake
Copper (Cu)	Cellular function disruption, enzyme activity inhibition
Selenium (Se)	Growth rate inhibition
Lead (Pb)	Nucleic acid and protein destruction, enzyme activity and transcription inhibition
Mercury (Hg)	Protein denaturing, enzyme activity and cell membrane destruction
Nickel (Ni)	Cell membrane disruption, enzyme activity hindered and oxidative stress
Silver (Ag)	Cell lysis, cell transduction and growth inhibition
Zinc (Zn)	Death, decreased biomass, growth inhibition

Considering the general mineralogy and composition of various tailings and e-wastes respectively, and comparing it to the metals shown in Table 2.7, it can be seen that many of the components found within these waste sources have the potential to negatively effect and inhibit bioleaching microorganisms. In some cases, the desired metals of value that are to be extracted may potentially also have negative effects on the bioleaching microbial community. In Huerta-Rosas et al. (2020), this is seen with the desired metal, silver, negatively affecting the bioleaching bacteria and fungi used to leach the silver and manganese-rich ore. In the study, metal tolerance was tested by including a set of experiments, which assessed different microorganisms' reactions to increasing silver concentrations. This information is valuable to have in order to better understand the dynamics of different microbial consortia and determine why certain microorganisms may be more present and active than others. Therefore, in having information available about the metal tolerances of a microbial community, a better understanding of the dynamics of community structure can be obtained (Igiri et al., 2018).

It is important to note, however, that possessing knowledge on a metal tolerance of a species does not necessarily indicate that tolerances of all strains are known. Cabrera et al. (2005) highlights this when comparing the results of their metal tolerance tests of *Acidithiobacillus ferrooxidans* and an *Acidiphilium sp.* to other strains, seeing the variation in maximum tolerated concentrations (MTC) of cadmium, copper, chromium, zinc and nickel. Not only were the MTC values varying, but also the order of metal tolerance. Furthermore, it was seen that the MTC values changed with leaching conditions, with a system of *A. ferrooxidans* alone showing different MTCs than a system of *At. ferrooxidans* and an *Acidiphilium sp.* Thus, it can be seen how microbial strain, microbial community and leaching conditions all play a role in a microorganism's ability to tolerate metals. For each community, it is advised to test the metal tolerance based on the specific strains of interest (Cabrera et al., 2005). However, in general, it was seen that toxicity followed the following trend: $Cr^{3+} > Cu^{2+} > Cd^{2+} > Ni^{2+} > Zn^{2+}$. This indicates that from the tested metals, chromium was seen to be the most toxic and zinc the least (Cabrera et al., 2005).

2.5 Bioleaching efficiency

The bioleaching efficiency is a significant concept that needs to be considered in bioleaching processes. It is the measure of the activity of the microorganisms and is used to compare different systems. Various factors can be used to test the bioleaching efficiency of an experiment. These include measuring or calculating the pH, redox potential (ORP), metal extraction, iron oxidation rate and acid production. Through research, different parameters are continuously being altered and tested in order to optimize the efficiency of bioleaching systems.

2.5.1 Indicators of efficiency

2.5.1.1 Metal recovery

This has been stated to be one of the most important parameters in testing bioleaching efficiency. It gives a value which is directly related to recovery of the metal value and when needed, can be compared to commercial applications to determine whether leaching is more efficient. Comparing different metal recovery percentages and associated leaching conditions allows for the potential for optimized processes to be designed.

2.5.1.2 Redox potential and pH

The pH and the ORP are additional parameters that have been measured in bioleaching experiments to assess the bioleaching activity. The pH is often a manipulated variable that is varied to test for the optimal value, but at the same time is monitored over the course of bioleaching. With the leaching of pyrite, decreasing pH has been seen to indicate more activity of sulfur oxidisers and in that way showcases the bioleaching efficiency (Bosecker, 1997).

In terms of ORP, its measurement can also indicate the activity of microorganisms, with higher ORPs generally associated with more oxidation occurring (Ahmadi et al., 2015). However, it has also recently been seen as a variable that could potentially be manipulated to achieve better bioleaching. According to Ahmadi et al. (2015), pyrite is better leached at a higher ORP (> 645 mV) while chalcopyrite and sphalerite are, conversely, better leached at a lower ORP (400 – 450 mV). This is corroborated in Zhang et al. (2020) which shows more active microorganisms leaching the pyritic phase at a higher ORP and the converse for the sphalerite phase. Ahmadi et al. (2015) goes on to recommend a two-stage process for bioleaching where the ORP is initially high to leach pyrite, and then later decreased to more efficiently leach other minerals. Furthermore, it is suggested that possible methods to alter the ORP are to change the mass transfer rate of oxygen by either changing air flowrate into reactors or regulating the stirring rate.

2.5.1.3 Iron oxidation rate

As described in Section 2.1.2, microbial-facilitated iron oxidation occurs when iron-oxidising microorganisms aid in the oxidation of ferrous iron to ferric iron. When conducting experiments, this oxidation can be monitored by recording the decrease in ferrous iron concentration and over the course of an experiment, the oxidation rate can thus be determined. Generally, continuously higher oxidation rates are linked to more active, vigorous microorganisms and thus comparing iron oxidation rates can be used as a measure of bioleaching efficiency for iron oxidisers. The same can be done for sulfur oxidisers by determining sulfur oxidation rates. It is noted that in leaching systems, abiotic oxidation also occurs where microorganisms are not involved. Abiotic iron oxidation was observed to be between 0.013 and 0.030 $g.L^{-1}.h^{-1}$ (average of 0.021 $g.L^{-1}.h^{-1}$) in systems with a pH above 5 and temperatures between 12.2 and 29.8°C. (Kirby et al., 1999).

Additionally, Singer and Stumm (1970) states that abiotic iron oxidation can be 10^6 times slower than microbial-facilitated iron oxidation at low pH values below 3.5. This study was conducted at 25°C.

Thus it is important to note that oxidation can still occur without the assistance of microorganisms (Kirby et al., 1999), albeit very slowly, and the rate in which it occurs is dependent on various factors such as pH and temperature.

2.5.1.4 Acid production

Another measure of bioleaching efficiency is the rate in which acid is produced. Depending on the microorganisms used, different inorganic or organic acids are produced. However, commonly, sulfuric acid is an acid that is formed and used to determine the efficiency of the process (Vera et al., 2022). Sulfuric acid production is facilitated by sulfur-oxidising microbes and therefore the activity of these microorganisms can be attributed to their ability to produce this acid. Acid production can be monitored via keeping track of parameters such as pH, sulfur sources and different component concentrations (Hong and Valix, 2014; Y.-H. Lin et al., 2010). It is noted that there can be complexities involved in determining acid production due to factors such as various intermediates or precipitates forming which remove acid components out of solution, or different minerals present being acid consuming or producing.

2.5.2 Factors affecting efficiency

Factors that affect the bioleaching efficiency can vary widely. They include pH, solids loading percentage/pulp density, temperature, hydraulic retention time (HRT), nutrients present, microorganisms used, inhibitory compounds, and the mineralogy of tailings (Ahmadi et al., 2015; Bryan et al., 2011; Huerta-Rosas et al., 2020; Mäkinen et al., 2020; Zhang et al., 2020). This section will detail information on six of these parameters: pH, temperature, solids loading, HRT, nutrients used and inhibitors present.

2.5.2.1 pH

The adjustment of the pH in bioleaching is a necessary condition for the growth of acidophilic microorganisms. A wide range of pH values are used in bioleaching systems with certain studies showing microbial activity at lows of 0.5 and highs of 3.5 (Plumb et al., 2008). The ability of a microorganism to withstand a low pH is dependent on the species and strain. In general, however, the pH is not increased to a value that is too high in order to limit the possibility of jarosite or other iron oxide precipitate formation. Jarosite may form at a pH of about 1 to 3, but more intensely in the upper part of the range. It decreases the availability of Fe^{3+} ions in solution for leaching as elements bond with the ions and thus reduce the bioleaching efficiency (Gahan et al., 2009). Conversely, very low pH < 1 are also generally avoided. This is due to the fact that many microorganisms are seen to be inhibited at a pH this low, with cessation or partial cessation of activity seen at a pH of 1.2 for a variety of species and strains (Yahya, 2016).

2.5.2.2 Temperature

Like pH, the temperature is a parameter where the optimum values are seen to vary widely based on microbial species and strain. Either mesophilic or moderately thermophilic microorganisms are utilised and each of these groups are seen to operate over a different range. Mesophilic bacteria operate around 30°C while moderately thermophilic microorganisms operate between about 40 - 50°C (Ahmadi et al., 2015; Zhang et al., 2014). A number of studies have preferred the use of moderately thermophilic microorganisms due to an increased reaction rate with an increase in temperature.

An increased rate leads to an increase in dissolution; however, higher temperatures also accelerate iron precipitation reactions (Ahmadi et al., 2015; Franzmann et al., 2005).

It should be noted that different strains of microorganisms in the same species may fall into different categories due to them having adapted to their environment at a particular temperature. In light of this, it can be noted that the microorganisms typically used in the bioleaching system of interest operate at a temperature range of about 30 - 50°C.

2.5.2.3 Solids loading

Solids loading, also commonly denoted as the pulp density, refers to the amount of solids that are present during bioleaching. In general, a decrease in pulp density is seen to increase microbial activity, with a higher ORP being recorded potentially due to the increase in gas-liquid mass transfer (Ahmadi et al., 2015). Additional challenges related to high solids loading rates are physical abrasion and increased concentration of potentially toxic metals in solution. However, it is desirable to maximise the solids loading to maximise mineral throughput (Ahmadi et al., 2015; Nemati and Harrison, 2000). Thus, a balance needs to be reached where the maximum pulp density which will not cause substantial microbial inhibition is used. Commercial systems generally target a solids loading of about 10 – 20%, though increasingly, the number is seen to be closer to 20% (Bryan et al., 2011; d'Hugues et al., 1997).

2.5.2.4 Hydraulic retention time

The hydraulic retention time (HRT) is defined as the average period of time that substrate and cells remain within a reactor. Theoretically, a shorter HRT would be desirable as it would mean obtaining the desired metal in a shorter period of time. Additionally, it would mean that the bioleaching microorganisms are in contact with potential inhibitors in the vessel for a shorter period of time. However, with a shorter retention time, there is a risk of microorganisms being washed out of the system without completing the desired leach. Thus, a balance needs to be reached where the HRT is long enough for bioleaching to take place appropriately, but short enough so that there is minimal negative inhibitory effects on the microorganisms (Ahmadi et al., 2015). Commercial systems generally target a HRT of about 6 – 7 days (Mäkinen et al., 2020; Neale et al., 2017).

2.5.2.5 Nutrients

Nutrients for bioleaching microorganisms can be supplied through media (0K, Norris, Autotrophic Basal Salt), trace element solution, various nutrient supplementations (for example, ferrous sulfate for iron oxidisers, a sulfur derivative for sulfur oxidisers and yeast extract for heterotrophs) and a mineral source (Centre for Bioprocess Engineering Research, 2018). The nutrients to be added is dependent on the microbial community that is used. The use of different nutrients at varying concentrations has been seen to drive communities into different consortia and could potentially be used to obtain a community which is dominant in particular microorganisms. This is seen in Liu et al. (2008) and Lin et al. (2010) where different concentrations of sulfur are seen to have an effect on the microorganisms as well as on the leaching efficiency of the systems. Additionally, it is seen that in stirred-tank reactors, nutrient provision is the third-largest operating cost after power consumption and pH control (Aswegen et al., 2007).

2.5.2.6 Inhibitors

As stated in previous sections, the presence of inhibitors has a big impact on the leaching ability and presence of microorganisms in the system. Inhibitors can enter the system through a variety of sources such as the mineral or compound being leached, the water source, or upstream processing (Dew et al., 1997). In terms of metals inhibitors, there are a variety which may have a negative effect on bioleaching microorganisms at high enough concentrations, and these include nickel and chromium (Cabrera et al., 2005; Igiri et al., 2018). Nickel is generally seen to dissociate into a +2 oxidation state (Benoit and Maier, 2013; Cabrera et al., 2005; Igiri et al., 2018).

Chromium has been seen to commonly dissociate into a 3+ or 6+ oxidation state, with Cr(VI) being an especially toxic and strong oxidant which is easily reduced into Cr(III) (Bodzek, 2015; Cabrera et al., 2005; Igiri et al., 2018).

In Anaya-Garzon et al. (2021), PCB leachate was analysed to determine the elements which are solubilised into the aqueous phase. The metal inhibitors with the highest concentrations were copper, aluminium, zinc, nickel, magnesium, manganese, tin and chromium, ordered from highest to lowest. At a PCB solids loading of 80 % (v/v), there was seen to be complete inhibition with no microbial growth occurring. At 40 % (v/v) and 60 % (v/v) growth and iron oxidation did occur, but at a decreased extent compared to the control containing no leachate. Interestingly, it was seen that after successive subcultures, the activity of the microorganisms was increased. This indicates the ability of the microorganisms to adjust to metals. Considering nickel and chromium, it was seen that 0.22 g/L and 0.008 g/L of the metals were present in the PCB leachate, respectively, at an initial 10% (w/v) of raw PCB. The chromium concentration being much lower than that of nickel is what is generally seen in raw PCBs and PCB leachate. However, it is widely reported that chromium a lot more inhibitory to bioleaching microorganisms than nickel, with inhibition of certain species (*L. ferriphilum*) occurring at concentrations as low as 0.52 mg/L (Cabrera et al., 2005; Johnson et al., 2017). Hence, being aware of the chromium (and nickel) concentrations is important as it could affect bioleaching microorganisms.

2.6 Identified gaps in current literature

Through the review of literature, it is clear to see that wastes such as tailings and e-wastes are growing, and with this growth is an increased risk of environmental degradation if these wastes are not properly managed. Additionally, it is seen that there is great potential for valuable metals to be extracted from these wastes through technologies such as bioleaching. In light of this, it is increasingly being considered to bioleach tailings and e-wastes together in order to decrease the ARD-forming potential of tailings while also using the produced lixiviant to extract valued metal from e-wastes like PCBs. However, research in this area is still in its infancy and more information is required to allow for waste leaching to become a more viable option commercially. More information is required on the effects of increased metal concentrations on the bioleaching microorganisms as in the process of leaching e-waste in particular, metal is solubilised into solution where it affects the microbes. These metals may potentially cause large shifts in the microbial community dynamics of a culture and the more that is understood, the better the possibility of the community being kept at the desired composition and efficiency. With regards to parameters such as microbial metal tolerance, many research studies have focused on the use of pure cultures or cultures with only a few microorganisms incorporated (Cabrera et al., 2005). While possessing information for particular microbes is valuable, it is noted that mixed microbial communities are seen to be more robust and are what are utilised in industrial applications. Thus, obtaining more information on the multifaceted microbial dynamics of mixed communities would be valuable.

Chapter 3: Defining the Research Project

3.1 Problem statement

Bioleaching is a process which can be used to extract various metals such as cobalt, nickel and copper from different secondary resources and wastes such as tailings and electronic wastes. Because the wastes and tailings that are used in the process are often of a low grade, a wide variety of metals, both desirable and undesirable, may be present. These metals have the potential to inhibit the activity of the microorganisms used in the process and therefore, obtaining information on metal tolerance levels for microbial communities used would be useful to determine how the bioleaching efficiency is affected by the various components in the waste. This would then help to ascertain the possibility of using certain microorganisms for different wastes. Additionally, knowledge on the metal tolerance levels of microorganisms would allow for a deeper understanding of the species present in a bioleaching microbial community, and having more knowledge on these microbes is beneficial for designing optimized bioleaching processes.

3.2 Objectives

The objectives of this project can be split into one main objective and two secondary objectives:

- Main Objective: To improve the understanding of bioleaching processes which may be used to recover metals from historic tailings material & other metallic wastes using mixed microbial communities.
- Sub-objective 1: To understand the potential inhibition mixed communities may experience from the inhibitory metals, nickel and chromium, which are present in wastes by determining microbial metal tolerance levels.
- Sub-objective 2: To track microbial community dynamics in response to the presence of the metal inhibitors, nickel and chromium, at varying concentrations.

3.3 Key research questions

- To what extent will nickel and chromium affect two different microbial bioleaching communities with substrate provision made for iron oxidisers alone?
- To what extent will nickel and chromium affect a microbial bioleaching community with substrate provision made for both iron and sulfur oxidisers?
- To what extent will nickel and chromium affect a microbial bioleaching community when subjected to varying concentrations of the inhibitory metals in the presence of tailings in 1L bioreactors?
- Over time, how will bioleaching microorganisms react to increasing concentrations of nickel and chromium when they become increasingly adapted and tolerant to these metals?

3.4 Hypothesis

During bioleaching, metals or metalloids are leached into solution. These include, but are not limited to, cobalt, nickel, copper, chromium, zinc, silver, cadmium and lead. Many of these can be considered inhibitory metals which will inhibit bioleaching microorganisms at high enough concentrations. Considering the bioleaching of electronic wastes and tailings, nickel and chromium are possible constituents which may have an inhibitory effect on bioleaching microorganisms at high enough concentrations. However, it is hypothesised that over an extended period in the presence of these metals, a microbial consortium can become increasingly tolerant of them, and in doing so, the initial consortium may experience a variety of changes in its composition.

3.5 Implications of project

Currently, there are commercial scale applications of bioleaching. However in these applications, there is not much precedence given to understanding how the complex microbial communities used work and how individual species within these communities react towards each other as well as to the components found in the bioleaching matrix. Thus, when bioleaching performance issues arise, it can be difficult to troubleshoot and find the reasons for the lack of efficiency. Exacerbating this problem is the desired shift towards the recovery of metals from wastes which often make bioleaching systems more complex with the additional components added to the system. In light of this, through this project, a better understanding of common microorganisms used in bioleaching is sought. With this knowledge, there is the potential for bioleaching systems to be designed where bioleaching efficiency and metal recovery is optimised and into which improved resilience is built.

Chapter 4: Materials and Methods

In this chapter, a detailed account is given of the procedures used to conduct research in this thesis. This includes a complete description of the different experiments performed in the various experimental blocks as well as a full description of the more generalized analytical methods performed across multiple experiments. In addition, information pertaining to the microorganisms and media used are detailed below.

4.1 Microbial consortia

Two mixed acidophilic microbial communities were used in the leaching experiments performed in this thesis. The first was a mixed moderately thermophilic biooxidation culture hereafter referred to as the BIOX™ culture. This culture was originally sourced from commercial gold biooxidation tanks and has been subsequently maintained in 1 L stirred tank reactors at 45°C at a pH of 1.3 in the Centre for Bioprocess Engineering Research (CeBER). The culture was kept on pyrite mineral at a 10% w/v solids loading in 0K medium, and was aerated at a rate of 2 L/min. Using a semi-continuous "draw-and-fill" method of operation where a portion of the reactor contents is removed tri-weekly and replaced with an appropriate amount of fresh pyrite and media, the culture was maintained at a residence time of 5 days. Throughout the period of time this culture was used, routine assessment of the culture was performed through the measurement of pH, redox potential and direct cell counts (methods detailed in Section 4.6). The culture consists of a variety of sulfur and iron-oxidizing bacteria and archaea including *L. ferriphilum*, *At. caldus* and *Ap. cupricumulans*. A detailed analysis of the microbial structure of both communities used can be seen in Chapters 5 – 7 (Smart et al., 2017a).

The second culture used was a mesophilic culture initially taken from the Kasese Cobalt Company Ltd. (KCC) bioleaching plant located in Uganda. The culture was transported and kept at the French geological survey (BRGM) on pyritic tailings (Bryan et al., 2011). The culture will hereafter be referred to as the BRGM-KCC microbial consortium. Once acquired in the CeBER labs where experimentation took place, the consortium was subcultured in flasks on increasing concentrations of a pyritic tailings (3% to 5% to 10%) until the time it was confirmed that the microorganisms were well-accustomed to a 10% w/v solids loading (Joulian et al., 2020). Stock cultures were then kept within aerated 1L stirred tank reactors at 35°C and at a pH of 1.3. A photograph of these stock reactors can be seen in

Figure 4.1 below. The aeration was kept at 2 L/min. 0K modified medium (0Km) was used and the culture remained on the pyritic tailings. These stock cultures were also supplemented with sulfuric acid and small amounts of limestone ($CaCO_3$) to control pH. The limestone also provided an inorganic carbon source for autotrophic species. This was to ensure the pH remained within an optimal range of about 1 – 1.3, never increasing beyond a maximum of 2. A "draw-and-fill" method of operation was also adopted with this culture tri-weekly to make up a residence time of 7 days. The stock culture was used to inoculate the small-scale tests performed, and later, was also used to inoculate the larger-scale bioreactor study described in a later section. This culture consists of microorganisms in the genera *Acidithiobacllus, Leptospirillum* and *Sulfobacillus* (Hubau et al., 2020).

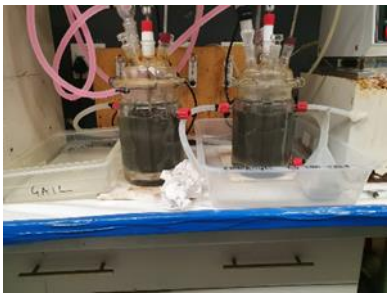

Figure 4.1: Photograph of BRGM-KCC stock cultures used for Microwell plate tests and to inoculate bioreactors

4.2 Media

0K and 0Km were used for the BIOX™ culture and BRGM-KCC cultures, respectively. The compositions of these two media can be seen in Table 4.1 below. The media used was acidified using sulfuric acid to a pH of 1.3. Additionally, 1 mL of a 1000× stock of a trace element solution (TES) consisting of 0.01 g/L $ZnSO_4.7H_2O$, 0.001 g/L $CuSO_4.5H_2O$, 0.001 g/L $MnSO_4.4H_2O$, 0.001 $CoSO_4.7H_2O$, 0.0005 g/L $Cr_2(SO_4)_3.15H_2O$, 0.0006 H_3BO_3, 0.0005 g/L $Na_2MoO_4.2H_2O$, 0.001 g/L $NiSO_4.6H_2O$, 0.001 g/L $Na_2SeO_4.10H_2O$ and 0.0001 g/L $Na_2WO_4.2H_2O$ was added to the acidified water used in experiments (Kolmert and Johnson, 2001). Deionised water was used to limit additional ions present. The media was sterilised at 121°C and 103 kPa for 20 minutes before use.

It is noted that the addition of many of these components have the potential to affect the osmotic pressure within the systems and induce osmotic stress for the microorganisms. However, many of these constituents are required for microbial metabolism, and their concentrations are not excessive (Centre for Bioprocess Engineering Research, 2018; Kolmert and Johnson, 2001). Thus, they do not negatively affect the microorganisms.

Table 4.1: Composition of 0K and 0Km media used for BIOX® and BRGM-KCC cultures respectively ((Centre for Bioprocess Engineering Research, 2018; Hubau et al., 2020)

Component	**Concentration (g/L)**	
	0K	**0Km**
$(NH_4)_2SO_4$	3	3.7
KCl	0.1	-
K_2HPO_4	0.5	-
$MgSO_4.7H_2O$	0.5	0.52
$Ca(NO_3)_2$	0.01	-
KOH	-	0.48
H_3PO_4 (85%)	-	0.8

4.3 Batch MicroWell Plate study (without sulfur)

4.3.1 Experimental setup

Small-scale batch experiments were performed using Greiner Bio-one CELLSTAR® 12 Well Suspension Culture Plates with a 4 mL total volume per well. Each well was filled with a 3 mL total working volume of the following nutrient mix:

- 5 g/L ferrous iron
- 5 g/L ferric iron
- Approx. 6.5 x 10^7 cells/mL inoculum
- Appropriate amount of nickel or chromium stock solution (depending on tested concentrations)
- Appropriate amount of 0K or 0Km (depending on tested concentrations)
- Appropriate amount of acidified deionised water used (depending on tested concentrations)

The ferrous iron was provided in the form of a ferrous sulfate heptahydrate ($FeSO_4 . 7H_2O$) stock solution of concentration 54 g/L. The ferric iron was provided in the form of a ferric sulfate hydrate ($Fe_2(SO_4)_3 . xH_2O$) stock solution of concentration 100 g/L. The hydration and concentration of the ferric sulfate hydrate solution was determined using the 1-10 phenanthroline assay detailed in Section 4.6.2. Ferric iron was added to better simulate the leaching environment that bioleaching microorganisms would experience when leaching different minerals. Considering the bioleaching of pyrite for example, both Fe^{2+} and Fe^{3+} would be present as mineral dissolution occurs and Fe^{2+} is oxidized to Fe^{3+} by the microbes. The ratio of Fe^{3+} to Fe^{2+} affects the redox potential which in turn influences the solubility of metal ions, the microbial activity and the extent to which iron oxidation occurs (Ahmadi et al., 2015).

These experiments were completed using the BIOX™ and BRGM-KCC consortia. The BIOX™ experiments were carried out in 45°C shaking incubators while the BRGM-KCC experiments were carried out in 35°C shaking incubators as these were the temperatures that the cultures had previously been maintained in. The starting pH within the wells was set at 1.3. In order to diminish losses caused by evaporation, each Microwell plate (MWP) incorporated the use of an AeraSeal™ film placed on top of the wells. These films minimise spillage, cross-contamination and evaporation, and allow for uniform air flow (Omega Biotek, 2021). Moreover, the MWPs were placed within humidified containers. These containers were placed in incubators shaking at a speed of 140 rpm. An annotated image of the MWP setup with and without the AeraSeal™ film and MWP cover can be seen in Figure 4.2 below.

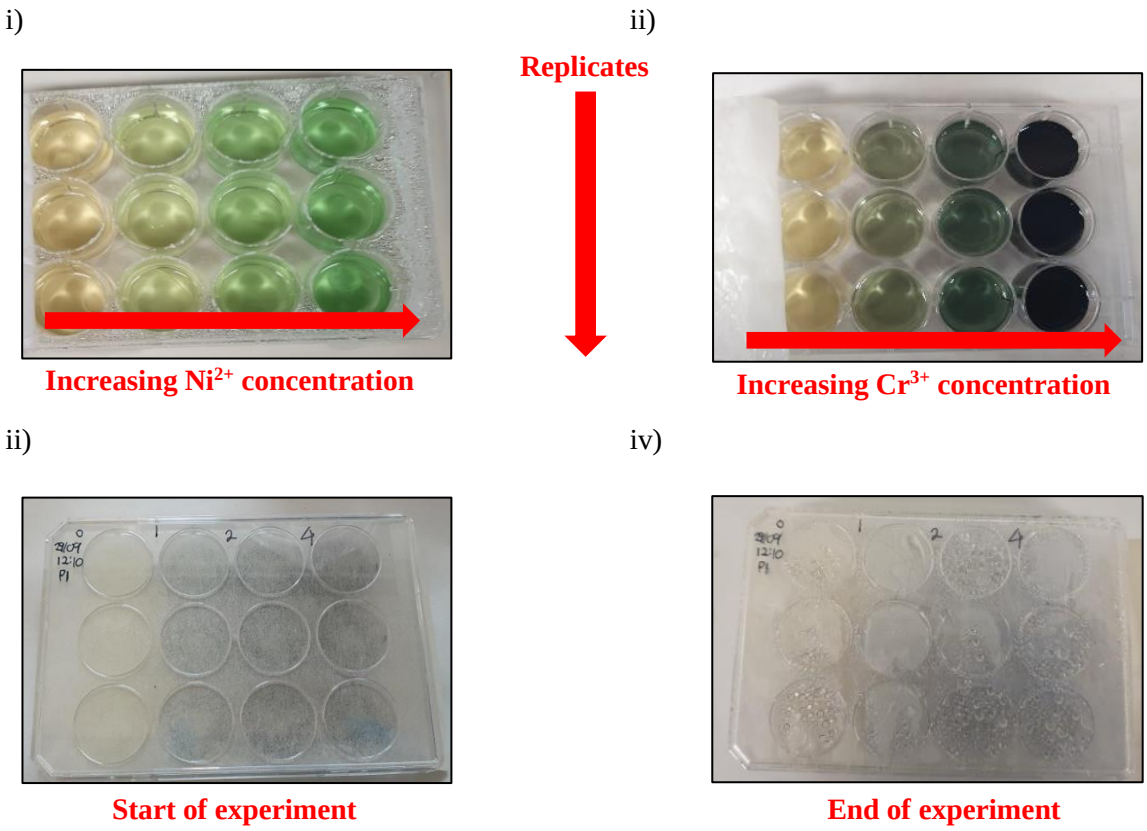

Figure 4.2: i) Example of MWP setup of a nickel test where increasing nickel concentrations are seen from left to right, and triplicates of the same concentration are seen from top to bottom. ii) Example of MWP chromium test setup similar to i) except with chromium used. iii) Example of MWP setup with AeraSeal™ film and cover at the start of an experiment. iv) Example of MWP setup at the end of an experiment after being in humidified container.

In this block of experiments, the effect of varying concentrations of both nickel and chromium on the BIOX® and BRGM-KCC cultures were tested. Starting with the BIOX® culture, a wide variety of concentrations were tested to get an initial broad understanding of how change in concentration affects the community. While the very first MWPs utilised concentrations based on literature, it is clear from literature that different communities and microorganisms can have widely different tolerance levels and even different strains of the same microorganism can react contrarily (Cabrera et al., 2005). Once these initial tests were completed, key concentrations were identified and at least three repeats of these concentrations were performed. These key concentrations were then also repeated using the BRGM-KCC culture. Table 4.2 shows the tested concentrations of nickel and chromium for the two microbial communities used.

Table 4.2: Tested concentrations of nickel and chromium for the BIOX® and BRGM-CC cultures (with key concentrations indicated by double tick check marks)

Concentration (g/L)	BIOX™ nickel tests	BIOX™ chromium tests	BRGM-KCC nickel tests	BRGM-KCC chromium tests
0	✓✓	✓✓	✓✓	✓✓
0.25	✓	✓		
0.5	✓✓	✓	✓✓	
0.75	✓	✓		
1	✓✓	✓✓	✓✓	✓✓
1.5		✓		
2	✓✓	✓✓	✓✓	✓✓
2.5		✓		
2.75		✓		
3		✓		
3.5		✓		
4	✓✓	✓✓	✓✓	✓✓
5		✓		
6	✓	✓		
7.5		✓✓		✓✓
8.5		✓		
9		✓		
10		✓		
20	✓			
30	✓			

The nickel used is in the form of a nickel sulfate hexahydrate ($NiSO_4$. $6H_2O$) stock solution of 100 g/L concentration and the chromium used is in the form of chromium sulfate hydrate ($Cr_2(SO_4)_3$. xH_2O). The hydration and concentration of the chromium sulfate was calculated using ICP-AES and a stock solution of concentration 50 g/L was used. Both solutions were sterilized and acidified to a pH of 1.3 prior to use in all experiments.

4.3.2 Sampling

During the course of the experiment, regular samples were taken. At each sampling point, 5 µL was removed to record ferrous iron concentration via the 1-10 phenanthroline colorimetric assay. Similarly, 5 µL was removed to measure cell density through direct cell counts (method described in Section 4.6.3). Cell counts were performed less frequently than iron assays. Once ferrous iron oxidation was completed, sampling for that assay was terminated. However, all other sampling was continued.

The experiments were set to last for a maximum of seven days. This is to ensure that there was sufficient time for cell numbers to increase to a suitable concentration where centrifugation at the end of the experiment would result in an adequate cell pellet with which DNA extraction and quantitative polymerase chain reaction analysis (qPCR) could be done successfully. Cell pellets were prepared for both the inocula and the end communities to ensure qPCR analysis at the start and at the end of the experiment could occur. Cell pelleting, DNA extraction and qPCR analysis are described in the analytical methods in Section 4.6. Triplicate wells were combined to form a single cell pellet for each concentration. This resulted in a total of 6 mL of sample being pelleted for each concentration with 2 mL aliquots being taken from each well. A schematic of this can be seen in Figure 4.3. In addition, the seven days also allowed ample time for the effects of the metal inhibitors to be seen in the microbial community.

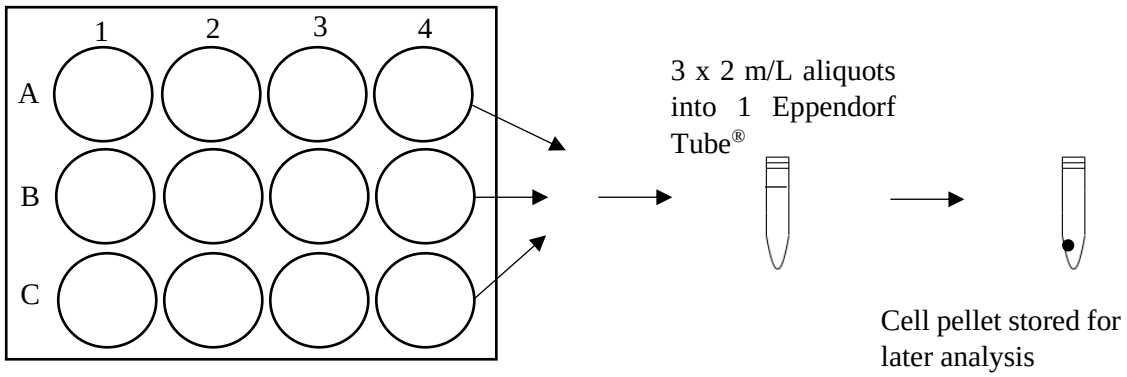

Figure 4.3: Schematic drawing of the MWP cell pelleting method

Redox potential and pH were measured throughout the course of the experiment once per day. Redox potential and pH were measured for all experiments in this research project apart from those performed using the BIOX® culture. For all MWP tests, duplicate MWPs were used to measure pH and redox potential. This was to avoid potential contamination during sampling. Ethanol and deionised water were used to ensure the probes were sterile and clean before sampling. A pH

4.4 Batch Microwell plate study (with sulfur)

4.4.1 Experimental setup

The experiments performed in this section were similarly set up to the experiments performed in Section 4.3 except for the added addition of a sulfur source. Experiments were also implemented in Greiner Bio-one CELLSTAR® 12 Well Suspension Culture Plates with a working volume of 3 mL. The nutrient mix placed in each well consisted of the following:

- 5 g/L ferrous iron
- 5 g/L ferric iron
- Approx. 6.5 x 10^7 cells/mL inoculum
- Appropriate amount of nickel or chromium stock solution (depending on tested concentrations)
- Appropriate amount of 0Km (depending on tested concentrations)
- Appropriate amount of acidified deionised water used (depending on tested concentrations)
- 0.5 w/v % tyndallised elemental sulfur

Only the BRGM-KCC culture was used for these experiments. The experiments took place at a starting pH of 1.3 and 35°C. The MWPs used were once again placed in humidified containers with an AeraSeal™ film used. The incubator rotated at a speed of 140 rpm.

Figure 4.4 shows a picture of the experiment setup.

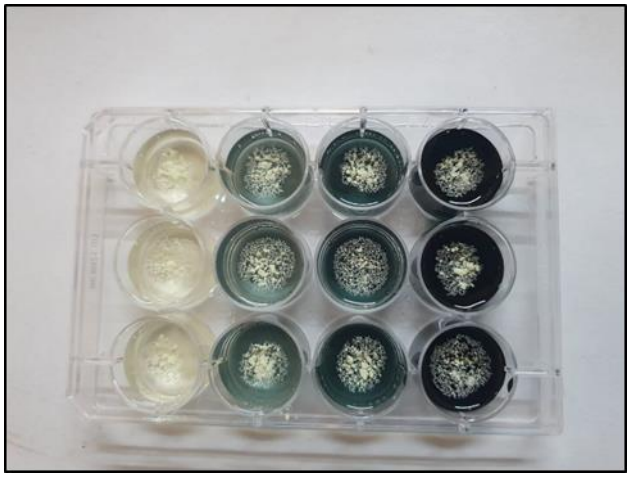

Figure 4.4: Photograph of MWP setup with tyndallised elemental sulfur (AeraSeal™ film and cover not included)

The same concentrations tested on the BRGM-KCC community in the MWP studies with no sulfur were tested in this section. These are 0 g/L, 0.5 g/L, 1 g/L, 2 g/L and 4 g/L for nickel, and 0 g/L, 1 g/L, 2 g/L, 4 g/L and 7.5 g/L for chromium. Experiments for all concentrations were replicated at least three times.

4.4.2 Sampling

Sampling was done in the same way as described in Section 4.3.2. Ferrous iron concentration was measured via the 1-10 phenanthroline colorimetric assay and direct cell counts were performed under phase contrast microscopy at 1000× magnification. Redox potential and pH were also measured throughout the course of the experiment. Cell pellets were made at the start of the experiments of the inoculum and at the end of the experiments of the end community. These were kept for later qPCR analysis. When sampling from the wells, care was taken to not disrupt or remove any of the elemental sulfur. Additionally, it was ensured that no sulfur was pelleted along with the cells at the end of the experiment. All experiments were a week in length.

4.5 Semi-continuous bioreactor study

4.5.1 Experimental setup

This experiment was a long term experiment that lasted for a period of 5 months (18 July 2022 to 18 December 2022). The tests were conducted in four glass 1 L (working volume) stirred tank reactors. As mentioned in Section 4.1, the four reactors used were inoculated from an established stock reactor and prior to the experiment commencement, the reactors were run for a period of 3 weeks to ensure the cultures had acclimatised to their new environment. The four reactors consisted of a control reactor (C-R), a nickel reactor (Ni-R), a chromium reactor (Cr-R) and a mixed reactor (Mixed-R) containing both nickel and chromium. The only difference between these reactors was in the metal inhibitor and concentration of inhibitor present. The different concentrations present were either based on results shown in previous MWP experiments (for C-R, Ni-R and Cr-R) or based on electronic waste printed circuit board (PCB) concentrations found in literature (for Mixed-R). More information pertaining to this can be seen in Section 4.5.3. Figure 4.5 shows a photograph of the reactor setup.

Figure 4.5: Photograph of bioreactor setup

Like the stock reactors, each of the experimental reactors were aerated at a rate of 2 L/min. In-line filters were used to prevent potential contamination through aeration. The reactors were maintained at a temperature of 35°C. This is because the optimum temperature for similar systems to obtain high ferrous iron oxidation while limiting precipitation has been recorded to be at this temperature (Anaya-Garzon et al., 2021; Hubau et al., 2020). Additionally, the optimal temperature of *L. ferriphilum*, which has been seen to be a major constituent of the BRGM-KCC consortium, is close to this temperature (Hubau et al., 2020). Jacketed vessels were used to ensure the temperature remained constant throughout the experiment and a heated waterbath circulated the warmed water through the vessels in a series system. A cooling system was also implemented in series where coolant at 2°C was used to minimize water loss from evaporation. Any water lost due to evaporation was manually replaced daily prior to sampling.

Within the reactors, four connected fin baffles were placed to improve mixing and prevent the formation of vortexes. Three-blade 45° axial flow impellers were used at a mixing rate of 650 rpm to ensure mineral remained in suspension (Hubau et al., 2020; Joulian et al., 2020). The impellers and spargers were positioned according to standard bioreactor dimensions to maximise mass transfer and mixing. Figure 4.6 displays a diagram of the typical bioreactor setup used. All equipment was sterilised prior to use.

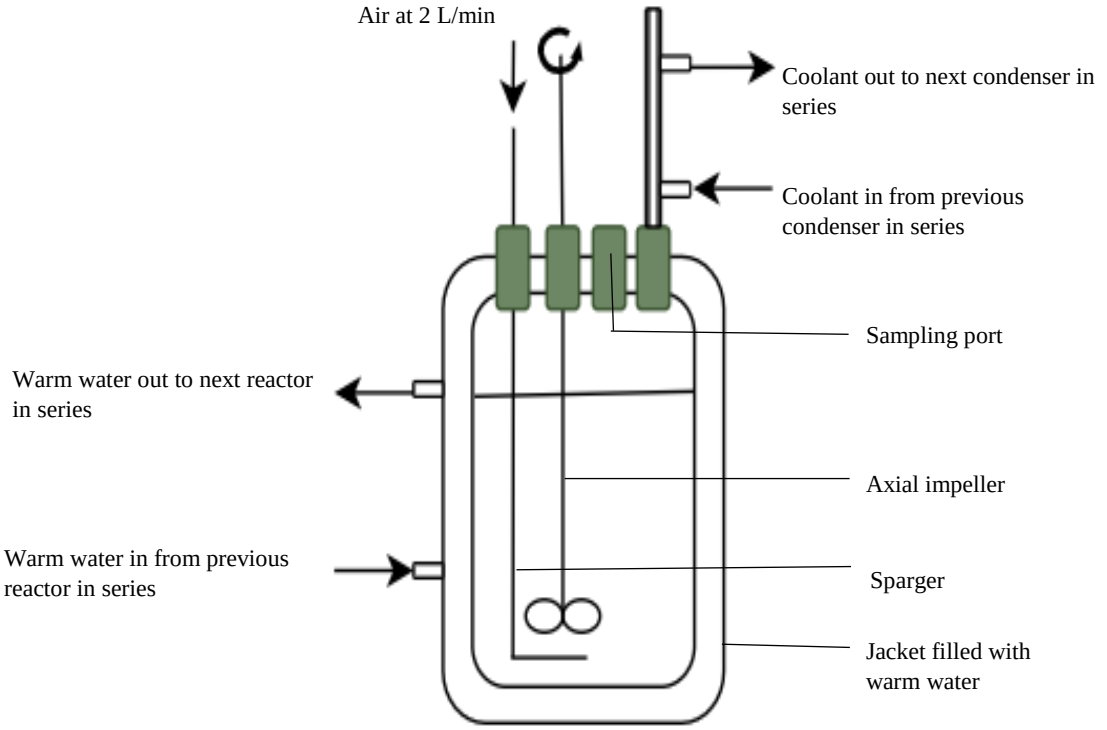

Figure 4.6: Schematic diagram of a bioreactor experimental setup

Within the reactors, at all times, the following components could be found at varying concentrations depending on the stage of the experiment:

- 0Km (in all reactors)
- Acidified deionised water (in all reactors)
- 10 w/v % pyritic tailings (in all reactors)
- Metal stock solution (nickel, chromium, both or none)
- Small amount of limestone ($CaCO_3$)
- Dissolved oxygen

Three times a week, a reactor feeding would occur where a third of the reactor contents would be removed and replaced with the appropriate amounts of the components listed above. This was to establish a seven day residence time. Generally, these feeding would occur on Monday, Wednesday and Friday. However, there were some feedings that deviated from this, though always keeping to a 3-day-a-week schedule.

4.5.2 Tailings characterisation

The tailings used in this experiment was originally sourced from a copper mine. A batch of the concentrate was then taken to the BRGM facilities and from there, 22 kg was shipped to the CeBER laboratories. The tailings concentrate is a pre-processed mineral that was fine enough to not require additional comminution steps. Before its use, the tailings was homogenised and divided up with the use of a riffle splitter. The tailings composition can be seen in Table 4.3 below and the characterization was done prior to experimentation. A combination of the following methods were used in the characterization of the tailings:

- BRGM – XRF (X-ray fluorescence)
- ALS (LR22015237) – XRF
- ALS (LR21096113) – ICP (Inductively Coupled Plasma)

Table 4.3: Characterization of a pyritic tailings using a combination of XRF and ICP techniques

		Sample A	**Sample B**	**Sample C**	**Average**	**Relative Standard Deviation**
Al_2O_3	%	8.2	8.3	8.3	8.27	0.5%
Total C	%	<0,1	0.02	0.06	0.04	50.0%
CaO	%	2.93	2.86	2.88	2.89	0.9%
Co	ppm	827	918	908	884.33	4.3%
Cu	ppm	1930	2300	2330	2186.67	7.8%
Fe	%	23.29	24.30	24.10	23.90	1.7%
Fe as pyrite	%	20.8	16.8	18.7	18.77	7.2%
Fe as other	%	2.49	7.50	5.40	5.13	34.3%
K_2O	%	1.91	1.89	1.87	1.89	0.7%
MgO	%	1.18	1.18	1.21	1.19	1.1%
MnO	%	0.107	-	-	0.11	0.0%
Na_2O	%	1.96	-	-	1.96	0.0%
P_2O_5	%	0.113	-	-	0.11	0.0%
S total	%	24.1	24.2	24.3	24.20	0.3%
S as sulfide	%	23,8	19.3	21.4	20.35	5.2%
S as sulfate	%	0.13	0.34	0.42	0.30	37.5%
S as elemental S	%	0.14	0.03	0.01	0.06	88.9%
SiO_2	%	30.4	30.9	31.1	30.80	0.9%
Pyrite*	%	44.6	36.1	40.1	40.27	7.2%

**Calculated value*

4.5.3 Nickel and chromium concentration rationale

As a co-processing approach is being studied, information pertaining to both tailings and printed circuit board (PCB) concentrations was necessary to acquire. Tailings were directly used in this experiment; however, PCBs were not and thus the information with regards to PCB composition was obtained from literature. This experiment was modelled as if there was 100% solubilisation of nickel and chromium into solution from PCB leaching (the highest possibility of microbial inhibition that could occur). The ratio of nickel to chromium was calculated by averaging values from a variety of literature sources (seen in Chapter 2) and was calculated to be a 1: 0.03 nickel to chromium ratio found in PCBs. Literature was also used to determine the typical solids loading of PCBs used as a starting point for the experiment. Nickel and chromium concentrations attributed to 10, 40, 60, 100, 200, 400 and 500 w/v% PCBs were tested during the course of the experiment in the mixed reactor. While it is highly unlikely that the higher concentrations will be reached when actual PCBs are being used, the concentrations were still increased to these values to test metal tolerance levels when it was seen that the culture was able to withstand the conditions. At the same time, it is feasible that PCB leachates may be recirculated in bioleaching systems resulting in the accumulation of metal in the aqueous phase at elevated concentrations. Table 4.4 shows the concentrations tested in each reactor. The concentrations were tested for a minimum of three weeks and if it was seen that the culture continued to function without issue and remained majorly unchanged, the concentration was increased. During the course of the experiment, the control reactor remained the same with no addition of extra nickel or chromium. This reactor was thus maintained similarly to the BRGM-KCC stock cultures.

Table 4.4: Tested concentrations of metals in Ni-R, Cr-R and Mixed-R

Weeks	**Nickel concentration in Ni-R (g/L)**	**Chromium concentration in Cr-R (g/L)**	**Mixed concentration in Mixed-R**	
			Nickel (g/L)	**Chromium (g/L)**
1 – 3	0.5	1	0.36	0.01
4 – 6	1	2	1.43	0.05
7 - 9	2	4	2.14	0.07
10 – 12	3	4	3.57	0.12
13 – 15	6	4	7.14	0.23
16 – 18	12	4	14.28	0.46
19 - 22	24	6	17.84	0.59

4.5.4 Sampling

Sampling occurred daily for the first 3 months and after this period, sampling occurred three times a week on feeding days. On days when feedings occurred, the removed supernatant was used for sampling. On days with no feedings, a 10 mL aliquot was removed for sampling. These 10 mL amounts were taken into account during feedings and the appropriate amount of tailings, media, metal stock solution and acidified deionized water was added to the reactors. Before sampling, deionized water was added to make up for water lost due to evaporation. Additionally, after the samples were removed from the reactors, they were left to settle for 1 hour to ensure sufficient separation of mineral from the supernatant.

Redox potential and pH were measured during samplings. Ferrous iron and total iron concentration was also measured using the 1-10 phenanthroline assay. Direct cell counts were performed where the planktonic or free bacteria cell numbers were totalled. Using the first and last feedings of the week, cell pelleting for qPCR analysis were performed. For cell pelleting only, samples were left to settle overnight to ensure the majority of fine mineral was separated out before DNA extraction and qPCR. Generally, 2 m/L aliquots were taken, however, at times when a culture was struggling, two to three rounds of pelleting was necessary to get a large enough pellet and thus a total of 4 to 6 m/L of sample was used. Throughout the sampling process, care was taken to make certain no cross contamination of samples occurred.

4.6 Analytical methods

4.6.1 Redox potential and pH

Redox potential was measured using a Metrohm Ion Analyser 827 pH lab meter fitted with a platinum-ring 3 M KCl electrode (Ag/AgCl reference). The redox potentials measured are reported relative to the standard hydrogen electrode (Eh values). A Metrohm standard of 650 mV was used. The pH was measured using a Metrohm 704 pH meter and probe. The meter was calibrated at a pH of 1.0 and 4.0.

4.6.2 Iron analysis

All iron assays were done using the 1-10 phenanthroline colorimetric assay using a spectrophotometer at a wavelength of 510 nm. With the addition of the 1-10 phenanthroline, ferrous iron forms a red-orange complex as the phenanthroline molecules chelate with ferrous iron ions. Ferrous iron absorbance can be measured at this time. With the addition of a spatula tip of hydroxylamine, all the ferric iron present is reduced to ferrous iron and forms a complexing agent with the 1-10 phenanthroline mix. Total iron can then be measured after ensuring the hydroxylamine is well mixed in the solution and has been left for 5 minutes in order for the full reaction to take place. Ferric iron can be calculated by subtracting ferrous iron concentration from total iron concentration. This method is accurate to values below 1 mg/L (Centre for Bioprocess Engineering Research, 2018).

4.6.3 Direct cell counts

Planktonic cell numbers were measured through the use of direct cell counts. A Thoma counting chamber was used with an Olympus BX40 Microscope at 1000× magnification under phase contrast. 1.3 µL of appropriately diluted sample was pipetted onto the Thoma counting chamber and a coverslip was carefully placed on the sample. An oil immersion objective was used at the required magnification. For each count, the cells in a quadrant were totalled. Equation 1 below was used to calculate the cell density in cells/mL. C_N is the cell concentration (cells/mL), C is the number of cells counted in the large squares, N_T is the total number of large squares (16), N_L is the number of large squares where cells were counted (4), D is the depth of the chamber (0.02 µm), A is the area, and d is the dilution.

$$C_N = \frac{C \times \left(\frac{N_T}{N_L}\right)}{D \times A} \times \frac{1}{d} \times 10^3 \tag{4.1}$$

This equation can be simplified into Equation 4.2:

$$C_N = 312500 \times d \tag{4.2}$$

4.6.4 Cell pelleting

Cell pelleting was used in all three experimental blocks. For the MWP experiments, 6 mL of sample was pelleted into a single 2 mL Eppendorf™ tube as shown in Figure 4.3. For the bioreactor samples, only 2 mL samples were used unless more was required due to a lower cell concentration. Cells were collected through high speed centrifugation at 14 000 × *g* for 15 minutes and the supernatant after each run was discarded. The pellets were then washed with 1 mL of 10 mM citrate buffer solution (0.22 mM sodium citrate dehydrate and 9.88 mM citric acid anhydrous at a pH of 2) by centrifugation again at 14 000 × *g* for 10 minutes repeatedly until no yellow colour was observed in the supernatant meaning soluble iron was no longer present. The cells were then washed twice with 1 mL of 1 x PBS to neutralize the pH. Finally, the cells were frozen at -20°C until DNA extraction occurred.

4.6.5 DNA extraction

Cells were re-suspended in 200 µL tissue lysis buffer with the addition of 50 µg lysozyme. This was then incubated for 15 minutes at 37°C. Using the Roche High Pure PCR template preparation kit, the protocol for the isolation of DNA from bacteria was then followed. The extracted DNA was quantified using a Nanodrop® ND-2000 (Thermo) spectrophotometer and samples were diluted to 10 ng/µL for qPCR. DNA samples were stored at -20°C for later qPCR analysis.

4.6.6 Quantitative polymerase chain reaction (qPCR) analysis

The qPCR analysis was performed for all experimental blocks. For the MWPs, the inoculum and the end community were analysed while for the bioreactors, key stages in the reactors' lifespans were analysed. These dates corresponded to the period just before a potential concentration increase, every three weeks. For the BIOX™ and BRGM-KCC cultures, the following analyses occurred:

- Universal bacteria (measuring all bacterial species)
- Universal archaea (measuring all archaeal species)
- *L. ferriphilum*
- *At. caldus*
- *Sb. benefaciens*
- *At. thioxidans*
- *Ap. cupricumulans*
- *Fp. acidiphilum*
- Archaea (JTC1/2)

Established specific primer sets were used in this analyses and conditions for qPCR were typical except for *Sb. benefaciens* which required a different primer concentration of 0.5 µM and an annealing temperature of 67°C. In creating what is known as a "mastermix" used for the qPCR reactions to take place, SYBR KAPA mix, forward primers, reverse primers and Ultra-Pure Millipore water was used. Table 4.5 shows detail on the primers used for qPCR analysis taken from Hedrich et al. (2016) and Tupikina et al. (2013).

Table 4.5: Primer sequences used for qPCR analysis (modified from Hedrich et al. (2016) and Tupikina et al. (2013))

Primer title	Group/species	Sequence (5' – 3')
Universal primers		
UniBactF335[a]	Universal bacteria	GAC TCC TAC GGG AGG CAG CA
UniBactR937[a]	Universal bacteria	TTG TGC GGG CCC CCG TCA AT
UniArchF343[a]	Universal archaea	ACG GGG IGC AIC AGG CG
UniArchR932[a]	Universal archaea	TGC TCC CCC GCC AAT TCC
Bacterial primers		
LH[a]	*Leptospirillum ferriphilum* strain LH	GGG GGC CTG AAT AAG GTC A
At.c[a]	*Acidithiobacillus caldus*	CGG ATC CGA ATA CGG TCT G
Sb1030F[b]	*Sulfobacillus benefaciens*	CAG CTC GTG TCG TGA GAT GT
Sb1265R[b]	*Sulfobacillus benefaciens*	ACT GAG GAT CCG TTT GCG G
At.t[a]	*Acidithiobacillus thiooxidans*	GGG TGC TAA TAT CGC CTG CT
Archaeal primers		
JTC3[a]	*Acidiplasma cupricumulans*	AAG CCT AAC TTC AGA AGG CCT G
Ferro[a]	*Ferroplasma acidiphilum*	GAA GCT TAA CTC CAG AAA GTC TG
JTC1/2[a]	*Thermoplasmatales* sp.	AGA AAA ATT CTC CCG CTC AAC GG

[a] Source: Tupikina et al. (2013); [b] Source: Hedrich et al. (2016)

4.7 Data handling

In this section, the approaches and calculations used to analyse reactor performance are explained.

4.7.1 Maximum volumetric iron oxidation rate

The maximum volumetric iron oxidation rate was calculated by recording the decrease in ferrous iron over time, specifically in the period where ferrous iron concentration decreased steeply with a constant slope. It was calculated using the following equation:

$$V_{max} = -\frac{[Fe^{2+}]_1 - [Fe^{2+}]_2}{t_1 - t_2} \quad (4.3)$$

where V_{max} is the maximum volumetric iron oxidation rate, $[Fe^{2+}]_1$ and $[Fe^{2+}]_2$ represent the ferrous iron concentrations at time 1 and time 2, respectively, and t_1 and t_2 represent time 1 and time 2, respectively. In the MWP tests, to get the average maximum volumetric iron oxidation rate, all V_{max} values for a single concentration from different tests were averaged.

4.7.2 Maximum specific growth rate

The maximum specific growth rate was calculated in batch tests considering the period of exponential growth. The calculation can be seen in Equation 4.4:

$$\mu_{max} = \frac{\ln\left(\frac{C_{N,1}}{C_{N,2}}\right)}{t_2 - t_1} \tag{4.4}$$

where μ_{max} is the maximum specific growth rate, $C_{N,1}$ is the cell density at time 1, $C_{N,2}$ is the cell density at time 2, t_2 is time 2 and t_1 is time 1. Similarly to $V_{max,}$ average values for μ_{max} were also obtained by averaging μ_{max} values for all tests at the different concentrations in the MWPs.

4.7.3 Apparent yield

In this project, the biomass yield per gram of iron oxidised was calculated. The apparent yield was calculated from the beginning of the experiment to the point where oxidation was completed by the quickest in the group (generally the control with no added metals). The calculation for the apparent yield can be seen below:

$$Y_{X/S} = -\frac{C_{N,2} - C_{N,1}}{[Fe^{2+}]_2 - [Fe^{2+}]_1} \tag{4.5}$$

where $Y_{X/S}$ is the apparent yield. In the MWP experiments, the average apparent yield for each metal concentration was calculated by averaging the values for all tests.

4.7.4 Standard deviation

When possible, deviation in data was calculated using standard deviation. The formula for calculating standard deviation can be seen below:

$$SD = \sqrt{\frac{\sum(x - \bar{x})^2}{n - 1}} \tag{4.6}$$

where SD is the standard from the mean, x is a data point, $\bar{x}$ is the mean and n represents the number of repeats.

Chapter 5: Batch Microwell plate tests without sulfur substrate

5.1 Introduction

In this chapter, small scale batch MWPs were used to test the metal tolerance of two similar mixed microbial consortia. The metal tolerance indicator used was the maximum tolerated concentration (MTC). The MTC in this case refers to the highest inhibitor concentration where microbial oxidation is still able to take place (Cabrera et al., 2005; Shylla et al., 2021). However, at and below this concentration, there is still the possibility of changes in microbial performance and issues with resilience; with some microorganisms affected more than others. In this chapter, different parameters are explored and studied to better understand the effect of two potential metal inhibitors (nickel and chromium) on various acidophilic bioleaching microorganisms. These parameters include microbial oxidation, microbial growth, redox potential, pH, and microbial speciation. This set of experiments also acted as a preliminary study to provide a starting point for the tolerance levels to be tested. A broad range was initially tested, and then the range was reduced and key concentrations were repeated a number of times and used in later studies performed.

In this block of experiments, sulfur was omitted as a substrate. This was done to explore the ability of iron-oxidisers in particular to withstand increasing concentrations of the metal inhibitors with little to no interference by active sulfur-oxidisers in a mixed microbial community. The results are presented and discussed in the sections below.

5.2 Results and Discussion

5.2.1 Microbial iron oxidation

5.2.1.1 BIOX® microbial consortium

As mentioned, the first tests conducted were done in order to gauge the approximate tolerance values of the BIOX® culture and to define key concentrations that would be used for the detailed investigation of both the BIOX® culture and the BRGM-KCC culture. The ferrous iron oxidation curves for the initial nickel tests can be seen in Figure 5.. These preliminary results collected across three concentration ranges with maxima of 30 g/L, 6 g/L and 0.75 g/L, indicate that at concentrations of nickel of 2 g/L and above, the iron-oxidisers within the culture are unable to fully oxidise ferrous iron into ferric iron. However, in the lowest concentration range (0.0 – 0.75 g/L), this oxidation occurs, but not as effectively as when no nickel is present as seen in Figure 5. iii). Interestingly, it can be seen when comparing the 0.0 g/L profiles that there is a level of variation in the Fe^{2+} oxidation profiles. This is thought to be attributed to slightly fluctuating inocula for different experimental runs (and therefore slightly different proportions of iron oxidizers), and is apparent for all concentrations tested. Hence, for the key concentrations a minimum of three runs were completed and all calculated parameters, like oxidation rates and growth rates, were based on average values obtained. Based on these tests, and some shown in Appendix B, the key concentrations of nickel selected to test further were 0 g/L, 0.5 g/L, 1 g/L, 2 g/L and 4 g/L as highlighted in Chapter 4.

A similar process was followed for the metal chromium where a broad range of 0.0 to 10.0 g/L was initially studied. These concentration curves can be seen in Figure 5.2. At a chromium concentration of 9.0 and 10.0 g/L, it is seen that microbial iron oxidation seems to cease while at 7.5 g/L oxidation occurred at a reduced rate. From these chromium tests and those in Appendix, the selected key concentrations were 0 g/L, 1 g/L, 2 g/L, 4 g/L and 7.5 g/L.

i)

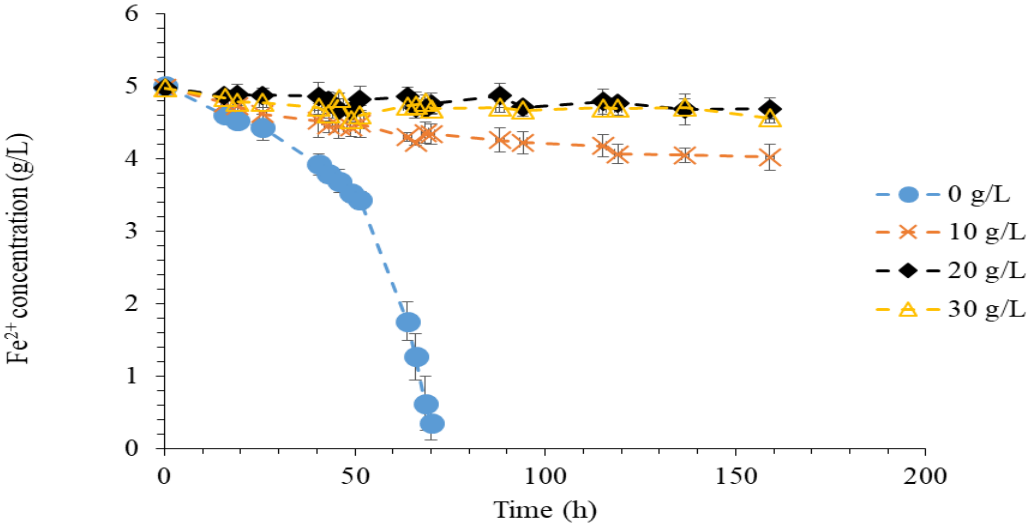

ii)

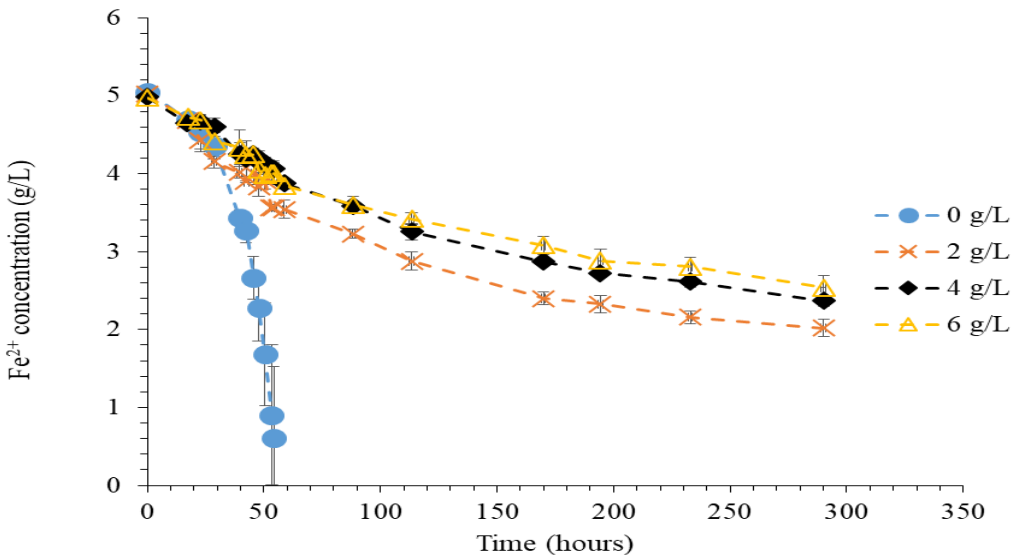

iii)

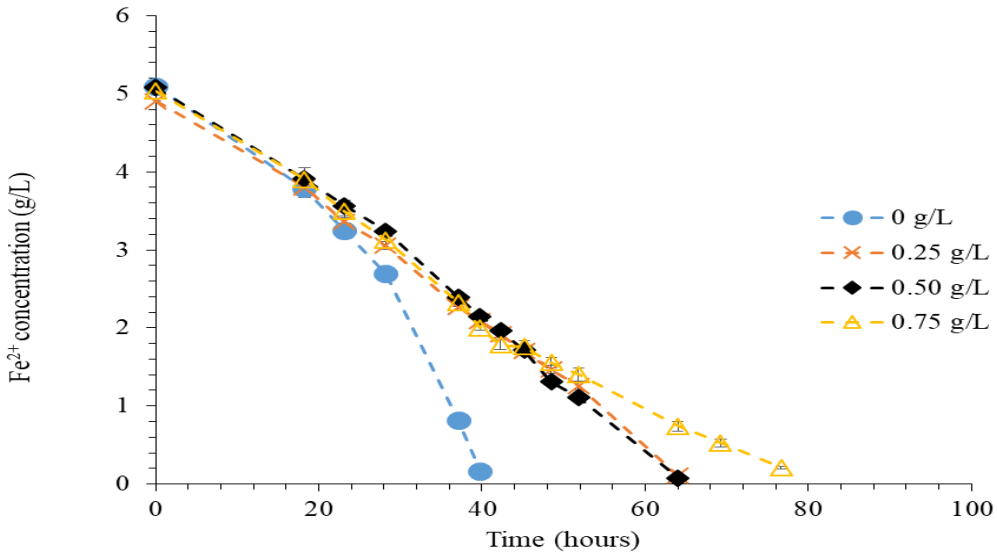

Figure 5.1: Initial broad-ranged nickel tolerance tests carried out to gauge the approximate tolerance of the BIOX® culture at 45°C for i) (range of 0 - 30 g/L), ii) (range of 0 - 6 g/L), and for iii) (range of 0 - 0.75 g/L)

i)

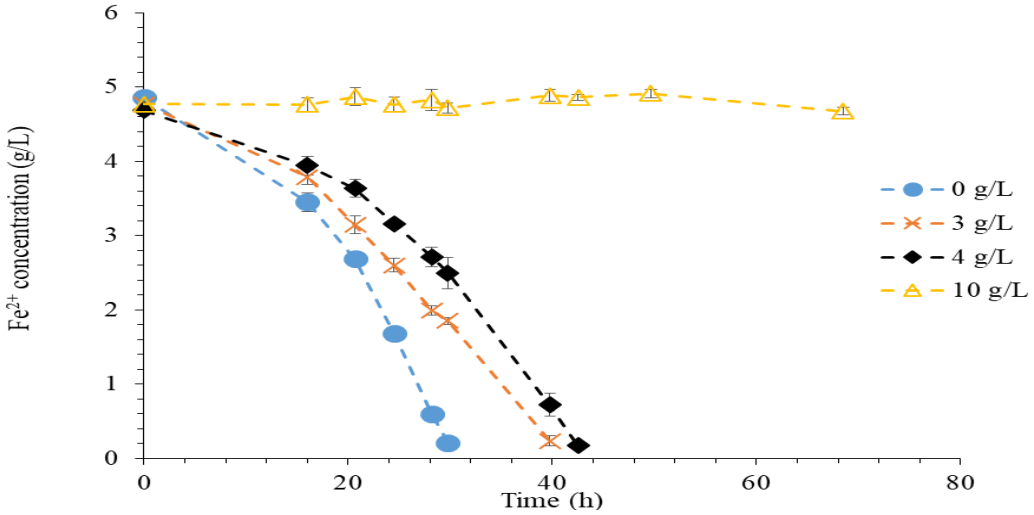

ii)

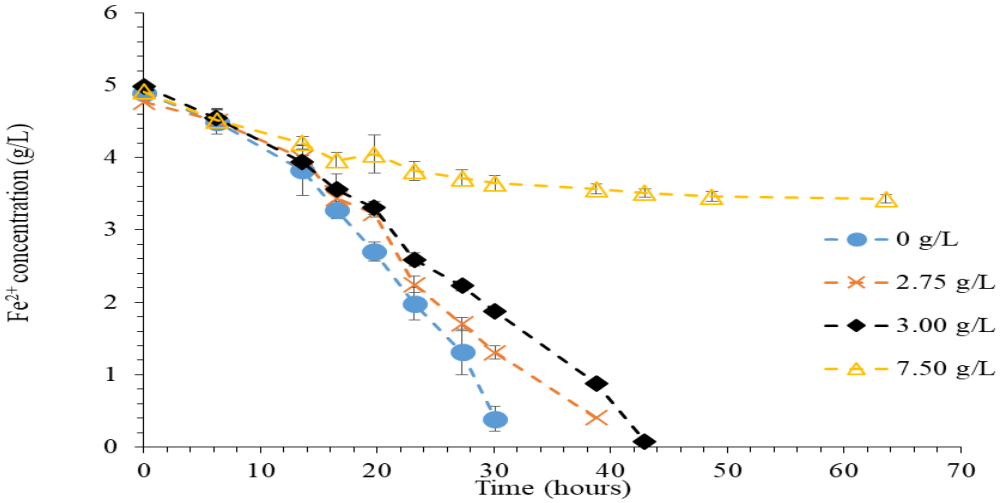

iii)

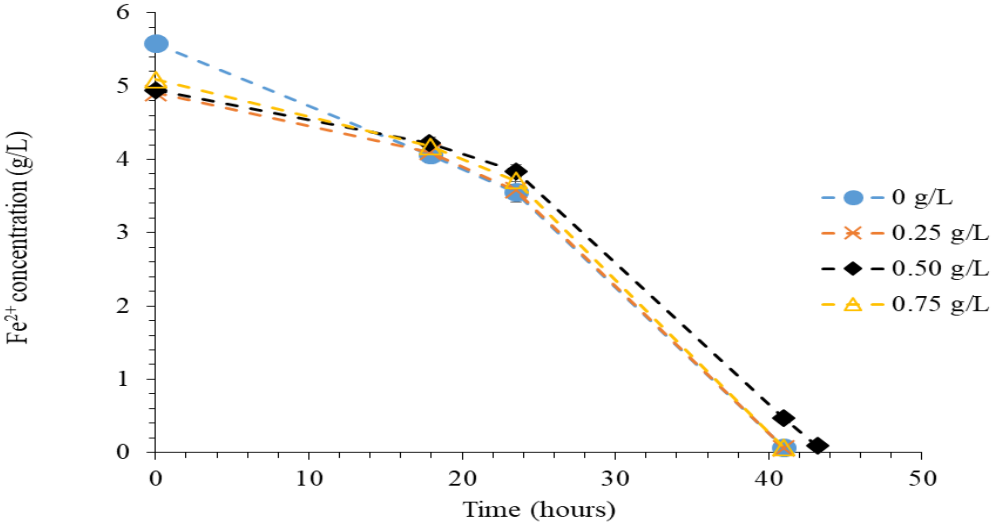

Figure 5.2: Initial broad-ranged chromium tolerance tests carried out to gauge the approximate tolerance of the BIOX® culture at 45°C for i) (range of 0 - 10 g/L), ii) (range of 0 - 9 g/L), and for iii) (range of 0 - 0.75 g/L)

Focusing on the key concentrations, Figure 5.4 and Figure 5.5 show examples of ferrous oxidation profiles across varying starting nickel and chromium concentrations (additional curves shown in Appendix B). As mentioned, at nickel concentrations above 2 g/L and chromium concentrations above 7.5 g/L, microbial ferrous iron oxidation does not proceed to completion. This indicates that at higher concentrations, the main iron oxidisers in the community are unable to oxidise iron in an iron-only medium. At 2 g/L for nickel and 7.5 g/L for chromium, it is seen that there is variation and in some cases oxidation goes to completion while in other cases, it does not. These variations are shown in Figure 5.4 and Figure 5.5. This may be an indication that at these concentrations, the oxidising ability of the microorganisms has reached a limit where it may or may not be able to oxidise iron and is thus considered to be the MTC. Therefore, the MTC for nickel is considered 2 g/L and for chromium it is considered 7.5 g/L. This is in contrast to literature sources that generally indicate chromium is more toxic to similar bioleaching microorganisms (Cabrera et al., 2005; Joulian et al., 2020; Tian et al., 2007; Wang et al., 2021). This could potentially be linked to the fact that different strains of the same microorganisms can be vastly different and some could have higher resistant levels to certain metals than others. Additionally, these differences could be as a result of the fact that no sulfur source was present for these tests. That would confirm the importance of different synergetic components within a bioleaching system, and demonstrate how a single element being excluded can change the way these complex microorganisms work.

In Figure 5.3, the average maximum volumetric Fe^{2+} oxidation rates for different concentrations of nickel and chromium are shown. For both metals, the rates are seen to decrease as the concentration of inhibitory metal increases. There is a sharp decrease in the Fe^{2+} oxidation rate achieved even when the smallest amount of nickel (0.5 g/L) is present, and between 0.5 and 2.0 g/L of Ni, it seems that the rate remains relatively constant with only a small decrease with an increase in nickel, with rates falling from 0.213 $g.L^{-1}.h^{-1}$ in the absence of Ni to between 0.069 and 0.055 $g.L^{-1}.h^{-1}$. At 4 g/L of nickel, the lowest rate of 0.018 $g.L^{-1}.h^{-1}$ is recorded. This oxidation is potentially abiotic as according to Searby (2006), moderately thermophilic culture temperatures have abiotic reaction rates that should not be considered negligible. Thus, there is the possibility that at 4 g/L nickel, microbial oxidation is minimal or has ceased. However in Searby (2006), the work was conducted at a temperature between 60 - 80°C, much higher than the 45°C of the BIOX® culture. Hence, these cultures cannot be compared to a great extent as temperature is seen to have a big impact on kinetics (Franzmann et al., 2005). Considering Kirby et al. (1999) which states an average abiotic rate of 0.021 $g.L^{-1}.h^{-1}$ at a pH above 5 and temperatures between 12.2 – 29.8°C, this may further show that abiotic iron oxidation is occurring to some extent because even at these lower temperatures, there's still a level of abiotic iron oxidation that is occurring. However, the oxidation reported on this study is at higher pH and at a pH above 3.5 and temperature of 25 °C, Singer and Stumm (1970) indicates that the oxidation rate is dependent on both temperature and pH. Thus, the rate of 0.021 $g.L^{-1}.h^{-1}$ may not necessarily apply. In Singer and Stumm (1970), it is also states that abiotic iron oxidation can be more than a factor of 10^6 times slower than microbial-facilitated iron oxidation at a low pH and 25°C. This substantiates what is stated in Searby (2006) that at lower, mesophilic temperatures, the abiotic iron oxidation rate is essentially negligible in comparison to microbial-facilitated iron oxidation.

The chromium oxidation rates in comparison to the nickel rates are faster at higher concentrations. Additionally, a steadier decline in rate is seen and at all tested concentrations of chromium, microbial-facilitated oxidation has occurred. Interestingly, at the MTC values for both metals, the oxidation rates were seen to be similar. At a concentration of 9 g/L chromium (information seen in Appendix), the calculated rate was seen to be 0.019 $g.L^{-1}.h^{-1}$, similar to that of the 4 g/L nickel rate which spiked down after the MTC was reached.

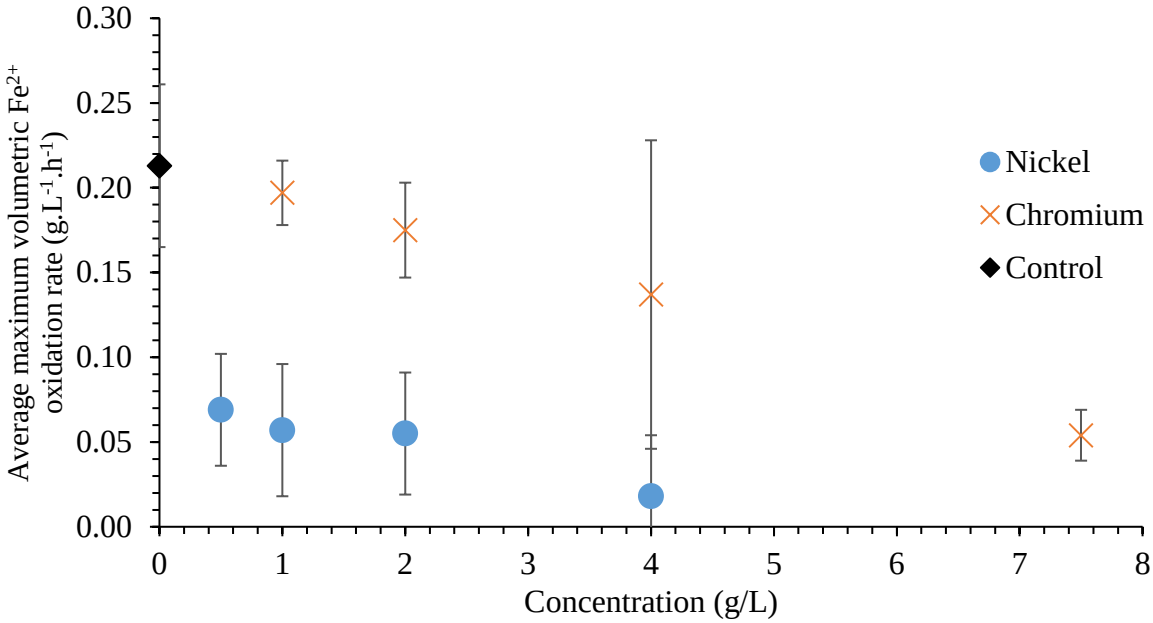

Figure 5.3: Average maximum volumetric ferrous iron oxidation rates for BIOX® culture exposed to increasing concentrations of $Ni^{2+}$and Cr^{3+} at 45°C

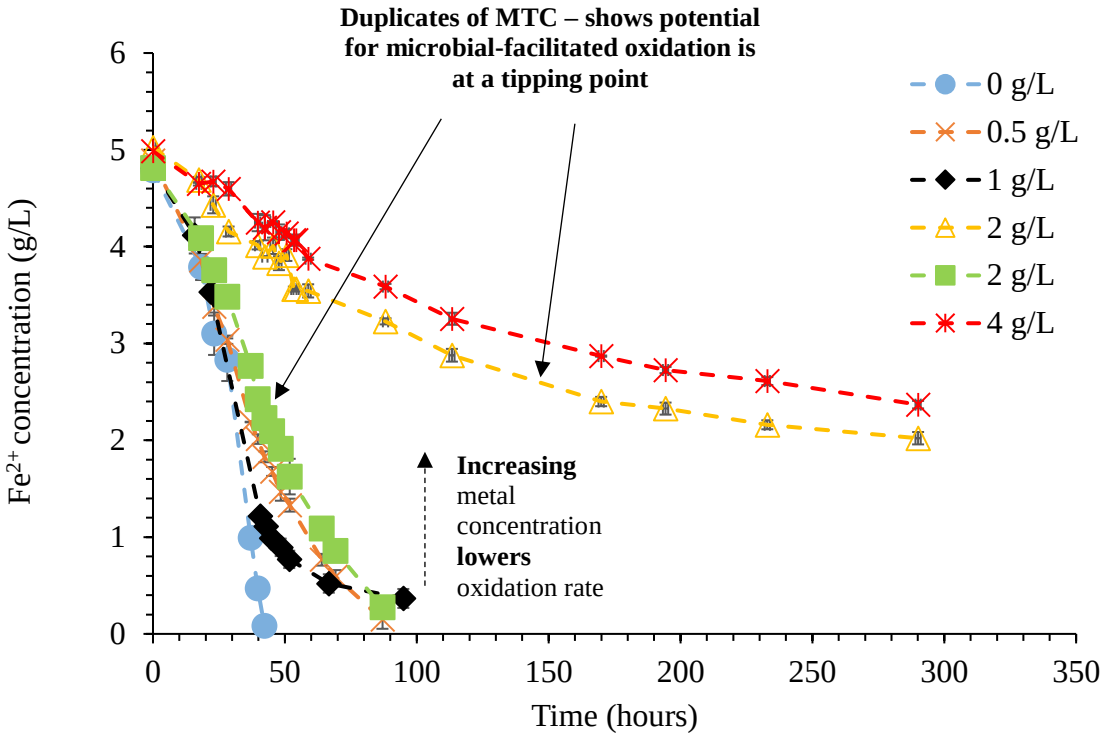

Figure 5.4: Annotated ferrous iron concentration profiles for key Ni^{2+} concentrations tested in MWPs with BIOX® culture at 45°C

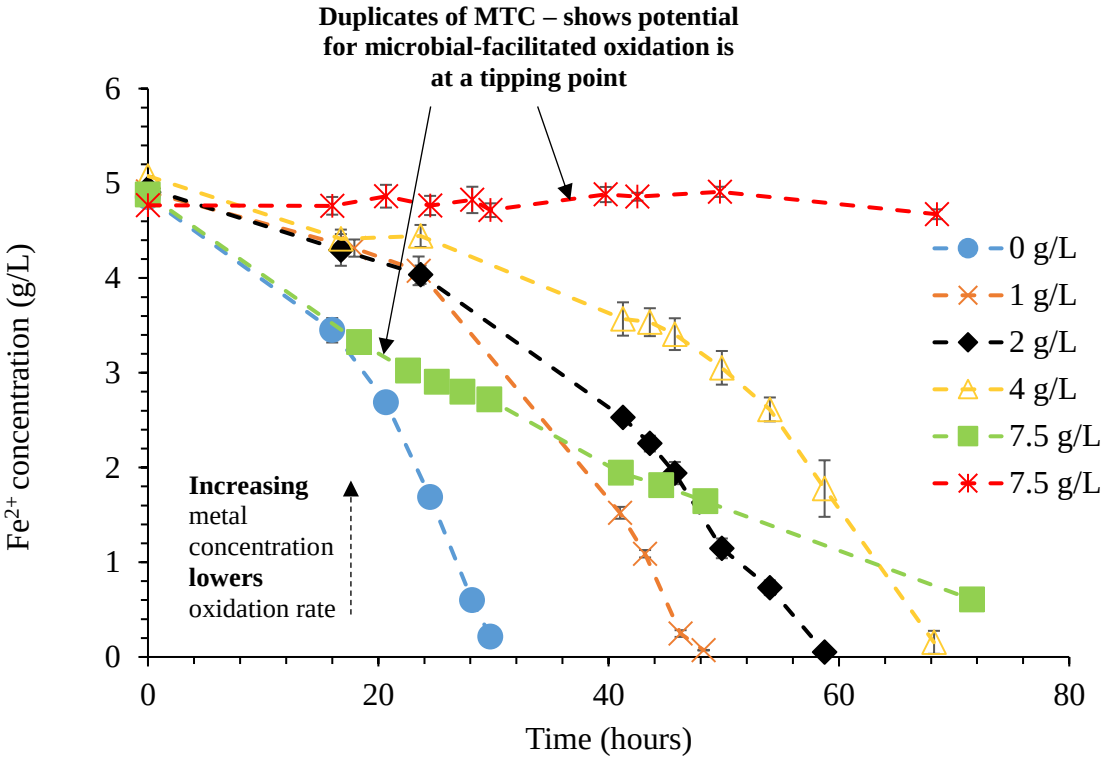

Figure 5.5: Annotated ferrous iron concentration profiles for key Cr^{3+} concentrations tested in MWPs with BIOX® culture at 45°C

5.2.1.2 BRGM-KCC™ microbial consortium

For the BRGM-KCC community, only the key concentrations were tested. Figure 5.7 and Figure 5.8 show a selection of nickel and chromium concentration profiles obtained. The MTC for chromium is seen to be the same as the BIOX® community at 7.5 g/L. However, the MTC for nickel is seen to be 4 g/L. This means that the BRGM-KCC community may be able to withstand higher concentrations of nickel, and is potentially alluding to the fact that different strains of a microbe can behave differently. However, these two ostensibly similar consortia are at different temperatures. In iron-only media at their respective temperatures, both communities are less tolerant towards nickel than chromium.

Figure 5.6 gives the average maximum volumetric ferrous iron oxidation rates for the BRGM-KCC community for nickel and chromium. Like the BIOX® culture, the rates decrease with an increasing inhibitor concentration. For nickel, the rates are generally higher than those of the BIOX® culture which corresponds with the fact that the BRGM-KCC community is more tolerant to nickel. However for chromium, the Fe^{2+} oxidation rates are lower. This means that even though both communities have the same chromium MTC, BIOX® community is slightly more tolerant of chromium at the tested temperatures. It is also noted that the control average rate with no metal inhibitor is lower than that of the BIOX® culture. This is likely due to the mesophilic nature of the culture which is maintained 10°C lower. Under mesophilic temperatures, low pH and ambient pressure, abiotic oxidation of ferrous iron is deemed negligible, or substantially lower than similar moderately thermophilic temperatures (Searby, 2006). Lower temperatures are often coupled with lower reaction rates. However, lower temperatures have lower energy requirements and thus a compromise needs to be reached where reaction rates are acceptable, but operating costs are kept at a minimum (Hubau et al., 2020; Joulian et al., 2020).

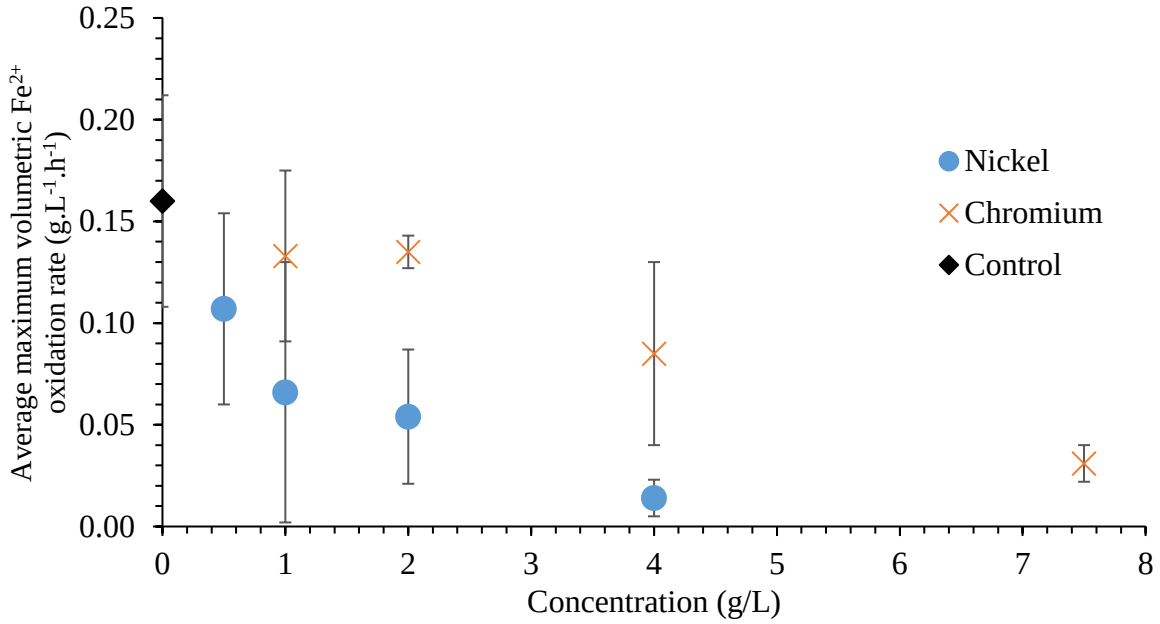

Figure 5.6: Average maximum volumetric ferrous iron oxidation rates for BRGM-KCC culture exposed to increasing concentrations of Ni^{2+} and Cr^{3+} at 35°C

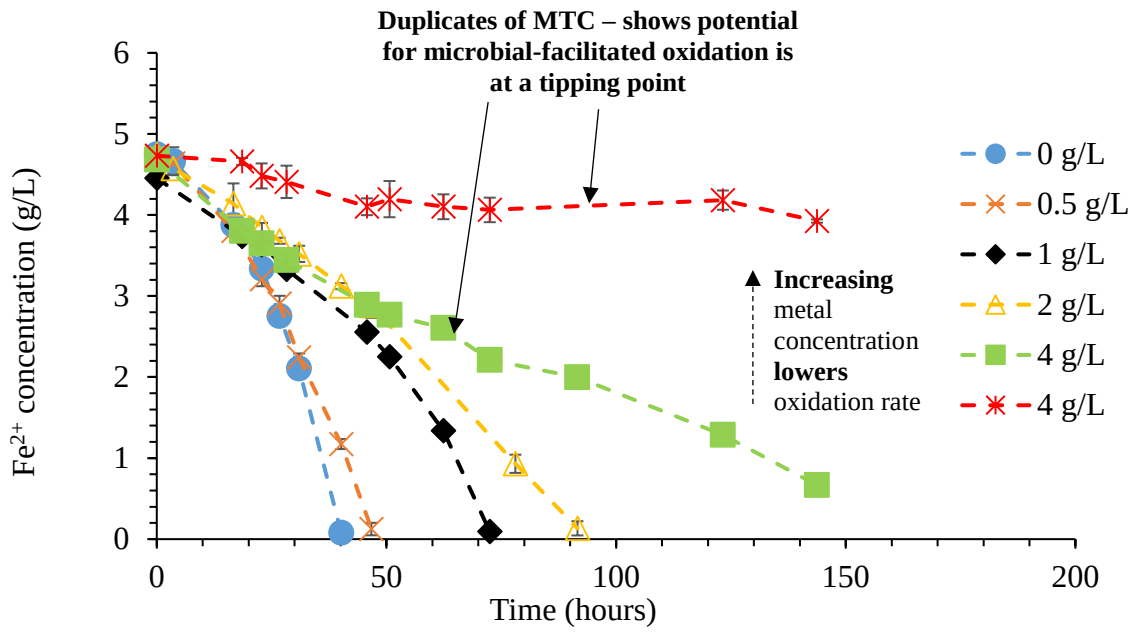

Figure 5.7: Annotated ferrous iron concentration profiles for key Ni^{2+} concentrations tested in MWPs with BRGM-KCC culture at 35°C

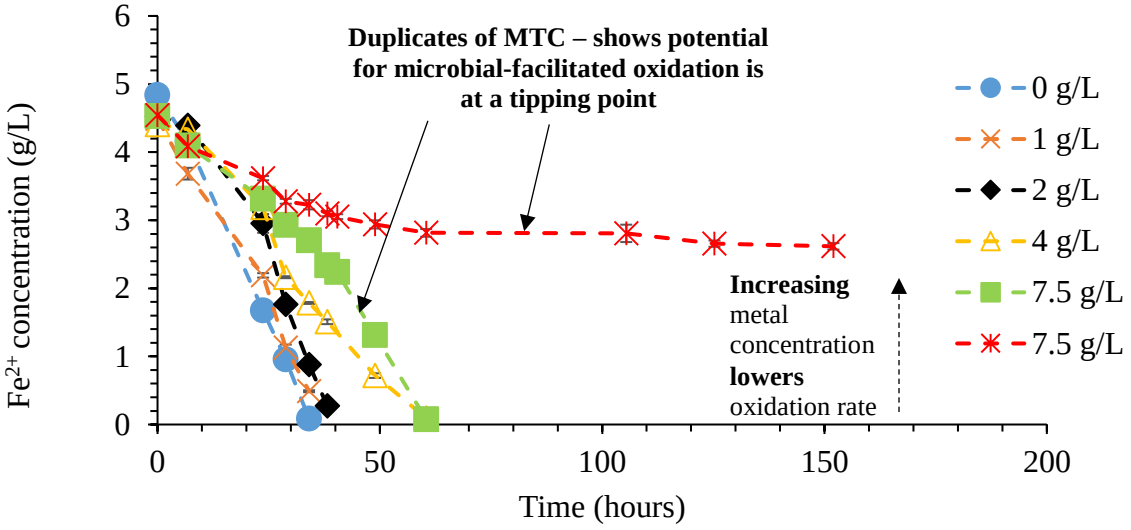

Figure 5.8: Annotated ferrous iron concentration profiles for key Cr^{3+} concentrations tested in MWPs with BRGM-KCC culture at 35°C

5.2.2 Microbial growth

5.2.2.1 BIOX® microbial consortium

During the course of the MWP tests, planktonic cell density was monitored to show the effect of varying inhibitor concentrations on microbial growth. As seen in Figure 5.9, when no nickel is present, the BIOX® community is able to grow substantially. However, at even the lowest concentrations of nickel, it was seen to be minimal to no growth that occurred. This indicates that the BIOX® community is particularly sensitive to the presence of nickel. According to Igiri et al. (2018), this could be as a result of cell membrane damage, enzyme activity inhibition or oxidative stress occurring for the bioleaching microorganisms. In contrast, Figure 5.10 shows that microbial growth occurs at elevated concentrations of chromium, with little to no growth only seen at 4 g/L and above. When chromium concentrations reach higher levels, there is the potential for growth inhibition, elongation of the lag phase and hindrance in oxygen uptake (Igiri et al., 2018). Note that additional cell density profiles for the repeat cultivations of the BIOX® culture and BRGM-KCC culture can be seen in Appendix B, with graphs shown in both the logarithmic and non-logarithmic scale.

An interesting finding is that even when growth was minimal for all nickel concentrations and higher chromium concentrations, oxidation occurred to some extent. This indicates that oxidation may take place without microbial growth as a potential stress response i.e. the energy generated by oxidation may be diverted to maintenance rather than growth. However, this is unsustainable in the long term for continuous bioleaching systems which require continuous biomass production. This finding corresponds with the calculated maximum specific growth rates and maximum iron oxidation rates which show that even when the growth rate is 0 $g.L^{-1}.h^{-1}$, there is still an oxidation rate for that metal inhibitor concentration (besides any potential abiotic oxidation that takes place). Table 5.1 shows the calculated parameters of the average maximum specific growth rate (μ_{max}) and average apparent biomass yield ($Y_{X/S}$) for different concentrations of nickel and chromium. Note that the average maximum specific growth rate was measured for the exponential growth phase, and the average apparent biomass yield was measured from the start of the experiment till the end of the Fe^{2+} oxidation period for the condition demonstrating the most rapid oxidation i.e. the first concentration to deplete Fe^{2+} (generally 0 g/L of the inhibitory metal Ni^{2+} or Cr^{3+}). All yields were measured over the same time period.

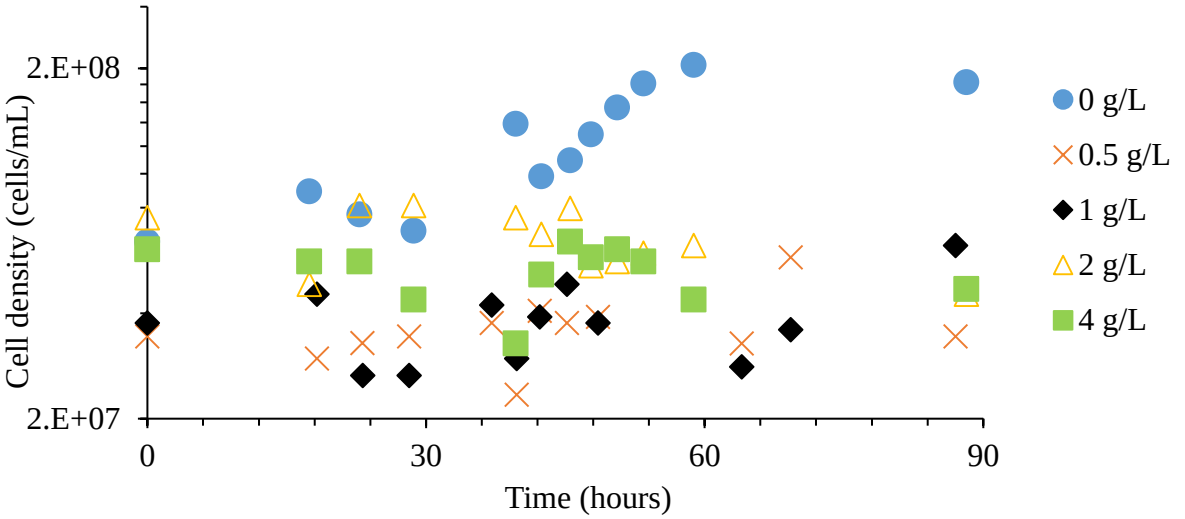

Figure 5.9: Cell density over time for changing Ni^{2+} concentrations using the BIOX® culture at 45°C (logarithmic scale used)

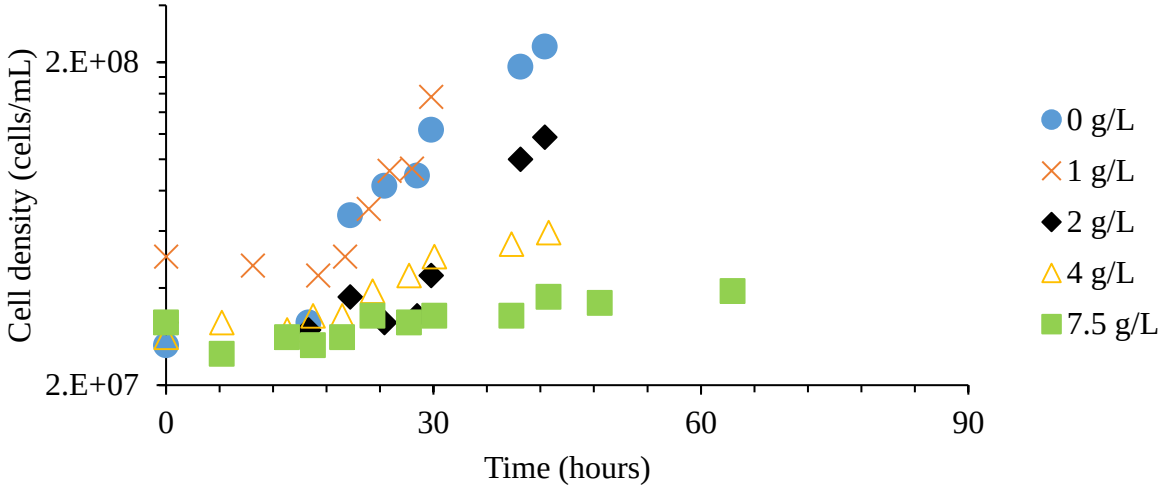

Figure 5.10: Cell density over time for changing Cr^{3+} concentrations using the BIOX® culture at 45°C (logarithmic scale used)

Table 5.1: Average maximum specific growth rates and apparent yields for BIOX® culture exposed to increasing concentrations of Ni^{2+} and Cr^{3+} at 45°C (parameters are measured over the exponential growth phase)

Ni^{2+} concentration (g/L)	**Average μ_{max} (h^{-1})**	**Average Apparent Yield ($x10^9$cells/g_{iron})**	**Cr^{3+} concentration (g/L)**	**Average μ_{max} (h^{-1})**	**Average Apparent Yield ($x10^9$cells/g_{iron})**
0	0.063 ± 0.023	17.7 ± 11.9	0	0.063 ± 0.023	17.7 ± 11.9
0.5	0.009 ± 0.008	7.46 ± 1.15	1	0.051 ± 0.008	12.1 ± 36.4
1	0	1.98 ± 4.02	2	0.033 ± 0.020	7.76 ± 1.10
2	0	0	4	0.034 ± 0.030	1.95 ± 9.62
4	0	0	7.5	0.001 ± 0.002	0

With increasing metal concentration, there is seen to be a decrease in μ_{max} and $Y_{X/S}$. Minimal growth is seen at nickel concentrations of 0.5 g/L; above this, no growth is seen. However, growth is seen for all chromium concentrations studied. This confirms that, in iron-only media, the microbes appear more tolerant to Cr^{3+} than Ni^{2+}.

5.2.2.1 BRGM-KCC microbial consortium

Figure 5.11 and Figure 5.12 show sample cell density profiles for varying concentrations of nickel and chromium (with additional profiles presented in Appendix B) while Table 5.2 shows the calculated average maximum specific growth rates and apparent yields. In comparison to the BIOX® community, it seems that the microorganisms are more nickel-tolerant as growth is seen, to some extent, for all concentrations (confirmed by all concentrations below 4 g/L having non-zero μ_{max} values in Table 5.2).

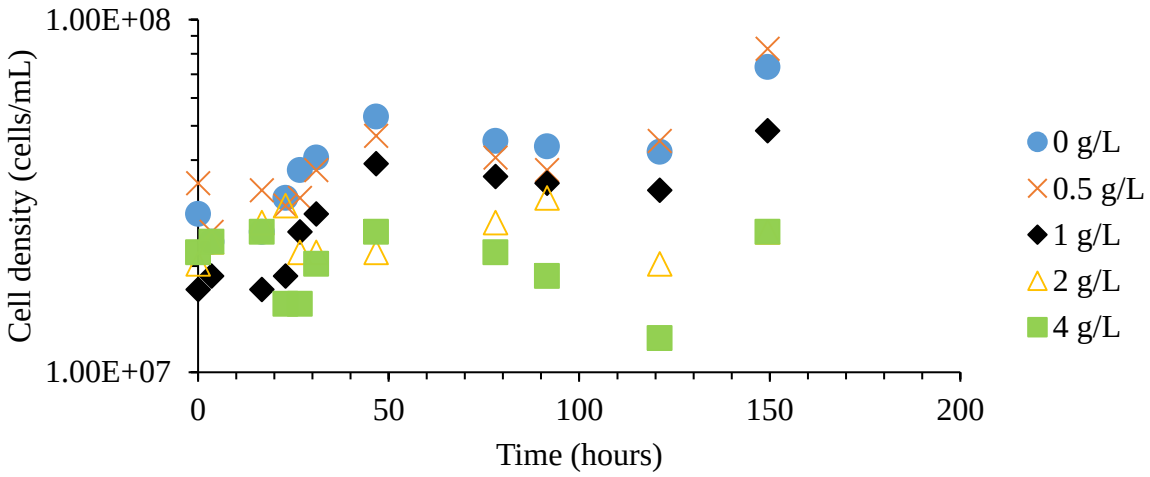

Figure 5.11: Cell density over time for changing Ni^{2+} concentrations using the BRGM-KCC culture at 35°C (logarithmic scale used)

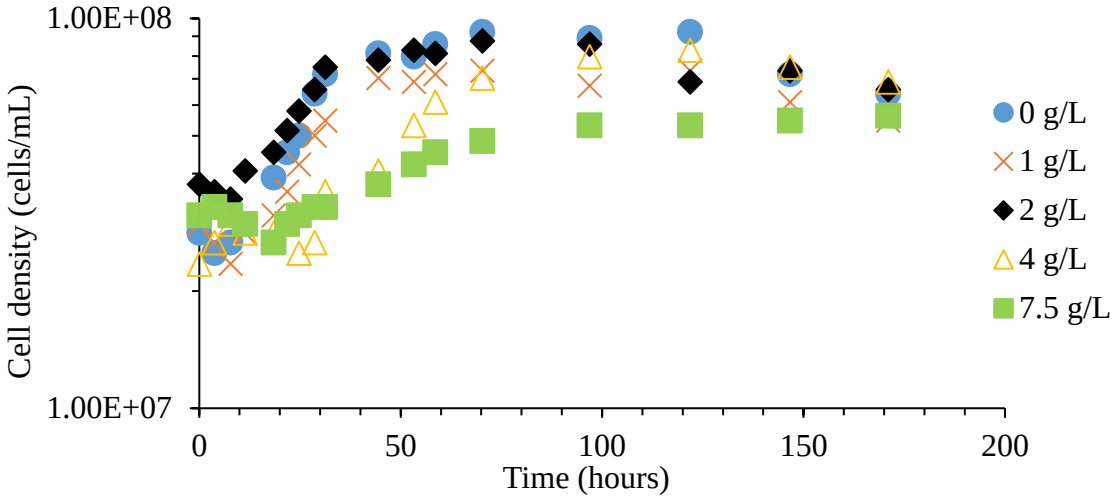

Figure 5.12: Cell density over time for changing Cr^{3+} concentrations using the BRGM-KCC culture at 35°C (logarithmic scale used)

Table 5.2: Average maximum specific growth rates and apparent yields for BRGM-KCC culture exposed to increasing concentrations of Ni^{2+} and Cr^{3+} (parameters are measured over the exponential growth phase)

Ni^{2+} concentration (g/L)	**Average μ_{max} (h^{-1})**	**Average Apparent Yield ($x10^9$cells/g_{iron})**	**Cr^{3+} concentration (g/L)**	**Average μ_{max} (h^{-1})**	**Average Apparent Yield ($x10^9$cells/g_{iron})**
0	0.031 ± 0.013	8.53	0	0.031 ± 0.013	8.53 ± 3.37
0.5	0.018 ± 0.002	5.55	1	0.029 ± 0.005	5.81 ± 5.19
1	0.011 ± 0.014	3.07	2	0.025 ± 0.006	3.18 ± 2.41
2	0.005 ± 0.009	0	4	0.021 ± 0.006	1.48 ± 1.24
4	0	0	7.5	0.005 ± 0.011	0

In contrast, it can be seen that the BIOX® community is able to grow better in the presence of chromium compared to the BRGM-KCC community when comparing the growth rates and yields. However, even when no chromium is present, there is a large difference. This is, again, likely due to the difference in temperatures as higher temperatures coincide with faster growth rates, up until T_{max} is reached (Franzmann et al., 2005; H. Lin et al., 2010). This is substantiated when comparing the cell density numbers in Figure 5.11 and Figure 5.12 to those in Figure 5.9 and Figure 5.10 which show when there is no inhibitor, the BIOX® culture is able to grow into the 10^8 cells/mL range while the BRGM-KCC community remains a magnitude lower in the 10^7 cells/mL range. Despite this, both cultures have shown at least a small amount of growth for all chromium concentrations considered and for both, only at a chromium concentrations of 7.5 g/L is there no longer any biomass produced per gram of iron oxidised.

5.2.3 Redox potential and pH

The redox potential and pH were two additional parameters measured during the course of this experimental block. These were only measured for the BRGM-KCC community. Figure 5.13 and Figure 5.14 show pH and redox potential profiles with increasing nickel concentration while Figure 5.15 and Figure 5.16 show pH and redox potential profiles with increasing chromium concentration. Since there is no sulfur in the system, there is no substrate for sulfur oxidisers and thus no acid production occurs.

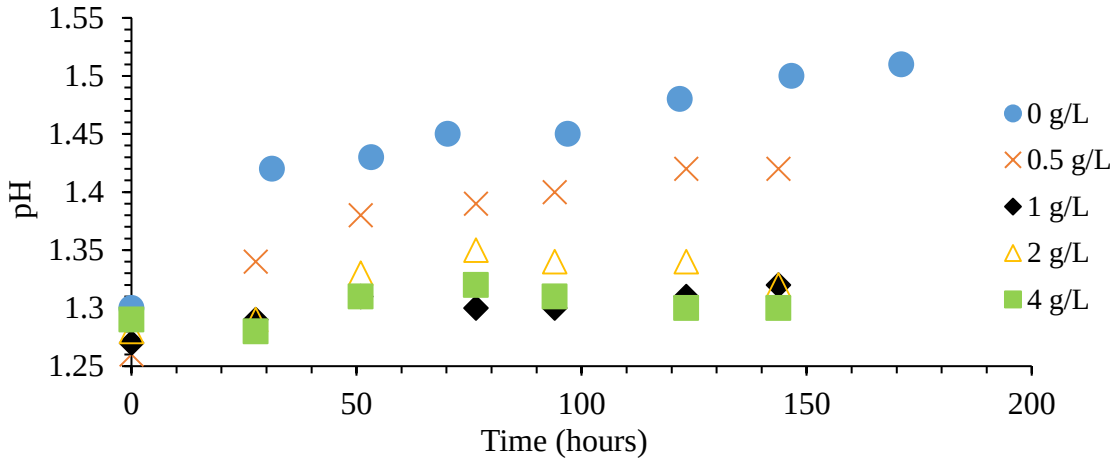

Figure 5.13: Change in pH over time for different Ni^{2+} concentrations using the BRGM-KCC culture at 35°C

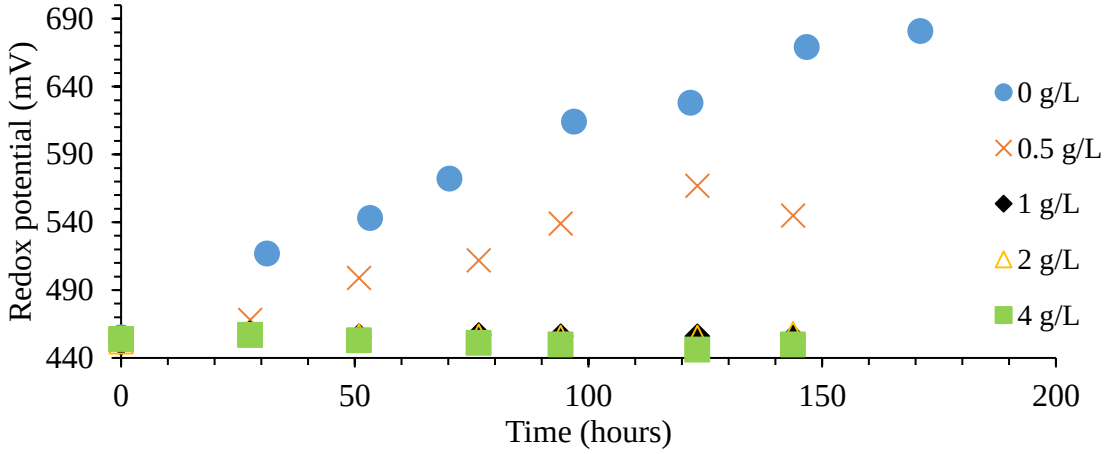

Figure 5.14: Change in redox potential over time for different Ni^{2+} concentrations using the BRGM-KCC culture at 35°C

This, coupled with the fact that acid is consumed during ferrous to ferric iron oxidation, results in an increase in pH seen in both nickel and chromium tests (Rawlings, 2005; Vera et al., 2022). The higher increase in pH for the chromium test corresponds with the fact that more iron oxidation occurs and hence there is more acid consumption. Additionally, there is also the potential of precipitate formation which could have added to increased pH. Examples of precipitates that may have formed which can increase pH with the reduction of OH^- ions include ferric hydroxide and Cr^{3+} hydroxide precipitates (Birk, 2018; Nordstrom and Alpers, 1999). While all the components required for these precipitates to form are present, they are generally seen to form at more basic conditions (pH of about 3.5 - 7) (Birk, 2018; Cruells and Roca, 2022).

This is because Fe^{3+} and Cr^{3+} mostly remains soluble at a lower pH. Thus if any precipitate has formed, it is likely to a small extent. Jarosite, another precipitate commonly seen in bioleaching, is generally formed at a lower pH of about 2 (Cruells and Roca, 2022). However, jarosite is yellow-brown and no evidence of this was observed in the MWPs (Cruells and Roca, 2022). Additionally, jarosite is often associated with a decrease in pH as H^+ ions are released in its formation (Cruells and Roca, 2022). However, this pH change did not occur.

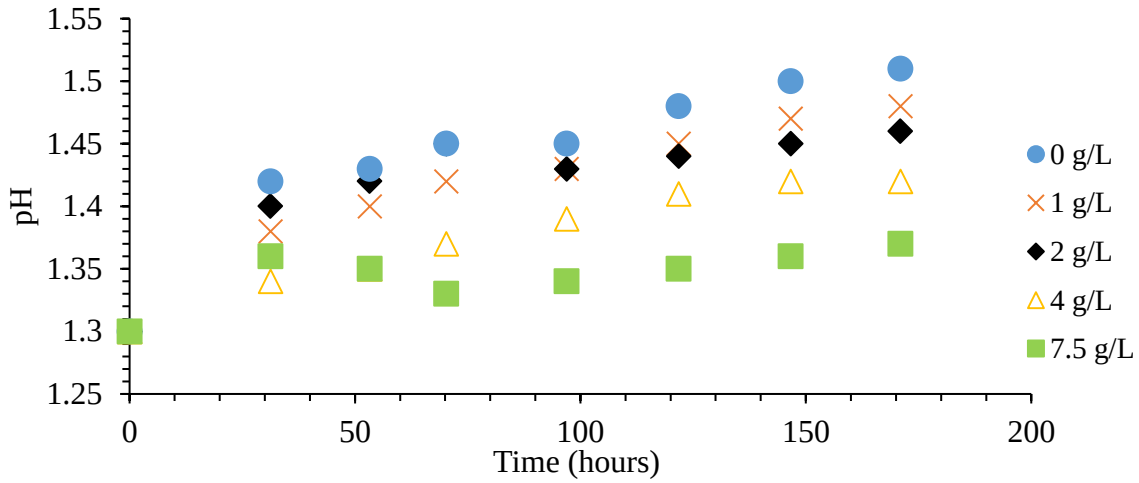

Figure 5.15: Change in pH over time for different Cr^{3+} concentrations using the BRGM-KCC culture at 35°C

Considering the redox potential, it would be assumed that strong iron oxidisers (such as *L. ferriphilum)* are present when no metal is added. This is because strong oxidisers are associated with higher redox potentials (Ahmadi et al., 2015). For nickel, the only concentration which saw an increase in redox potential is 0.5 g/L. This indicates that for higher concentrations when iron oxidation took place, the oxidation was likely done by weak iron oxidisers and this is another reason why iron oxidation at higher nickel concentration could be lower. This may also allude to the fact that the stronger iron oxidisers are more inhibited by nickel.

For chromium, the redox potentials seen in Figure 5.16 were substantially higher for the concentrations tested, suggesting that strong iron oxidisers are able to withstand higher concentrations of chromium and therefore iron oxidation is able to occur more efficiently with higher oxidation rates as seen in Section 5.2.1.2. This is expanded on in Section 5.2.4.

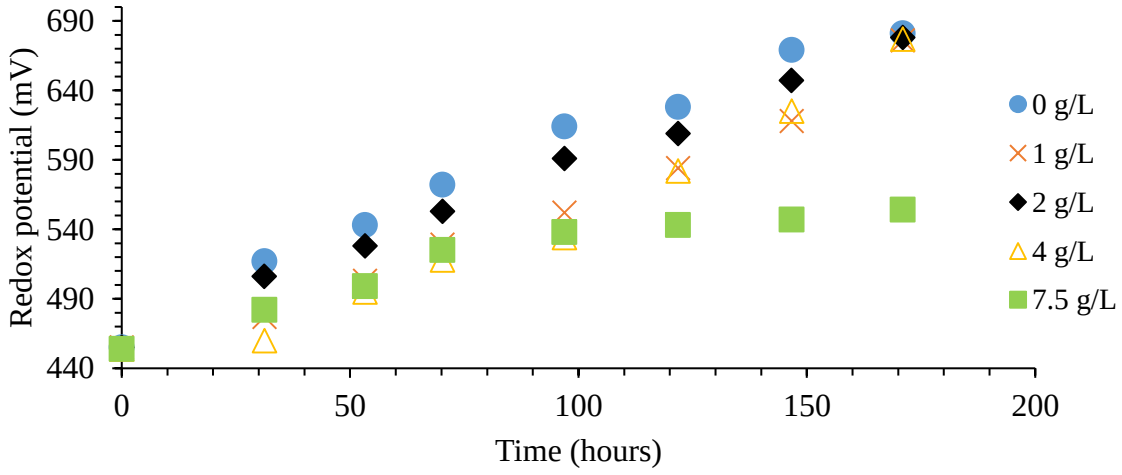

Figure 5.16: Change in redox potential over time for different Cr^{3+} concentrations using the BRGM-KCC culture at 35°C

5.2.4 Microbial speciation

5.2.4.1 BIOX® microbial consortium

Figure 5.17 shows the percentage species abundance of the BIOX® culture at the start of an experiment (inoculum) and at the end of an experiment after exposure to nickel and chromium. The experiment duration was dependent on when iron oxidation was complete, but was continued until a maximum of 1 week if oxidation did not go to completion. The initial BIOX® community in the inoculum consisted predominantly of *L. ferriphilum* (1.50 x 10^7 cells/mL), with lesser amounts of *At. caldus, Fp. acidiphilum* and an unknown bacterium. In all conditions, the *L. ferriphilum* cell numbers and relative abundance decreased, with the percentage decrease reaching up to 88% for 1 and 2 g/L of chromium. It is noted here that the relative abundance (seen in Figure 5.17) and the cell numbers/cell density (seen in Table 5.3) are different. Information on the cell numbers can be seen in Section 5.3 where it is discussed in more detail. Interestingly, there was also a decrease of *L. ferriphilum* in the metal-free test. This indicates that even in test conditions with iron-only media, *L. ferripilum* may not possess all that it requires to thrive. As ferrous iron becomes less available, *L. ferriphilum* numbers will drop. This knowledge can be used to control *L. ferriphilum* levels, along with the control of pH (Ojumu and Petersen, 2011; Smith and Johnson, 2018). *L. ferriphilum* is seen to be at especially low concentrations in the chromium tests. Repeatedly, it has been seen in literature that this microbe is very sensitive to a variety of components, including chromium, nickel and thiocyanate (Edward et al., 2018; Johnson et al., 2017).

Interestingly, the highest levels of oxidation compared to all other nickel and chromium tests occurs when the BIOX® culture is in the presence of chromium and therefore, it is assumed that another microbe other than *L. ferriphilum* is also a good iron oxidiser. Thus, there is the potential that the not well-documented archaeon JTC1/2 is an effective iron oxidiser. This is substantiated in the nickel tests which show lesser amounts of JTC1/2 and has less iron oxidation occurring. Additionally, the iron-oxidising archaeon, *Ap. cupricumulans* can be seen to be at high levels in the nickel tests and low levels in the chromium tests. This points to the fact that it has a higher tolerance towards nickel than chromium. The fact that *Ap. cupricumulans* is at low amounts for chromium and not nickel further corresponds to weaker iron oxidation taking place in the nickel tests. This is because *Ap. cupricumulans* is a weak iron oxidiser, and experiments show that at initial iron concentrations greater than 1 g/L of ferrous iron, there is incomplete iron oxidation by *Ap. cupricumulans* occurs. The ferric iron production rate by *Ap. cupricumulans* is reported to be less than 0.03 h^{-1} at a pH higher than 1.5. This is less than half the rate achieved by *L. ferriphilum* (0.07 h^{-1}) under the same conditions (Smart et al., 2017a).

Considering *Sb. benefaciens*, *At. caldus* and *At. thiooxidans*, the numbers for each are low, except for *Sb. benefaciens* which is particularly high in chromium tests reaching a high of 4.66 x 10^7 cells/mL (an increase of over 10^3 times from the inoculum) in a chromium concentration of 1 g/L. This is to be expected. This is because *Sb. benefaciens* is a facultative anaerobic Firmicute which is able to oxidise iron as well as sulfur (Johnson et al., 2008). *At. caldus* and *At. thiooxidans* are obligate sulfur oxidisers and therefore requires a sulfur source to grow. It has been documented that *At. caldus* and *Sb. benefaciens* are often in competition, and generally it appears that when one begins to dominate, the other would decrease in number (Bryan et al., 2011). This is seen in the nickel concentrations where *Sb. benefaciens* number decrease with an increase in *At. caldus.*

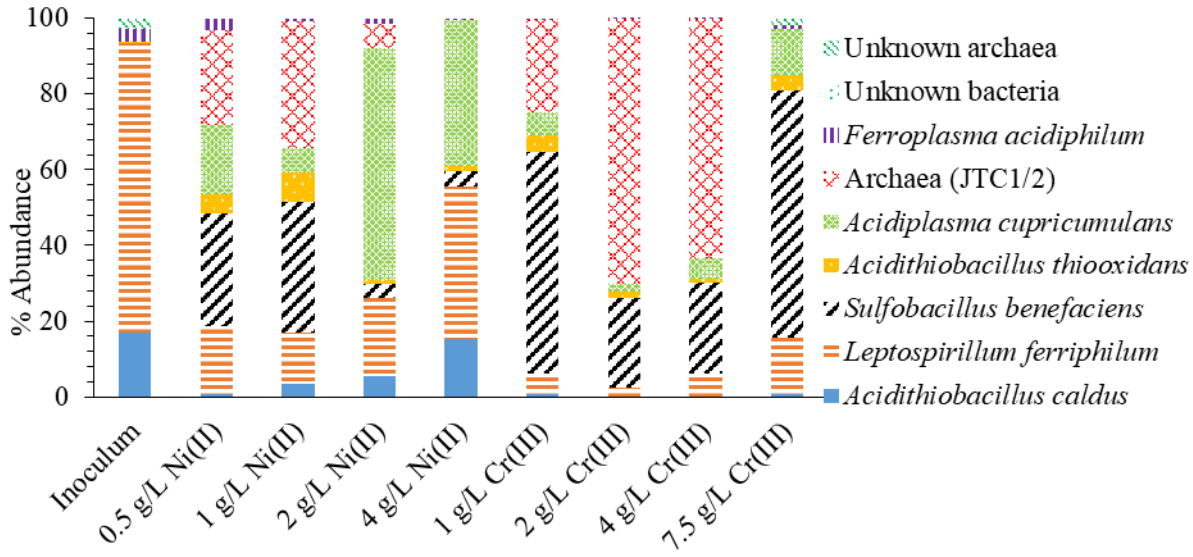

Figure 5.17: Graphical representation of the percentage species abundance of the BIOX® culture exposed to different concentrations of Ni^{2+} and Cr^{3+} following cell culture, compared with the inoculum

5.2.4.2 BRGM-KCC microbial consortium

Figure 5.18 shows the percentage species abundance of the BRGM-KCC culture for nickel and chromium at the start of an experiment (inoculum) and at the end of an experiment. The inoculum seen in Figure 5.18 consists mainly of *L. ferriphilum* and *Sb. benefaciens,* with smaller proportions of *At. caldus* and unknown archaea. When no metal inhibitor is present, the composition of the culture remains mostly unchanged, with the presence of the bacterium *At. thioxidans*, the archaeon *Fp. acidiphilum* and unknown archaea slightly increasing. As stated in Sections 5.2.1 and 5.2.2, it can be seen that *L. ferriphilum* in this culture is more tolerant to nickel with numbers even increasing from 1.11 x 10^7 cells/mL to 4.40 x 10^7 cells/mL in the presence of 0.5 g/L of nickel. Species cell numbers can be seen in Section 5.3 and are explained in more detail. At concentrations higher than this, both the numbers and the relative abundance decrease, but not at the same extent as the BIOX® culture.

In contrast, chromium at all concentrations is seen to have a detrimental effect on a few bioleaching microorganisms with *L. ferriphilum* and *Ap. cupricumulans* in particular showing a substantial decrease in cell numbers. *At. caldus* also decreases in cell number, but it is an obligate sulfur oxidiser and thus it cannot be inferred if the decrease is due to metal inhibition or lack of a growth substrate. In contrast to the BIOX® community which showed an increase in the unspecified archaeon JTC1/2 in the presence of chromium, the BRGM-KCC culture shows an increase in cell number and relative abundance of the archaeon *Fp. acidiphilum* with cell number increases of more than 100 times being seen. This occurred at lower concentrations of chromium (1 g/L and 2 g/L), and at higher concentrations, there was still an increase in this archaeon, but to a lesser degree. As seen in Section 5.2.3, the redox potential for the chromium tests using the BRGM-KCC culture is particularly high in comparison to the other tests. This generally indicates that strong iron oxidisers are present (Ahmadi et al., 2015; Huerta-Rosas et al., 2020). However, the presence of *L. ferriphilum*, a strong iron oxidiser, is low in the chromium tests. Thus it is thought that another microorganism, perhaps *Fp. acidiphilum*, acts as a good iron oxidiser achieving high iron oxidation rates, rates higher than those seen by *L. ferriphilum* in the presence of chromium.

Once again, it is seen that *Sb. benefaciens* cell numbers increase in nickel tests. However, there was a decrease in cell numbers at all chromium concentrations. Despite this decrease, the relative abundance of *Sb. benefaciens* remains high at higher chromium concentrations indicating that while still being affected, the extent of inhibition may be lower than other microbes. Of note is the increased presence of *At. thiooxidans* in all iron-only media tests. While *At. thioxidans* is mesophilic (an added reason why it's presence is seen more in the BRGM-KCC culture), it solely uses sulfur oxidation as an energy and electron source and therefore one would expect it not to be present, or present at low amounts (Quatrini and Johnson, 2016; Yang et al., 2019). Yet, its presence is seen (especially at a chromium concentration of 4 g/L). This is potentially due to a small amount of sulfur carry-over that occurred when removing the culture from its stock source, especially in the 4 g/L of chromium. Coupled with this is the fact that *At. thioxidans* may be able to tolerate some amount of the metal inhibitors in solution.

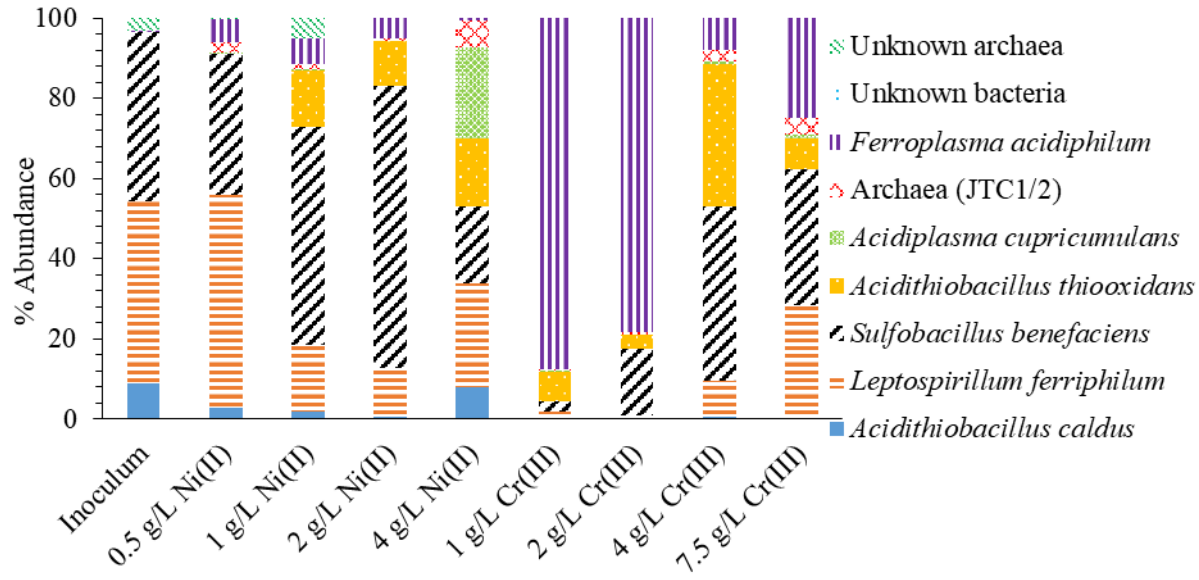

Figure 5.18: Graphical representation of the percentage species abundance of the BRGM-KCC culture exposed to different concentrations of Ni^{2+} and Cr^{3+} following cell culture, compared with the inoculum

5.3 Integrated results and discussion

Heat maps showing the growth of each microbial species as well as calculated oxidation rates can be seen in Table 5.3 and Table 5.4 for the BIOX® and BRGM-KCC cultures respectively. The tables have been split into iron oxidisers and sulfur oxidisers, with iron oxidation data shown for the iron-oxidising microorganisms. As mentioned, while *Sb. benefaciens* has been seen in literature to be able to oxidise both iron and sulfur, it is seen to be a weak iron oxidiser, and has been seen to be in competition with sulfur oxidisers (Bryan et al., 2011; Johnson et al., 2008; Zhang et al., 2021). Thus, it has been placed in the sulfur oxidiser section in Table 5.3 and Table 5.4. Figure 5.19 shows a key for the heat maps displayed in Table 5.3 and Table 5.4. Values nearest to the initial inoculum size of each microorganism are shown as a yellowish hue, values that have shown a decrease in numbers are shown as a reddish hue, and values where the numbers have increased are shown as a greenish hue. This scaling is done relative to each microorganism's inoculum and other differing concentrations. Hence, in cases where multiple values are above the inoculum cell density, a greener hue will appear for the values which show a larger extent of growth. All values besides the inoculum are obtained from the end of the experimentation period.

Considering the BIOX® culture, it can be seen that the total iron oxidiser cell density decreased for all concentrations of nickel and chromium, and only increased when no additional inhibitor was added. This shows the general sensitivity to nickel and chromium of the iron-oxidising microorganisms in the BIOX® culture. Interestingly, iron oxidation rates for chromium were seen to be higher than those for nickel, yet there is a distinct redder hue in the iron oxidiser chromium section indicating a greater decrease in cell density than the nickel section. This seems to indicate that chromium is inflicting a stress response in the microorganisms, requiring the cells to utilise additional iron for energy; however, this energy is not being used for cell growth. This shows how iron oxidation is not necessarily an indication of a microorganism thriving, and in long term, continuous operations, a community actively oxidising iron while not experiencing growth may not be ideal for sustained processing. Conversely, exposing microorganisms to sub-lethal concentrations of metals can also be beneficial to the process as energy consumption is increased when they are required to dedicate energy to cell repair and other metabolic processes to deal with the inhibitors.

Not all microorganisms experienced a decrease in numbers, with *Sb. benefaciens* cell number increasing substantially. Additionally, the lesser known Archaea JTC1/2 and *At. thiooxidans* are also seen to increase, indicating that, like *Sb. benefaciens*, they potentially may play a greater role in oxidation that is currently known or expected. It should be noted that these MWP tests have their limitations with their small scale. Due to their scale, they are more susceptible to larger variations and thus minor differences should not be overplayed.

The BRGM-KCC culture differs from the BIOX® culture as an increase in the total iron oxidiser cell density was observed in the control, and for 0.5 g/L and (minimally) 1 g/L for nickel, and 1 g/L and 2 g/L for chromium. This shows that at the lower inhibitor concentrations, the more commonly known iron oxidisers continue to thrive. At concentrations above 0.5 g/L for nickel, it is seen that the pH and redox potential remains relatively constant. This corresponds to the iron oxidiser numbers seen in the heat map which remain similar or decrease. However, the same is not seen for higher concentrations of chromium where even though a decrease in numbers is seen, the pH and redox potential is still seen to increase. Additionally, it is seen that even with the lower iron oxidiser cell densities than nickel for 4 g/L and 7.5 g/L chromium, the oxidation rates remain higher. This may indicate that other microorganisms are oxidising the iron more than *L. ferriphilum* whose numbers are seen to decrease at all concentrations of chromium (showing its lack of tolerance to this inhibitor). However, it is more likely that a smaller population of *L. ferriphilum* is oxidising the iron under stress conditions because the oxidising ability of *L. ferriphilum* is believed to outweigh that of the other iron oxidising microorganisms. In the BRGM-KCC culture, *Ap. cupricumulans, Fp. acidiphilum, At. thiooxidans* and Archaea JTC1/2 see increases for all chromium concentrations, and unlike with the BIOX® culture, *Sb. benefaciens* sees only decreases. This means that the three former microorganisms are likely all more tolerant to the metal. While *Ap. cupricumulans, Fp. acidiphilum* and possibly Archaea JTC1/2 are contributing to the oxidation of iron in the BRGM-KCC chromium tests, as mentioned, it is still likely *L. ferriphilum* that is facilitating the majority of the oxidation.

Fp. acidiphilum is seen to perform well in the BRGM-KCC reactors in comparison to other microorganisms. Its high cell numbers are potentially due to it being a known mesophilic microorganism, coupled with the fact that it is opportunistic and utilises organic carbon produced by other microorganisms (Bryan et al., 2011; Smart et al., 2017a). *Ap. cupricumulans*, a moderately thermophilic microorganism, was also seen to increase in cell number in nickel and chromium test, but to a lesser extent than *Fp. acidiphilum* (Golyshina, 2014). This could be linked to the fact that its optimum temperature is higher than that of *Fp. acidiphilum*,

As seen in Figure 5.14 and Figure 5.16, the redox potential reaches highs near 690 mV for both nickel and chromium tests. For the nickel test, only when no inhibitor is present is the redox this high. Since

there is *L. ferriphilum* growth for this concentration, it can be assumed the strong oxidiser is mostly responsible for the oxidation that occurs. However, in the chromium tests with the decrease in *L. ferriphilum* numbers, there is potentially another strong oxidiser present. Since it is known that *Ap. cupricumulans* is a weaker oxidiser, it then alludes to the fact that *Fp. acidiphilum* or Archaea JTC1/2 is a strong oxidiser (Smart et al., 2017a). It should be noted that there is also the potential for the dying *L. ferriphilum* to be responsible for some of the oxidation taking place. This could be as a form of stress response where oxidation still occurs (as described in Section 5.2.2.1).

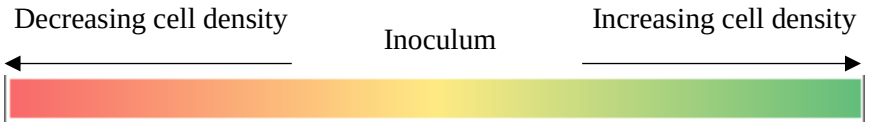

Figure 5.19: Heat map key showing cell density; yellows represent cell density values near the inoculum, red represents decreasing cell density, and green represents increasing cell density

*Table 5.3: Species-specific growth heat map and oxidation data for BIOX® culture**

Microorganism	Inoculum (cell/mL)	Growth (cells/mL)								
		Dominant iron oxidisers								
			Nickel				Chromium			
		0 g/L	0.5 g/L	1 g/L	2 g/L	4 g/L	1 g/L	2 g/L	4 g/L	7.5 g/L
Leptospirillum ferriphilum	1.50E+07	1.23E+06	9.50E+06	3.76E+06	1.46E+07	8.23E+06	4.45E+06	1.82E+06	1.73E+06	5.78E+06
Acidiplasma cupricumulans	6.60E+02	1.33E+08	9.84E+06	1.82E+06	4.29E+07	7.83E+06	4.89E+06	1.73E+06	1.62E+06	4.76E+06
Ferroplasma acidiphilum	7.08E+05	3.96E+06	1.72E+06	2.17E+05	1.10E+06	7.78E+04	4.41E+05	1.73E+05	5.32E+04	2.91E+05
Total	**1.57E+07**	**1.38E+08**	**2.11E+07**	**5.79E+06**	**5.86E+07**	**1.61E+07**	**9.78E+06**	**3.72E+06**	**3.40E+06**	**1.08E+07**
Iron Oxidation rate ($g.L^{-1}.h^{-1}$)		**0.213 ± 0.005**	**0.069 ± 0.003**	**0.057 ± 0.004**	**0.055 ± 0.004**	**0.018 ± 0.011**	**0.197 ± 0.002**	**0.175 ± 0.003**	**0.137 ± 0.009**	**0.054 ± 0.015**
		Dominant sulfur oxidisers								
Sulfobacillus benefaciens[a]	6.47E+03	4.13E+06	1.58E+07	9.71E+06	2.67E+06	8.11E+05	4.66E+07	1.85E+07	7.19E+06	2.54E+07
Acidithiobacillus caldus	3.29E+06	6.99E+04	4.18E+05	1.02E+06	3.82E+06	3.09E+06	4.69E+05	6.46E+04	5.21E+04	3.15E+05
Acidithiobacillus thiooxidans	3.43E+04	5.97E+05	2.60E+06	2.16E+06	7.17E+05	2.87E+05	3.56E+06	1.25E+06	2.54E+05	1.70E+06
		Unknown								
Archaea (JTC1/2)	7.31E+03	4.23E+06	1.32E+07	9.44E+06	4.50E+06		1.93E+07	5.46E+07	1.88E+07	

**Growth values represented (besides the inoculum) are from the end of the experiment; total iron oxidiser cell densities are only shown due to the focus on iron oxidation; grey blocks represent values where qPCR errors occurred. [a]Sulfobacillus benefaciens is both a sulfur and iron-oxidising bacterium. It has been placed in the sulfur oxidiser section as it is considered a weak iron oxidiser (Johnson et al., 2008).*

*Table 5.4: Species-specific growth heat map and oxidation for BRGM-KCC culture**

Microorganism	Inoculum (cell/mL)	Growth (cells/mL)								
		Iron oxidisers								
			Nickel				Chromium			
		0 g/L	0.5 g/L	1 g/L	2 g/L	4 g/L	1 g/L	2 g/L	4 g/L	7.5 g/L
Leptospirillum ferriphilum	1.11E+07	3.68E+07	4.40E+07	7.97E+06	3.04E+06	6.51E+06	1.14E+06	3.15E+05	1.14E+06	1.76E+06
Acidiplasma cupricumulans	2.62E+02	6.73E+05	2.86E+05	2.02E+05	3.45E+04	5.63E+06	3.88E+04	1.67E+04	5.98E+04	6.86E+04
Ferroplasma acidiphilum	9.89E+04	1.23E+06	4.83E+06	3.15E+06	1.29E+06	1.64E+05	5.06E+07	2.82E+07	1.02E+06	1.55E+06
Total	**1.12E+07**	**3.87E+07**	**4.91E+07**	**1.13E+07**	**4.37E+06**	**1.23E+07**	**5.18E+07**	**2.85E+07**	**2.21E+06**	**3.38E+06**
Iron Oxidation rate ($g.L^{-1}.h^{-1}$)		**0.160 ± 0.005**	**0.107 ± 0.005**	**0.066 ± 0.006**	**0.054 ± 0.003**	**0.014 ± 0.009**	**0.133 ± 0.004**	**0.135 ± 0.007**	**0.085 ± 0.005**	**0.031 ± 0.009**
		Sulfur oxidisers								
Sulfobacillus benefaciens[a]	1.04E+07	1.84E+07	2.92E+07	2.63E+07	1.75E+07	4.77E+06	1.49E+06	5.98E+06	5.44E+06	2.11E+06
Acidithiobacillus caldus	2.21E+06	6.13E+06	2.24E+06	9.60E+05	1.56E+05	1.97E+06	2.85E+04	2.37E+04	6.42E+04	2.78E+04
Acidithiobacillus thiooxidans	5.62E+03	1.87E+06		6.83E+06	2.79E+06	4.26E+06	4.25E+06	1.24E+06	4.43E+06	4.69E+05
		Unknown								
Archaea (JTC1/2)	1.91E+03	1.55E+05	2.14E+06	5.62E+05	1.50E+05	1.69E+06	2.57E+05	1.78E+05	3.57E+05	2.63E+05

**Growth values represented (besides the inoculum) are from the end of the experiment; total iron oxidiser cell densities are only shown due to the focus on iron oxidation; grey blocks represent values where qPCR errors occurred; [a]Sulfobacillus benefaciens is both a sulfur and iron-oxidising bacterium. It has been placed in the sulfur oxidiser section as it is considered a weak iron oxidiser (Johnson et al., 2008).*

5.4 Conclusions

In this chapter, MWP tests were performed in sulfur-free media using two microbial communities, the BIOX™ and the BRGM-KCC culture. These tests were done to determine the MTCs for these two microbial communities for nickel and chromium, and to determine the effects of these metals on the community as a whole as well as on individual species within the community. Considering the BIOX® community, results show that the MTC for nickel is 2 g/L and for chromium it is 7.5 g/L. For the BRGM-KCC community, the MTCs for nickel and chromium were 4 g/L and 7.5 g/L respectively. Despite the fact that the cultures were able to oxidise ferrous iron to ferric iron up until their MTCs, it was determined that growth was not always able to occur at these concentrations. This indicates that in a commercial setting even when oxidation is occurring, microbial growth may not be directly coupled with this oxidation. For a sustainable continuous system, continuous biomass production is required at a rate greater than or equal to the rate that biomass is lost from the system through continuous flow. Additionally, the experiments performed showed the importance of the components found in a bioleaching matrix. With the omission of a single component such as a sulfur source, one can see how the microbial composition of the community is changed. Therefore, it is important to consider all potential components found within a bioleaching system, and take note of the potential inhibition that can take place within the system in order to understand how inhibitors interact with different species. Further, it is important to understand the potential for de-coupling of energy generation through oxidation and growth and to ensure sufficient growth to support a stable oxidising system.

Chapter 6: Batch Microwell plate tests with sulfur substrate

6.1 Introduction

In this chapter, small scale batch MWPs were used to test the metal tolerance of the BRGM-KCC microbial consortium in the presence of elemental sulfur. Similarly to the previous chapter, the metal tolerance indicator used was the maximum tolerated concentration (MTC). In this chapter, once again different parameters are explored and studied to better understand the effect of two potential metal inhibitors (nickel and chromium) on various acidophilic bioleaching microorganisms. These parameters include microbial oxidation, microbial growth, redox potential, pH and microbial speciation. Only key concentrations identified in Chapter 5 have been explored in this set of experiments.

The inclusion of elemental sulfur as an additional growth substrate was to explore the tolerance of both iron and sulfur-oxidising microorganisms to increasing concentrations of the metal inhibitors in a mixed microbial community. The results are discussed in the sections below.

6.2 Results and Discussion

6.2.1 Microbial iron oxidation

In Figure 6.1, the average maximum volumetric iron oxidation rates collected over replicate runs are presented as averages, on exposure to different concentrations of nickel and chromium. The same trend of decreasing oxidation rates with increasing concentrations of metals is observed for the nickel and chromium tests. This is similar to in the trends seen in the MWP tests with no sulfur present discussed in Chapter 5. However, some differences are apparent upon further review of the results.

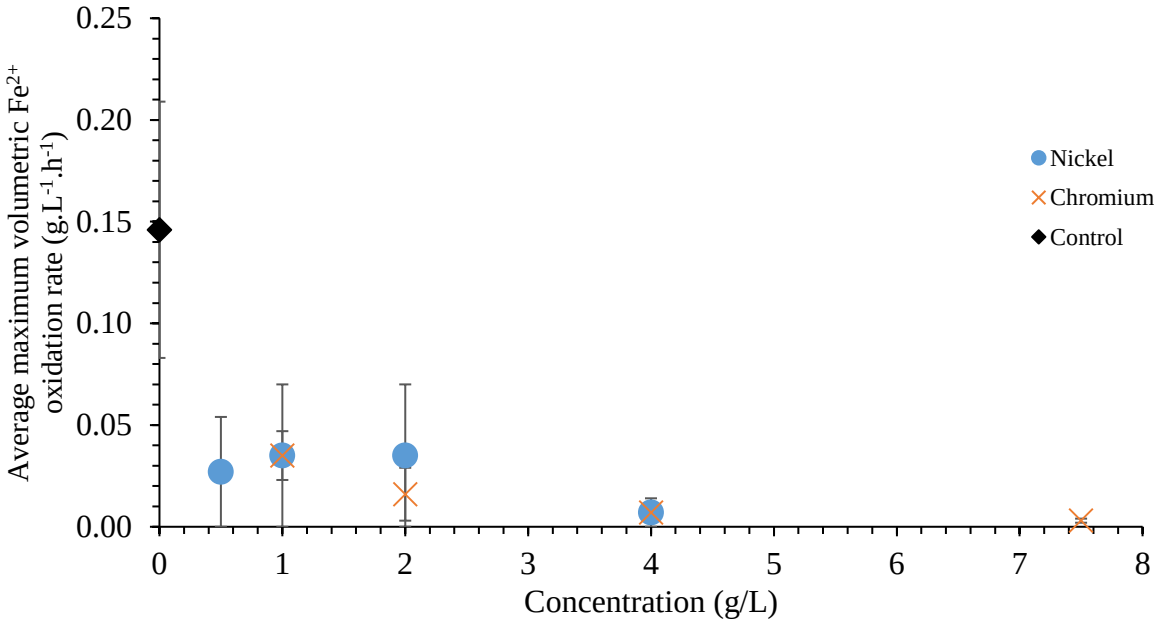

Figure 6.1: Average maximum volumetric ferrous iron oxidation rates for BRGM-KCC culture exposed to increasing concentrations of Ni^{2+} and Cr^{3+} in media containing iron and sulfur

For the nickel tests, it can be seen that at a low concentration and when no nickel is present (0 and 0.5 g/L nickel added), the rate of iron oxidation is lower when there is iron and sulfur present in the media in comparison to when only iron is present (0.146 and 0.074 $g.L^{-1}.h^{-1}$ *vs* 0.160 and 0.107 $g.L^{-1}.h^{-1}$, respectively). This could potentially be due to the fact that in the presence of a sulfur source, sulfur-oxidisers with the ability to weakly oxidise iron (e.g. some microorganisms in the *Sulfobacillus* genus according to Johnson et al. (2008) and Zhang et al. (2021)) may out compete obligate iron-oxidisers when nickel is present at low concentrations.

In contrast, at higher nickel concentrations, it is seen that more oxidation occurs when sulfur is present compared to iron-only tests. This could be as a result of a number of mechanisms. Potentially, the dominant microorganisms, though weaker iron oxidisers, are better able to tolerate nickel. Alternatively, the resistance mechanisms that are activated at a higher nickel concentration require more energy, and sulfur is able to provide more of this energy than iron. Additionally, this difference could be due to the fact that the presence of more H^+ ions in solution allows for these ions to be bound to binding sites on cells rather than metal ions which in turn may decrease toxicity for nickel (Gadd and Griffiths, 1977).

Interestingly, in the presence of sulfur it is seen that any added amount of chromium severely affects the iron oxidation rates achieved at a much greater extent to any addition of nickel. This is in opposition to the iron-only tests where nickel was more inhibiting to iron oxidisers than chromium. This shows how the addition of a single component can have a marked effect, either positive or negative, on a bioleaching system.

At 2 g/L of chromium, an iron oxidation rate of 0.016 $g.L^{-1}.h^{-1}$ is seen. This equates to the minimum Fe^{2+} oxidation rate achieved in tests without sulfur. However, at 4 and 7.5 g/L of chromium, the Fe^{2+} oxidation rates decrease further to 0.007 ± 0.004 $g.L^{-1}.h^{-1}$ and 0.003 ± 0.001 $g.L^{-1}.h^{-1}$, respectively, i.e. minimal oxidation is taking place. These extremely low iron oxidation rate values suggest intense inhibition of iron-oxidisers at elevated chromium levels, and potentially increased precipitation reactions occurring which strongly interfere with iron oxidation. Precipitation reactions may remove the ferric iron leach agent from the solution phase or disrupt the iron oxidation by directly affecting the microbes or by forming a layer which blocks oxygen from entering the system. The precipitate may be formed at higher chromium and pH levels, and a picture of its potential occurrence can be seen in Figure 6.2. The higher the chromium concentration, the greater the extent of the precipitation which in turn causes even higher pH levels. A pH as high as 2.57 can be seen in Figure 6.10. This is substantially higher than maximum pH of 1.51 seen in the iron-only tests. The exact reaction mechanisms resulting in the formation of the precipitate are unknown since it has not been further analysed and goes beyond the scope of this study. However, since it formed at higher chromium concentrations, and only formed in tests where sulfur was present, it is thought to be a precipitate involving these components. Additionally, there is the potential for species in the 0Km media to be involved as literature states components like aqueous ammonia and hydroxides can form precipitates with Cr^{3+} under certain conditions, and the precipitates formed are of a grey-greenish/bluish colour (as seen in Figure 6.2) (Birk, 2018).While these precipitates have generally been observed to form at higher pH values (3.5 – 7), it is not theoretically impossible for them to have occurred in the test conditions (Birk, 2018; Nordstrom and Alpers, 1999). It is noted that what appears to be a precipitate may also be elemental sulfur which has not sunk to the bottom of the well. This may occur because there is limited or no growth on the sulfur which may result in the sulfur not sinking.

Now considering the MTC values, it was seen that the MTC value for nickel is > 4 g/L and the MTC value for chromium is < 2 g/L. Figure 6.3 and Figure 6.4 show example iron oxidation profiles for nickel and chromium tests respectively and other profiles can be seen in Appendix B. In Figure 6.3, at even the highest concentration of 4 g/L nickel, iron oxidation still occurs and this is why it is thought that the MTC is greater than 2 g/L. In Figure 6.4, the two 2 g Cr^{3+}/L profiles do not see full oxidation and it is thus thought that only at a concentration lower than this will the MTC be reached. In comparison to the iron-only tests, it is seen that the nickel MTC increased while the chromium MTC decreased. Once again this indicates how a change in a single component such as the addition of sulfur may strongly impact a microbial consortium.

Figure 6.2: Picture of MWP Cr^{3+} test with sulfur at the start of the test and at the end of the test where a film/potential precipitate is formed at a higher Cr^{3+} concentration

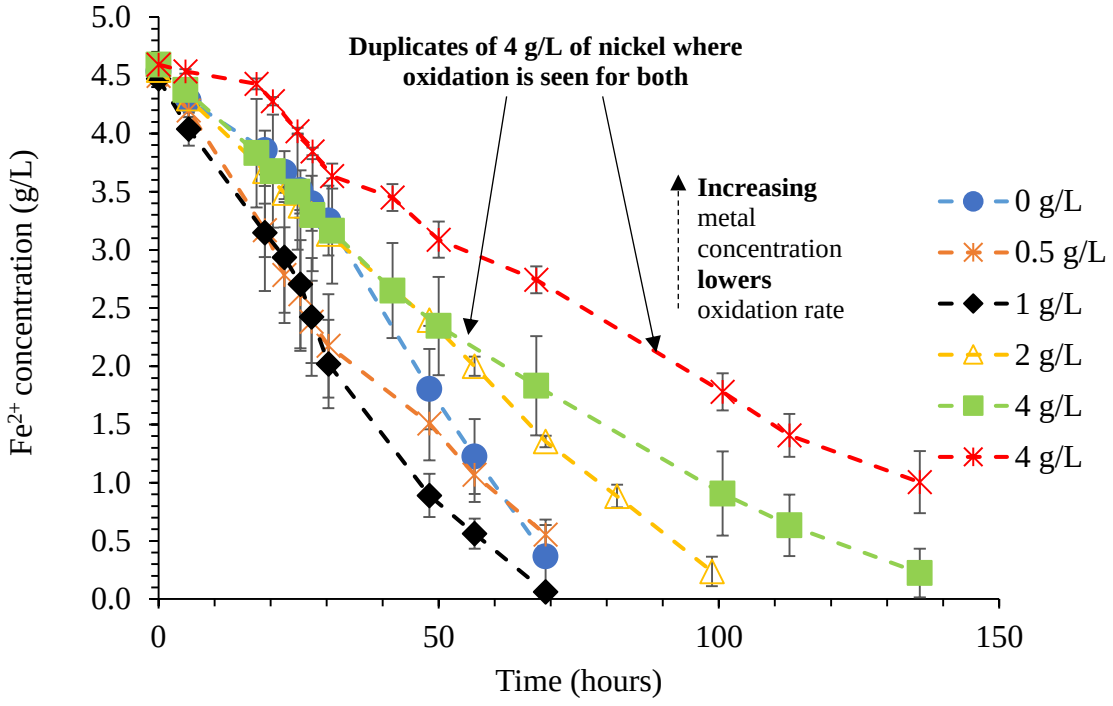

Figure 6.3: Annotated ferrous iron concentration profiles for key Ni^{2+} concentrations tested in MWPs with BRGM-KCC culture in media containing iron and sulfur

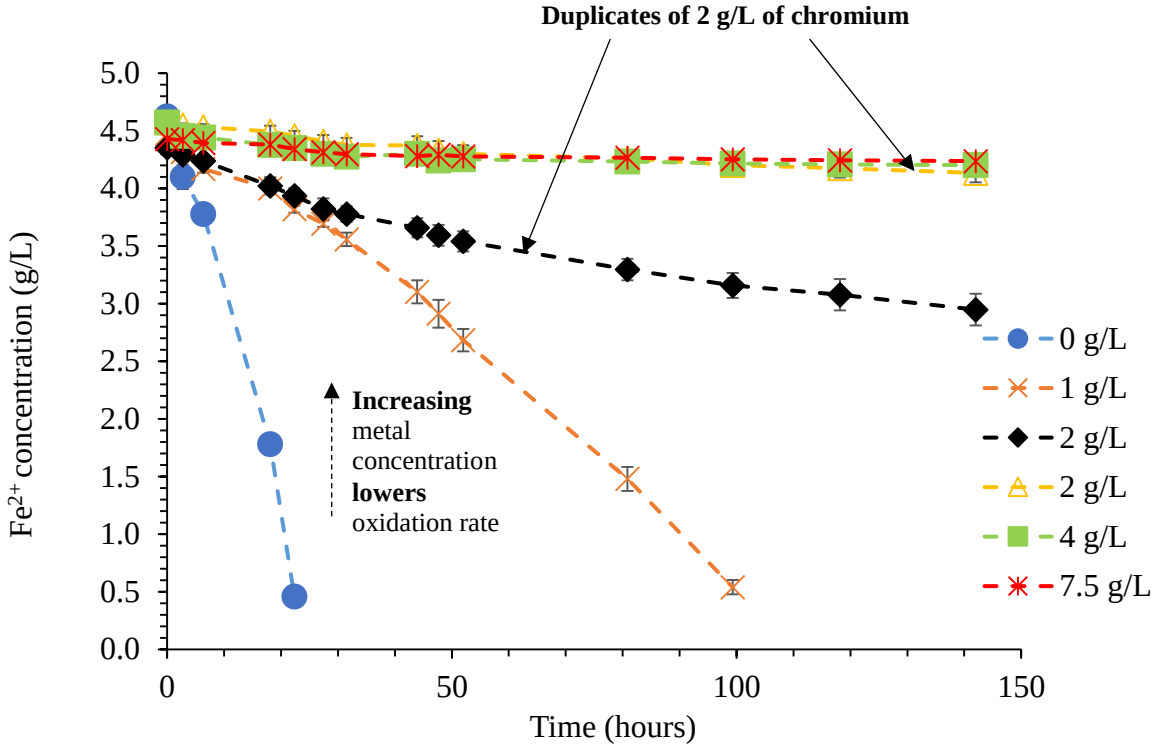

Figure 6.4: Annotated ferrous iron concentration profiles for key Cr^{2+} concentrations tested in MWPs with BRGM-KCC culture in media containing iron and sulfur

6.2.2 Microbial growth

Comparing Figure 6.5, Figure 6.6 and Table 6. to Figure 5.9, Figure 5.10 and Table 5.4 (all growth-related information), it can be seen that BRGM-KCC microbial growth is elevated in the presence of sulfur, compared to in its absence, when nickel is added. In contrast, growth decreased in the presence of sulfur, compared to in its absence, when chromium is present. When both nickel and chromium is not present, the tests with sulfur show a higher average maximum specific growth rate and average apparent yield than those without sulfur, with an increase of about 0.034 h^{-1} and 22.27 x 10^9 cells/g_{iron} seen respectively. A comparison of maximum specific growth rates and yield coefficients between the two experimental blocks can be seen in Figure 6.7. This large difference clearly shows the benefit of ensuring there is sufficient sulfur for both sulfur and iron oxidisers when there is no presence of chromium. All growth curves used in the calculation of average values can be seen in Appendix B.

For nickel, a higher growth rate and yield compared to when no metal is added is seen at all concentrations, except at the average maximum specific growth rate value of 4 g/L (about 0.004 h^{-1} lower than the 0 g/L value of 0.065 ± 0.047 h^{-1}). This trend is not seen in the iron oxidation data where a decrease in the average oxidation rates is seen with an increase in nickel concentration. This could potentially be as a result of the fact that as the concentrations increase, the iron-oxidising microorganisms decrease in number, but there is still an increase in the microbes which are capable of oxidising sulfur. This suggests that low concentrations of nickel may actually stimulate growth.

For chromium, there is only seen to be minimal growth at 1 g/L with an average maximum specific growth rate of 0.005 ± 0.013 h^{-1} at this concentration. All other concentrations show no growth and when viewing Figure 6.6, it is seen that there is even a death phase with cell numbers decreasing. The information in Figure 6.6, Figure 6.7 and Table 6. clearly indicate that the microbes are greatly affected by chromium at all tested concentrations in the presence of sulfur, and corresponds to oxidation data as there is no oxidation occurring at concentrations above 1 g/L and no growth is also seen at these concentrations. At 1 g/L of chromium, even though there is a small amount of growth that is seen, the yield is seen to be 0. Additionally, oxidation is also seen to take place at this concentration to near completion in Figure 6.4, but at a slow rate. This could indicate that in the presence of sulfur at 1 g/L of chromium, iron-oxidising microorganisms are able to grow to a small extent, but not high enough to sustain and yield continuous iron oxidation. This is substantially different in the iron-only tests where a high level of growth is seen at 1 g/L.

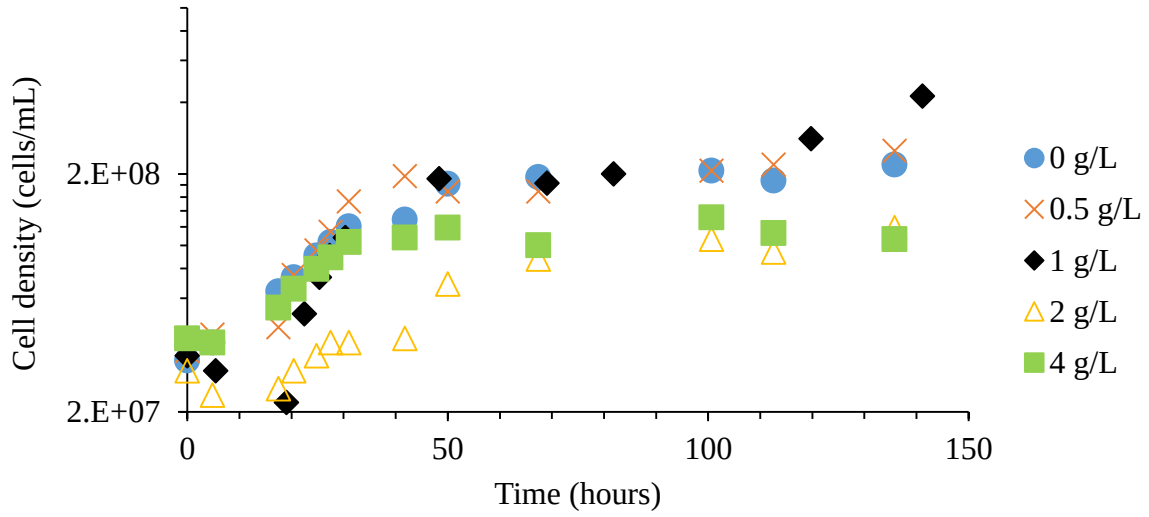

Figure 6.5: Cell density over time for changing Ni^{2+} concentrations in media containing sulfur (logarithmic scale used)

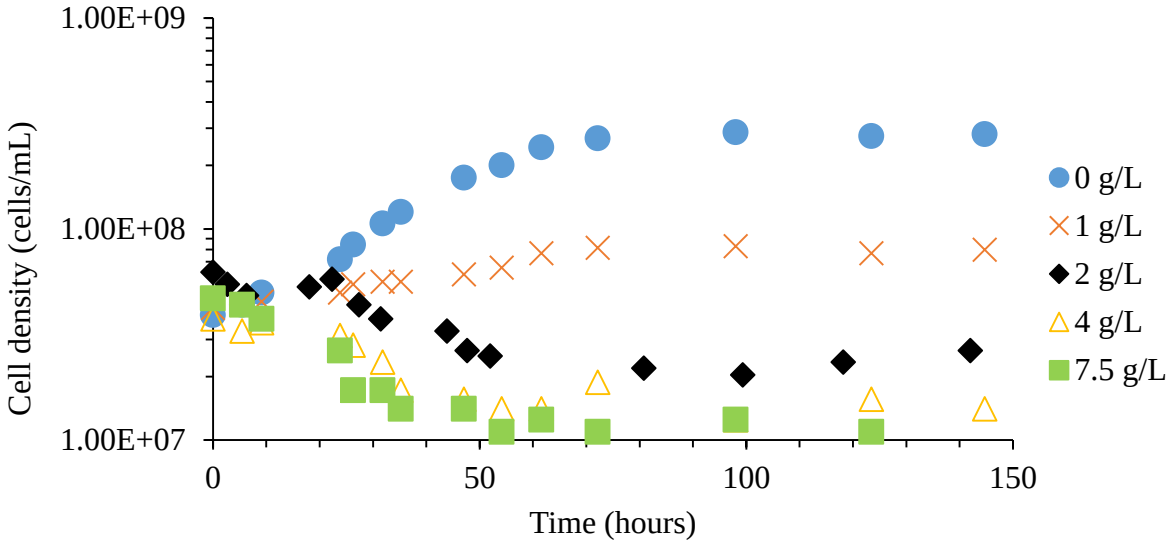

Figure 6.6: Cell density over time for changing Cr^{3+} concentrations in media containing sulfur (logarithmic scale used)

Table 6.1: Average maximum specific growth rates and apparent yields for BRGM-KCC culture exposed to increasing concentrations of Ni^{2+} and Cr^{3+} in media containing sulfur (parameters are measured over the exponential growth phase)

Ni^{2+} concentration (g/L)	**Average μ_{max} (h^{-1})**	**Average Apparent Yield ($x10^9$cells/g_{iron})**	**Cr^{3+} concentration (g/L)**	**Average μ_{max} (h^{-1})**	**Average Apparent Yield ($x10^9$cells/g_{iron})**
0	0.065 ± 0.047	30.8 ± 12.6	0	0.065 ± 0.047	30.8 ± 12.6
0.5	0.126 ± 0.035	50.0 ± 17.4	1	0.005 ± 0.013	0
1	0.111 ± 0.065	39.3 ± 23.6	2	0	0
2	0.076 ± 0.046	33.0 ± 24.6	4	0	0
4	0.061 ± 0.053	41.0 ± 34.7	7.5	0	0

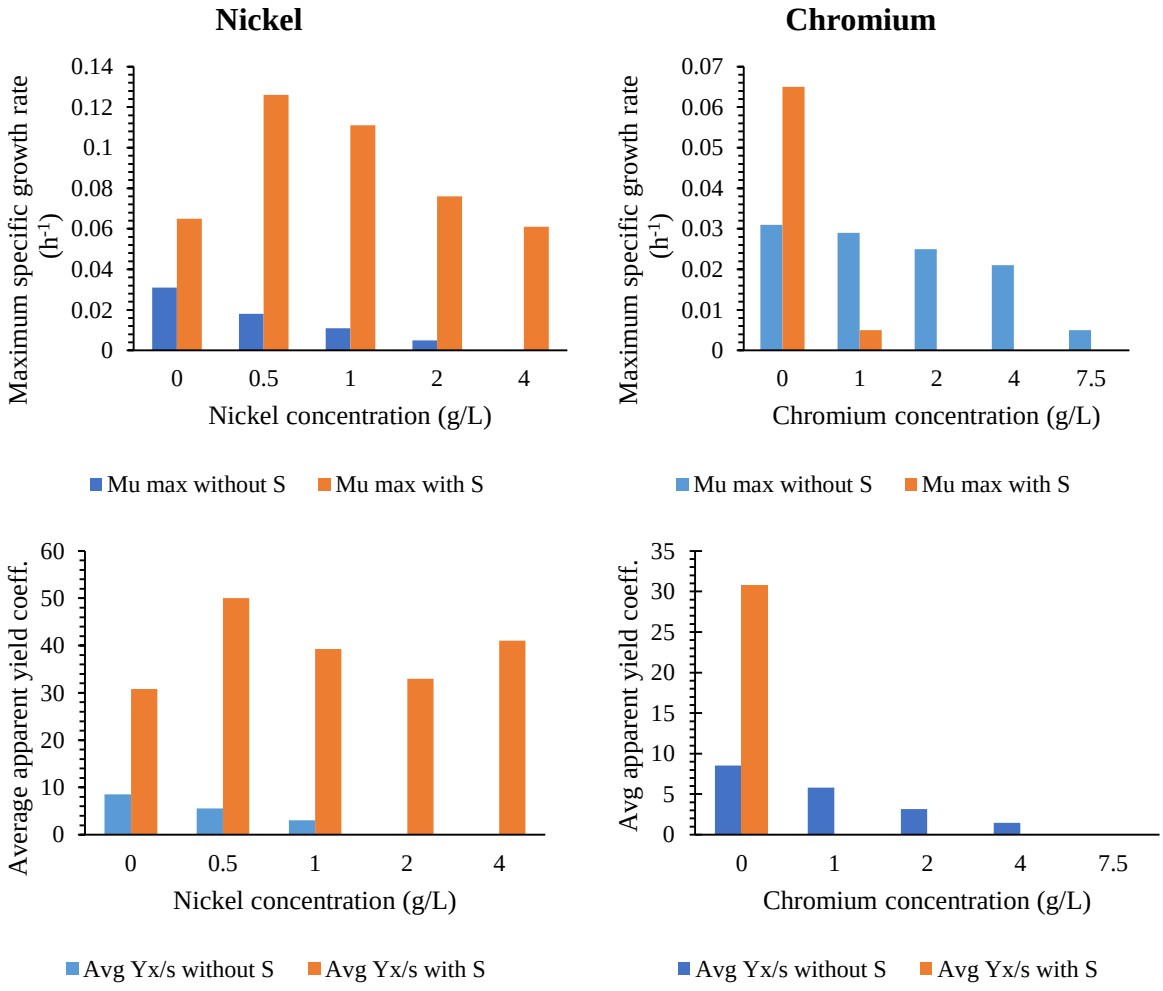

Figure 6.7: Comparison of maximum specific growth rate and average yield coefficient for tests with and without sulfur using the BRGM-KCC culture at 35°C

6.2.3 Redox potential and pH

In Figure 6.6 and Figure 6.9, the change in pH over time is seen in the presence of increasing nickel concentrations. Interestingly, the pH is seen to continuously increase for all test cases, similarly to tests where sulfur is not present. The highest increase is seen when 0 g/L of nickel is added, despite the fact that sulfur is present and thus acid-producing sulfur oxidation is occurring. This shows that at the conditions in this small scale, the extent of iron oxidation (with acid consumption) is potentially higher than the sulfur oxidation occurring (with acid production) (Chandra and Gerson, 2010). It should be noted, however, that the form of sulfur used (elemental sulfur) amongst other factors may attribute to this, and in the presence of a sulfidic mineral like pyrite the results may be different.

Similarly to the pH, redox potential for the nickel tests is seen to increase at all concentrations of nickel, again with 0 g/L seeing the greatest increase. Highs of 537 mV (Ag/AgCl reference) are reached. This is not considered particularly high for strong iron oxidisers which, as mentioned in Chapter 5, are able to reach highs of above 645 mV (Ahmadi et al., 2015). Thus, it is possible that there are weak iron oxidisers which are also present and/or strong iron oxidisers are present in low numbers. At 4 g/L of nickel, the redox potential has the lowest increase. This corresponds to iron oxidation data which shows the lowest rate of iron oxidation at this concentration.

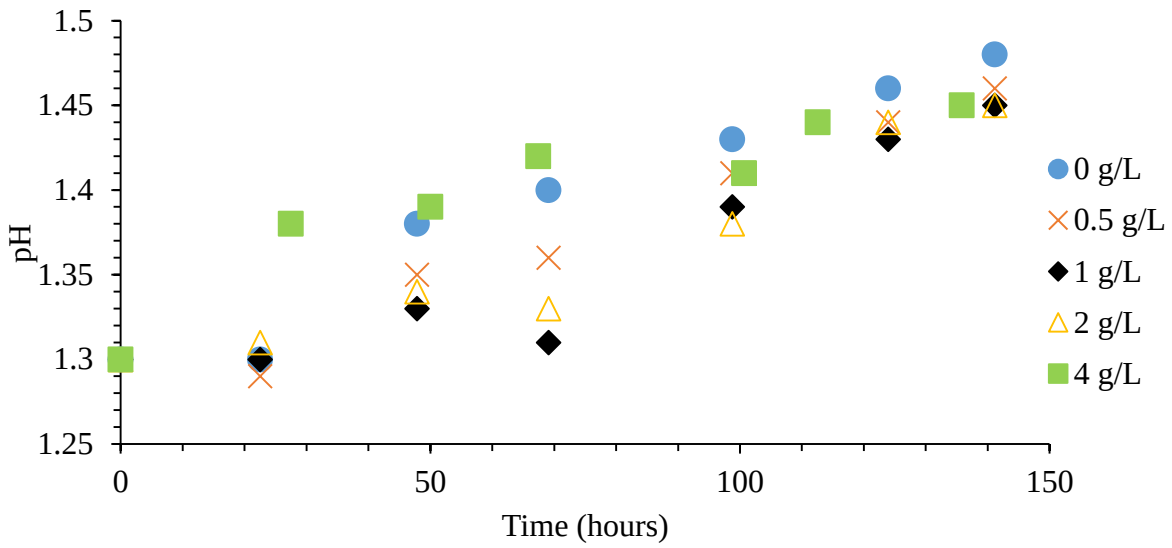

Figure 6.8: Change in pH over time for different Ni^{2+} concentrations using the BRGM-KCC culture in media containing sulfur

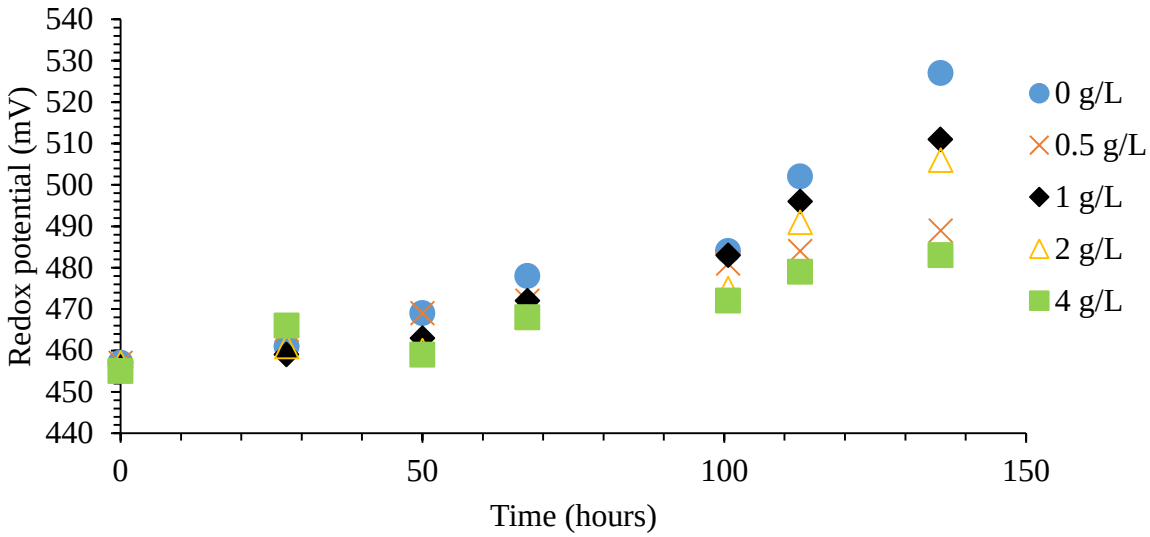

Figure 6.9: Change in redox potential over time for different Ni^{2+} concentrations using the BRGM-KCC culture in media containing sulfur

Considering Figure 6.10, pH profiles for the chromium tests, it is seen that the pH greatly increases in the presence of any amount of chromium, with a high of 2.57 reached in 7.5 g/L of chromium. Since minimal iron oxidation is taking place one would think the pH would not increase at this level. However, it is likely that a precipitate has formed (as mentioned in Section 6.2.1), which results in the high pH values. It is noted that the precipitate formation was not validated in this study.

Figure 6.11 shows the change in redox potential for the chromium tests. Unlike with the nickel tests, the redox potential is seen to decrease at a concentration of 2 g/L and above. Generally, if it was a case where oxidation was just inhibited, then the redox potential would likely remain constant. However, with the decrease, it indicates that a reductive reaction was taking place involving the iron ions in solution (as redox potential is a function of the Fe^{3+}/Fe^{2+} ratio), and this further corroborates the formation of a precipitate (Yue et al., 2014).

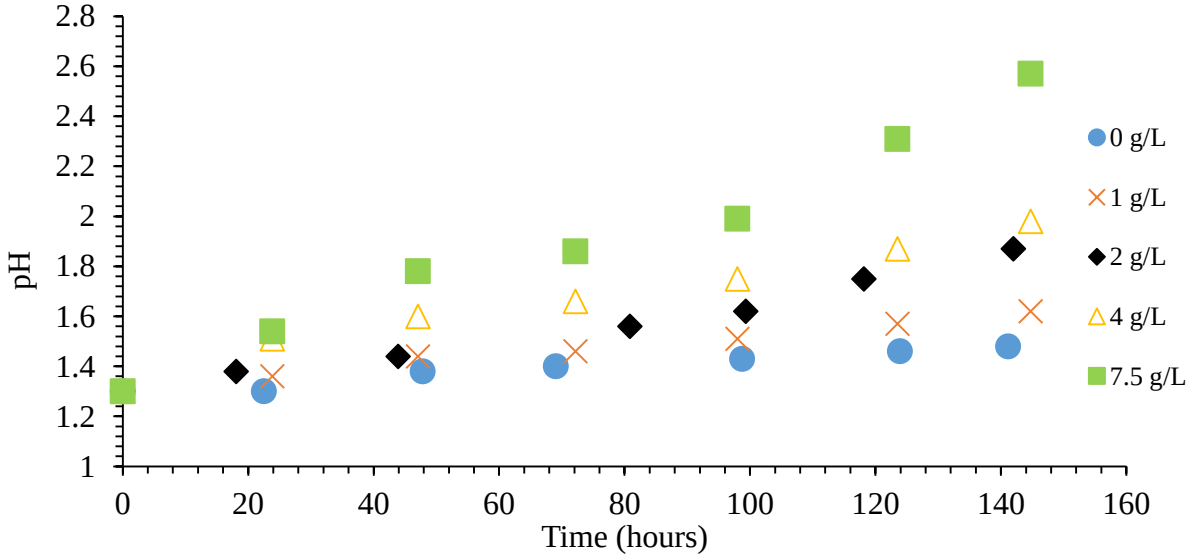

Figure 6.10: Change in pH over time for different Cr^{3+} concentrations using the BRGM-KCC culture in media containing sulfur

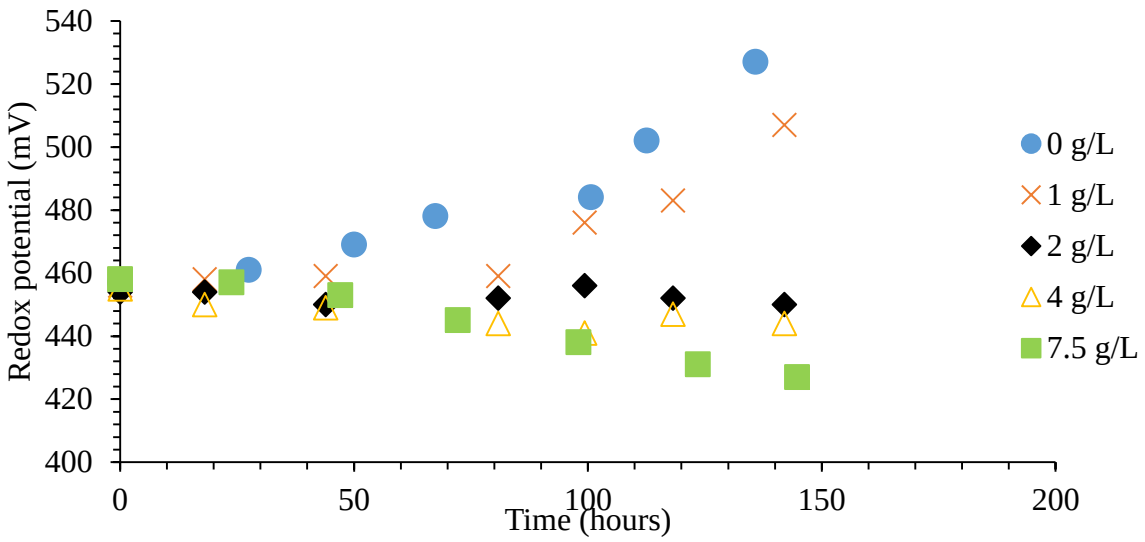

Figure 6.11: Change in redox potential over time for different Cr^{3+} concentrations using the BRGM-KCC culture in media containing sulfur

6.2.4 Microbial speciation

Figure 6.12 shows the species abundance of the BRGM-KCC community for nickel and chromium tests where the inoculum and end community composition can be seen. Similarly to the information shown in Chapter 5, this section refers to both relative abundance and cell numbers. It is important to once again note that there is a difference. While the cell numbers may decrease, it is possible that the abundance increases as a larger decrease is seen in other species and vice versa. Thus, these two values are discussed together for a more all-encompassing discussion.

The inoculum used consisted largely of *L. ferriphilum*, with smaller proportions of *Fp. acidiphilum* and *At. caldus.* A major proportion of the inoculum is seen to be unidentified bacteria and a small proportion unidentified archaea. An example of a potential microbe that could represent the unidentified bacteria fraction would be *Sulfobacillus thermosulfidooxidans*. This moderately thermophilic sulfur oxidiser is able to operate near the temperature used in the MWP tests (35°C) and could therefore potentially represent a portion of the unidentified bacteria (Vardanyan et al., 2019). However, it was not possible to look for this organism due to project constraints, although qPCR probes do exist.

Considering that when no metal inhibitor is present and the nickel tests, it is seen that there is no substantial change in the microbial composition at the end of the testing period. The abundance changes that do occur consist generally of an increase in *At. caldus*, a decrease in *L. ferriphilum*, an increase in *Fp. acidiphilum* and a decrease in the unidentified microorganisms, all to differing extents depending on the nickel concentration. It is noted that while the abundance of *L. ferriphilum* decreases, its numbers still increase from the inoculum size at all nickel concentrations except 4 g/L where a decrease of 0.29 x 10^7 cells/mL from 1.31 x 10^7 cells/mL occurs as seen in Figure 6.13. This indicates that while *L. ferriphilum* shows positive growth, there is a higher rate of growth for *Fp. acidiphilum*, and *At. caldus* in particular. This is expected as there is sulfur in the media and it is likely that a large portion of sulfur oxidation that is occurring can be attributed to this microbe. In the system, *L. ferriphilum* and *Fp. acidiphilum* are the main known iron-oxidising microorganisms present. *Fp. acidiphilum* is able to increase to similar levels as that of *L. ferriphilum*. Possible reasons for this include *Fp. acidiphilum* being more tolerant to nickel in the experimental conditions or that *Fp. acidiphilum* is potentially able to utilise cellular exudates and detritus for growth unlike *L. ferriphilum*, a chemolithotroph microorganism sensitive to organic acids produced (Golyshina, 2014; Pivovarova et al., 2002; Vardanyan et al., 2019). Therefore, their numbers are expected to increase with an increasing number of obligate lithotrophs. Often, *Fp. acidiphilum* are seen at their highest numbers in terminal reactors in industrial continuous stirred tank reactors (Smart et al., 2017b).

In contrast to the nickel tests, the addition of chromium changes the composition of the consortium substantially as seen in Figure 6.12. At 1 g/L of chromium, the composition consists mainly of *At. caldus* > *Fp. acidiphilum* > *Sb. benefaciens* > *L. ferriphilum* in order of highest to lowest abundance. All microorganisms also see an increase in cell number at this concentration, apart from *L. ferriphilum* which decreases by 7.17 x 10^7 g/L as seen in Figure 6.13. This may indicate that even at the lowest concentrations, in the presence of sulfur, *L. ferriphilum* is severely inhibited by chromium, demonstrated by growth inhibition, elongation of the lag phase and hindrance of oxygen uptake (Igiri et al., 2018).

At concentrations above 1 g/L, *Sb. benefaciens* becomes the most abundant microorganism and an increase in its cell density is seen for every concentration, even at 7.5 g/L of chromium where a substantial increase of 4.38 x 10^6 cells/mL is seen. Its increase in the presence of chromium is also seen in tests where sulfur is not present, but at a lower rate. This increase is expected as the microorganism is a faculative and is able to utilise both sulfur and iron in a system. The presence of *Ap. cupricumulans*, Archaea JTC1/2, and unidentified archaea and bacteria are also seen to appear in Figure 6.12. *Ap. cupricumulans* and Archaea JTC1/2 increase in terms of relative abundance and cell density indicating they may be able to tolerate chromium. The increasing presence of *Ap. cupricumulans* (a weak iron oxidiser) at higher chromium concentrations coupled with the decreasing numbers of *L. ferriphilum* (a strong iron oxidiser) could have caused the lower iron oxidation and redox potential seen in higher chromium concentration tests (Edward et al., 2022; Golyshina, 2014; Smart et al., 2017a; Vardanyan et al., 2019).

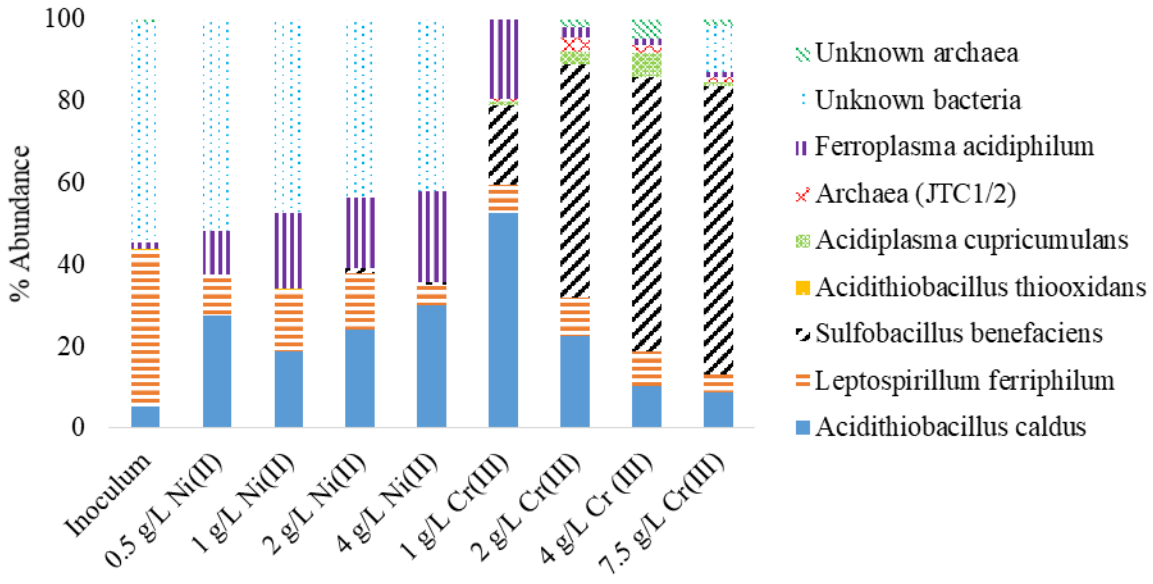

Figure 6.12: Graphical representation of the percentage species abundance of the BRGM-KCC culture exposed to different concentrations of Ni^{3+} and Cr^{3+} in media containing sulfur

6.3 Integrated results and discussion

Heat maps showing the growth of each microbial species as well as calculated oxidation rates can be seen in Table 6.2. The tables have been split into iron oxidisers and sulfur oxidisers, with iron oxidation data shown for the iron-oxidising microorganisms. Figure 6.13 provides a key for the heat map. Values nearest to the initial inoculum size of each microorganism are shown as a yellowish hue, values that have shown a decrease in numbers are shown as a reddish hue, and values where the numbers have increased are shown as a greenish hue. This scaling is done relative to each microorganism's inoculum and other differing concentrations. Hence, in cases where multiple values are above the inoculum cell density, a greener hue will appear for the values which show a larger extent of growth. All values besides the inoculum are obtained from the end of the experimentation period.

Table 6.2 once again clearly indicates that in the test conditions, chromium is generally more toxic to the microorganisms. This is apparent due to the reddish hue that can be seen for most microorganisms. Considering the total number of iron oxidisers for different nickel concentrations, at all concentrations an increase in the cell number can be seen in Table 6.2. This is not the case for the chromium tests which only sees a slight increase of 0.98×10^7 cells/mL. Hence, it is once again seen that in MWP tests in the presence of sulfur, most iron oxidisers are more inhibited by chromium than nickel. However, *Ap. cupricumulans* does seem to be an exception. While an increase in this microbe is seen in both tests, its cell numbers increase more in the presence of chromium.

This could potentially be because there is less competition in the chromium tests and *Ap. cupricumulans* is able to feed on more dead cells. Alternatively, this may indicate it is more inhibited by nickel. The increased numbers of *Ap. cupricumulans* may be a reason that the redox potential remains relatively low since *Ap. cupricumulans* is considered a weaker iron oxidiser in comparison to other microorganisms such as *L. ferriphilum* (Smart et al., 2017a). Alternatively, the low redox potentials could be as a result of the low overall iron-oxidiser cell density.

Similarly to the iron oxidisers in nickel solution, the sulfur oxidisers seem to be able to withstand the increasing concentrations, with the total growth increasing at all concentrations where the information is available. It is noted that some information is missing where qPCR yielded poor results. This is likely due to the low copy numbers in the samples. Thus, total sulfur oxidiser cell numbers are unable to be obtained. Considering the relative abundance of archaeon JTC1/2 in Figure 6.12, it is generally seen to be at low levels in comparison to other microbes. The relative abundance of the archaeon can increase slightly in the chromium tests. In Table 6.2, while there is an increase in the cell numbers of this archaeon at all concentrations for both nickel and chromium tests (but especially in the presence of chromium), the numbers are still low in comparison to other microorganisms. Additionally, it is seen that the numbers are greater in the presence of chromium compared to nickel indicating that it may be more tolerant to chromium. This could also be as a result of the fact that other microbes are more inhibited by chromium and JTC1/2, which is less affected by the chromium, is able to capitalize on nutrients and energy source becoming more available.

As a whole, the iron oxidiser which shows the highest level of growth for all concentrations in the nickel tests is *Fp. acidiphilum* with a maximum growth of 9.84 x 10^7 cells/mL at 1 g/L. At 1 g/L of chromium, this is also found with the archaeon outperforming other microorganisms. However, thereafter, *Ap. cupricumulans* becomes the microorganism with the largest growth in numbers. The trend of *Fp. acidiphilum* exhibiting more growth is also seen in tests described in Chapter 5 (nickel tests 1 g/L and above, and all chromium tests). This indicates the resilience of the species to both nickel and chromium in a variety of test conditions. Its wide temperature and pH operating range (15 - 45°C and 1.3 – 2.2) allow it to be able to thrive in numerous environments, and the conditions of the experiment sit well within the operating range (Golyshina et al., 2000). Interestingly, studies such as that described in Pivovarova et al. (2002) mention the need for yeast extract as a growth factor. However, in this study, *Fp. acidiphilum* was able to grow without its presence. This may further allude to the robustness of *Fp. acidiphilum* which seems to be able to grow in many conditions. It is also noted that the presence of archaea in acidophilic, low to moderate temperature environments has seen a rise in industrial mineral biooxidation plants (Smart et al., 2017b). This may be explained by the robustness of certain archaea and its ability to utilise the waste produced by other microbes as energy.

For the sulfur oxidisers, the microorganism showing the largest growth in numbers is *At. caldus* for all nickel concentrations and chromium concentrations up until 1 g/L. Above this, *Sb. benefaciens* shows the strongest growth. Bryan et al. (2011) mentions competition between these two sulfur oxidisers, where the growth of one is linked to the decrease in the other. This is seen to an extent in Figure 6.12 where the nickel tests have a higher relative abundance and cell numbers of *At. caldus*, but at higher concentrations of chromium, the opposite is seen. This may indicate that in the experimental conditions with no added metal, with multiple concentrations of nickel and with low concentrations of chromium, *At. caldus* is able to outcompete *Sb. benefaciens*. However, once *At. caldus* becomes inhibited by chromium, *Sb. benefaciens* which is more tolerant to the metal, is able to thrive.

It should be noted that elemental sulfur has a low solubility (Franzmann et al. 2005); this may limit access to sulfur in solution for planktonic bacteria and archaea which affects growth and sulfur oxidation.

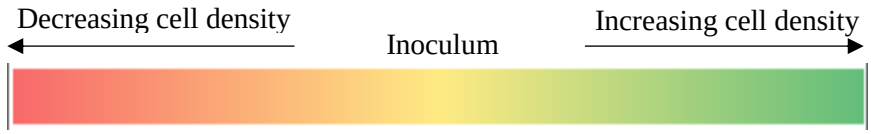

Figure 6.13: Heat map key showing cell density; yellows represent cell density values near the inoculum, red represents decreasing cell density, and green represents increasing cell density

*Table 6.2: Species-specific growth heat map and oxidation data for BRGM-KCC culture in media containing sulfur**

Microbes	**Inoculum (cell/mL)**	**Growth (cells/mL)**								
		Dominant iron oxidisers								
			Nickel				**Chromium**			
		0 g/L	0.5 g/L	1 g/L	2 g/L	4 g/L	1 g/L	2 g/L	4 g/L	7.5 g/L
Leptospirillum ferriphilum	1.31E+07	6.43E+07	2.69E+07	8.01E+07	4.83E+07	1.02E+07	5.93E+06	2.51E+06	9.09E+05	2.87E+05
Acidiplasma cupricumulans	1.21E+03	1.45E+04	1.52E+04	1.92E+04	1.89E+04	1.07E+04	9.11E+05	8.44E+05	6.54E+05	6.87E+04
Ferroplasma acidiphilum	6.07E+05	8.20E+07	2.83E+07	9.90E+07	6.21E+07	4.40E+07	1.67E+07	6.59E+05	1.69E+05	8.69E+04
Total	**1.38E+07**	**1.46E+08**	**5.52E+07**	**1.79E+08**	**1.10E+08**	**5.43E+07**	**2.36E+07**	**4.01E+06**	**1.73E+06**	**4.43E+05**
Iron Oxidation rate (g/L/h)		**0.146 ± 0.063**	**0.074 ± 0.027**	**0.095 ± 0.035**	**0.068 ± 0.035**	**0.058 ± 0.007**	**0.035 ± 0.012**	**0.016 ± 0.013**	**0.007 ± 0.004**	**0.003 ± 0.001**
		Dominant sulfur oxidisers								
Sulfobacillus benefaciens[a]	1.83E+04	1.77E+07	1.79E+05	4.41E+05	4.32E+06	1.13E+06	1.66E+07	1.51E+07	7.34E+06	4.40E+06
Acidithiobacillus caldus	1.86E+06	7.06E+07	7.39E+07	9.99E+07	8.64E+07	6.01E+07	4.53E+07	5.98E+06	1.13E+06	5.43E+05
Acidithiobacillus thiooxidans	2.06E+04	1.89E+05	2.72E+05	3.57E+05		2.06E+05				
Total	**1.90E+06**	**8.85E+07**	**7.43E+07**	**1.01E+08**		**6.14E+07**				
		Unknown								
Archaea (JTC1/2)	1.87E+03	3.77E+04	2.15E+04	3.57E+04	3.26E+04	1.61E+04	5.06E+05	9.22E+05	2.26E+05	6.90E+04

**Growth values represented (besides the inoculum) are from the end of the experiment; grey blocks represent values where qPCR errors occurred.*

[a]Sulfobacillus benefaciens is both a sulfur and iron-oxidising bacterium. It has been placed in the sulfur oxidiser section as it is considered a weak iron oxidiser (Johnson et al., 2008).

6.4 Conclusions

In this chapter, MWP tests were performed in media containing tyndallised elemental sulfur using the BRGM-KCC culture. These tests were done to determine the MTCs of nickel and chromium when both iron and sulfur oxidisers were catered to, and to determine the effects of these metals on the community as a whole as well as the effects on individual members within the community. Results indicate that the MTC value for nickel is > 4 g/L and the MTC value for chromium is < 2 g/L. This differs from the tests where no sulfur was added with the nickel MTC being 4 g/L and the chromium MTC being 7.5 g/L. At all nickel concentrations, microbial growth and iron oxidation occurred indicating that the culture as a whole was able to withstand nickel at even the highest tested concentration. In contrast, growth and iron oxidation ceased above 1 g/L chromium, indicating severe inhibition due to chromium.

Interestingly, it is seen that when sulfur is present, chromium is more toxic to the culture than nickel, but when sulfur is absent, the opposite is seen. This difference illustrates the substantial effect the components in a bioleaching system can make to the microorganisms and their performance, and highlights the importance in understanding the material being leached and how different components can affect critical microorganisms in a system.

It is important to note the limitations of small scale batch MWP studies such as those described in this chapter as well as Chapters 5. These batch, small scale tests are more sensitive to small variations in factors such as inoculum microbial composition. Hence, in the next chapter, a larger scale, semi-continuous experiment is described where more information on the effects of nickel and chromium on the BRGM-KCC culture can be seen.

Chapter 7: Semi-continuous bioreactor study

7.1 Introduction

In this chapter, the results of a study of a set of semi-continuous reactors lasting over a period of 5 months are presented and discussed. Similarly to Chapters 5 and 6, the experiment explored the microbial metal tolerance of the BRGM-KCC microbial consortium. Here, this was done in the presence of a pyritic tailings mineral, and no other iron or sulfur source was added. This experiment was performed in 1 L glass bioreactors and a semi-continuous draw-and-fill setup was used. The analysis done includes the iron oxidation and dissolution from the tailings material, microbial growth, redox potential, pH, and microbial speciation. Four test conditions were considered: a control with no added metal, a nickel experiment (0 – 24 g Ni^{2+}/L), a chromium experiment (0 – 6 g Cr^{3+}/L) and a mixed metal experiment (0 – 18 g Ni^{2+}/L and 0 – 0.6 g Cr^{3+}/L). In each experiment with metals, the metal concentrations in each bioreactor were increased after a minimum of 3 weeks, depending on the performance of the microorganisms.

This chapter explores the effect of continuous exposure to increasing concentrations of nickel and chromium on the bioleaching microorganisms, and determines whether they adapt to the metals over time.

7.2 Results and Discussion

7.2.1 Microbial iron oxidation and pyrite dissolution

In Figure 7.1, the ferrous iron concentration over the course of the experiment is shown. The nickel reactor will be represented by the code, Ni-R, the chromium reactor will be represented by the code, Cr-R, and the mixed reactor containing both nickel and chromium will be represented by the code, Mixed-R. Note that the vertical lines represent periods when the nickel and chromium concentrations were increased. The red lines denote increases in all reactors besides the control while the blue lines denote increases in only the nickel reactor and mixed reactor. This was done to allow additional time for the culture in Cr-R to adjust to the conditions as the culture did not perform well with increasing concentrations of chromium. The concentrations in the seven segments shown in Figure 7. are given in Table 7.. The concentrations in the mixed reactor are based on nickel and chromium concentrations within PCBs. Multiple literature sources were used to obtain average values of nickel and chromium, and a ratio of 1:0.03 nickel to chromium was obtained. Each set of nickel and chromium concentrations in the mixed reactor were then based on different PCB solid loadings (10, 40, 60, 100, 200, 400 and 500 w/v% PCBs). More detail is provided in Chapter 4. It is also noted that the small spikes in concentrations are a result of the draw-and-fill technique used where feedings cause dilution of the iron.

Table 7.1: Tested concentrations of metals in Ni-R, Cr-R and Mixed-R

Weeks	Nickel concentration in Ni-R (g/L)	Chromium concentration in Cr-R (g/L)	Mixed concentration in Mixed-R	
			Nickel (g/L)	Chromium (g/L)
1 – 3	0.5	1	0.36	0.01
4 – 6	1	2	1.43	0.05
7 - 9	2	4	2.14	0.07
10 – 12	3	4	3.57	0.12
13 – 15	6	4	7.14	0.23
16 – 18	12	4	14.28	0.46
19 - 22	24	6	17.84	0.59

In Figure 7.1, the ferrous iron concentration is seen to increase to approximately 4.3 g/L initially at approximately Day 3, but quickly settles to about 0.250 g/L by Day 6. This initial spike is on introduction of fresh mineral tailings, establishment of the active microbial culture and when the system was stabilizing to the dilution rate of the experiment. The ferrous iron concentration in the control, Ni-R and Mixed-R was maintained around 0.25 g/L for the remainder of the experiment. However, further spikes in the Fe^{2+} concentration were observed in Cr-R. At the 54 day mark, after the concentration in Cr-R was increased to 4 g/L, the ferrous iron concentration increased to a maximum of 1.627 g/L in Cr-R. This is likely due to the iron oxidisers in the reactor experiencing adverse effects of an increased chromium concentration with reduced Fe^{2+} oxidation rates in the elevated concentration for about 12 days. The dissolution of pyrite produces ferrous iron (Equation 7.1) (Schippers and Sand, 1999; Vera et al., 2022):

$$FeS_2 + 6Fe^{3+} + 3H_2O \rightarrow {S_2O_3}^{2-} + 7Fe^{2+} + 6H^+ \quad (7.1)$$

The ferrous iron is subsequently oxidised to ferric iron by iron-oxidising microorganisms in Equation 7.2:

$$2Fe^{2+} + \frac{1}{2}O_2 + 2H^+ \rightarrow 2Fe^{3+} + H_2O \quad (7.2)$$

Thus, when there are spikes of ferrous iron, the iron oxidisers are likely under stress and are not oxidising the ferrous iron faster than it is reduced at the mineral surface. This, in turn, reduces the ferric iron concentration in the system and reduces the dissolution of pyrite.

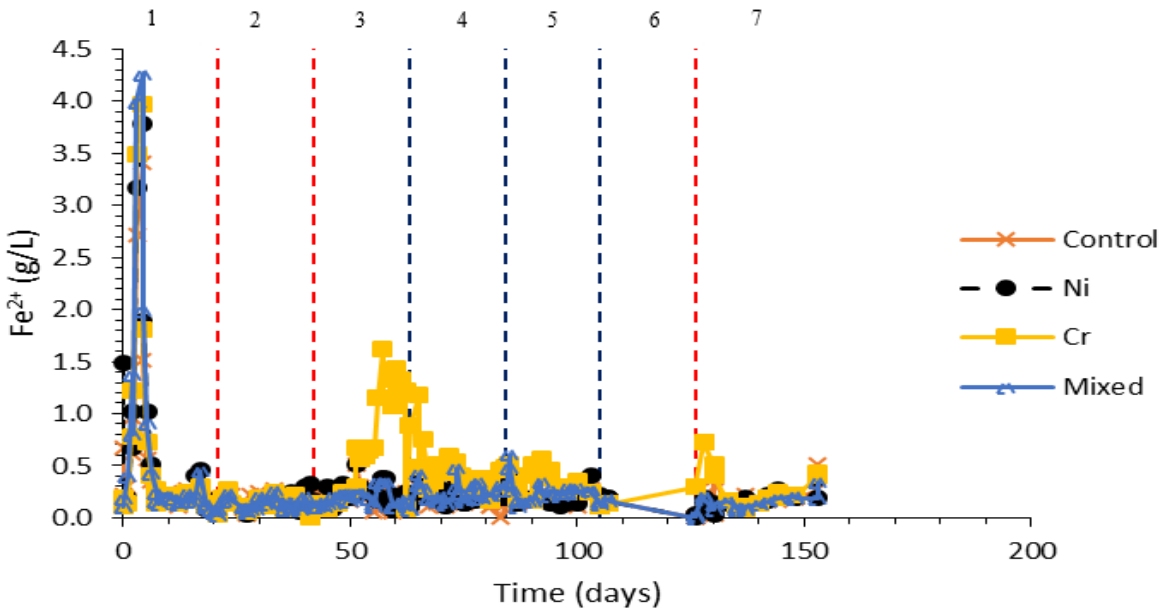

Figure 7.1: Ferrous iron concentrations over the period of the experiment. Vertical lines represent where metal (nickel & chromium) concentrations were increased. Red lines indicate where metal concentration increased in all non-control bioreactors; Blue lines indicate where metal concentration increased in all bioreactors except the chromium bioreactor and the control. Numbers on top represent the following concentrations in each reactor: (1) 0.5 g/L in Ni-R, 1 g/L in Cr-R, 0.36 g Ni^{2+}/L & 0.01 g Cr^{3+}/L in Mixed-R. (2) 1 g/L in Ni-R, 2 g/L in Cr-R, 1.43 g Ni^{2+}/L & 0.05 g Cr^{3+}/L in Mixed-R. (3) 2 g/L in Ni-R, 4 g/L in Cr-R, 2.14 g Ni^{2+}/L & 0.07 g Cr^{3+}/L in Mixed-R. (4) 3 g/L in Ni-R, 4 g/L in Cr-R, 3.57 g Ni^{2+}/L & 0.12 g Cr^{3+}/L in Mixed-R. (5) 6 g/L in Ni-R, 4 g/L in Cr-R, 7.14 g Ni^{2+}/L & 0.23 g Cr^{3+}/L in Mixed-R. (6) 12 g/L in Ni-R, 4 g/L in Cr-R, 14.28 g Ni^{2+}/L & 0.46 g Cr^{3+}/L in Mixed-R. (7) 24 g/L in Ni-R, 6 g/L in Cr-R, 17.84 g Ni^{2+}/L & 0.59 g Cr^{3+}/L in Mixed-R

This stress response is also seen in Figure 7.2 which shows the total iron concentration over the course of the experiment. At around the 54 day mark, the total iron concentration begins to decrease to a value near zero, indicating that the iron in solution is very low in Cr-R and thus minimal dissolution of the pyrite is occurring. The clear struggle of the microorganisms in Cr-R to handle a chromium concentration of 4 g/L is also seen when considering microbial growth and other parameters, discussed in later sections. Cr-R was maintained at 4 g/L chromium for an additional 9 weeks, to determine whether the microorganisms in the reactor would acclimatise to the chromium and return to the original oxidation levels given sufficient time.

Interestingly, it can be seen in Figure 7.1 that at about 67 days into the experiment, the ferrous iron level in Cr-R drops to just above the same level as it was at originally before the concentration was changed to 4 g/L. However, the total iron concentration remains low (Figure 7.2). Hence, the decrease in ferrous iron concentration is attributed to a decrease in pyrite dissolution and not that the iron oxidisers have started to once again oxidise iron efficiently. Therefore, it can be said that in terms of iron oxidation, the microorganisms in the BRGM-KCC community are likely unable to maintain iron oxidation at chromium concentrations of 4 g/L and above.

Considering the control where no extra metal is added, Ni-R and Mixed-R, it is seen in Figure 7.1 and Figure 7.2 that their ferrous and total iron concentrations remain relatively unchanged for most of the experiment, with a slight change starting to occur at around 126 days. At this point, Ni-R and Mixed-R begin to show a decrease in the total iron concentration, indicating reduced leaching, potentially due to the elevated metal concentrations. Since there is no similar decrease in the control culture, the decrease can be attributed to inhibitory effects of the metals. Despite this difference, the cultures in these reactors are still seen to oxidise iron, indicating that the culture can tolerate nickel concentrations, up to the 24 g/L tested. This is in line with literature where similar microorganisms were used and concentrations up to 30 g/L were tolerated (Cabrera et al., 2005).

As mentioned, in Mixed-R there is a combination of nickel and chromium, based on the concentrations of these components in PCBs. The oxidation behaviour in this reactor is similar to that of Ni-R, with only slight variations seen. This indicates that the overall oxidation interaction between nickel and chromium in the reactor at concentrations seen in PCBs is potentially negligible. However, the additional metals found within PCBs could alter the microbial interaction with nickel and chromium. As seen in previous chapters, the addition or removal of a single component from a bioleaching system can play a large role in how the microorganisms react and perform.

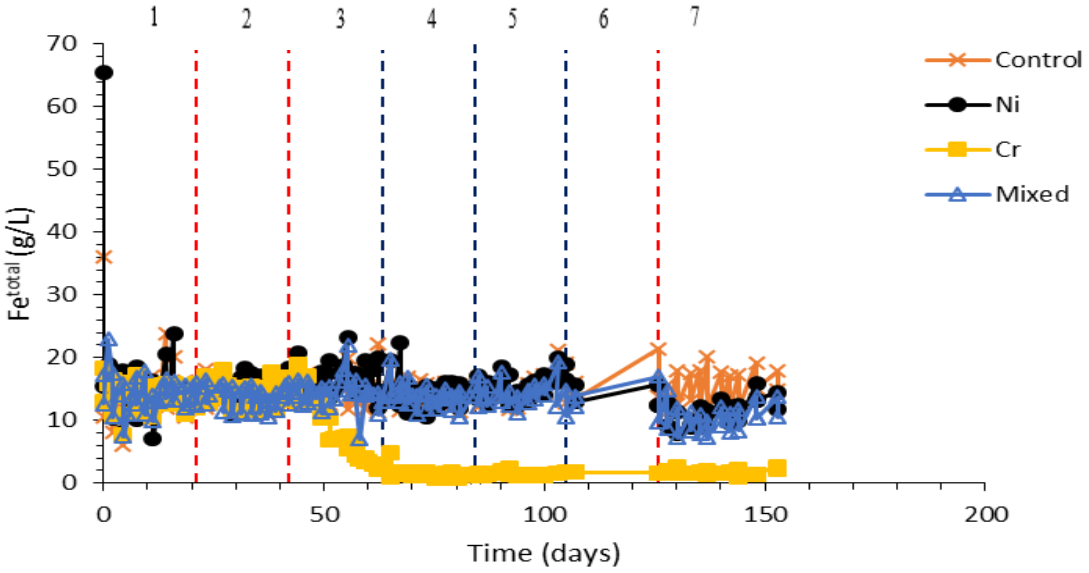

Figure 7.2: Total iron concentrations over the period of the experiment. Vertical lines represent where metal (nickel & chromium) concentrations were increased. Red lines indicate where metal concentration increased in all non-control bioreactors; Blue lines indicate where metal concentration increased in all bioreactors except the chromium bioreactor and the control. Numbers on top represent the following concentrations in each reactor: (1) 0.5 g/L in Ni-R, 1 g/L in Cr-R, 0.36 g Ni^{2+}/L & 0.01 g Cr^{3+}/L in Mixed-R. (2) 1 g/L in Ni-R, 2 g/L in Cr-R, 1.43 g Ni^{2+}/L & 0.05 g Cr^{3+}/L in Mixed-R. (3) 2 g/L in Ni-R, 4 g/L in Cr-R, 2.14 g Ni^{2+}/L & 0.07 g Cr^{3+}/L in Mixed-R. (4) 3 g/L in Ni-R, 4 g/L in Cr-R, 3.57 g Ni^{2+}/L & 0.12 g Cr^{3+}/L in Mixed-R. (5) 6 g/L in Ni-R, 4 g/L in Cr-R, 7.14 g Ni^{2+}/L & 0.23 g Cr^{3+}/L in Mixed-R. (6) 12 g/L in Ni-R, 4 g/L in Cr-R, 14.28 g Ni^{2+}/L & 0.46 g Cr^{3+}/L in Mixed-R. (7) 24 g/L in Ni-R, 6 g/L in Cr-R, 17.84 g Ni^{2+}/L & 0.59 g Cr^{3+}/L in Mixed-R

In Figure 7.3, the average iron dissolution rate is seen. While there is variation seen across the period of the experiment, it is seen that some time into the experiment at about Day 40, the average iron dissolution rates for all the reactors except Cr-R remain in the range of about 0.02 to 0.01 $g.L^{-1}.h^{-1}$. Cr-R at Day 40 is seen to diverge from the rest of the reactors, with a decrease to a value near zero. This, again, indicates that at 4 g/L of chromium, the BRGM-KCC culture is unable to sustain iron oxidation and thus essentially no dissolution of pyrite occurs. At Day 125, Ni-R and Mixed-R remain at a similar average iron dissolution rate, but the control reactor experiences a slight increase. The deviation of Ni-R and Mixed-R from the control is potentially due to the cultures within these reactors beginning to experience the adverse effects of the metal inhibitors, but not to the extent where the iron dissolution rate is heavily impacted.

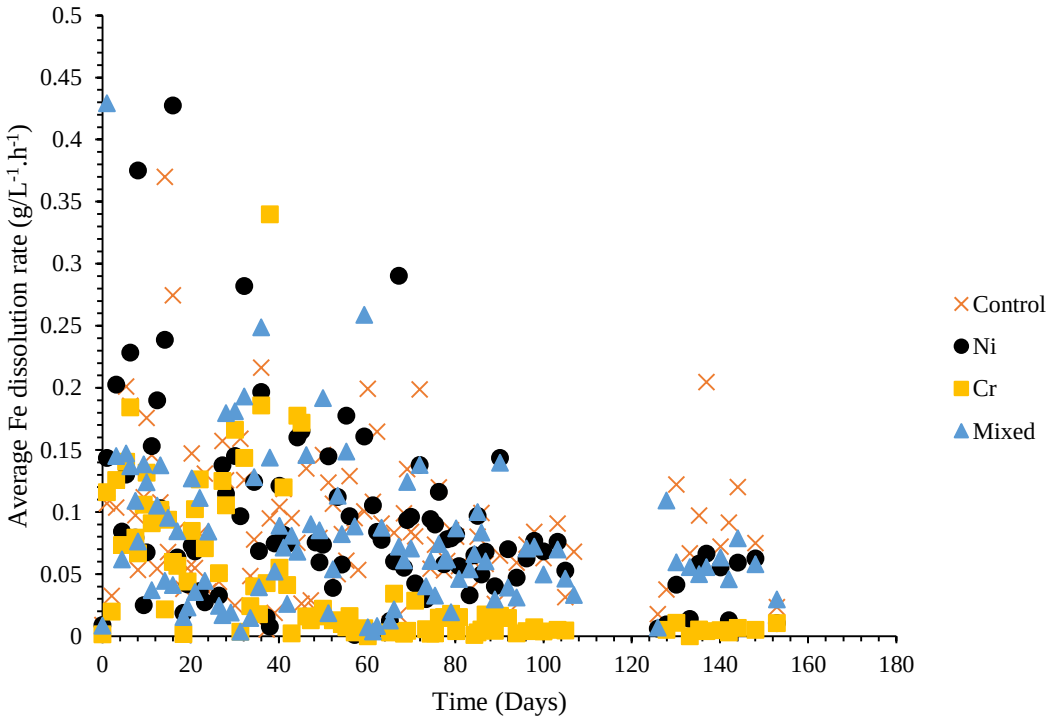

Figure 7.3: Total iron dissolution rate over the period of the experiment.

7.2.2 Microbial growth

In Figure 7.4, the total cell numbers in each reactor over the course of the experiment are seen. From Day 10 (where the numbers have all stabilized) to Day 41 where the metal concentration is increased for the 2nd time, the numbers remain similar. Thereafter, the cell density for Cr-R decreases, further demonstrating inhibition of the BRGM-KCC community at chromium concentrations of 4 g/L and above. The decrease is seen to continue until Day 70 where it begins to increase for a short period of time. During this time, the community may be acclimating to the excess chromium. Soon after this increase, the cell number in Cr-R began to fall again, along with the cell numbers in all the other reactors. As mentioned in Section 7.2.1, this decrease seen in all reactors has been attributed to technical issues related to O_2 availability. Once these issues were resolved, the numbers in Cr-R increased and a new constant at around 3.75 x 10^8 cell/mL was reached. At this point, the concentration of chromium was increased to 6 g/L which resulted in the cell density decreasing again.

Considering Ni-R and Mixed-R, the numbers are seen to remain relatively similar to the control reactor's numbers throughout the course of the experiment. Only after the final concentration change is a slight deviation from the control seen, with the numbers in Ni-R and Mixed-R decreasing. A decrease is also seen in the total iron concentration (Figure 7.2), showing that a decrease in numbers collates with a decrease in the dissolution of iron into solution.

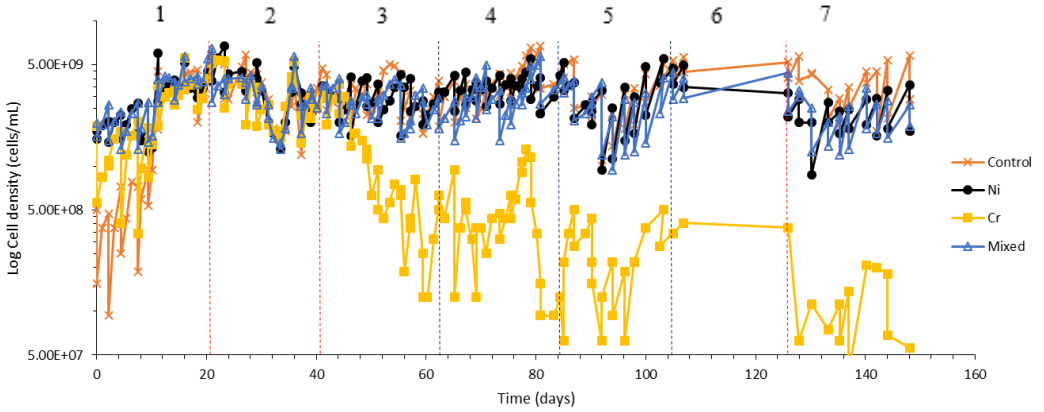

Figure 7.4: Cell density over the period of the experiment (logarithmic scale used). Vertical lines represent where metal (nickel & chromium) concentrations were increased. Red lines indicate where metal concentration increased in all non-control bioreactors; Blue lines indicate where metal concentration increased in all bioreactors except the chromium bioreactor and the control. Numbers on top represent the following concentrations in each reactor: (1) 0.5 g/L in Ni-R, 1 g/L in Cr-R, 0.36 g Ni^{2+}/L & 0.01 g Cr^{3+}/L in Mixed-R. (2) 1 g/L in Ni-R, 2 g/L in Cr-R, 1.43 g Ni^{2+}/L & 0.05 g Cr^{3+}/L in Mixed-R. (3) 2 g/L in Ni-R, 4 g/L in Cr-R, 2.14 g Ni^{2+}/L & 0.07 g Cr^{3+}/L in Mixed-R. (4) 3 g/L in Ni-R, 4 g/L in Cr-R, 3.57 g Ni^{2+}/L & 0.12 g Cr^{3+}/L in Mixed-R. (5) 6 g/L in Ni-R, 4 g/L in Cr-R, 7.14 g Ni^{2+}/L & 0.23 g Cr^{3+}/L in Mixed-R. (6) 12 g/L in Ni-R, 4 g/L in Cr-R, 14.28 g Ni^{2+}/L & 0.46 g Cr^{3+}/L in Mixed-R. (7) 24 g/L in Ni-R, 6 g/L in Cr-R, 17.84 g Ni^{2+}/L & 0.59 g Cr^{3+}/L in Mixed-R

7.2.3 Redox potential and pH

Figure 7.5 shows the change in pH over the course of the experiment. When the pH exceeded a value of 2, sulfuric acid was added to decrease the pH to a value between 1 and 1.3. For the majority of the experimental time, Ni-R, Mixed-R and the control reactors remained at a pH between 1 and 1.3, with few outliers seen. After the final increase in Ni^{2+} concentration, the pH of Ni-R and Mixed-R increased above the control pH, suggesting that, at 24 g/L of nickel in Ni-R and 17.84 and 0.59 g/L of nickel and chromium respectively in Mixed-R, some inhibition decreased the production of H^+ ions. The overall reaction for the dissolution of pyrite is (Schippers and Sand, 1999; Vera et al., 2022):

$$FeS_2 + 12Fe^{3+} + \frac{1}{2}O_2 + 7H_2O \rightarrow 2{SO_4}^{2-} + 13Fe^{2+} + 14H^+ \quad (7.3)$$

Equation 7.3 shows that acid is produced and therefore the pH decreases. Thus, with the overall increase of pH in Ni-R and Mixed-R, it suggests reduced pyrite dissolution as a result of the increased metal concentrations.

When considering the pH profile of Cr-R, the inhibitory effect of chromium is seen. At 4 g/L of chromium, the pH continues to increase. Apart from the likely inhibition of the microorganisms, the high pH levels may be a result of precipitate formation. In Chapter 6, a precipitate was reported to form at higher concentrations of chromium in the presence of sulfur. Additionally, it is known for jarosite to form at higher pH levels, causing there to be a decrease in the availability of Fe^{3+} ions (Gahan et al., 2009). This is potentially another reason that the pH is increasing, and that the dissolution of pyrite decreases as seen in Section 7.2.1 as there is less Fe^{3+} to attack pyrite grains.

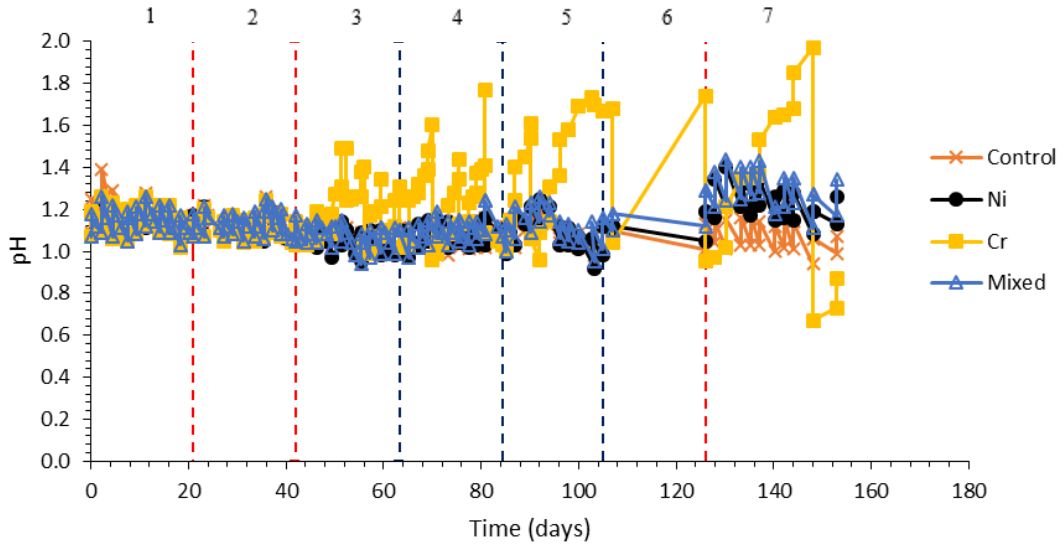

Figure 7.5: Change in pH over the course of the experiment. Vertical lines represent where metal (nickel & chromium) concentrations were increased. Changed wording: Red lines indicate where metal concentration increased in all non-control bioreactors; Blue lines indicate where metal concentration increased in all bioreactors except the chromium bioreactor and the control. Numbers on top represent the following concentrations in each reactor: (1) 0.5 g/L in Ni-R, 1 g/L in Cr-R, 0.36 g Ni^{2+}/L & 0.01 g Cr^{3+}/L in Mixed-R. (2) 1 g/L in Ni-R, 2 g/L in Cr-R, 1.43 g Ni^{2+}/L & 0.05 g Cr^{3+}/L in Mixed-R. (3) 2 g/L in Ni-R, 4 g/L in Cr-R, 2.14 g Ni^{2+}/L & 0.07 g Cr^{3+}/L in Mixed-R. (4) 3 g/L in Ni-R, 4 g/L in Cr-R, 3.57 g Ni^{2+}/L & 0.12 g Cr^{3+}/L in Mixed-R. (5) 6 g/L in Ni-R, 4 g/L in Cr-R, 7.14 g Ni^{2+}/L & 0.23 g Cr^{3+}/L in Mixed-R. (6) 12 g/L in Ni-R, 4 g/L in Cr-R, 14.28 g Ni^{2+}/L & 0.46 g Cr^{3+}/L in Mixed-R. (7) 24 g/L in Ni-R, 6 g/L in Cr-R, 17.84 g Ni^{2+}/L & 0.59 g Cr^{3+}/L in Mixed-R

In Figure 7.6, the redox potential for each reactor is plotted. The redox potential generally remains between 600 and 700 mV (Ag/AgCl) in all reactors up until about Day 46. Thereafter the concentration in Cr-R was changed to 4 g/L. This indicates the likely presence of strong iron oxidisers performing the iron oxidation and provides an ideal environment for pyrite dissolution as pyrite is better leached in high redox environments (above 645 mV) (Ahmadi et al., 2015).

After 46 days, the redox potential of Cr-R decreases to around 450 mV. This is likely due to inhibition of strong iron oxidisers, and a decrease in the Fe^{3+} concentrations as the redox potential is a function of the ferric ion concentration.

Again, a deviation of Ni-R and Mixed-R from the control is seen in the redox profile towards the end of the experiment after the final increase in metal concentration. However, this change is minimal and the redox potential in these two reactors remains in a range indicating the strong iron oxidisers are at work, though slightly below the ideal pyrite dissolution redox potential of 645 mV.

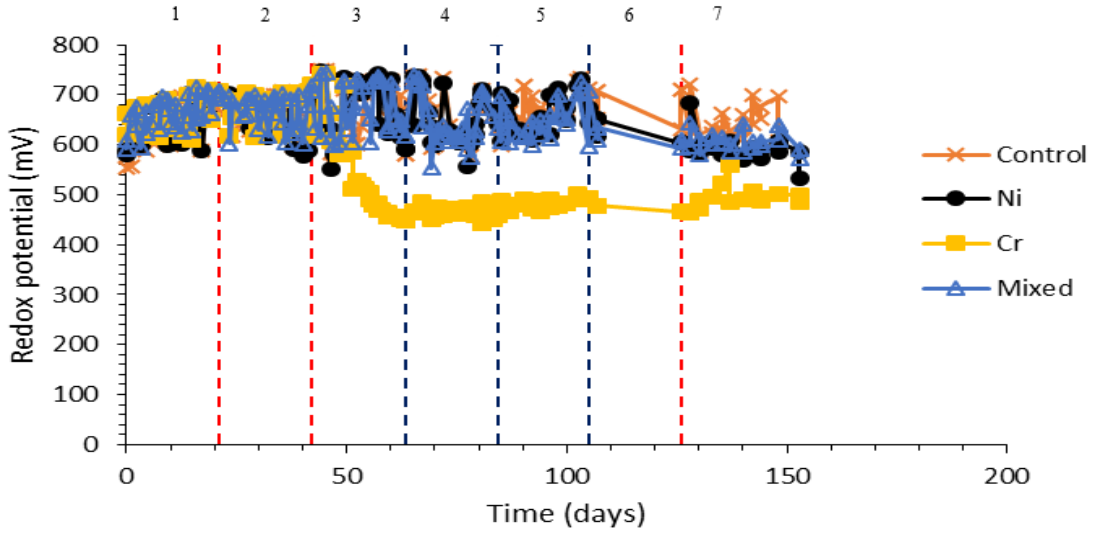

Figure 7.6: Change in redox potential over the course of the experiment. Vertical lines represent where metal (nickel & chromium) concentrations were increased. Changed wording: Red lines indicate where metal concentration increased in all non-control bioreactors; Blue lines indicate where metal concentration increased in all bioreactors except the chromium bioreactor and the control. Numbers on top represent the following concentrations in each reactor: (1) 0.5 g/L in Ni-R, 1 g/L in Cr-R, 0.36 g Ni^{2+}/L & 0.01 g Cr^{3+}/L in Mixed-R. (2) 1 g/L in Ni-R, 2 g/L in Cr-R, 1.43 g Ni^{2+}/L & 0.05 g Cr^{3+}/L in Mixed-R. (3) 2 g/L in Ni-R, 4 g/L in Cr-R, 2.14 g Ni^{2+}/L & 0.07 g Cr^{3+}/L in Mixed-R. (4) 3 g/L in Ni-R, 4 g/L in Cr-R, 3.57 g Ni^{2+}/L & 0.12 g Cr^{3+}/L in Mixed-R. (5) 6 g/L in Ni-R, 4 g/L in Cr-R, 7.14 g Ni^{2+}/L & 0.23 g Cr^{3+}/L in Mixed-R. (6) 12 g/L in Ni-R, 4 g/L in Cr-R, 14.28 g Ni^{2+}/L & 0.46 g Cr^{3+}/L in Mixed-R. (7) 24 g/L in Ni-R, 6 g/L in Cr-R, 17.84 g Ni^{2+}/L & 0.59 g Cr^{3+}/L in Mixed-R

7.2.4 Microbial speciation

In this section, the relative species abundance of the BRGM-KCC culture at certain points in the experiment is presented and discussed. It is noted that the relative abundance is not the same as the cell numbers for each species. Information on the species-specific cell numbers can be seen in Section 7.3.

Figure 7.7 to Figure 7.10 show the relative abundance of the different species in the BRGM-KCC community over the course of the reactor experiments. At the beginning of the experiment (Day 0), the relative abundance for all reactors except for the control is seen to be similar. The inoculum for all reactors was the same and therefore it is a likely an analytical issue that occurred. For Ni-R, Cr-R and Mixed-R, the microorganism in highest abundance is *L. ferriphilum* with *At. caldus* and a small amount of *Fp. acidiphilum* making up the balance. In the control reactor, the amount of *At. caldus* present is similar, but the majority is made up of *Fp. acidiphilum*. However by Day 11 after the culture had stabilised in the reactor, the relative abundance changed so that the control had a similar makeup to the other reactors. The high relative abundance of *L. ferriphilum* is to be expected in the control and at low concentrations of metals as the conditions align with the growth of this microbe. Additionally, it is seen that, with the presence of *At.caldus*, there is the lack of presence of *Sb. benefaciens* in accordance with the competition reportec between these species (Bryan et al., 2011). This indicates that at 35°C in a system with a pyritic tailings source, *At. caldus* dominated as the sulfur oxidiser over *Sb. benefaciens*. However, from Day 105 onwards, the control reactor showed an abundance of an unidentified bacterium. This unidentified bacterium could potentially be *Sb. thermosulfidooxidans*, and it has been seen in the analysis of long-term continuous bioleaching systems using the BRGM-KCC culture that *Sb. thermosulfidooxidans* and another microbe in the *Sulfobacillus* sp. became present (Joulian et al., 2020). This finding, however, was in a system containing nickel, whereas the control does not contain elevated concentrations of the metal. Further, these micro-organisms have been seen to dominate in column experiments on low grade whole ore that are not inoculated (Tupikina et al., 2013).

If the unidentified bacteria is indeed *Sb. thermosulfidooxidans*, this would lead one to postulate that this increase in the relative abundance of the microbe would occur naturally in such systems. In addition, later in the experiment it is seen that the unidentified bacteriim has a greater relative abundance in Ni-R and Mixed-R than in the control. Again, if this microbe is indeed *Sb. thermosulfidooxidans*, it shows that it is better able to deal with nickel than other sulfur oxidisers and this corresponds with literature that used the same culture (Joulian et al., 2020).

Interestingly, it is seen that at high concentrations of nickel in Ni-R and Mixed-R, *L. ferriphilum* still makes up a large proportion of the culture. In previous work using the BRGM-KCC culture, the relative abundance of the microbe is seen to be significantly reduced in the presence of nickel (Joulian et al., 2020). This work was done at nickel concentrations of 2.3 g/L, far below the concentrations that were reached in this study. It is not entirely clear the reason for this difference seen in the relative abundance, but there could likely be another factor such as temperature or potentially another component in the mineral leached which has caused this to occur. There is also the potential that the *L. ferriphilum* in this study was given ample time to adjust to nickel and thus became more tolerant to the metal.

Considering chromium, it is seen in Figure 7.9 that on Day 85 and onwards the relative abundance of *L. ferriphilum* drops significantly. This is approximately 43 days since Cr-R was changed to a concentration of 4 g/L. Interestingly, at Day 62 (20 days after the change to 4 g/L), while the cell numbers have decreased as seen in Figure 7.4, the relative abundance of *L. ferriphilum* remains unchanged, taking up the highest proportions of the cell numbers. This could potentially indicate that chromium is not immediately inhibitory to *L. ferriphilum*. Alternatively, the *L. ferriphilum* identified may be less active but not yet washed out of the draw-and-fill reactor. The performance of *L. ferriphilum* in the presence of chromium seen in this study corresponds to other studies where chromium is shown to be very inhibitory, more so than nickel (Cabrera et al., 2005; Johnson et al., 2017).

In Figure 7.9, there is also a decreased presence of *At. caldus* in Cr-R, and an increased presence of *Sb. benefaciens.* This once again shows how these competing sulfur oxidisers are rarely seen to both thrive in the same system. Additionally, it shows that *Sb. benefaciens* is likely less sensitive to chromium than *At. caldus.* In Cr-R after the MTC of 4 g/L is reached, the relative abundance of *At. thiooxidans* is seen to increase, especially at Day 85. A similar pattern is seen for archaeon JTC 1/2 and *Ap. cupricumulans* in Cr-R, but to a lesser extent. These are both increases in relative abundance and cell numbers. These correlate to the decrease in other microorganisms like *L. ferriphilum* which use up available components in the media. It is noted though that the cell number increase is minimal and soon after increasing, they decrease at the end of the experiment when the chromium concentration is increased to 6 g/L. More information on the change in cell numbers can be seen in Section 7.3.

Considering *Fp. acidiphilum*, towards the end of the experiment, its relative abundance in all reactors increases, though particularly in Cr-R. Taking note of its cell numbers, its values are also seen to increase or at least remain steady. As mentioned, the increase in the microbe in control as well as the other reactors shows that in long term systems, *Fp. acidiphilum* presence is likely to be seen. This is potentially due to its mixotrophic nature and its ability to deal with elevated concentrations of nickel and chromium (Golyshina, 2014; Pivovarova et al., 2002).

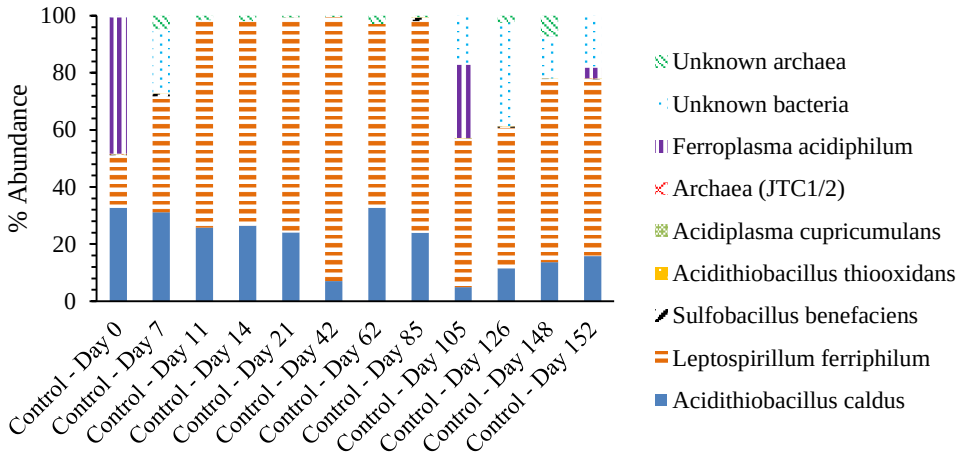

Figure 7.7: Graphical representation of the percentage species abundance of the BRGM-KCC culture over the course of the experiment where there is no exposure to metals in a system containing pyritic tailings

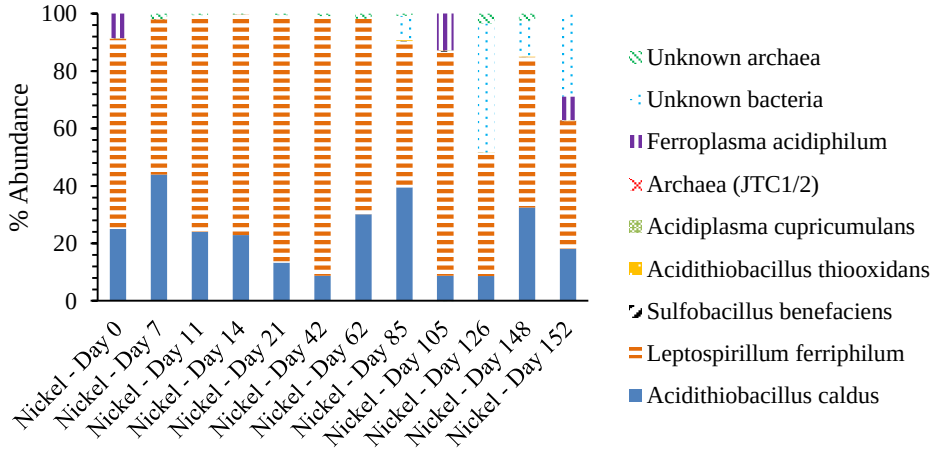

Figure 7.8: Graphical representation of the percentage species abundance of the BRGM-KCC culture in Ni-R exposed to increasing concentrations of Ni^{2+} in a system containing pyritic tailings

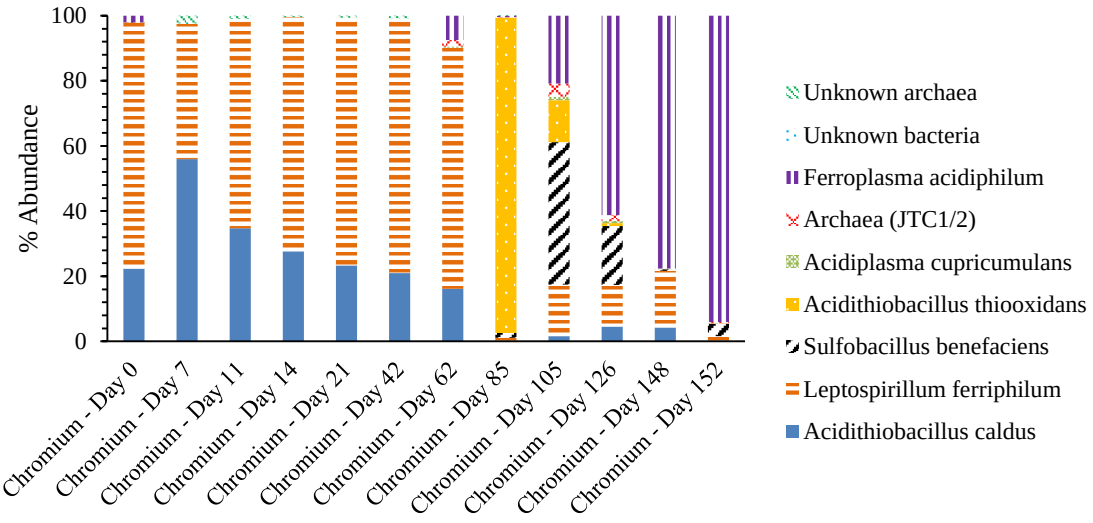

Figure 7.9: Graphical representation of the percentage species abundance of the BRGM-KCC culture in Cr-R exposed to increasing concentrations of Cr^{3+} in a system containing pyritic tailings

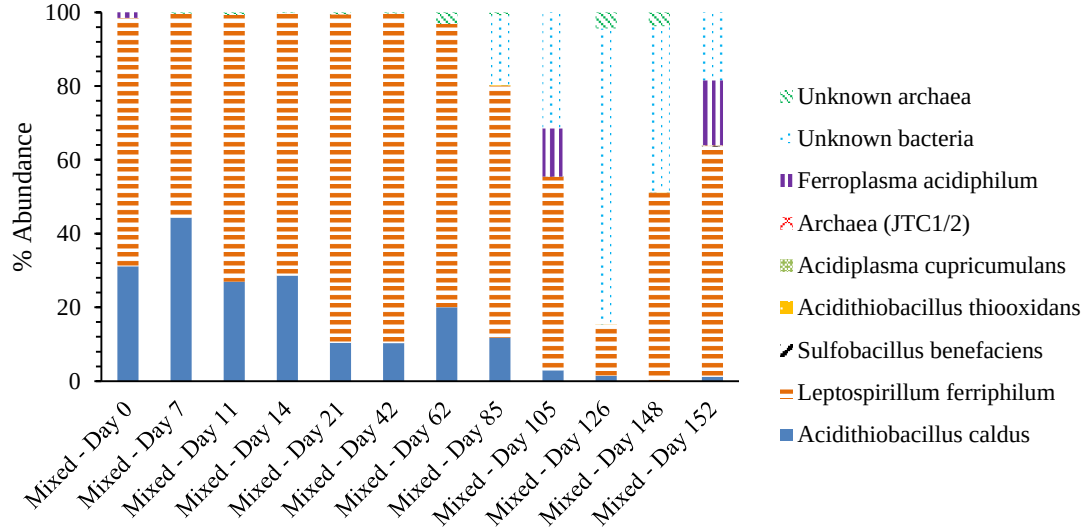

Figure 7.10: Graphical representation of the percentage species abundance of the BRGM-KCC culture in Mixed-R exposed to increasing concentrations of Ni^{2+} and Cr^{3+} in a system containing pyritic tailings

7.3 Integrated results and discussion

In Figure 7.12 to Figure 7.16, the species-specific cell numbers can be seen for different bacteria and archaea in the BRGM-KCC culture over the course of the experiment. Figure 7.12 shows information for *At. caldus* and in the control and Ni-R, the numbers remain relatively unchanged over the course of the experiment. A similar trend can be seen when considering *L. ferriphilum*, archaeon JTC 1/2 and *Fp. acidiphilum.* This indicates that these microorganisms are not affected by concentrations of nickel up to 24 g/L. These microorganisms (excluding JTC 1/2) make up the majority of the BRGM-KCC culture in the control and Ni-R, and their unchanging numbers thus correspond with the information seen throughout Sections 7.2 where iron oxidation, overall cell growth, pH and redox potential remain relatively steady. This is unusual for *L. ferriphilum* which has seen to be sensitive to higher concentrations of nickel, and this was seen in Chapter 6 where there was a decrease of about 0.29×10^7 cells/mL. However, the presence of pyrite coupled with the fact that the system is well-mixed and aerated allows for better growth and performance of the microorganisms in comparison to the MWP plates.

In contrast, in Cr-R a significant drop in the *At. caldus* and *L. ferriphilum* numbers occurs after the chromium concentration is changed to 4 g/L. This shows the great extent to which these microbes are negatively affected by chromium at concentrations 4 g/L and above. The drop in the strongly-oxidising *L. ferriphilum* is seen with the drop in the redox potential to the 400s and the drop in the iron dissolution and oxidation that occurs. While it is clear that chromium can have a strong inhibitory effect on *At. caldus* and *L. ferriphilum*, literature has shown that the inhibitory effects of chromium can occur at much lower concentrations. Johnson et al. (2017) indicate that at concentrations of 0.52 mg/L of chromium, *L. ferriphilum* is already inhibited by chromium. This is not seen in this study and once again this may be because of the time that allowed the microbes to adjust to chromium. Similarly to this study, the study described in Johnson et al. (2017) occurred in 1L aerated bioreactors with *At. thiooxidans*, *At caldus* and *L. ferriphilum*, amongst others, being present. However, the pH maintained at a value of 2 and this may be a reason why the tolerance of *L. ferriphilum* was lower. In more acidic environments (containing more H^+ ions) it has been recorded that microorganisms may have less cell binding sites available for inhibitory metals and thus are less affected by the toxins. As Cr-R was maintained at a pH of between 1 and 1.3 as opposed to 2, there is the potential that the microorganism are less affected by the presence of chromium. Another possible reason for the discrepancy could be simply that different strains of a microorganism behave differently, or due to external factors such as the leached mineral being different and tests being run at different temperatures (30°C and 40°C *vs* the 35°C used in the present study).

For Mixed-R, the *At. caldus* numbers are only really seen to diverge from the control and Ni-R after the final change to 17.84 g/L nickel and 0.59 g/L chromium. Since there is no drop in Ni-R at 24 g/L, and no drop in Cr-R at 2 g/L, it can be assumed that the decrease in Mixed-R is attributed to the combination of nickel and chromium in the reactor. This is possibly an aggregate, multiple stress effect that occurs where a mixture is seen to be more inhibitory than individual components.

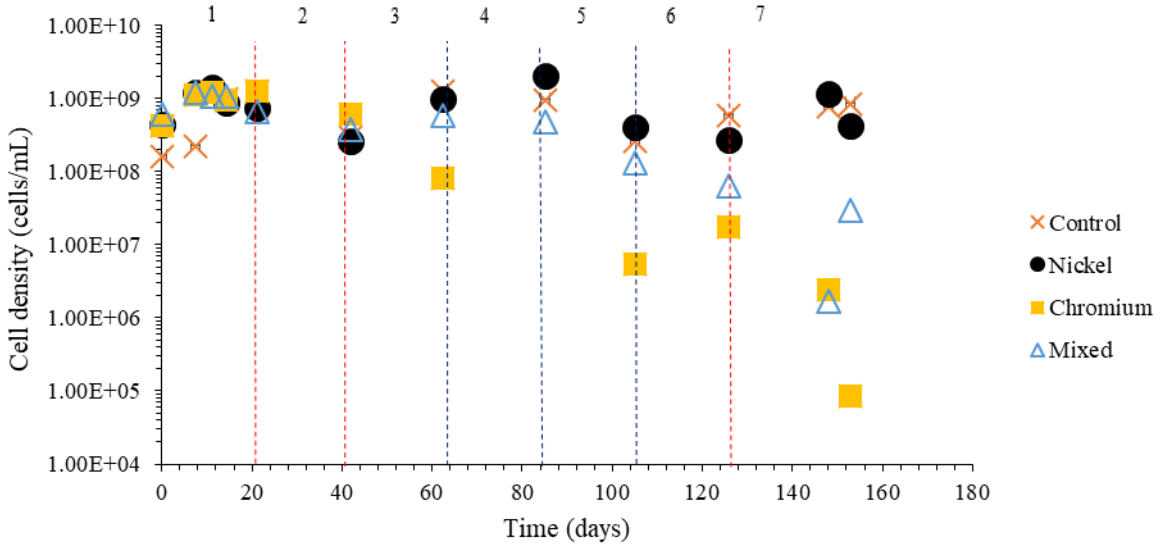

Figure 7.11: Calculated cell density of At. caldus over the period of the experiment (logarithmic scale used). Vertical lines represent where metal (nickel & chromium) concentrations were increased. Red lines indicate where metal concentration increased in all non-control bioreactors; Blue lines indicate where metal concentration increased in all bioreactors except the chromium bioreactor and the control. Numbers on top represent the following concentrations in each reactor: (1) 0.5 g/L in Ni-R, 1 g/L in Cr-R, 0.36 g Ni^{2+}/L & 0.01 g Cr^{3+}/L in Mixed-R. (2) 1 g/L in Ni-R, 2 g/L in Cr-R, 1.43 g Ni^{2+}/L & 0.05 g Cr^{3+}/L in Mixed-R. (3) 2 g/L in Ni-R, 4 g/L in Cr-R, 2.14 g Ni^{2+}/L & 0.07 g Cr^{3+}/L in Mixed-R. (4) 3 g/L in Ni-R, 4 g/L in Cr-R, 3.57 g Ni^{2+}/L & 0.12 g Cr^{3+}/L in Mixed-R. (5) 6 g/L in Ni-R, 4 g/L in Cr-R, 7.14 g Ni^{2+}/L & 0.23 g Cr^{3+}/L in Mixed-R. (6) 12 g/L in Ni-R, 4 g/L in Cr-R, 14.28 g Ni^{2+}/L & 0.46 g Cr^{3+}/L in Mixed-R. (7) 24 g/L in Ni-R, 6 g/L in Cr-R, 17.84 g Ni^{2+}/L & 0.59 g Cr^{3+}/L in Mixed-R

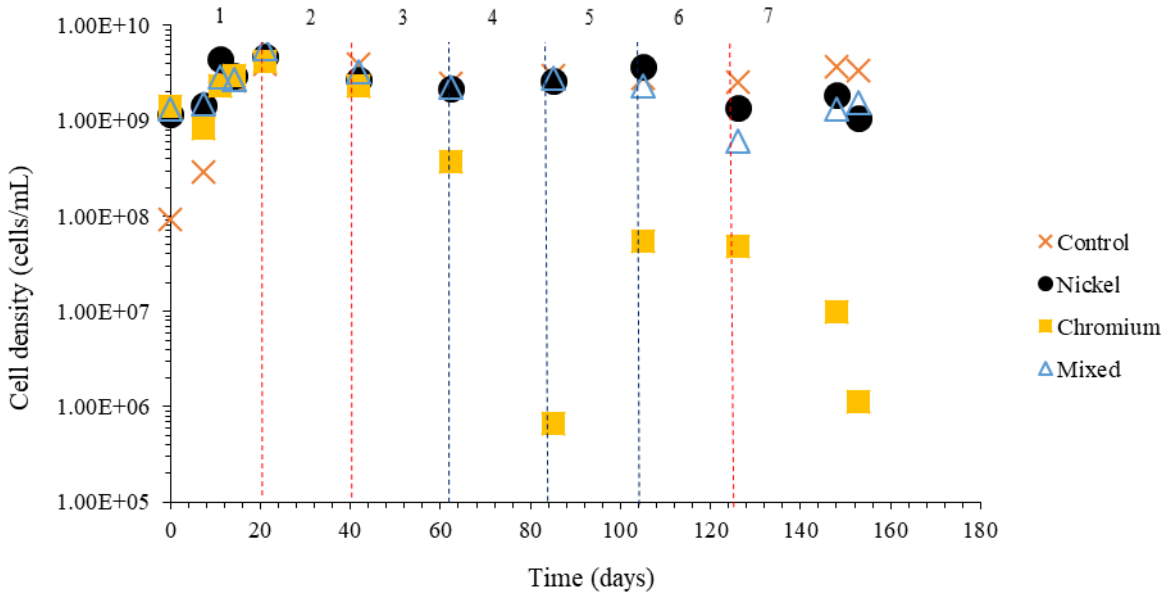

Figure 7.12: Calculated cell density of L. ferriphilum over the period of the experiment (logarithmic scale used). Vertical lines represent where metal (nickel & chromium) concentrations were increased. Red lines indicate where metal concentration increased in all non-control bioreactors; Blue lines indicate where metal concentration increased in all bioreactors except the chromium bioreactor and the control. Numbers on top represent the following concentrations in each reactor: (1) 0.5 g/L in Ni-R, 1 g/L in Cr-R, 0.36 g Ni^{2+}/L & 0.01 g Cr^{3+}/L in Mixed-R. (2) 1 g/L in Ni-R, 2 g/L in Cr-R, 1.43 g Ni^{2+}/L & 0.05 g Cr^{3+}/L in Mixed-R. (3) 2 g/L in Ni-R, 4 g/L in Cr-R, 2.14 g Ni^{2+}/L & 0.07 g Cr^{3+}/L in Mixed-R. (4) 3 g/L in Ni-R, 4 g/L in Cr-R, 3.57 g Ni^{2+}/L & 0.12 g Cr^{3+}/L in Mixed-R. (5) 6 g/L in Ni-R, 4 g/L in Cr-R, 7.14 g Ni^{2+}/L & 0.23 g Cr^{3+}/L in Mixed-R. (6) 12 g/L in Ni-R, 4 g/L in Cr-R, 14.28 g Ni^{2+}/L & 0.46 g Cr^{3+}/L in Mixed-R. (7) 24 g/L in Ni-R, 6 g/L in Cr-R, 17.84 g Ni^{2+}/L & 0.59 g Cr^{3+}/L in Mixed-R

In Figure 7.13, *Sb. benefaciens* numbers in all the reactors are seen. Again, the control remains relatively constant. The microbe numbers in Ni-R also remain relatively constant until 6 g/L of nickel is reached and then begin to drop. The numbers in Mixed-R gradually increase and the numbers in Cr-R do the same until the concentration is changed to 6 g/L. The increase in Mixed-R and Cr-R correspond to decreases in *At. caldus* numbers, showing the competition taking place. However, at higher chromium concentrations *Sb. benefaciens* is unable to tolerate the chromium levels and the numbers also decrease.

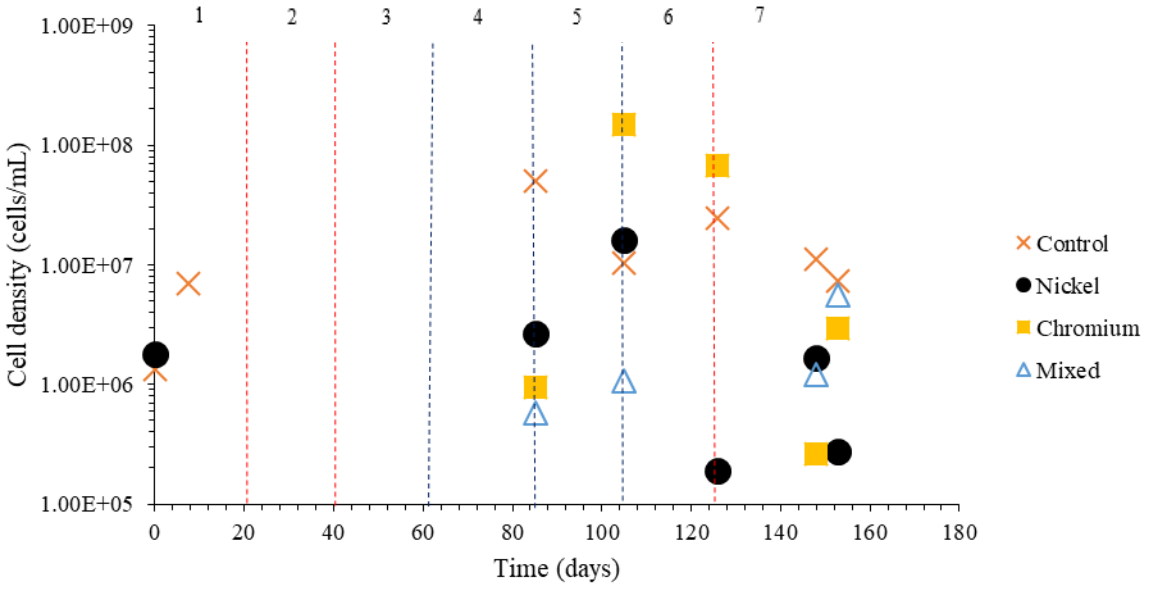

Figure 7.13: Calculated cell density of Sb. benefaciens over the period of the experiment (logarithmic scale used). Vertical lines represent where metal (nickel & chromium) concentrations were increased. Red lines indicate where metal concentration increased in all non-control bioreactors; Blue lines indicate where metal concentration increased in all bioreactors except the chromium bioreactor and the control. Numbers on top represent the following concentrations in each reactor: (1) 0.5 g/L in Ni-R, 1 g/L in Cr-R, 0.36 g Ni^{2+}/L & 0.01 g Cr^{3+}/L in Mixed-R. (2) 1 g/L in Ni-R, 2 g/L in Cr-R, 1.43 g Ni^{2+}/L & 0.05 g Cr^{3+}/L in Mixed-R. (3) 2 g/L in Ni-R, 4 g/L in Cr-R, 2.14 g Ni^{2+}/L & 0.07 g Cr^{3+}/L in Mixed-R. (4) 3 g/L in Ni-R, 4 g/L in Cr-R, 3.57 g Ni^{2+}/L & 0.12 g Cr^{3+}/L in Mixed-R. (5) 6 g/L in Ni-R, 4 g/L in Cr-R, 7.14 g Ni^{2+}/L & 0.23 g Cr^{3+}/L in Mixed-R. (6) 12 g/L in Ni-R, 4 g/L in Cr-R, 14.28 g Ni^{2+}/L & 0.46 g Cr^{3+}/L in Mixed-R. (7) 24 g/L in Ni-R, 6 g/L in Cr-R, 17.84 g Ni^{2+}/L & 0.59 g Cr^{3+}/L in Mixed-R

At. thiooxidans numbers can be seen in Figure 7.14. The sulfur oxidiser sees an increase in numbers in the control and Ni-R. The high numbers associated with multiple sulfur oxidisers (*At. caldus*, *Sb. benefaciens* and *At. thiooxidans*) in the control, Ni-R and Mixed-R can be seen with the decreasing pH between feedings. This shows that generally, sulfur-oxidising microorganisms are not affected by nickel. Though in Figure 7.14, it is noted that *At. thiooxidans* numbers begin to decrease at 6 g/L of nickel unlike the other sulfur oxidisers. This may indicate that it is the sulfur oxidiser that is least tolerant to nickel, or that in the experimental conditions, the other sulfur oxidisers are able to outcompete the microbe.

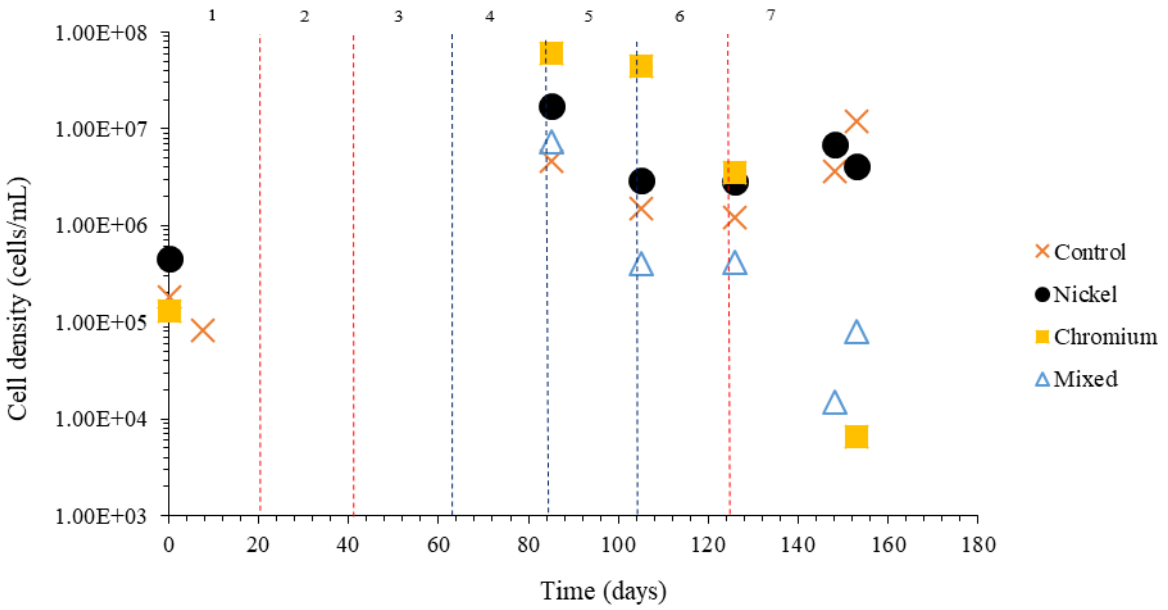

Figure 7.14: Calculated cell density of At. thiooxidans over the period of the experiment (logarithmic scale used). Vertical lines represent where metal (nickel & chromium) concentrations were increased. Red lines indicate where metal concentration increased in all non-control bioreactors; Blue lines indicate where metal concentration increased in all bioreactors except the chromium bioreactor and the control. Numbers on top represent the following concentrations in each reactor: (1) 0.5 g/L in Ni-R, 1 g/L in Cr-R, 0.36 g Ni^{2+}/L & 0.01 g Cr^{3+}/L in Mixed-R. (2) 1 g/L in Ni-R, 2 g/L in Cr-R, 1.43 g Ni^{2+}/L & 0.05 g Cr^{3+}/L in Mixed-R. (3) 2 g/L in Ni-R, 4 g/L in Cr-R, 2.14 g Ni^{2+}/L & 0.07 g Cr^{3+}/L in Mixed-R. (4) 3 g/L in Ni-R, 4 g/L in Cr-R, 3.57 g Ni^{2+}/L & 0.12 g Cr^{3+}/L in Mixed-R. (5) 6 g/L in Ni-R, 4 g/L in Cr-R, 7.14 g Ni^{2+}/L & 0.23 g Cr^{3+}/L in Mixed-R. (6) 12 g/L in Ni-R, 4 g/L in Cr-R, 14.28 g Ni^{2+}/L & 0.46 g Cr^{3+}/L in Mixed-R. (7) 24 g/L in Ni-R, 6 g/L in Cr-R, 17.84 g Ni^{2+}/L & 0.59 g Cr^{3+}/L in Mixed-R

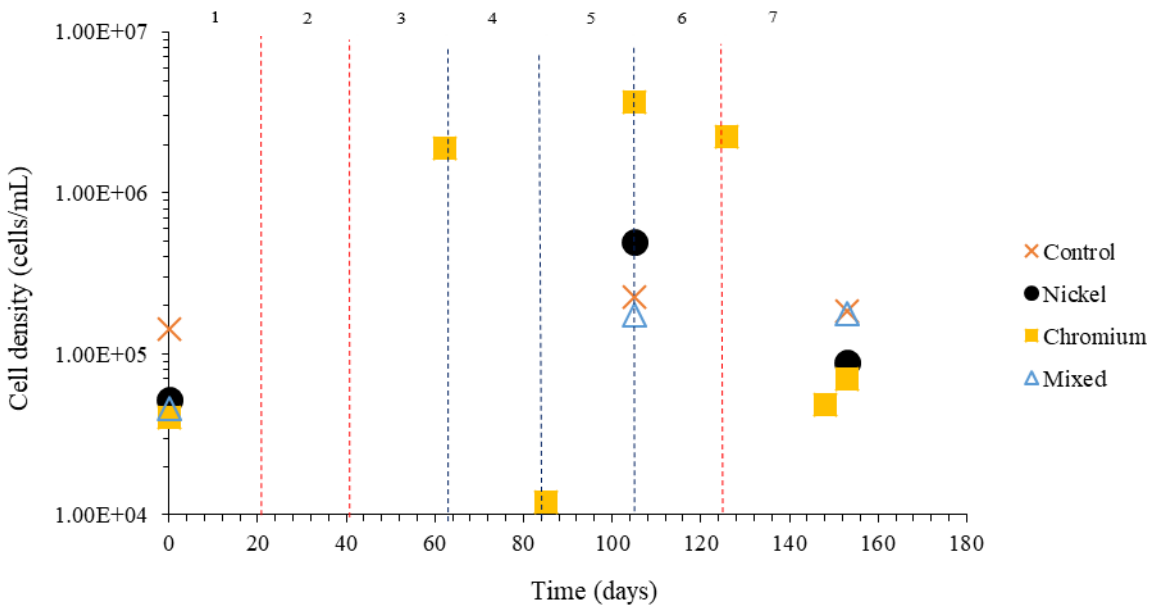

Figure 7.15: Calculated cell density of Ap. cupricumulans over the period of the experiment (logarithmic scale used). Vertical lines represent where metal (nickel & chromium) concentrations were increased. Red lines indicate where metal concentration increased in all non-control bioreactors; Blue lines indicate where metal concentration increased in all bioreactors except the chromium bioreactor and the control. Numbers on top represent the following concentrations in each reactor: (1) 0.5 g/L in Ni-R, 1 g/L in Cr-R, 0.36 g Ni^{2+}/L & 0.01 g Cr^{3+}/L in Mixed-R. (2) 1 g/L in Ni-R, 2 g/L in Cr-R, 1.43 g Ni^{2+}/L & 0.05 g Cr^{3+}/L in Mixed-R. (3) 2 g/L in Ni-R, 4 g/L in Cr-R, 2.14 g Ni^{2+}/L & 0.07 g Cr^{3+}/L in Mixed-R. (4) 3 g/L in Ni-R, 4 g/L in Cr-R, 3.57 g Ni^{2+}/L & 0.12 g Cr^{3+}/L in Mixed-R. (5) 6 g/L in Ni-R, 4 g/L in Cr-R, 7.14 g Ni^{2+}/L & 0.23 g Cr^{3+}/L in Mixed-R. (6) 12 g/L in Ni-R, 4 g/L in Cr-R, 14.28 g Ni^{2+}/L & 0.46 g Cr^{3+}/L in Mixed-R. (7) 24 g/L in Ni-R, 6 g/L in Cr-R, 17.84 g Ni^{2+}/L & 0.59 g Cr^{3+}/L in Mixed-R

In Figure 7.15, *Ap. cupricumulans* numbers over the course of the experiment are shown. Generally, there are low numbers for this microbe, except for a stage where the numbers are high in Cr-R. This is possibly opportunistic as this increase coincides with a decrease in *L. ferriphilum*, another iron oxidiser. Even with the increased presence of this microbe, there is still seen to be little iron oxidation occurring in the reactor. This is because this microbe is considered a weak iron-oxidising archaeon. In Figure 7.16, *Fp. acidiphilum* numbers in Cr-R remain high and constant, though not as high as what *L. ferriphilum* is able to achieve in favourable conditions. With the increasing *Ap. cupricumulans* and *Fp. acidiphilum*, the iron oxidation is still unable to reach as high levels as seen with *L. ferriphilum* early in the experiment when it was not inhibited by chromium. This would then make it seem that *Fp. acidiphilum* is not actually a strong iron oxidiser as with its number remaining high, there is still minimal iron oxidation and the redox potential remains low. However, this could also be due to the fact that there are low overall cell numbers in the reactor and even if *Fp. acidiphilum* was a strong oxidiser, it still would not be able to oxidise iron to the extent to increase the redox potential to a higher level. In all reactors, *Fp. acidiphilum* numbers do not drop and this shows the microorganism's robustness and ability to handle high metal concentrations.

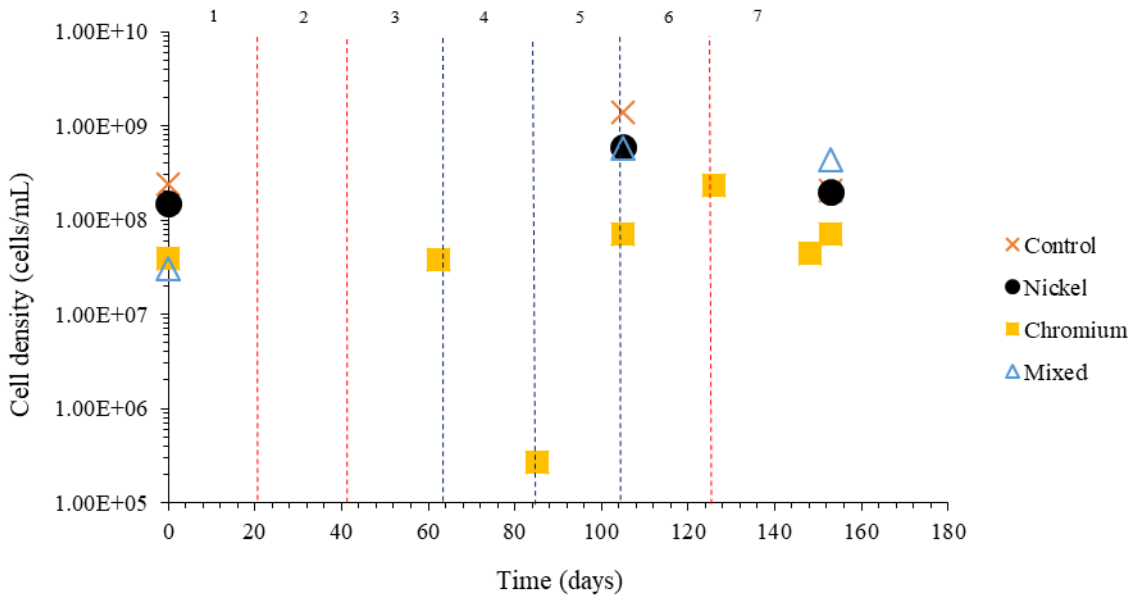

Figure 7.16: Calculated cell density of Fp. acidiphilum over the period of the experiment (logarithmic scale used). Vertical lines represent where metal (nickel & chromium) concentrations were increased. Red lines indicate where metal concentration increased in all non-control bioreactors; Blue lines indicate where metal concentration increased in all bioreactors except the chromium bioreactor and the control. Numbers on top represent the following concentrations in each reactor: (1) 0.5 g/L in Ni-R, 1 g/L in Cr-R, 0.36 g Ni^{2+}/L & 0.01 g Cr^{3+}/L in Mixed-R. (2) 1 g/L in Ni-R, 2 g/L in Cr-R, 1.43 g Ni^{2+}/L & 0.05 g Cr^{3+}/L in Mixed-R. (3) 2 g/L in Ni-R, 4 g/L in Cr-R, 2.14 g Ni^{2+}/L & 0.07 g Cr^{3+}/L in Mixed-R. (4) 3 g/L in Ni-R, 4 g/L in Cr-R, 3.57 g Ni^{2+}/L & 0.12 g Cr^{3+}/L in Mixed-R. (5) 6 g/L in Ni-R, 4 g/L in Cr-R, 7.14 g Ni^{2+}/L & 0.23 g Cr^{3+}/L in Mixed-R. (6) 12 g/L in Ni-R, 4 g/L in Cr-R, 14.28 g Ni^{2+}/L & 0.46 g Cr^{3+}/L in Mixed-R. (7) 24 g/L in Ni-R, 6 g/L in Cr-R, 17.84 g Ni^{2+}/L & 0.59 g Cr^{3+}/L in Mixed-R

Figure 7.17 shows the cell density of the archaeon JTC 1/2 over the course of the experiment. The control, Ni-R and Mixed-R remain unchanged. However, Cr-R generally increases until the concentration in the reactor is changed to 6 g/L of chromium where it proceeds to decrease. This shows that the microbe is likely very tolerant to nickel, but not as tolerant to chromium.

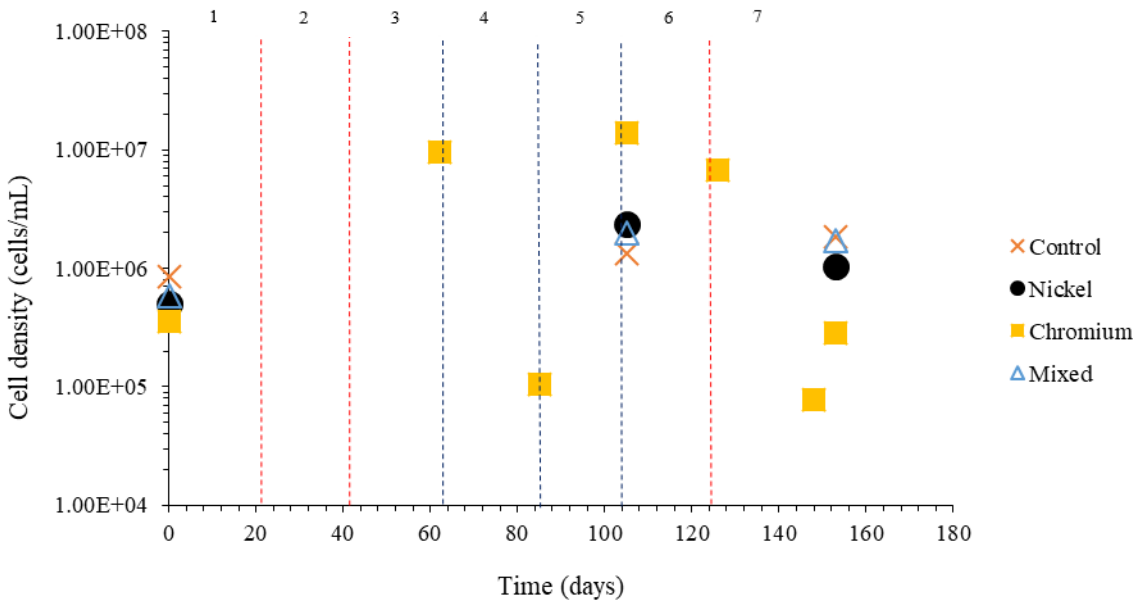

Figure 7.17: Calculated cell density of Archaeon JTC 1/2 over the period of the experiment (logarithmic scale used). Vertical lines represent where metal (nickel & chromium) concentrations were increased. Red lines indicate where metal concentration increased in all non-control bioreactors; Blue lines indicate where metal concentration increased in all bioreactors except the chromium bioreactor and the control. Numbers on top represent the following concentrations in each reactor: (1) 0.5 g/L in Ni-R, 1 g/L in Cr-R, 0.36 g Ni^{2+}/L & 0.01 g Cr^{3+}/L in Mixed-R. (2) 1 g/L in Ni-R, 2 g/L in Cr-R, 1.43 g Ni^{2+}/L & 0.05 g Cr^{3+}/L in Mixed-R. (3) 2 g/L in Ni-R, 4 g/L in Cr-R, 2.14 g Ni^{2+}/L & 0.07 g Cr^{3+}/L in Mixed-R. (4) 3 g/L in Ni-R, 4 g/L in Cr-R, 3.57 g Ni^{2+}/L & 0.12 g Cr^{3+}/L in Mixed-R. (5) 6 g/L in Ni-R, 4 g/L in Cr-R, 7.14 g Ni^{2+}/L & 0.23 g Cr^{3+}/L in Mixed-R. (6) 12 g/L in Ni-R, 4 g/L in Cr-R, 14.28 g Ni^{2+}/L & 0.46 g Cr^{3+}/L in Mixed-R. (7) 24 g/L in Ni-R, 6 g/L in Cr-R, 17.84 g Ni^{2+}/L & 0.59 g Cr^{3+}/L in Mixed-R

7.4 Conclusions

In this chapter, a semi-continuous bioreactor test was conducted for the period of 5 months. Four reactors were used in the experiment, a control reactor with no added metal, a nickel reactor (Ni-R) where increasing concentrations of nickel was added, a chromium reactor (Cr-R) where increasing concentrations of chromium was added and a mixed reactor (Mixed-R) where a combination of nickel and chromium was added. The combinations used in Mixed-R was based on increasing PCB compositions at different solid loading rates. This experiment was done to test the ability of the BRGM-KCC microbial community to withstand increasing concentrations of metals in a bioreactor system where tailings have been incorporated. The tailings used was pyritic in nature.

Results from the tests indicate that the BRGM-KCC culture is able to withstand the very high nickel concentration of 24 g/L. At this concentration, growth, iron oxidation and acid production are all seen to occur. However, there is seen to be slight deviations from the control with the amount of total iron in solution slightly increasing, and the cell density slightly decreasing. This could indicate that microorganisms may be starting to be negatively affected by nickel to the extent where performance is beginning to decrease. This cannot be validated because it is unknown whether the performance would continue to drop or would begin to rise after some time adapting to the high nickel concentrations.

Contrarily, chromium was shown to inhibit the BRGM-KCC culture at just 4 g/L. In the mixed reactor, it was seen that generally, the microorganisms were able to withstand all concentrations of nickel and chromium studied, up to 18 g/L nickel and 0.6 g/L chromium, but some microbial species present did experience detrimental effects linked to the combination of the two metals being present. In Mixed-R, it was seen that nickel and chromium concentrations equivalent to 500 w/v% PCBs can still be tolerated by the microbes.

Another important observation is the extent in which the microorganisms are able to adapt to a metal after experiencing a large extent of inhibition. For nickel, the BRGM-KCC community as a whole only showed a very small extent of inhibition towards the end of the experiment. However for chromium, a drastic drop in performance was recorded. Results show that to a small extent, the community was able to increase in number, though no increased iron oxidation or pyrite dissolution was recorded. This indicates that the BRGM-KCC community is likely unable to fully adapt to increased chromium concentrations, but changes in the community can occur to at least slightly increase cell numbers. Knowledge on the ability for microorganisms to adjust to metals in solution can be used in the design of robust bioleaching systems to allow for higher efficiency recoveries.

Chapter 8: Conclusions and Recommendations

8.1 Conclusions

In recent times, the use of mine wastes has been increasingly investigated. This is because of a decrease in primary minerals, coupled with a push towards improved resource efficiency and more sustainable production practices in the mining sector. By utilising biohydrometallurgical methods such as bioleaching, wastes such as tailings and electronic wastes (e-wastes) can be reduced or made increasingly inert or less reactive, benefitting the environment, while at the same time allowing valuable metals to be extracted from these wastes as critical raw materials for technology components. Processing wastes is not without its challenges, with one of the biggest associated drawbacks being the variety of impurities within the wastes which affect the bioleaching microorganisms used in the extraction process. In mine wastes, metal impurities are key. While the metals may be valuable to retrieve, there is potential for them to inhibit bioleaching microorganisms when at high concentrations. Currently, limited information is available on the extent to which various metals found within tailings (and e-wastes especially) affect acidophilic microbes used in bioleaching, especially considering mixed microbial communities where many microorganisms are present. Thus, the aim of this project was to determine changes that may occur when mixed communities are exposed to two metals found within wastes, nickel and chromium.

In this project, a number of studies were completed to determine the extent to which nickel and chromium affected microbial Fe- and S-oxidising communities consisting of *L. ferriphilum, At. caldus, Fp. acidiphilum, Ap. cupricumulans, Sb. benefaciens, At. thioxidans,* Archaeon JTC1/2, and others. In small-scale tests carried out in multi-well plates in sulfur-free media, two microbial communities were used; the BIOX® community operating at 45°C and the BRGM-KCC community operating at 35°C. The BIOX® community was seen to have a maximum tolerated concentration (MTC) of 2 g/L for nickel and 7.5 g/L for chromium. The BRGM-KCC community was seen to have a MTC of 4 g/L for nickel and 7.5 g/L for chromium. The results from these tests showed that in iron-only media, these communities are able to handle a higher concentration of chromium than nickel. This finding is interesting because this is the opposite of what has been reported in literature. This then indicates the great extent to which a single component in a bioleaching matrix can change the community dynamics and microbial performance. Another important finding from these tests was the way in which iron oxidation and microbial growth can be decoupled. Considering the iron-oxidising *L. ferriphilum, Ap. cupricumulans* and *Fp. acidiphilum*, it was seen that the rate of iron oxidation was faster in the presence of chromium than in the presence of nickel. However, the numbers of these microbes are less than in the nickel tests. This shows that, in the presence of metal inhibitors, these microorganisms may experience a stress response where iron oxidation is increased to supply more energy for maintenance. Therefore, microbial growth is not always required to achieve iron oxidation. This knowledge allows for the potential of bioleaching systems to be prepared and controlled to maximise iron oxidation by inducing a stress response. However, this may not be sustainable for long periods of times if the microbes are unable to adapt to the metal inhibitors.

In small-scale tests where both sulfur and iron were present in media using the BRGM-KCC culture, the MTCs changed with the MTC in nickel tests increased to above 4 g/L while the MTC in chromium tests decreased to below 2 g/L. This means that the presence of sulfur can substantially change the manner in which microorganisms function, and again, highlights the importance of being aware of the components in a bioleaching matrix as a single components can change the performance and functioning of a community substantially. A commonality in this set of tests as well as the tests where no sulfur is present is the increase in numbers of *Fp. acidiphilum*. This increased presence of *Fp. acidiphilum* is also seen in industrial bioreactors. This is likely because this microbe is able to utilise organic material produced by other microbes and dead cells, and an increase in *Fp. acidiphilum* often occurs with an increase in obligate lithotrophs. With the presence of *Fp. acidiphilum* being seen increasingly in commercial bioleaching reactors, it is an important microbe to investigate and study further.

An additional finding in this project relates to the presence of *At. caldus* and *Sb. benfaciens.* These microbes have been seen in literature to be in competition, and the same can be seen in the tests performed for this project (Bryan et al., 2011). Generally, *At. caldus* was seen to outcompete *Sb. benefaciens* with *Sb.benefaciens* decreasing in number while *At. caldus* cell numbers grow. However, when *At. caldus* is inhibited or is not provided with an essential substrate (sulfur) and the numbers decrease, *Sb. benefaciens* numbers are able to grow, even in the presence of metal inhibitors.

In the semi-continuous bioreactors, the level tolerance of bioleaching microbes was tested, along with their potential adapt to nickel and chromium. Four reactors were commissioned for this test, a control where no additional metal inhibitors were added, a nickel reactor where only nickel was added, a chromium reactor where only chromium was added and a mixed reactor where nickel and chromium were added at a ratio matching those found in waste printed circuit boards (PCBs) at increasing solid loading rates. The results indicate that the BRGM-KCC community is most inhibited by chromium, with the chromium reactor experiencing a large drop in cell numbers, iron oxidation and pyrite dissolution at concentrations above 4 g/L. Once it was clear that the culture was affected by the chromium concentration, the concentration was maintained at 4 g/L to determine whether the culture could adapt and recover. There were a number of iterations where the cell numbers began to rise, but that was not sustained and the numbers dropped again until a new "steady-state" was achieved, albeit lower than the initial value. This indicates that the culture as a whole is unable to fully adapt to concentrations of chromium 4 g/L and above.

Conversely, the culture is able to tolerate concentrations of nickel up to 24 g/L in the nickel reactor, with there still being oxidation and cell growth. The same is seen in the mixed reactor (reaching a maximum nickel and chromium concentration of 18 g/L and 0.6 g/L, respectively) where overall cell density and iron oxidation is similar to that of the control reactor. Interestingly, it was seen that *Fp. acidiphilum* is the only microbe that was able to maintain its number throughout the course of the experiment in the chromium reactor. Once again, this shows the robust-nature of *Fp. acidiphilum* and the importance in gaining understanding on the microbe which will likely continue to be one seen in industrial applications of bioleaching. In order to maximise the amount of metals that can be extracted from wastes, it is beneficial to devote time to understanding *Fp. acidiphilum* and all the other microorganisms found in bioleaching consortia.

8.2 Recommendations

The following are recommendations to improve or complement the findings of this project:

- While a lot of information is able to be obtained from the MWP experiments, it is important for these test to be repeated at a larger scale in flasks or, preferably, bioreactors. This is because the MWP are seen to be more sensitive to variations in the inoculum due to the small volumes held by them.
- Considering the semi-continuous bioreactor study, it is recommended that the experiment be repeated (for a longer period of time) to validate the results obtained in this project, and to determine at what point the BRGM-KCC culture would be severely impacted by nickel (in the nickel reactor) and a combination of nickel and chromium (in the mixed reactor). This is because there is the potential for microorganisms to be exposed to a high concentration of metal. The metal may not necessarily directly originate from the material being leached (e.g. tailings and e-waste), but may potentially come from recycled streams where the accumulation of metal inhibitors that are already in solution could affect bioleaching microorganisms. In order to maximise metal recovery, it is beneficial for the metal concentrations in solution to be high. In ferric leaching systems, especially if e-waste is perhaps the sole/main leached material, ideally the volume being purged out of the system should be minimised to decrease the fresh iron requirements.
- It is recommended that more metals found within PCBs be examined. These metals include copper, cobalt, iron and aluminium. It is noted that some information is available on the effects of copper, cobalt and iron on the community.
- Finally, it is recommended that more work be done using actual PCBs. While it is valuable to understand the effect of single components on a community, it is also important to investigate how a culture would be affected in real PCB leachate which contains more metals and thus, the metal-to-metal and microbe-to-metal interactions may be different.

References

Abhilash, D., Tabassum, S., Ghosh, A., Meshram, P., van Hullebusch, E., 2021. Microbial Processing of Waste Shredded PCBs for Copper Extraction Cum Separation-Comparing the Efficacy of Bacterial and Fungal Leaching Kinetics and Yields. Metals - Open Access Metallurgy Journal 317. https://doi.org/10.3390/met11020317

Abraham R, M., Tumwebaze, S., 2017. Water contamination with heavy metals and trace elements from Kilembe copper mine and tailing sites in Western Uganda; implications for domestic water quality. Chemosphere 169, 281–287. https://doi.org/10.1016/j.chemosphere.2016.11.077

Adiguzel, D., Tuylu, S., Eker, H., 2022. Utilisation of tailings in concrete products: A review. Construction and Building Materials 360, 129574. https://doi.org/10.1016/j.conbuildmat.2022.129574

Ahmadi, A., Khezri, M., Abdollahzadeh, A.A., Askari, M., 2015. Bioleaching of copper, nickel and cobalt from the low grade sulfidic tailing of Golgohar Iron Mine, Iran. Hydrometallurgy 154, 1–8. https://doi.org/10.1016/j.hydromet.2015.03.006

Anaya-Garzon, J., Hubau, A., Joulian, C., Guezennec, A.-G., 2021. Bioleaching of E-Waste: Influence of Printed Circuit Boards on the Activity of Acidophilic Iron-Oxidizing Bacteria. Frontiers in Microbiology 12.

Andeobu, L., Wibowo, S., Grandhi, S., 2021. A Systematic Review of E-Waste Generation and Environmental Management of Asia Pacific Countries. Int J Environ Res Public Health 18, 9051. https://doi.org/10.3390/ijerph18179051

Annamalai, M., Gurumurthy, K., 2019. Enhanced bioleaching of copper from circuit boards of computer waste by Acidithiobacillus ferrooxidans. Environ Chem Lett 17, 1873–1879. https://doi.org/10.1007/s10311-019-00911-y

Arshadi, M., Mousavi, S.M., 2015. Multi-objective optimization of heavy metals bioleaching from discarded mobile phone PCBs: Simultaneous Cu and Ni recovery using Acidithiobacillus ferrooxidans. Separation and Purification Technology 147, 210–219. https://doi.org/10.1016/j.seppur.2015.04.020

Aswegen, P., van Niekerk, J., Olivier, J., 2007. The BIOXTM Process for the Treatment of Refractory Gold Concentrates, in: Biomining. pp. 1–33. https://doi.org/10.1007/978-3-540-34911-2_1

Bas, A.D., Deveci, H., Yazici, E.Y., 2013. Bioleaching of copper from low grade scrap TV circuit boards using mesophilic bacteria. Hydrometallurgy 138, 65–70. https://doi.org/10.1016/j.hydromet.2013.06.015

Belle, G., Fossey, A., Esterhuizen, L., Moodley, R., 2021. Contamination of groundwater by potential harmful elements from gold mine tailings and the implications to human health: A case study in Welkom and Virginia, Free State Province, South Africa. Groundwater for Sustainable Development 12, 100507. https://doi.org/10.1016/j.gsd.2020.100507

Benoit, S.L., Maier, R.J., 2013. Nickel Ions in Biological Systems, in: Kretsinger, R.H., Uversky, V.N., Permyakov, E.A. (Eds.), Encyclopedia of Metalloproteins. Springer, New York, NY, pp. 1501–1505. https://doi.org/10.1007/978-1-4614-1533-6_75

Birk, J.P., 2018. Characteristic Reactions of Chromium Ions (Cr3+) [WWW Document]. Chemistry LibreTexts. URL https://chem.libretexts.org/Bookshelves/Analytical_Chemistry/Supplemental_Modules_(Analytical_C

hemistry)/Qualitative_Analysis/Characteristic_Reactions_of_Select_Metal_Ions/Characteristic_Reactions_of_Chromium_Ions_(Cr) (accessed 12.18.23).

Bodzek, M., 2015. 15 - Membrane technologies for the removal of micropollutants in water treatment, in: Basile, A., Cassano, A., Rastogi, N.K. (Eds.), Advances in Membrane Technologies for Water Treatment, Woodhead Publishing Series in Energy. Woodhead Publishing, Oxford, pp. 465–517. https://doi.org/10.1016/B978-1-78242-121-4.00015-0

Bosecker, K., 1997. Bioleaching: metal solubilization by microorganisms. FEMS Microbiol Rev 20, 591–604. https://doi.org/10.1111/j.1574-6976.1997.tb00340.x

Bruins, M.R., Kapil, S., Oehme, F.W., 2000. Microbial Resistance to Metals in the Environment. Ecotoxicology and Environmental Safety 45, 198–207. https://doi.org/10.1006/eesa.1999.1860

Bryan, C.G., Joulian, C., Spolaore, P., El Achbouni, H., Challan-Belval, S., Morin, D., d'Hugues, P., 2011. The efficiency of indigenous and designed consortia in bioleaching stirred tank reactors. Minerals Engineering 24, 1149–1156. https://doi.org/10.1016/j.mineng.2011.03.014

Bryan, C.G., Watkin, E.L., McCredden, T.J., Wong, Z.R., Harrison, S.T.L., Kaksonen, A.H., 2015. The use of pyrite as a source of lixiviant in the bioleaching of electronic waste. Hydrometallurgy 152, 33–43. https://doi.org/10.1016/j.hydromet.2014.12.004

Bryan, C.G., Williamson, B.J., Całus-Moszko, J., van Haute, Q., Guezennec, A.-G., Gaydardzhiev, S., Wavrer, P., Frączek, R., 2020. CEReS – co-processing of coal mine & electronic wastes: Novel resources for a sustainable future. Hydrometallurgy 197, 105444. https://doi.org/10.1016/j.hydromet.2020.105444

Cabrera, G., Gómez, J.M., Cantero, D., 2005. Influence of heavy metals on growth and ferrous sulfate oxidation by Acidithiobacillus ferrooxidans in pure and mixed cultures. Process Biochemistry 40, 2683–2687. https://doi.org/10.1016/j.procbio.2004.12.005

Centre for Bioprocess Engineering Research, 2018. CeBER Laboratory Methods Manual.

Chakraborty, S.C., Qamruzzaman, M., Zaman, M.W.U., Alam, M.M., Hossain, M.D., Pramanik, B.K., Nguyen, L.N., Nghiem, L.D., Ahmed, M.F., Zhou, J.L., Mondal, Md.Ibrahim.H., Hossain, M.A., Johir, M.A.H., Ahmed, M.B., Sithi, J.A., Zargar, M., Moni, M.A., 2022. Metals in e-waste: Occurrence, fate, impacts and remediation technologies. Process Safety and Environmental Protection 162, 230–252. https://doi.org/10.1016/j.psep.2022.04.011

Chandra, A.P., Gerson, A.R., 2010. The mechanisms of pyrite oxidation and leaching: A fundamental perspective. Surface Science Reports 65, 293–315. https://doi.org/10.1016/j.surfrep.2010.08.003

Choi, M.-S., Cho, K.-S., Kim, D.-S., Kim, D.-J., 2004. Microbial recovery of copper from printed circuit boards of waste computer by Acidithiobacillus ferrooxidans. J Environ Sci Health A Tox Hazard Subst Environ Eng 39, 2973–2982.

Coram, N.J., Rawlings, D.E., 2002. Molecular relationship between two groups of the genus Leptospirillum and the finding that Leptospirillum ferriphilum sp. nov. dominates South African commercial biooxidation tanks that operate at 40 degrees C. Appl Environ Microbiol 68, 838–845. https://doi.org/10.1128/aem.68.2.838-845.2002

Costa, F.R., Nery, G.P., Carneiro, C. de C., Kahn, H., Ulsen, C., 2022. Mineral characterization of low-grade gold ore to support geometallurgy. Journal of Materials Research and Technology 21, 2841–2852. https://doi.org/10.1016/j.jmrt.2022.10.085

Cox, D.P., Lindsey, D.A., Singer, D.A., Diggles, M.F., 2003. Sediment-Hosted Copper Deposits of the World: Deposit Models and Database (Open-File Report No. 2003–107), Open-File Report. US Geological Survey Publication.

Cruells, M., Roca, A., 2022. Jarosites: Formation, Structure, Reactivity and Environmental. Metals 12, 802. https://doi.org/10.3390/met12050802

d'Hugues, P., Cezac, P., Cabral, T., Battaglia, F., Truong-Meyer, X.M., Morin, D., 1997. Bioleaching of a cobaltiferous pyrite: A continuous laboratory-scale study at high solids concentration. Minerals Engineering 10, 507–527. https://doi.org/10.1016/S0892-6875(97)00029-0

Dew, D.W., Lawson, E.N., Broadhurst, J.L., 1997. The BIOX® Process for Biooxidation of Gold-Bearing Ores or Concentrates, in: Rawlings, D.E. (Ed.), Biomining: Theory, Microbes and Industrial Processes. Springer Berlin Heidelberg, Berlin, Heidelberg, pp. 45–80. https://doi.org/10.1007/978-3-662-06111-4_3

Dissanayake, V., 2014. Electronic Waste, in: Wexler, P. (Ed.), Encyclopedia of Toxicology (Third Edition). Academic Press, Oxford, pp. 568–572. https://doi.org/10.1016/B978-0-12-386454-3.00565-0

Edward, C.J., Kotsiopoulos, A., Harrison, S.T.L., 2022. Ferrous iron oxidation kinetics of Acidiplasma cupricumulans, a key archaeon in the mineral biooxidation consortium: Impact of nutrient availability, ferric iron and thiocyanate. Hydrometallurgy 211, 105890. https://doi.org/10.1016/j.hydromet.2022.105890

Edward, C.J., Kotsiopoulos, A., Harrison, S.T.L., 2018. Low-level thiocyanate concentrations impact on iron oxidation activity and growth of Leptospirillum ferriphilum through inhibition and adaptation. Res Microbiol 169, 576–581. https://doi.org/10.1016/j.resmic.2018.10.003

Ehrlich, H.L., 2002. How microbes mobilize metals in ores: A review of current understandings and proposals for further research. Mining, Metallurgy & Exploration 19, 220–224. https://doi.org/10.1007/BF03403273

European Union, 2023. Critical raw materials - European Commission [WWW Document]. URL https://single-market-economy.ec.europa.eu/sectors/raw-materials/areas-specific-interest/critical-raw-materials_en (accessed 2.8.24).

Franzmann, P.D., Haddad, C.M., Hawkes, R.B., Robertson, W.J., Plumb, J.J., 2005. Effects of temperature on the rates of iron and sulfur oxidation by selected bioleaching Bacteria and Archaea: Application of the Ratkowsky equation. Minerals Engineering, Selected papers from Bio and Hydrometallurgy '05, Cape Town, South Africa 18, 1304–1314. https://doi.org/10.1016/j.mineng.2005.04.006

Gadd, G.M., Griffiths, A.J., 1977. Microorganisms and Heavy Metal Toxicity. Microbial Ecology 4, 303–317.

Gahan, C.S., Sundkvist, J.-E., Sandström, Å., 2009. A study on the toxic effects of chloride on the biooxidation efficiency of pyrite. Journal of Hazardous Materials 172, 1273–1281. https://doi.org/10.1016/j.jhazmat.2009.07.133

Gangwar, C., Choudhari, R., Chauhan, A., Kumar, A., Singh, A., Tripathi, A., 2019. Assessment of air pollution caused by illegal e-waste burning to evaluate the human health risk. Environment International 125, 191–199. https://doi.org/10.1016/j.envint.2018.11.051

Gao, S., Cui, X., Zhang, S., 2020. Utilisation of Molybdenum Tailings in Concrete Manufacturing: A Review. Applied Sciences 10, 138. https://doi.org/10.3390/app10010138

Gao, X., Jiang, L., Mao, Y., Yao, B., Jiang, P., 2021. Progress, Challenges, and Perspectives of Bioleaching for Recovering Heavy Metals from Mine Tailings. Adsorption Science & Technology 2021, 1–13. https://doi.org/10.1155/2021/9941979

Gehrke, T., Telegdi, J., Thierry, D., Sand, W., 1998. Importance of Extracellular Polymeric Substances from Thiobacillus ferrooxidans for Bioleaching. Appl Environ Microbiol 64, 2743–2747. https://doi.org/10.1128/AEM.64.7.2743-2747.1998

Golyshina, O., 2014. The Family Ferroplasmaceae. The Prokaryotes: Other Major Lineages of Bacteria and The Archaea 29–34. https://doi.org/10.1007/978-3-642-38954-2_325

Golyshina, O.V., Pivovarova, T.A., Karavaiko, G.I., Kondratéva, T.F., Moore, E.R., Abraham, W.R., Lünsdorf, H., Timmis, K.N., Yakimov, M.M., Golyshin, P.N., 2000. Ferroplasma acidiphilum gen. nov., sp. nov., an acidophilic, autotrophic, ferrous-iron-oxidizing, cell-wall-lacking, mesophilic member of the Ferroplasmaceae fam. nov., comprising a distinct lineage of the Archaea. International Journal of Systematic and Evolutionary Microbiology. https://doi.org/10.1099/00207713-50-3-997

Gou, M., Zhou, L., Then, N.W.Y., 2019. Utilisation of tailings in cement and concrete: A review. Science and Engineering of Composite Materials 26, 449–464. https://doi.org/10.1515/secm-2019-0029

Gu, W., Bai, J., Dai, J., Zhang, C., Yuan, W., Wang, J., Wang, P., Zhao, X., 2014. Characterization of Extreme Acidophile Bacteria (Acidithiobacillus ferrooxidans) Bioleaching Copper from Flexible PCB by ICP-AES. Journal of Spectroscopy 2014, e269351. https://doi.org/10.1155/2014/269351

Halim, L., Suharyanti, Y., 2020. E-Waste: Current Research and Future Perspective on Developing Countries. International Journal of Industrial Engineering and Engineering Management 1, 25. https://doi.org/10.24002/ijieem.v1i2.3214

Harahuc, L., Lizama, H.M., Suzuki, I., 2000. Selective Inhibition of the Oxidation of Ferrous Iron or Sulfur in Thiobacillus ferrooxidans. Appl Environ Microbiol 66, 1031–1037.

Harrison, S., Broadhurst, J.L., Opitz, A., Fundikwa, B., Stander, H.-M., Mostert, L., Juarez, Amaral Filho, J., Kotsiopoulos, A., 2020. An Industrial Ecology Approach to Sulfide-containing Mineral Wastes to Minimise ARD Formation Part 2: Design for Disposal and Extraction of Products of Value.

Harrison, S.T.L., 2018. Towards sustainable development of mineral resources: The role of Biohydrometallurgy.

Harrison, S.T.L., Franzidis, J.P., van Hille, R.P., Mokone, T., Broadhurst, J., Kazadi-Mbamba, C., Opitz, A., Chiume, R., Vries, E., Stander, H., Jera, M., 2013. Evaluating Approaches to and Benefits of Minimising the Formation of Acid Rock Drainage Through Management of the Disposal of Sulphidic Waste Rock and Tailings: Report to the Water Research Commission. Water Research Commission.

Hartwig, T., Owor, M., Muwanga, A., Zachmann, D., Pohl, W., 2005. Lake George as a Sink for Contaminants Derived from the Kilembe Copper Mining Area, Western Uganda. Mine Water and the Environment 24, 114–123. https://doi.org/10.1007/s10230-005-0082-2

Hedrich, S., Guézennec, A.-G., Charron, M., Schippers, A., Joulian, C., 2016. Quantitative Monitoring of Microbial Species during Bioleaching of a Copper Concentrate. Frontiers in Microbiology 7.

Hong, Y., Valix, M., 2014. Bioleaching of electronic waste using acidophilic sulfur oxidising bacteria. Journal of Cleaner Production 65, 465–472. https://doi.org/10.1016/j.jclepro.2013.08.043

Hubau, A., Minier, M., Chagnes, A., Joulian, C., Silvente, C., Guezennec, A.-G., 2020. Recovery of metals in a double-stage continuous bioreactor for acidic bioleaching of printed circuit boards (PCBs). Separation and Purification Technology 238, 116481. https://doi.org/10.1016/j.seppur.2019.116481

Huerta-Rosas, B., Cano-Rodríguez, I., Gamiño-Arroyo, Z., Gómez-Castro, F.I., Carrillo-Pedroza, F.R., Romo-Rodríguez, P., Gutiérrez-Corona, J.F., 2020. Aerobic processes for bioleaching manganese and silver using microorganisms indigenous to mine tailings. World J Microbiol Biotechnol 36, 124. https://doi.org/10.1007/s11274-020-02902-6

Idrees, N., Tabassum, B., Abd Allah, E.F., Hashem, A., Sarah, R., Hashim, M., 2018. Groundwater Contamination with Cadmium Concentrations in Some West U.P. Regions, India. Saudi Journal of Biological Sciences 25. https://doi.org/10.1016/j.sjbs.2018.07.005

Igiri, B.E., Okoduwa, S.I.R., Idoko, G.O., Akabuogu, E.P., Adeyi, A.O., Ejiogu, I.K., 2018. Toxicity and Bioremediation of Heavy Metals Contaminated Ecosystem from Tannery Wastewater: A Review. Journal of Toxicology 2018, 1–16. https://doi.org/10.1155/2018/2568038

Ilyas, S., Lee, J., Chi, R., 2013. Bioleaching of metals from electronic scrap and its potential for commercial exploitation. Hydrometallurgy 131–132, 138–143. https://doi.org/10.1016/j.hydromet.2012.11.010

IndustriALL, 2019. What are tailings dams? [WWW Document]. IndustriALL. URL http://www.industriall-union.org/why-you-need-to-know-about-tailings-dams (accessed 5.13.21).

Ionescu, D., Heim, C., Polerecky, L., Thiel, V., de Beer, D., 2015. Biotic and abiotic oxidation and reduction of iron at circumneutral pH are inseparable processes under natural conditions. Geomicrobiology Journal 32, 221–230. https://doi.org/10.1080/01490451.2014.887393

Johnson, D.B., Hedrich, S., Pakostova, E., 2017. Indirect Redox Transformations of Iron, Copper, and Chromium Catalyzed by Extremely Acidophilic Bacteria. Frontiers in Microbiology 8.

Johnson, D.B., Joulian, C., d'Hugues, P., Hallberg, K.B., 2008. Sulfobacillus benefaciens sp. nov., an acidophilic facultative anaerobic Firmicute isolated from mineral bioleaching operations. Extremophiles 12, 789–798. https://doi.org/10.1007/s00792-008-0184-4

Joulian, C., Fonti, V., Chapron, S., Bryan, C.G., Guezennec, A.-G., 2020. Bioleaching of pyritic coal wastes: bioprospecting and efficiency of selected consortia. Research in Microbiology, Special Issue on International BiohydrometallurgySymposium (IBS) 2019 171, 260–270. https://doi.org/10.1016/j.resmic.2020.08.002

Kaliyaraj, D., Rajendran, M., Angamuthu, V., Antony, A.R., Kaari, M., Thangavel, S., Venugopal, G., Joseph, J., Manikkam, R., 2019. Bioleaching of heavy metals from printed circuit board (PCB) by Streptomyces albidoflavus TN10 isolated from insect nest. Bioresources and Bioprocessing 6, 47. https://doi.org/10.1186/s40643-019-0283-3

Kinnunen, P.H.-M., Kaksonen, A.H., 2019. Towards circular economy in mining: Opportunities and bottlenecks for tailings valorization. Journal of Cleaner Production 228, 153–160. https://doi.org/10.1016/j.jclepro.2019.04.171

Kirby, C.S., Thomas, H.M., Southam, G., Donald, R., 1999. Relative contributions of abiotic and biological factors in Fe(II) oxidation in mine drainage. Applied Geochemistry 14, 511–530. https://doi.org/10.1016/S0883-2927(98)00071-7

Kolmert, Å., Johnson, D.B., 2001. Remediation of acidic waste waters using immobilised, acidophilic sulfate-reducing bacteria. Journal of Chemical Technology & Biotechnology 76, 836–843. https://doi.org/10.1002/jctb.453

Lin, H., Huang, M., Huang, H., 2010. Effect of Temperature on Bioleaching Heavy Metals from Sewage Sludge, in: 2010 4th International Conference on Bioinformatics and Biomedical Engineering. Presented at the 2010 4th International Conference on Bioinformatics and Biomedical Engineering, pp. 1–4. https://doi.org/10.1109/ICBBE.2010.5518083

Lin, Y.-H., Juan, M.-L., Huang, H.-L., Tsai, H.-Y., Lin, P.H.-P., 2010. Influence of Sulfur Concentration on Bioleaching of Heavy Metals from Industrial Waste Sludge. Water Environment Research 82, 2219–2228.

Liu, Y.-G., Zhou, M., Zeng, G.-M., Wang, X., Li, X., Fan, T., Xu, W.-H., 2008. Bioleaching of heavy metals from mine tailings by indigenous sulfur-oxidizing bacteria: Effects of substrate concentration. Bioresource Technology 99, 4124–4129. https://doi.org/10.1016/j.biortech.2007.08.064

Makaula, D.X., 2019. Developing quantitative approaches to determine microbial colonisation and activity in mineral bioleaching and characterisation of acid rock drainage. University of Cape Town.

Mäkinen, J., Salo, M., Khoshkhoo, M., Sundkvist, J.-E., Kinnunen, P., 2020. Bioleaching of cobalt from sulfide mining tailings; a mini-pilot study. Hydrometallurgy 196, 105418. https://doi.org/10.1016/j.hydromet.2020.105418

Maluleke, M.D., Kotsiopoulos, A., Govender-Opitz, E., Harrison, S.T.L., 2024a. Exploring microbial adaptation of immobilised acidophilic cultures to improve microbial oxidation rates and copper tolerance in e-waste bioleaching. Minerals Engineering 207, 108560. https://doi.org/10.1016/j.mineng.2023.108560

Maluleke, M.D., Kotsiopoulos, A., Govender-Opitz, E., Harrison, S.T.L., 2024b. Microbial immobilisation and adaptation to Cu2+ enhances microbial Fe2+ oxidation for bioleaching of printed circuit boards in the presence of mixed metal ions. Research in Microbiology 175, 104148. https://doi.org/10.1016/j.resmic.2023.104148

McCarthy, T.S., 2011. The impact of acid mine drainage in South Africa. South African Journal of Science 107, 01–07. https://doi.org/10.4102/sajs.v107i5/6.712

Mindat.org, Hudson Institute of Mineralogy, 2021. Kilembe Mine, Toro, Kasese, Western Region, Uganda [WWW Document]. mindat.org. URL https://www.mindat.org/loc-19036.html (accessed 5.13.21).

Minetek, 2023. JAGERSFONTEIN: TAILINGS DAM FAILURE [WWW Document]. Minetek. URL https://minetek.com/jagersfontein-tailings-dam-failure/

Monitor, 2021. The haunting legacy of Kilembe mines [WWW Document]. Monitor. URL https://www.monitor.co.ug/uganda/special-reports/the-haunting-legacy-of-kilembe-mines-1759168 (accessed 7.21.23).

Mori de Oliveira, C., Bellopede, R., Tori, A., Marini, P., 2022. Study of Metal Recovery from Printed Circuit Boards by Physical-Mechanical Treatment Processes. Materials Proceedings 5, 121. https://doi.org/10.3390/materproc2021005121

Morin, D., Lips, A., Pinches, T., Huisman, J., Frias, C., Norberg, A., Forssberg, E., 2005. BioMinE-EUROPEAN PROJECT DEDICATED TO THE DEVELOPMENT OF BIOTECHNOLOGY FOR METAL-BEARING MATERIALS IN EUROPE.

Musisi, F., 2017. Uganda: Kilembe: How the Once Vibrant Copper Mines Ended Up in Ruins. The Monitor.

Mwesigye, A.R., Young, S.D., Bailey, E.H., Tumwebaze, S.B., 2016. Population exposure to trace elements in the Kilembe copper mine area, Western Uganda: A pilot study. Science of The Total Environment 573, 366–375. https://doi.org/10.1016/j.scitotenv.2016.08.125

Neale, J., Seppälä, J., Laukka, A., Aswegen, P., Barnett, S., Gericke, M., 2017. The MONDO Minerals Nickel Sulfide Bioleach Project: From Test Work to Early Plant Operation. Solid State Phenomena 262, 28–32. https://doi.org/10.4028/www.scientific.net/SSP.262.28

Nemati, M., Harrison, S., 2000. Effect of solid loading on thermophilic bioleaching of sulfide minerals. Journal of Chemical Technology and Biotechnology 75, 526–532. https://doi.org/10.1002/1097-4660(200007)75:7<526::AID-JCTB249>3.0.CO;2-4

Ngoma, E., Borja, D., Smart, M., Shaik, K., Kim, H., Petersen, J., Harrison, S., 2018. Bioleaching of arsenopyrite from Janggun mine tailings (South Korea) using an adapted mixed mesophilic culture. Hydrometallurgy 181. https://doi.org/10.1016/j.hydromet.2018.08.010

Nie, H., Yang, C., Zhu, N., Zhang, T., Zhang, Y., Xing, Y., 2015. Isolation of Acidithiobacillus ferrooxidans strain Z1 and its bioleaching mechanism of copper from waste printed circuit boards. Journal of Chemical Technology and Biotechnology 90. https://doi.org/10.1002/jctb.4363

Nordstrom, D., Alpers, C., 1999. Geochemistry of acid mine waters, in: The Environmental Geochemistry of Mineral Deposits. Part A. Processes, Methods, and Health Issues. pp. 133–160.

Ojumu, T.V., Petersen, J., 2011. The kinetics of ferrous ion oxidation by Leptospirillum ferriphilum in continuous culture: The effect of pH. Hydrometallurgy 106, 5–11. https://doi.org/10.1016/j.hydromet.2010.11.007

Omega Biotek, 2021. Plate sealing film, AeraSeal [WWW Document]. VWR. URL https://in.vwr.com/store/product/22982176/plate-sealing-film-aeraseal (accessed 2.9.24).

Owen, J.R., Kemp, D., Lèbre, É., Svobodova, K., Pérez Murillo, G., 2020. Catastrophic tailings dam failures and disaster risk disclosure. International Journal of Disaster Risk Reduction 42, 101361. https://doi.org/10.1016/j.ijdrr.2019.101361

Owor, M., Hartwig, T., Muwanga, A., Zachmann, D., Pohl, W., 2007. Impact of tailings from the Kilembe copper mining district on Lake George, Uganda. Environ Geol 51, 1065–1075. https://doi.org/10.1007/s00254-006-0398-7

Perlatti, F., Martins, E.P., de Oliveira, D.P., Ruiz, F., Asensio, V., Rezende, C.F., Otero, X.L., Ferreira, T.O., 2021. Copper release from waste rocks in an abandoned mine (NE, Brazil) and its impacts on ecosystem environmental quality. Chemosphere 262, 127843. https://doi.org/10.1016/j.chemosphere.2020.127843

Pivovarova, T.A., Kondrat'eva, T.F., Batrakov, S.G., Esipov, S.E., Sheichenko, V.I., Bykova, S.A., Lysenko, A.M., Karavaiko, G.I., 2002. Phenotypic Features of Ferroplasma acidiphilum Strains YT and Y-2. Microbiology 71, 698–706. https://doi.org/10.1023/A:1021436107979

Plumb, J.J., Muddle, R., Franzmann, P.D., 2008. Effect of pH on rates of iron and sulfur oxidation by bioleaching organisms. Minerals Engineering 21, 76–82. https://doi.org/10.1016/j.mineng.2007.08.018

Punia Bangar, S., Suri, S., Trif, M., Ozogul, F., 2022. Organic acids production from lactic acid bacteria: A preservation approach. Food Bioscience 46, 101615. https://doi.org/10.1016/j.fbio.2022.101615

Quatrini, R., Johnson, D.B., 2016. Acidophiles: Life in Extremely Acidic Environments. Caister Academic Press.

Rawlings, D.E., 2011. Biomining (Mineral Bioleaching, Mineral Biooxidation), in: Reitner, J., Thiel, V. (Eds.), Encyclopedia of Geobiology, Encyclopedia of Earth Sciences Series. Springer Netherlands, Dordrecht, pp. 182–185. https://doi.org/10.1007/978-1-4020-9212-1_34

Rawlings, D.E., 2005. Characteristics and adaptability of iron- and sulfur-oxidizing microorganisms used for the recovery of metals from minerals and their concentrates. Microb Cell Fact 4, 13. https://doi.org/10.1186/1475-2859-4-13

Rawlings, D.E., Johnson, D.B., 2007. The microbiology of biomining: development and optimization of mineral-oxidizing microbial consortia. Microbiology (Reading) 153, 315–324. https://doi.org/10.1099/mic.0.2006/001206-0

Roberto, F.F., Schippers, A., 2022. Progress in bioleaching: part B, applications of microbial processes by the minerals industries. Appl Microbiol Biotechnol 106, 5913–5928. https://doi.org/10.1007/s00253-022-12085-9

Sand, W., Gerke, T., Hallmann, R., Schippers, A., 1995. Sulfur chemistry, biofilm, and the (in)direct attack mechanism — a critical evaluation of bacterial leaching. Appl Microbiol Biotechnol 43, 961–966. https://doi.org/10.1007/BF00166909

Schippers, A., 2007. Microorganisms Involved in Bioleaching and Nucleic Acid-Based Molecular Methods for Their Identification and Quantification, in: Donati, E.R., Sand, W. (Eds.), Microbial Processing of Metal Sulfides. Springer Netherlands, Dordrecht, pp. 3–33. https://doi.org/10.1007/1-4020-5589-7_1

Schippers, A., Hedrich, S., Vasters, J., Drobe, M., Sand, W., Willscher, S., 2014. Biomining: Metal Recovery from Ores with Microorganisms, in: Schippers, A., Glombitza, F., Sand, W. (Eds.), Geobiotechnology I: Metal-Related Issues, Advances in Biochemical Engineering/Biotechnology. Springer, Berlin, Heidelberg, pp. 1–47. https://doi.org/10.1007/10_2013_216

Schippers, A., Sand, W., 1999. Bacterial Leaching of Metal Sulfides Proceeds by Two Indirect Mechanisms via Thiosulfate or via Polysulfides and Sulfur. Appl Environ Microbiol 65, 319–321.

Searby, G., 2006. An investigation of the kinetics of thermophilic microbial ferrous iron oxidation in continuous culture. University of Cape Town.

Shylla, L., Barik, S., Joshi, S., 2021. Characterization and bioremediation potential of native heavy-metal tolerant bacteria isolated from rat-hole coal mine environment. Archives of Microbiology 203, 1–14. https://doi.org/10.1007/s00203-021-02218-5

Singer, P.C., Stumm, W., 1970. Acidic Mine Drainage: The Rate-Determining Step. Science 167, 1121–1123. https://doi.org/10.1126/science.167.3921.1121

Smart, M., Harrison, S., Edward, C., 2017a. Recycling bioremediated cyanidation tailings wastewater within the biooxidation circuit for gold recovery: impact on process performance and water management.

Smart, M., Huddy, R., Edward, C., Fourie, C., Shumba, T., Iron, J., Harrison, S., 2017b. Linking Microbial Community Dynamics in BIOX® Leaching Tanks to Process Conditions: Integrating Lab and Commercial Experience. Solid State Phenomena 262, 38–42. https://doi.org/10.4028/www.scientific.net/SSP.262.38

Smart, M., Huddy, R., Edward, C., Fourie, C., Trust, S., Iron, J., Harrison, S., 2017c. Linking Microbial Community Dynamics in BIOX® Leaching Tanks to Process Conditions: Integrating Lab and Commercial Experience. Solid State Phenomena 262, 38–42. https://doi.org/10.4028/www.scientific.net/SSP.262.38

Smith, J.R., Luthy, R.G., Middleton, A.C., 1988. Microbial Ferrous Iron Oxidation in Acidic Solution. Journal (Water Pollution Control Federation) 60, 518–530.

Smith, S.L., Johnson, D.B., 2018. Growth of Leptospirillum ferriphilum in sulfur medium in co-culture with Acidithiobacillus caldus. Extremophiles 22, 327–333. https://doi.org/10.1007/s00792-018-1001-3

Song, Z., Song, G., Tang, W., Yan, D., Zhao, Y., Zhu, Y., Wang, J., Ma, Y., 2021. Molybdenum contamination dispersion from mining site to a reservoir. Ecotoxicology and Environmental Safety 208, 111631. https://doi.org/10.1016/j.ecoenv.2020.111631

Suzuki, G., Someya, M., Matsukami, H., Tue, N., Uchida, N., Huu Tuyen, L., Viet, P., Takahashi, S., Tanabe, S., Brouwer, A., Takigami, H., 2016. Comprehensive evaluation of dioxins and dioxin-like compounds in surface soils and river sediments from e-waste-processing sites in a village in northern Vietnam: Heading towards the environmentally sound management of e-waste. Emerging Contaminants 2. https://doi.org/10.1016/j.emcon.2016.03.001

Tapia, J., Dueñas, A., Cheje, N., Soclle, G., Patiño, N., Ancalla, W., Tenorio, S., Denos, J., Taco, H., Cao, W., Alexandrino, D.A.M., Jia, Z., Vasconcelos, V., Carvalho, M. de F., Lazarte, A., 2022. Bioleaching of Heavy Metals from Printed Circuit Boards with an Acidophilic Iron-Oxidizing Microbial Consortium in Stirred Tank Reactors. Bioengineering (Basel) 9, 79. https://doi.org/10.3390/bioengineering9020079

Tenywa, G., 2013. Ghost of copper mining still haunts environment [WWW Document]. New Vision. URL https://www.newvision.co.ug/articledetails/undefined (accessed 7.21.23).

Tian, J., Wu, N., Li, J., Liu, Y., Guo, J., Yao, B., Fan, Y., 2007. Nickel-Resistant Determinant from Leptospirillum ferriphilum. Appl Environ Microbiol 73, 2364–2368. https://doi.org/10.1128/AEM.00207-07

Tupikina, O.V., Minnaar, S.H., van Hille, R.P., van Wyk, N., Rautenbach, G.F., Dew, D., Harrison, S.T.L., 2013. Determining the effect of acid stress on the persistence and growth of thermophilic microbial species after mesophilic colonisation of low grade ore in a heap leach environment. Minerals Engineering 53, 152–159. https://doi.org/10.1016/j.mineng.2013.07.015

Uchida, N., Matsukami, H., Someya, M., Tue, N., Huu Tuyen, L., Viet, P., Takahashi, S., Tanabe, S., Suzuki, G., 2018. Hazardous metals emissions from e-waste-processing sites in a village in northern Vietnam. Emerging Contaminants 4. https://doi.org/10.1016/j.emcon.2018.10.001

United Nations, 2021. Take Action for the Sustainable Development Goals [WWW Document]. United Nations Sustainable Development. URL https://www.un.org/sustainabledevelopment/sustainable-development-goals/ (accessed 5.13.21).

Vardanyan, A., Vardanyan, N., Khachatryan, A., Zhang, R.-Y., Sand, W., 2019. Adhesion to Mineral Surfaces by Cells of Leptospirillum, Acidithiobacillus and Sulfobacillus from Armenian Sulfide Ores. Minerals 9, 69. https://doi.org/10.3390/min9020069

Vera, M., Schippers, A., Hedrich, S., Sand, W., 2022. Progress in bioleaching: fundamentals and mechanisms of microbial metal sulfide oxidation – part A. Appl Microbiol Biotechnol 106, 6933–6952. https://doi.org/10.1007/s00253-022-12168-7

Wang, Q., Zhang, B., Yu, S., Xiong, J., Yao, Z., Hu, B., Yan, J., 2020. Waste-Printed Circuit Board Recycling: Focusing on Preparing Polymer Composites and Geopolymers. ACS Omega 5, 17850–17856. https://doi.org/10.1021/acsomega.0c01884

Wang, S., Liu, T., Xiao, X., Luo, S., 2021. Advances in microbial remediation for heavy metal treatment: a mini review. J Leather Sci Eng 3, 1. https://doi.org/10.1186/s42825-020-00042-z

Watling, H., 2016. Microbiological Advances in Biohydrometallurgy. Minerals 6, 49. https://doi.org/10.3390/min6020049

Wu, W., Liu, X., Zhang, X., Zhu, M., Tan, W., 2018. Bioleaching of copper from waste printed circuit boards by bacteria-free cultural supernatant of iron–sulfur-oxidizing bacteria. Bioresources and Bioprocessing 5, 10. https://doi.org/10.1186/s40643-018-0196-6

Xia, M., Bao, P., Liu, A., Wang, M., Shen, L., Yu, R., Liu, Y., Chen, M., Li, J., Wu, X., Qiu, G., Zeng, W., 2018. Bioleaching of low-grade waste printed circuit boards by mixed fungal culture and its community structure analysis. Resources, Conservation and Recycling 136, 267–275. https://doi.org/10.1016/j.resconrec.2018.05.001

Yahya, M., 2016. Design and Performance Evaluation of a Solar Assisted Heat Pump Dryer Integrated with Biomass Furnace for Red Chilli. International Journal of Photoenergy 2016, 1–14. https://doi.org/10.1155/2016/8763947

Yamane, L., Espinosa, D., Tenório, J., 2011. Bioleaching of copper from electronic scrap. Rem: Revista Escola de Minas 64, 327–333. https://doi.org/10.1590/S0370-44672011000300011

Yang, L., Zhao, D., Yang, J., Wang, W., Chen, P., Zhang, S., Yan, L., 2019. Acidithiobacillus thiooxidans and its potential application. Appl Microbiol Biotechnol 103, 7819–7833. https://doi.org/10.1007/s00253-019-10098-5

Yang, Y., Chen, S., Li, S., Chen, M., Chen, H., Liu, B., 2014. Bioleaching waste printed circuit boards by Acidithiobacillus ferrooxidans and its kinetics aspect. Journal of Biotechnology 173, 24–30. https://doi.org/10.1016/j.jbiotec.2014.01.008

Ye, M., Li, G., Yan, P., Ren, J., Zheng, L., Han, D., Sun, S., Huang, S., Zhong, Y., 2017. Removal of metals from lead-zinc mine tailings using bioleaching and followed by sulfide precipitation. Chemosphere 185, 1189–1196. https://doi.org/10.1016/j.chemosphere.2017.07.124

Yue, G., Zhao, L., Olvera, O.G., Asselin, E., 2014. Speciation of the H2SO4–Fe2(SO4)3–FeSO4–H2O system and development of an expression to predict the redox potential of the Fe3+/Fe2+ couple up to 150°C. Hydrometallurgy 147–148, 196–209. https://doi.org/10.1016/j.hydromet.2014.05.008

Zeng, X., Zheng, L., Xie, H., Lu, B., Xia, K., Chao, K., Li, W., Yang, J., Lin, S., Li, J., 2012. Current Status and Future Perspective of Waste Printed Circuit Boards Recycling. Procedia Environmental Sciences, The Seventh International Conference on Waste Management and Technology (ICWMT 7) 16, 590–597. https://doi.org/10.1016/j.proenv.2012.10.081

Zhang, L., Wu, J., Wang, Y., Wan, L., Mao, F., Zhang, W., Chen, X., Zhou, H., 2014. Influence of bioaugmentation with Ferroplasma thermophilum on chalcopyrite bioleaching and microbial community structure. Hydrometallurgy 146, 15–23. https://doi.org/10.1016/j.hydromet.2014.02.013

Zhang, R., Hedrich, S., Jin, D., Breuker, A., Schippers, A., 2021. Sulfobacillus harzensis sp. nov., an acidophilic bacterium inhabiting mine tailings from a polymetallic mine. International Journal of Systematic and Evolutionary Microbiology 71. https://doi.org/10.1099/ijsem.0.004871

Zhang, R., Hedrich, S., Römer, F., Goldmann, D., Schippers, A., 2020. Bioleaching of cobalt from Cu/Co-rich sulfidic mine tailings from the polymetallic Rammelsberg mine, Germany. Hydrometallurgy 197, 105443. https://doi.org/10.1016/j.hydromet.2020.105443

Zhao, H., Yang, C., Zhang, X., Zhang, Y., Qiu, G., 2021. Chapter 7 - Industrial application for chalcopyrite bioleaching, in: Zhao, H., Yang, C., Zhang, X., Zhang, Y., Qiu, G. (Eds.), Biohydrometallurgy of Chalcopyrite. Elsevier, pp. 211–231. https://doi.org/10.1016/B978-0-12-821880-8.00002-6

Zhao, W., Xu, J., Fei, W., Liu, Z., He, W., Li, G., 2023. The reuse of electronic components from waste printed circuit boards: a critical review. Environmental Science: Advances 2, 196–214. https://doi.org/10.1039/D2VA00266C

Appendix A: Analytical methods

A.1 Iron standard curve

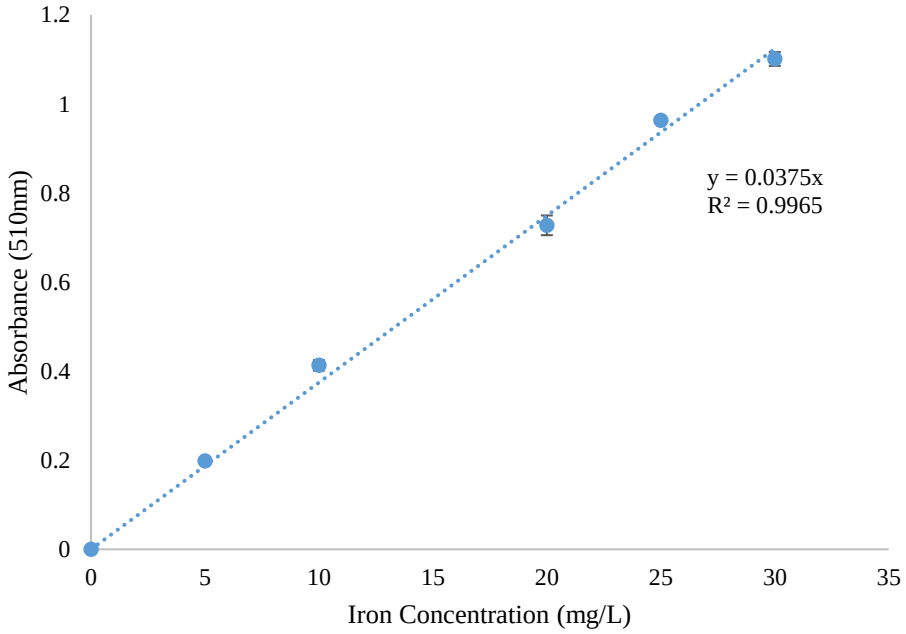

Figure A-1: Iron standard curve generated using a 100 mg/L stock solution of ferrous sulfate. This standard curve is used for the calculation of ferrous and total iron concentration.

Appendix B: Supplementary results

B.1 Batch Microwell plate tests without sulfur substrate

Several rounds of Microwell plate (MWP) tests were completed in order to calculate the average values reported in the results and discussion. These tests are seen in the figures below.

B.1.1 Initial BIOX® chromium tests (testing a wide range of concentrations from literature to determine key concentrations)

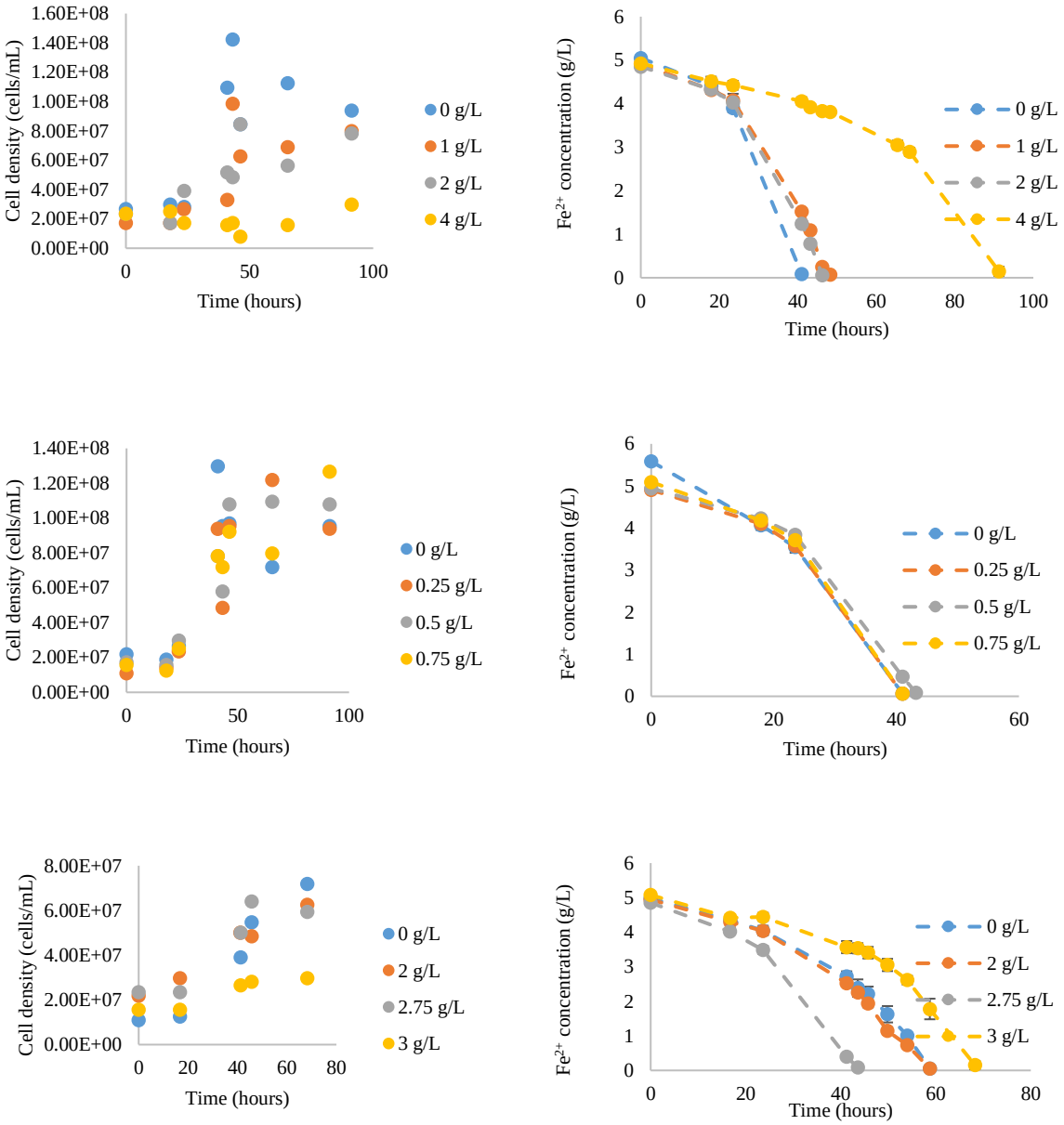

Figure B.1.1 A: Cell density and iron oxidation graphs using BIOX® culture

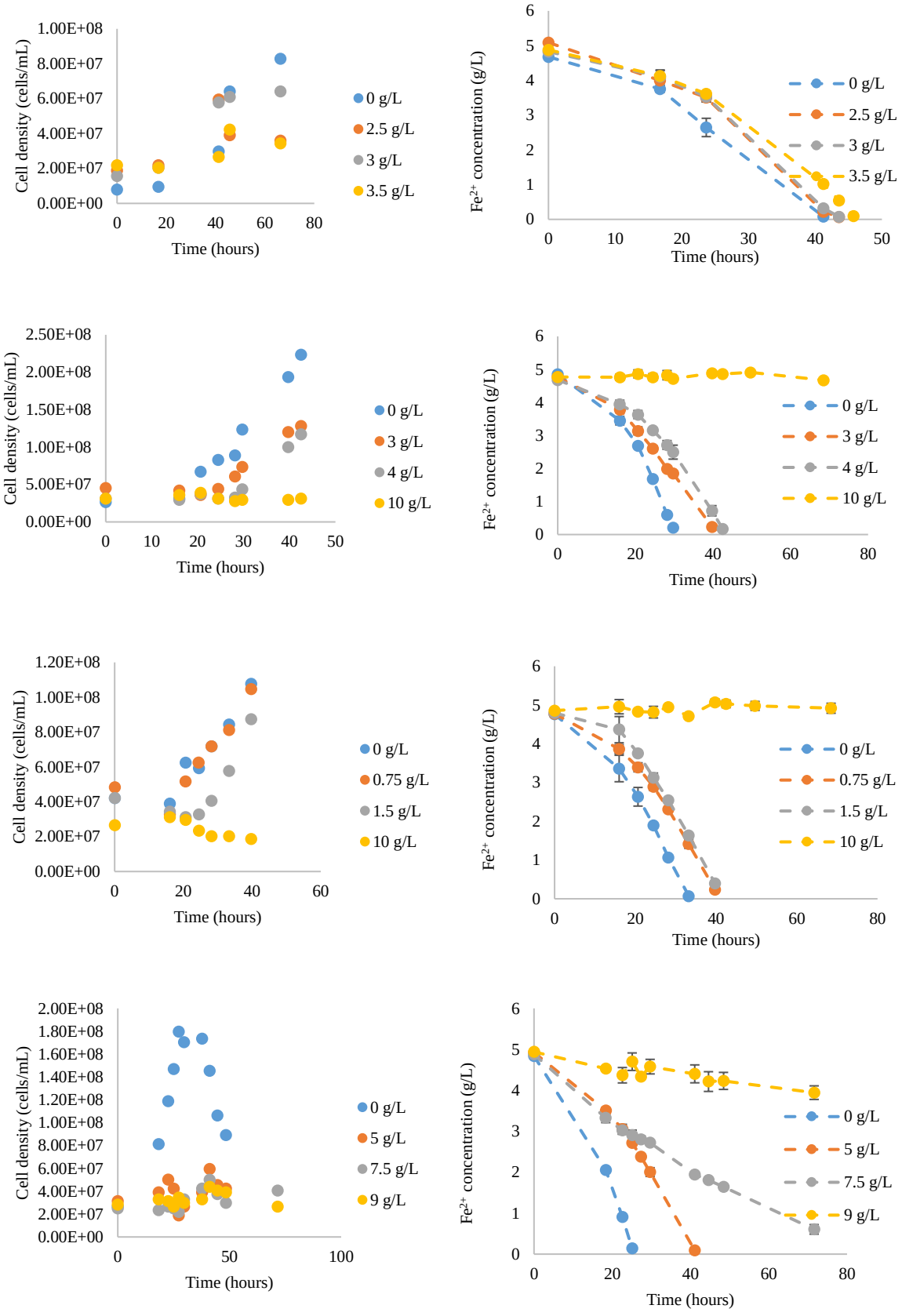

Figure B.1.1 B: Cell density and iron oxidation graphs using BIOX® culture continued (B)

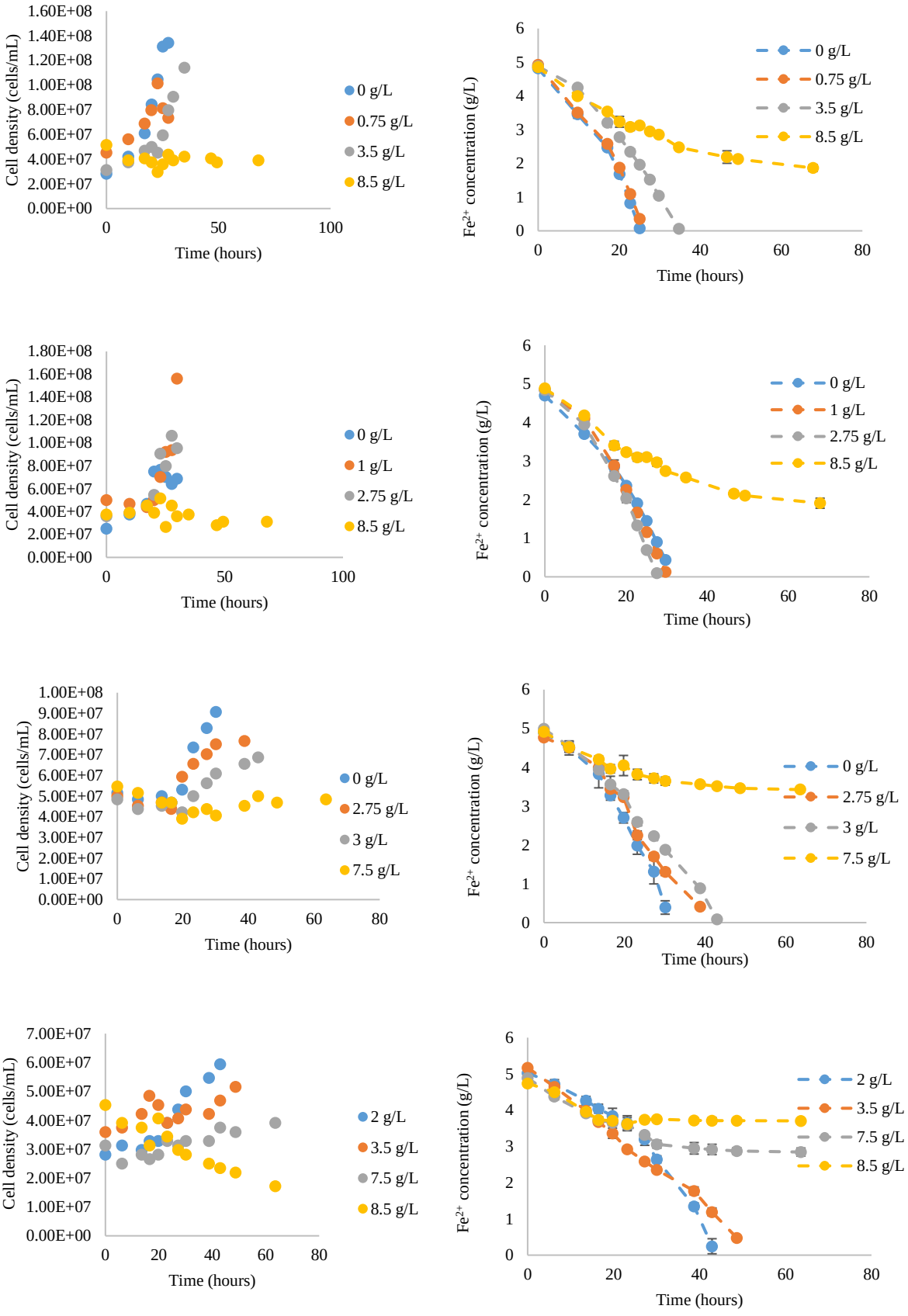

Figure B.1.1 C: Cell density and iron oxidation graphs using BIOX® culture continued (C)

B.1.2 BRGM-KCC chromium tests (key concentrations tested only)

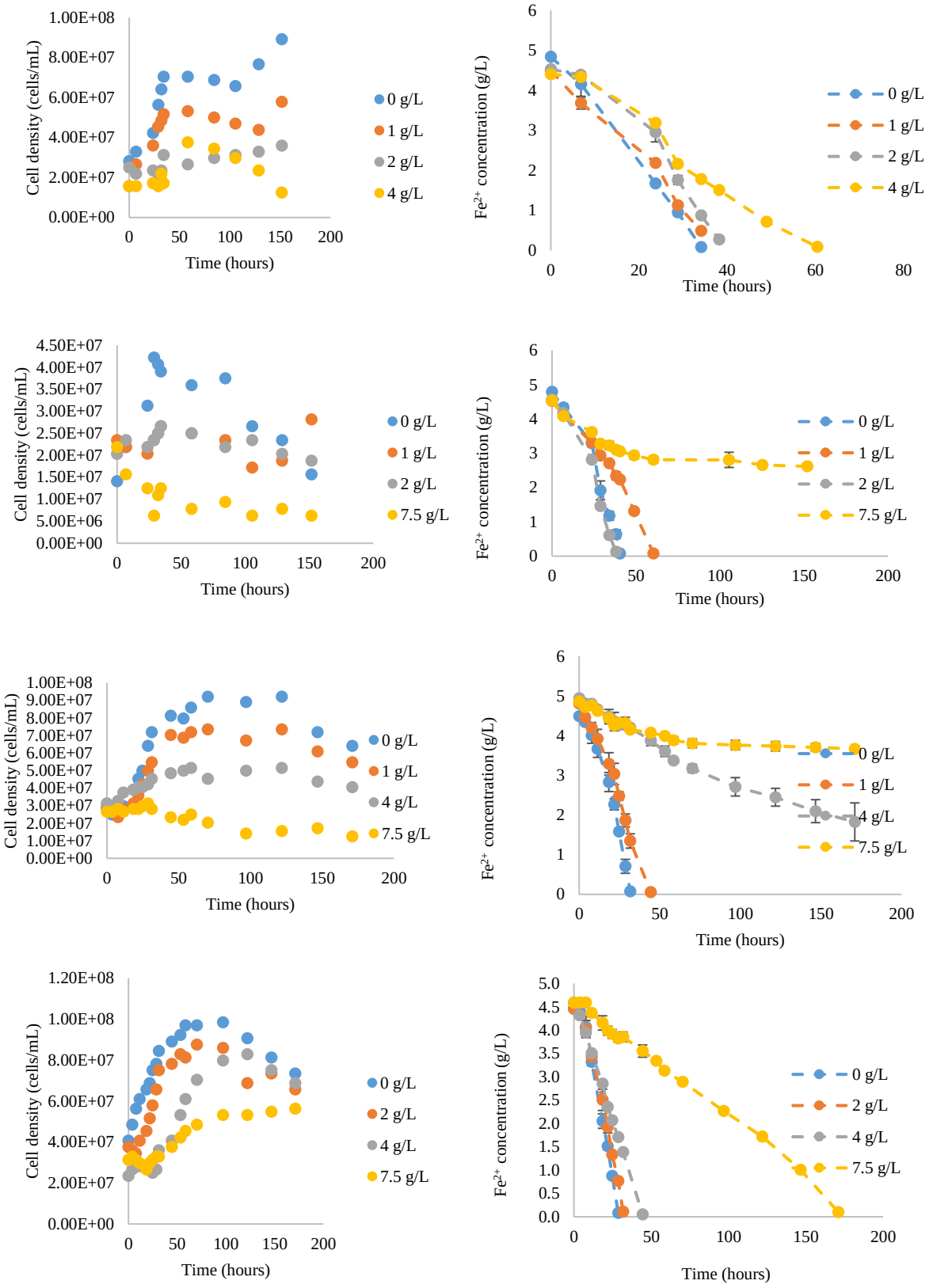

Figure B.1.2: Cell density and iron oxidation graphs using BRGM-KCC culture

B.1.3 Initial BIOX® nickel tests (testing a wide range of concentrations from literature to determine key concentrations)

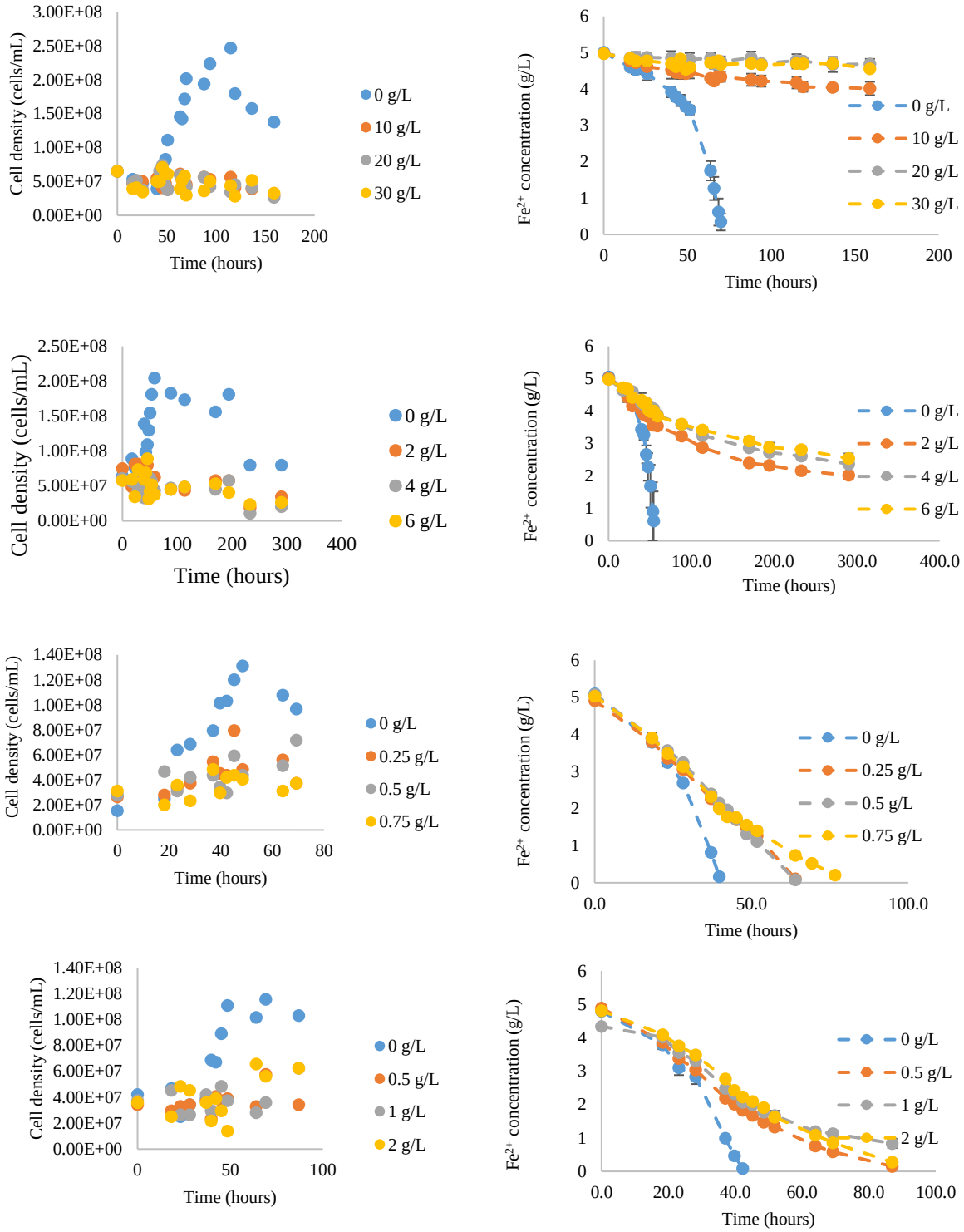

Figure B.1.3 A: Cell density and iron oxidation graphs using BIOX® culture (A)

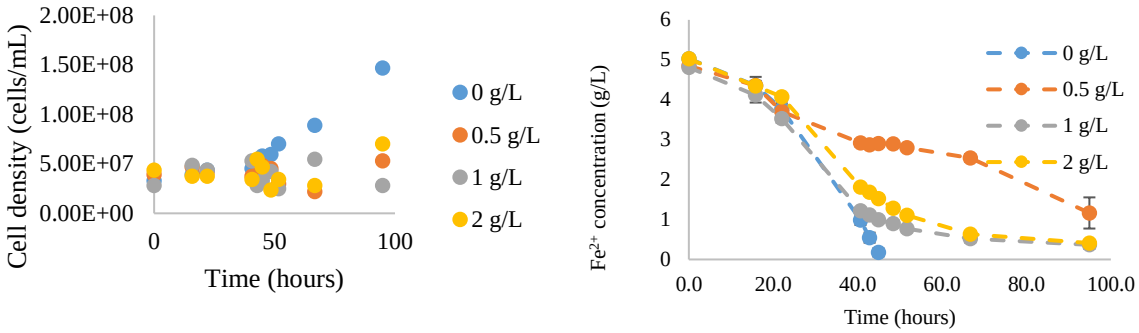

Figure B.1.3 B: Cell density and iron oxidation graphs using BIOX® culture continued (B)

B.1.4 BRGM-KCC nickel tests (key concentrations tested only)

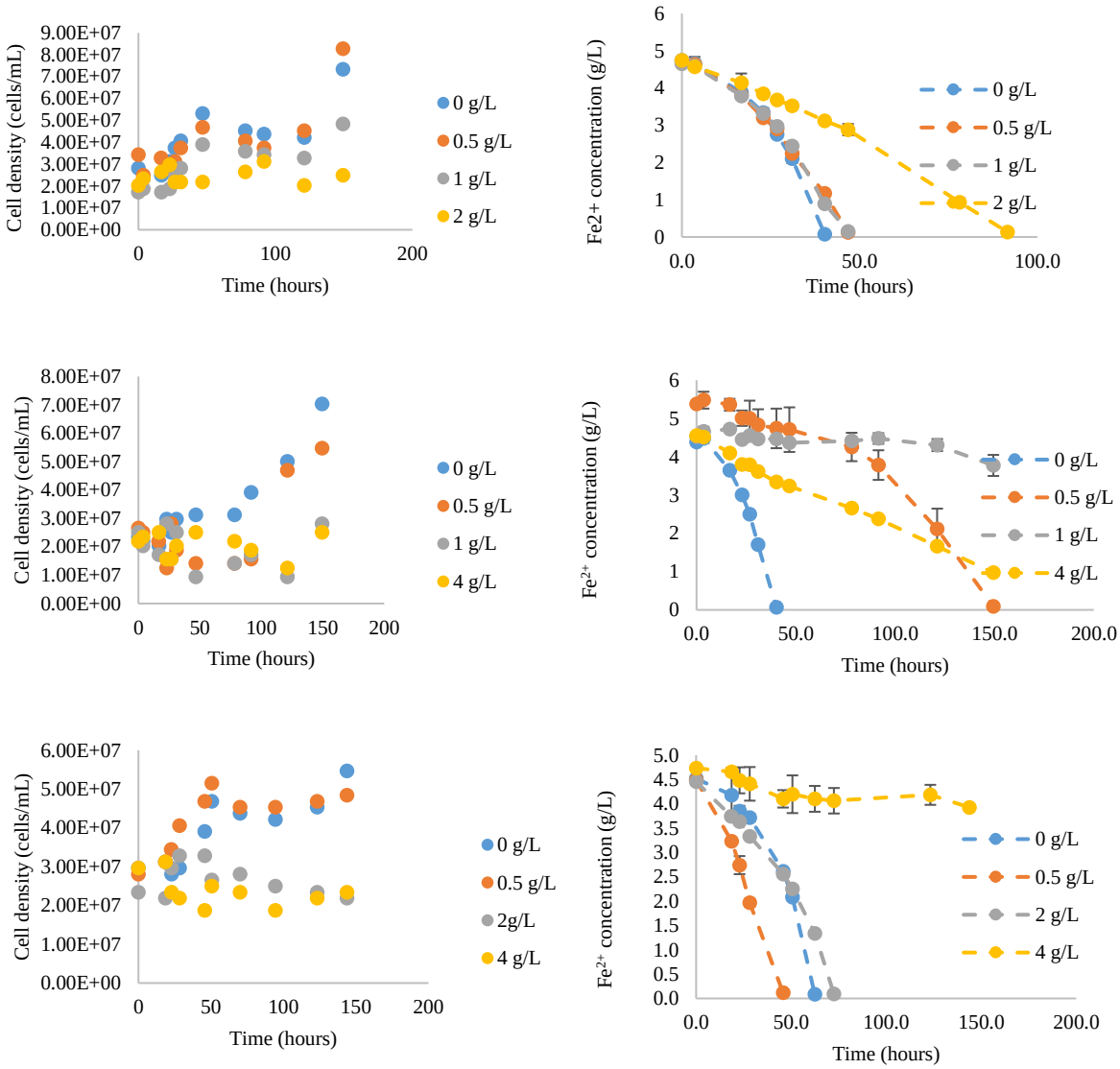

Figure B.1.4 A: Cell density and iron oxidation graphs using BRGM-KCC culture (A)

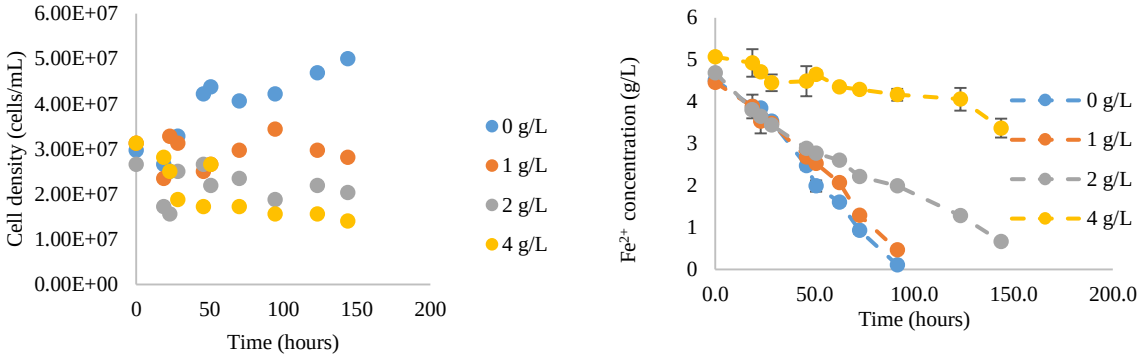

Figure B.1.4 B: Cell density and iron oxidation graphs using BRGM-KCC culture continued (B)

B.1.5 Average maximum volumetric ferrous iron oxidation rates (BIOX®)

Table B.1.5: Average maximum volumetric ferrous iron oxidation rates for BIOX® culture exposed to increasing concentrations of Ni^{2+} and Cr^{3+} at 45°C

Ni^{2+} concentration (g/L)	**Average maximum volumetric Fe^{2+} oxidation rate ($g.L^{-1}.h^{-1}$)**	**Cr^{3+} concentration (g/L)**	**Average maximum volumetric Fe^{2+} oxidation rate ($g.L^{-1}.h^{-1}$)**
0	0.213 ± 0.048	0	0.213 ± 0.048
0.5	0.069 ± 0.033	1	0.197 ± 0.019
1	0.057 ± 0.039	2	0.175 ± 0.028
2	0.055 ± 0.036	4	0.137 ± 0.091
4	0.018 ± 0.036	7.5	0.054 ± 0.015

B.1.6 Average maximum volumetric ferrous iron oxidation rates (BRGM-KCC)

Table B.1.5: Average maximum volumetric ferrous iron oxidation rates for BRGM-KCC culture exposed to increasing concentrations of Ni^{2+} and Cr^{3+} at 35°C

Ni^{2+} concentration (g/L)	**Average maximum volumetric Fe^{2+} oxidation rate ($g.L^{-1}.h^{-1}$)**	**Cr^{3+} concentration (g/L)**	**Average maximum volumetric Fe^{2+} oxidation rate ($g.L^{-1}.h^{-1}$)**
0	0.160 ± 0.052	0	0.160 ± 0.052
0.5	0.107 ± 0.047	1	0.133 ± 0.042
1	0.066 ± 0.064	2	0.135 ± 0.008
2	0.054 ± 0.033	4	0.085 ± 0.045
4	0.014 ± 0.009	7.5	0.031 ± 0.009

B.2 Batch Microwell plate tests with sulfur substrate

Several rounds of MWP tests were completed in order to calculate the average values reported in the results and discussion. These tests are seen in the figures below.

B.2.1 BRGM-KCC chromium tests (key concentrations tested only)

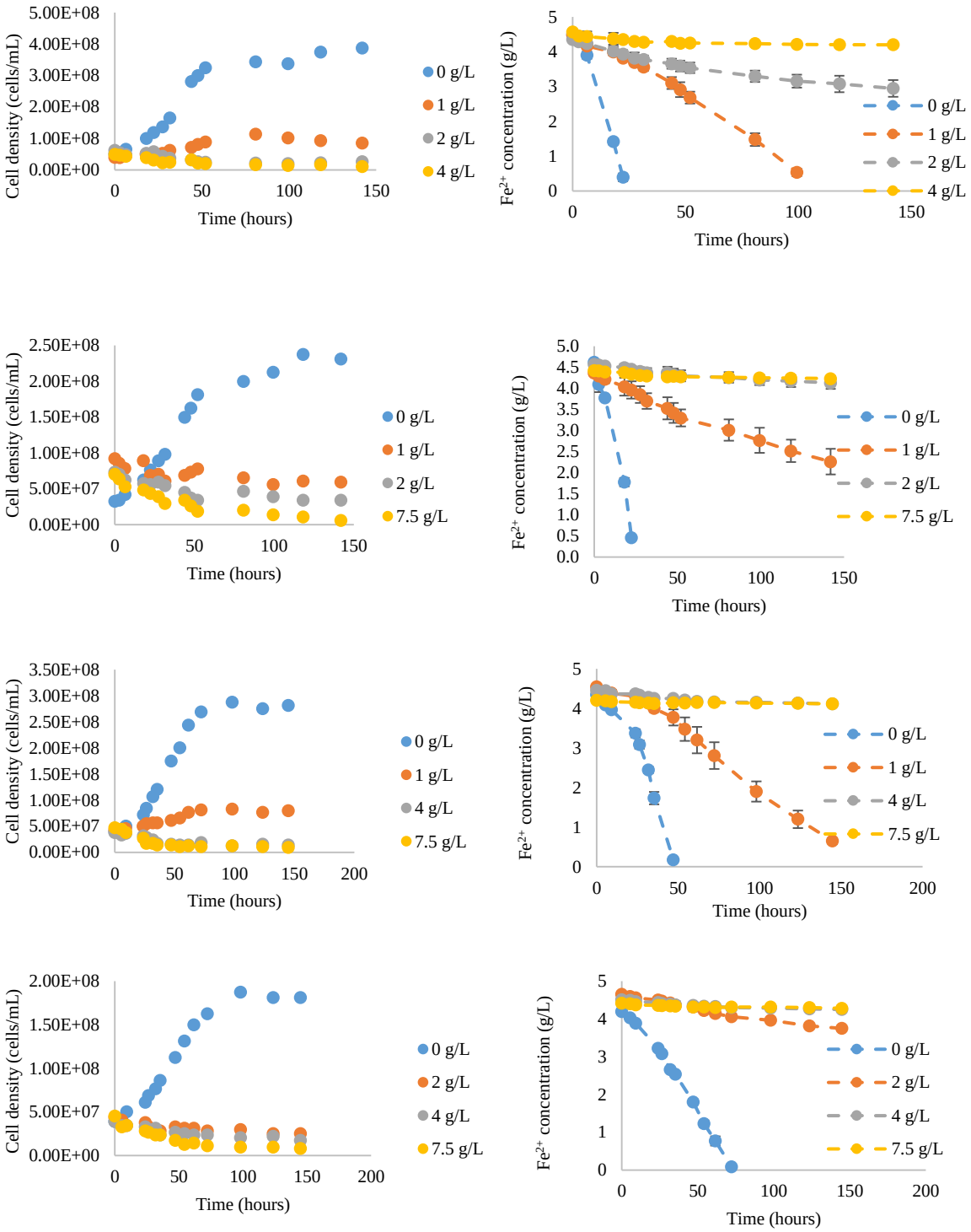

Figure B.2.1: Cell density and iron oxidation graphs using BRGM-KCC culture

B.2.2 BRGM-KCC nickel tests (key concentrations tested only)

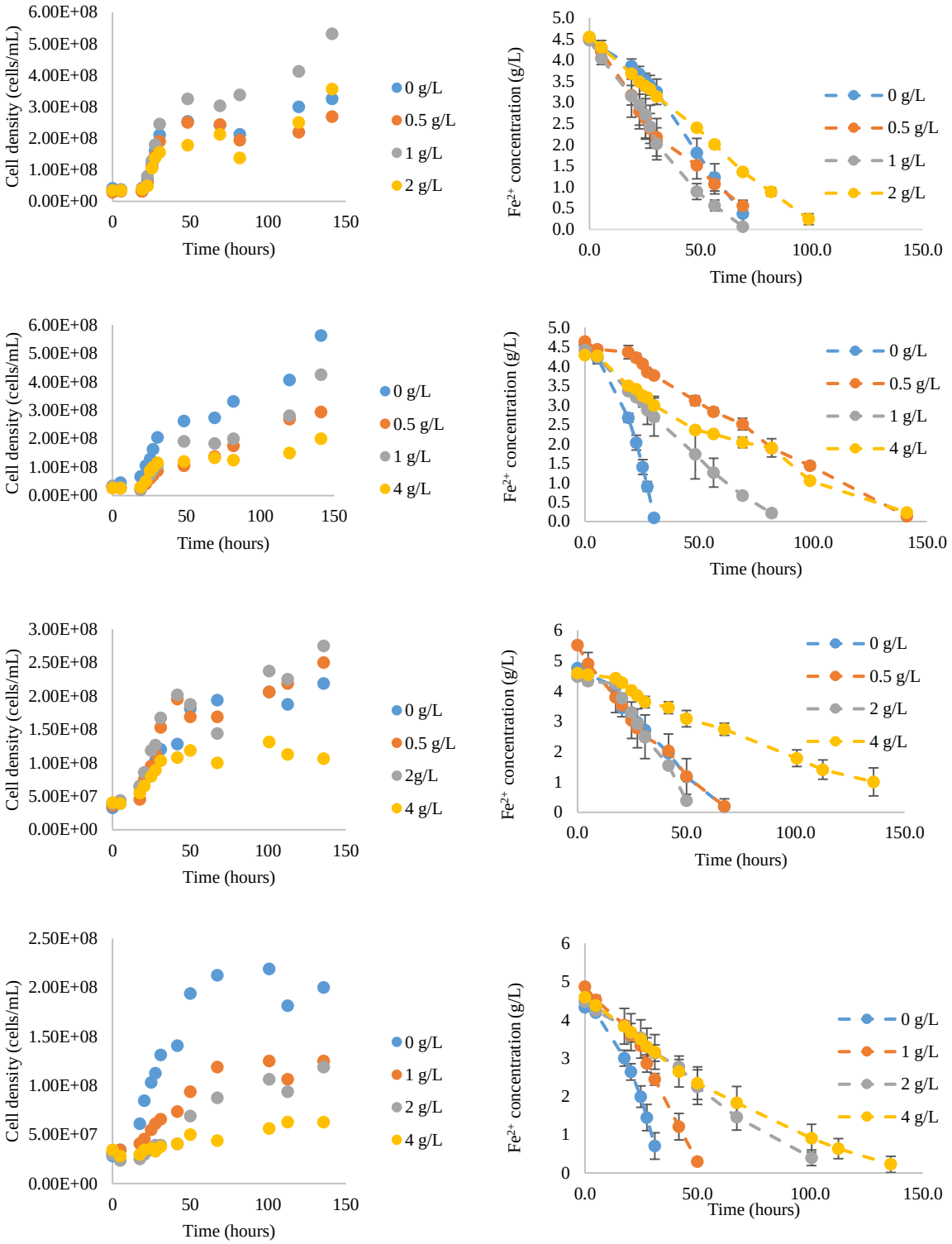

Figure B.2.2: Cell density and iron oxidation graphs using BRGM-KCC culture

B.2.3 Average maximum volumetric ferrous iron oxidation rates

Table B.2.1: Average maximum volumetric ferrous iron oxidation rates for BRGM-KCC culture exposed to increasing concentrations of Ni^{2+} and Cr^{3+} in media containing iron and sulfur

Ni^{2+} concentration (g/L)	**Average maximum volumetric Fe^{2+} oxidation rate ($g.L^{-1}.h^{-1}$)**	**Cr^{3+} concentration (g/L)**	**Average maximum volumetric Fe^{2+} oxidation rate ($g.L^{-1}.h^{-1}$)**
0	0.146 ± 0.063	0	0.146 ± 0.063
0.5	0.074 ± 0.027	1	0.035 ± 0.012
1	0.095 ± 0.035	2	0.016 ± 0.013
2	0.068 ± 0.035	4	0.007 ± 0.004
4	0.058 ± 0.007	7.5	0.003 ± 0.001

B.3 Semi-continuous bioreactor study

Table B.3: List of nickel and chromium concentrations for different PCB solids loading (highlighted is what was used)

PCB solids loading (w/v %)	Ni concentration (g/L)	Cr concentration (g/L)
0.5	0.0178	0.0006
1	0.0357	0.0012
2	0.0714	0.0023
3	0.1071	0.0035
4	0.1428	0.0046
5	0.1784	0.0058
6	0.2141	0.0069
7	0.2498	0.0081
8	0.2855	0.0093
9	0.3212	0.0104
10	0.3569	0.0116
20	0.7138	0.0231
30	1.0707	0.0347
40	1.4276	0.0463
50	1.7845	0.0578
60	2.1414	0.0694
80	2.8552	0.0925
100	3.5690	0.1157
200	7.1379	0.2313
300	10.7069	0.3470
400	14.2758	0.4626
500	17.8448	0.5783
800	28.5516	0.9252